

DESIGN OF WEIRS ON PERMEABLE ANISOTROPIC POROUS MEDIUM

A DISSERTATION

Submitted in partial fulfillment of the
requirements for the award of the degree

of

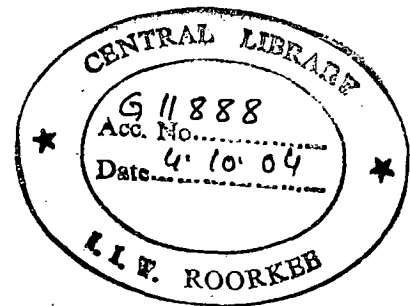
MASTER OF TECHNOLOGY

in

IRRIGATION WATER MANAGEMENT

By

TEK BAHADUR KARKI



WATER RESOURCES DEVELOPMENT TRAINING CENTRE
INDIAN INSTITUTE OF TECHNOLOGY ROORKEE
ROORKEE-247 667 (INDIA)

JUNE, 2004

CANDIDATE'S DECLARATION


I hereby declare that the dissertation entitled “**DESIGN OF WEIRS ON PERMEABLE ANISOTROPIC POROUS MEDIUM**” is being submitted by me in partial fulfillment of requirement for the award of degree of “**Master of Technology in IRRIGATION WATER MANAGEMENT**” and submitted in the Water Resources Development Training Centre, Indian Institute of Technology, Roorkee, is an authentic record of my own work carried out during the period from July, 2003 to June, 2004 under the guidance of **Dr. G.C. Mishra**, Professor, Water Resources Development Training Centre, Indian Institute of Technology, Roorkee.

The matter embodied in the dissertation has not been submitted by me for the award of any other degree.


(Tek Bahadur Karki)

Roorkee, Dated: June 30, 2004

This is to certify that the above statement made by the candidate is correct to the best of my knowledge.


(Dr.G.C. Mishra)
Professor, WRDTC,
Indian Institute of Technology, Roorkee
Uttaranchal, India.

ACKNOWLEDGMENTS

On the occasion of completion of the work reported in this dissertation the author has great pleasure in expressing his profound gratitude and indebtedness to Dr. G.C. Mishra, Professor, Water Resources Development Centre, Indian Institute of Technology Roorkee, for his inspiring guidance, constant encouragement and immense help. The author has all appreciation for his deep understanding, untiring enthusiasm and the great care he took in bringing up the dissertation to its present form.

The author is also grateful to Dr. U.C. Chaube, Professor and Head of Department of Water Resources Development Centre for his valuable support and kind help extended during all stages of this work.

The author expresses his sincere thanks to the faculty and the staff of the Water Resources Development Centre for their immense help during the preparation of this dissertation. The author is specially thankful to his friends and colleagues Er. Gir Bahadur K.C. and all trainee officers of 47th WRD and 23rd

IWM batch for their help and co-operation at different stages of this work.

The author is very much grateful to the Indian Council for Culture Relations, Government of India for awarding Fellowship to pursue his study in India.

The author is equally grateful to the Department of Irrigation, Ministry of Water Resources, His Majesty's Government of Nepal for granting study leave to complete his M.Tech. Degree.

The author acknowledges forbearance, never-ending support and immense patience, of his wife Mrs. Ranjana Karki and son Master Saket Karki, which have their own significance in completion of his M.Tech. Degree.

Tek Bahadur Karki

CONTENTS

	Page No.
CANDIDATE'S DECLARATION	(i)
ACKNOWLEDGEMENTS	(ii)
CONTENTS	(iv)
NOTATION	(vi)
ABSTRACT	(ix)
CHAPTER 1. INTRODUCTION ...	1
CHAPTER 2. REVIEW OF LITERATURE ...	4
2.1 General ...	4
2.2 Field and Laboratory Investigations ...	4
2.3 Summary of Literature ...	6
CHAPTER 3. FLOW UNDER A FLAT BOTTOMED WEIR ON ANISOTROPIC POROUS MEDIUM OF INFINITE DEPTH ...	8
3.1 General ...	8
3.2 Statement of the Problem ...	8
3.3 Analysis ...	9
3.4 Results and Discussion ...	15
3.5 Conclusion ...	26
CHAPTER 4. DESIGN OF TOE STRUCTURE FOR CONTROLLING THE EXIT GRADIENT ...	28
4.1 General ...	28
4.2 Statement of the Problem ...	28
4.3 Analysis ...	28
4.4 Results and Discussion ...	35
4.5 Conclusion ...	37

CHAPTER 5.	DESIGN OF DOWNSTREAM FILTER		
	BLANKET FOR A WEIR	...	39
	5.1 General	...	39
	5.2 Statement of the Problem	...	39
	5.3 Analysis	...	40
	4.4 Results and Discussion	...	45
	4.5 Conclusion	...	46
CHAPTER 6.	GENERAL DISCUSSIONS		
	AND CONCLUSIONS	...	47
APPENDIX-I.	FLOW REGION TRANSFORMATION	...	51
APPENDIX-II.	RELATIONSHIPS BETWEEN EXIT		
	GRADIENTS IN ORIGINAL AND		
	TRANSFORMED DOMAINS	...	54
APPENDIX-III.	FORTRAN PROGRAM	...	57
APPENDIX-IV	REFERENCES	...	79

NOTATION

The following symbols are used in this dissertation:

$B()$	=	complete beta function;
$B_x(), B_t()$	=	incomplete beta function;
b	=	width of weir in actual anisotropic flow domain ;
b_1, b_2	=	width of upstream and down stream blanket respectively, in actual anisotropic flow domain ;
\bar{b}	=	width of weir in fictitious isotropic flow domain ;
\bar{b}_1, \bar{b}_2	=	width of upstream and down stream blanket respectively, in fictitious isotropic flow domain ;
C	=	constant ;
	=	point of intersection of horizontal floor and downstream face of sheet pile in chapter 3;
	=	point of intersection of horizontal floor and upstream face of sheet pile in chapter 4;
D	=	point corresponding to the tip of sheet pile;
E	=	point of intersection of horizontal floor and upstream face of sheet pile in chapter 3;
\bar{d}	=	absolute value for \bar{s}_1 corresponding to depth of toe in fictitious isotropic flow domain ;
F_g	=	gravitational force;
F_s	=	seepage force;
H	=	Upstream head of water;
I_E	=	Exit gradient in anisotropic flow domain;
\bar{I}_E	=	Exit gradient in fictitious isotropic flow domain;
i	=	$\sqrt{-1}$;
k	=	$\sqrt{k_\mu k_\lambda}$; (equivalent coefficient of permeability of the fictitious homogeneous isotropic flow domain);
k_μ, k_λ	=	Principle coefficient of permeability in the direction of μ and λ , respectively;
m	=	parameter;

mf	=	magnification coefficient for transforming the value of exit gradient from fictitious isotropic flow region to actual anisotropic flow domain.
N	=	k_{μ}/k_{λ}
M, M_1, M_2, M_3	=	constants;
N, N_1, N_2, N_3	=	constants;
P	=	pressure
r_1, r_2, r_3	=	transformation coefficients to transfer the horizontal length, vertical length and the ratio of horizontal and vertical length from actual anisotropic flow domain to a fictitious isotropic flow region;
s	=	embedded length of sheet pile in actual anisotropic flow domain;
\bar{s}	=	embedded length of sheet pile in fictitious isotropic flow domain;
s1	=	embedded depth of toe structure in actual anisotropic flow domain;
$\bar{s}1$	=	embedded depth of toe structure in fictitious isotropic flow domain;
t	=	parametric plane;
w	=	complex potential = $\phi+i\Psi$
x_2	=	top width of toe structure in actual anisotropic flow domain in chapter 4
$\bar{x}2$	=	top width of toe wall in fictitious isotropic flow domain in chapter 4
x_1+x_2	=	bottom width of toe wall in actual anisotropic flow domain in chapter 4
$\bar{x}1 + \bar{x}2$	=	bottom width of toe wall in fictitious isotropic flow domain in chapter 4
x, y, \bar{x}, \bar{y}	=	cartesian co-ordinates;
$Z_B, Z_C, Z_D, Z_E,$		

$Z_{\bar{F}}, Z_{\bar{G}}, Z_{\bar{H}},$	=	z coordinates in fictitious isotropic flow domain corresponding to the points $\bar{B}, \bar{C}, \bar{D}, \bar{E}, \bar{F}, \bar{G}, \bar{H}$, respectively;
μ, λ	=	Cartesian co-ordinates;
α	=	b/s ratio;
$\bar{\alpha}$	=	$\frac{\bar{b}}{s}$;
θ	=	angle made by maximum coefficient of permeability with downstream horizontal boundary;
β	=	parameter;
β_1	=	parameter
β_2	=	parameter;
ν	=	parameter;
γ	=	angle in units of π made by embedded length of sheet pile with upstream horizontal boundary in fictitious isotropic flow domain;
	=	angle in units of π made by scoured surface with downstream face of sheet pile in chapter 5
γ_w	=	unit weight of water;
δ	=	angle in degrees made by scoured surface with the horizontal in chapter 5;
ϕ	=	velocity potential function;
Ψ	=	stream function;

Note : *Additional notations are defined locally wherever they occur.*

ABSTRACT

Field and laboratory tests indicate that most natural and man-made porous media exhibit directional variation in permeability. However, in general practice, hydraulic structures are designed based on the analysis of flow through isotropic porous media. The analyses have shown that the anisotropy may have considerable influence on the pressure and exit gradient distributions. This dissertation is therefore primarily concerned with the development of the charts, as design aids, for pressure at key points and exit gradient distributions for a flat bottomed weir with a vertical sheet pile on anisotropic porous medium. The analysis is done by transforming the anisotropic flow region into a fictitious isotropic domain and applying Schwarz-Christoffel transformation to the transformed region. The results obtained in transformed region are retransformed to the actual anisotropic flow domain and the charts are developed.

In general, as a thumb rule, a filter blanket is provided in downstream of a weir for a length of D to $2D$, where D is the anticipated depth of scour measured from the downstream bed of the river. A method to find the length of filter blanket is not yet available. An analytical method for obtaining the length of filter blanket is suggested in the dissertation.

The scope and nature of work undertaken is presented in Chapter 1. This is followed by a review of literature in chapter 2, which embraces the pertinent theory of seepage in anisotropic porous media and the provision of filter blanket downstream the weir.

Chapter 3 deals with the analysis for flat bottomed weir with a vertical sheet pile on anisotropic porous medium of infinite depth. Numerical results are presented for uplift pressure at key points and exit gradient distribution for various position of sheet pile and different degree of anisotropy. The results are compared with those of Khosla et al, for the particular case in which maximum and minimum coefficient of permeability ratio is one. The inclination of the direction of coefficient of permeability and the ratio of maximum and minimum coefficient of permeability have considerable influence on the pressure and exit gradient distribution.

Chapter 4 deals with the problems in a weir on anisotropic flow domain where maximum exit gradient becomes infinite when downstream sheet pile is vertical. The analyses are made for the provision of exit gradient controlling device (a concrete block

with certain shape) and the numerical results for obtaining the size and shape of such device are given.

Chapter 5 deals with the design of a filter blanket for a weir on isotropic porous media of infinite depth. The analysis is carried out applying Schwarz-Christoffel transformation. The exit gradient distribution corresponding to straight line scour of the downstream reservoir boundary is analysed. Numerical results for the length of the filter blanket are given for various ratio of weir width and length of sheet pile. The ratio of width of weir and the length of downstream vertical sheet pile has considerable influence on the length of filter blanket.

Finally, in Chapter 6, the results presented in earlier chapters are discussed and the important conclusions of the study are summarised.

CHAPTER 1

INTRODUCTION

Weirs are the most extensively used hydraulic structure for diversion of river flows for different purposes .A weir founded on porous medium is designed for surface and sub-surface flow conditions. The design from surface flow consideration is primarily concerned with the fixation of waterway, pond level, and effective dissipation of excess energy of water flowing over the structure. The weir floor is also subjected to forces due to seepage flow through the porous foundation underneath. The seepage flow causes uplift pressure under the apron and tends to lift the soil particles at the exit. Therefore, the weir floor is designed to ensure safety against uplift pressure and undermining.

Most of the theoretical analyses of ground water flow problems assume the porous medium to be isotropic and homogeneous with respect to coefficient of permeability. However, from the field and laboratory tests, it has been found that most natural and man-made soil deposits are anisotropic with respect to permeability to a considerable degree. Flow through anisotropic media is generally analysed by first transforming the anisotropic actual flow domain to a fictitious isotropic flow region by a suitable co-ordinate transformation and then applying a method of solution to the transformed section. From the solution of the problem in the transformed region, the solution for the actual problem in the anisotropic region can be obtained.

In cases, the directions of principle coefficients of permeability are different from the vertical and horizontal directions, the actual flow domain loses its shape in the transformed section and a vertical sheet pile changes into inclined one. In such cases, depending upon the degree of anisotropy, analyses to design the elements of the weir from sub surface flow consideration namely total floor length, thickness of the floor, and the depth of the downstream sheet pile, are required to be carried out accordingly.

Several methods are available for finding solutions to the problems of flow through isotropic media. Some of the methods that are used are conformal mapping, finite difference method, finite element method, graphical approach, Fourier series, analogue

method etc. For anisotropic porous media, these methods can be made use of after the anisotropic flow domain is transformed to a fictitious isotropic flow region.

The present work is primarily concerned with the analysis of flow under a flat bottomed weir in homogeneous anisotropic porous media and evaluation of pressure and exit gradient distribution for various position of a vertical sheet pile. Velocity potential curves and exit gradient distribution curves, as design aid, comparable to the curves given by Khosla are prepared for different degrees of anisotropy. For weirs on inclined stratified foundation soil, where the provision of a vertical sheet pile of any length still results in infinite exit gradient, a toe structure as exit gradient controlling device has been suggested. Analysis has been made to work out the shape and size of the toe structure. In addition, an analysis has been done to find the length of downstream filter blanket for a weir in isotropic homogeneous flow domain. All these analyses are done applying the Schwarz – christoffel transformation.

The scheme of the presentation in the dissertation is as follows:

Chapter 2 presents a review of literature.

Chapter 3 presents a study of flow under a flat bottomed weir with a vertical sheet pile resting on homogeneous anisotropic porous medium of infinite depth. Numerical results are presented in nondimensional form for pressure head at key points of the weir and exit gradient distribution for various degree of anisotropy. The results show that the inclination of the maximum coefficient of permeability with the horizontal and the degree of anisotropy have considerable influence on the pressure distribution and on the magnitude and location of the maximum exit gradient. The results are presented in the form of curves so that they can be used as design aids. The results are compared with the results presented by Khosla, et al (1954) for the particular case in which the degree of anisotropy is 1 (which represents the isotropic flow domain).

Chapter 4 deals with design of toe structure for controlling exit gradient in anisotropic medium. When the direction of maximum coefficient of permeability is inclined at an angle greater than 0 and less than $\pi/2$ with the horizontal (measured clockwise from downstream horizontal bed) then for a structure with downstream vertical sheet pile the value of maximum exit gradient becomes infinite. In this chapter, an attempt has been made to bring the value of maximum exit gradient within the desired

value by providing a suitable toe structure. Numerical results are given in nondimensional form for the exit gradient distribution.

Chapter 5 deals with design of downstream filter length assuming straight line profile of the scour.

In Chapter 6, the results presented in earlier chapters are discussed and important conclusions of the present studies are summarized.

It is hoped that the analyses and results presented will be assistance to a Design Engineer for designing the weirs in anisotropic porous medium of infinite depth.

CHAPTER 2

REVIEW OF LITERATURE

2.1 General

Weirs on permeable foundation are designed for both surface and sub-surface flow conditions. The criteria for design for sub-surface flow conditions are that the hydraulics structure should be safe against uplift pressure and should not fail due to undermining. These criteria are satisfied when the submerged weight of the structure at any section is equal to the uplift pressure acting at that section and the maximum exit gradient is less than the permissible exit gradient.

The analyses which have impact on the present study are: the case of confined flow under a weir having a vertical sheet pile and resting on porous medium of infinite depth (Khosla, et al, 1954); confined flow under a depressed weir (Pavlosky (vide Harr, 1962)); the case of an inclined sheet pile in a semi-infinite horizontal porous medium (Verigin (vide Harr, 1962)); confined and unconfined flows through anisotropic porous media (Mishra, 1972).

In reality, soil is seldom isotropic and homogeneous. According to Casagrande (1940) soils in their natural undisturbed condition are always anisotropic with regard to permeability even if they convey to the eye the impression of being entirely uniform in character.

2.2 Field and Laboratory Investigations

Many field and laboratory permeability tests on soils show evidence of anisotropy of a considerable degree. The various factors that are responsible for the directional variation of permeability are:

- i) particle shape and orientation (Graton and Fraser, 1935; Dapples and Rominger, 1945) (vide Krizek and Anand, 1968)
- ii) natural and artificial stratification (Massland, 1957) and
- iii) soil structure.

The carefully conducted permeability tests by Fancher, et al (vide Muskat, 1937) on oil sands have shown significant anisotropic properties of the sand. Out of the 65 pairs of samples tested, 46 pairs gave permeabilities parallel to the bedding planes greater than those normal to the bedding planes. The ratio of high to low permeability ranged from 1 to 40. In some cases, the permeability normal to the bedding plane exceeded that parallel to it, the maximum ratio of the two values being 7.3.

Arnovici (1947) (vide Krizek and Anand, 1968) conducted permeability tests on 15 soil samples and reported a maximum coefficient of anisotropy (ratio of maximum and minimum coefficient of permeability) 3.0.

Reeve and Kirkham(1951) (vide Krizek and Anand, 1968) used various methods of measurement of permeability such as: the auger hole method, the peizometer method, the tube method and laboratory tests. They noticed marked evidence of anisotropy.

Johnson and Houghes (1948) (vide Krizek and Anand, 1968) and Johnson and Breton (1951) (vide Krizek and Anand, 1968) measured the permeability of natural rock piece obtained from oil well cores in interval through 180°. Anisotropic permeability conditions were found and some consistency was observed in the directions of maximum and minimum coefficients of permeability.

Mansur and Dietrich (1965) conducted pumping test on a 16 inches diameter and 100 feet deep well located in the alluvial valley of the Arkansas river, to determine the coefficient of horizontal permeability and ratio of the coefficients of horizontal and vertical permeabilities, viz k_H / k_V . The ratio k_H / k_V was determined by two methods. In the first method, k_H / k_V was found by comparing the potential distribution around the test well with that around a similar well in a three-dimensional electrical analogy model. In the second method, Muskat's equation, which relates the flow from a partially penetrating well to that of a fully penetrating well, was made use of. The analyses of the pumping test data revealed that the coefficient of horizontal permeability is twice the coefficient of vertical permeability.

The extensive investigations carried out by De Ridder and Wit (1965) in the polder 'De Oude korendijk', were aimed at the determination of vertical and horizontal conductivity. These quantities were determined by (a) transmission of the tidal waves, (b) pumping tests, (c) laboratory tests on core samples from borings and (d) calculation from

mechanical analysis of core samples and disturbed samples obtained from bailer borings. From the laboratory tests on undisturbed samples, it was found that the horizontal conductivity of the core samples exceeded the vertical conductivity by 2 to 4 times.

Dagan (1967) and Boulton (1970) analysed the pumping test data collected by Wenzel at the Grand Island Nebraska. Dagan's analysis of the test data shows an average degree of anisotropy of 7.5.

Theoretical analysis concerned with anisotropic porous media, collected during the review of the literature is given in appendices A-I and A-II.

A properly designed stilling basin forms an integral part of a barrage/weir apron. It helps to dissipate excess energy of flow. However, some undissipated energy is generally carried over to the unprotected river bed, which causes scour. The shape and extent of scour depends upon type of soil, Froude number of flow, dimensions of stilling basin and basin appurtenances. Ample evidence is available in literature to conclude that the shape of scour downstream of stilling basins, founded on cohesionless soils, resemble arc of a circle or an aerofoil.

The scour profile downstream of various barrages, falls and regulators in the model studies carried out at Irrigation Research Institute, Roorkee (Sharma, 1972,1975) resemble the shape of aerofoil or arc of a circle.

The scour profiles, observed in the downstream side of Sambeek and Grave barrage, as reported by Leliavsky (1955), resemble the shape of an aerofoil.

This change in the boundary flow domain causes the redistribution of the exit gradient and may reduce the design factor of safety against piping in some cases. Therefore, usually a filter blanket for a length of one to times of the anticipated scour depth is provided just downstream of the structure to arrest the vertical movement of the bed particles.

2.3 Summary of Literature

From the foregoing review of literature, it can be concluded that: many field and laboratory tests give indication that most soils are anisotropic to a considerable degree with respect to their permeability. The degree of anisotropy in some cases is as high as 40.

The problems of seepage under a weir in anisotropic porous media can be solved by a suitable co-ordinate transformation of the actual anisotropic flow domain into a fictitious isotropic domain.

Solutions for flow characteristics under a stepped weir with inclined sheet pile in isotropic flow domain have been given by Mishra (1972). This is the transformed case of an actual anisotropic flow domain into a fictitious isotropic one. There is a need to analyse the flow characteristics under a weir in actual anisotropic flow domain itself, and study the effect of degree of anisotropy.

From the available solutions it is concluded that when a sheet pile makes an angle $0 < \gamma < \pi/2$ with the horizontal measured from upstream side in anti clockwise direction in an isotropic (fictitious or real) flow domain the maximum exit gradient becomes infinite. There is a need to design a structure so as to contain the exit gradient within limit.

The shape of scour, downstream of different hydraulic structures resemble arc of a circle or an aerofoil. Generally, a filter blanket is provided in downstream of a weir as extra safety measure to encounter the reduction in factor of safety against piping due to redistribution of exit gradient under scour and there is a need for finding the suitable length of the filter blanket.

CHAPTER 3

FLOW UNDER A FLAT BOTTOMED WEIR WITH A VERTICAL SHEET PILE ON ANISOTROPIC POROUS MEDIUM OF INFINITE DEPTH

3.1 General

Mostly, the porous media under hydraulic structures extend to a depth, which is very large in compared to the widths of the hydraulic structures. In such cases, a study on flow through porous medium of infinite depth is pertinent.

Taking a soil of infinite depth, two-dimensional steady flow beneath a weir with vertical sheet pile has been analysed by Khosla, et al (1954). Also, Khosla has developed curves to find i) the uplift pressure at key points along the base of a flat bottomed weir with a vertical sheet pile at various position and ii) the maximum exit gradient .The Khosla's curves are only applicable to a homogeneous isotropic porous medium of infinite depth.

Mishra (1972) has analysed the flow characteristics under a stepped weir with inclined sheet pile, which corresponds to the transformed fictitious isotropic flow domain of an actual anisotropic flow domain.

In this chapter an analysis of flow under a flat bottomed weir on an anisotropic porous medium with a vertical sheet pile, that may be located anywhere along the bottom, is carried out. Extensive sets of curves depicting pressure and exit gradient distributions are presented so that the flow characteristics can be obtained directly for the structure on anisotropic medium.

3.2 Statement of the Problem

Fig.3.1 (a) shows a flat bottomed weir with a vertical sheet pile in an anisotropic flow domain. The direction of maximum coefficient of permeability makes an angle θ with the horizontal axis ox measured in clockwise direction. k_μ and k_λ are the magnitude of the maximum and minimum coefficients of permeabilities, respectively. b_1 and b_2 are the widths of the upstream and downstream apron respectively, b is the total

width of the apron and s is the length of the vertical sheet pile. H is the height of water at the upstream side and there is no water in downstream side or H is the head difference that causes the flow. It is required to find the pressures at key points i.e. at points C, D and E shown in figure 3.1(a) and exit gradient distributions, for b_1/b ratio ranging from 0 to 1. The analyses are to be carried out for $\frac{k_\mu}{k_\lambda} = 1, 2, 4 \text{ and } 10$, $\theta = 0^\circ, 30^\circ, 60^\circ, 120^\circ$ and 150° and for b/s ratio = 1, 2, 3, 4, 5, 10 and 15. The ratio $b_1/b = 0$ corresponds to a weir with an upstream sheet pile and $b_1/b = 1$ represent a weir with a downstream sheet pile.

3.3 Analysis

First, the real anisotropic flow domain is transformed into fictitious isotropic flow domain using the relations given in appendix I.

Let the flow domain in x, y co-ordinate system be transformed into \bar{x}, \bar{y} co-ordinate system and that a vertical sheet pile in x, y co-ordinate system make an angle $\gamma\pi$ with \bar{x} axis (measured from upstream side in anti clockwise direction) in the fictitious flow domain in \bar{x}, \bar{y} co-ordinate system. Let the new length of the oblique sheet pile in the fictitious flow domain be \bar{s} and the new widths corresponding to b_1, b_2 and b be \bar{b}_1, \bar{b}_2 and \bar{b} , respectively. The transformed section in fictitious isotropic flow domain of the weir given in fig.3.1 (a) is shown in fig.3.1 (b).

The weir in fictitious isotropic flow domain has been analysed by Mishra (1972) using the Schwarz-christoffel transformation. The same approach is applicable here.

The results obtained are then transferred to the corresponding points in the actual anisotropic flow domain. The values of exit gradients obtained in fictitious flow domain are multiplied by the magnification factor given in appendix-II to get the values of exit gradient in the actual flow domain at the corresponding points.

The transformed fictitious isotropic flow region in z plane is mapped onto the lower half of an auxiliary t plane and then the complex potential plane is mapped onto the lower half of the auxiliary t plane. From these two conformal mappings, the relationship between w and z plane is obtained. The Schwarz-Christoffel transformation for mapping the polygon \overline{AEDCG} onto the lower half of the auxiliary t plane shown in fig.3.1 (d) is given by

$$z = M_1 \int \frac{(t-m)}{(t+1)^{1-\gamma} (1-t)^\gamma} dt + N_1 \quad \dots (3.3.1)$$

The vertices $\bar{A}, \bar{E}, \bar{D}, \bar{C}, \bar{G}$ being mapped onto $-\infty, -1, m, 1, \infty$, respectively.

In eq. 3.3.1, M_1 and N_1 are the constants to be determined. Let the point \bar{B} and \bar{F} be mapped onto the points $t = -\beta_1$ and β_2 , respectively. The parameters β_1 and β_2 can be found from eq. 3.3.1 when the constants M_1, m and N_1 are known. To find the constants M_1 and N_1 and the relationship between the transformation parameters and dimension of the structure, the integration between consecutive vertices are carried out. The constant N_1 is governed by the lower limit of integration.

i) Integration between vertices \bar{E} and \bar{D} ($-1 \leq t \leq m$)

For point \bar{E} , $Z_{\bar{E}} = 0$ and $t = -1$; and for point \bar{D} , $Z_{\bar{D}} = \bar{s} e^{(1-\gamma)ix}$ and $t = m$.

Applying these conditions

$$Z_{\bar{D}} = M_1 \int_{-1}^m \frac{t-m}{(t+1)^{1-\gamma} (1-t)^\gamma} dt + 0$$

$$\text{or } \bar{s} e^{(1-\gamma)ix} = M_1 \int_{-1}^m \frac{t-m}{(t+1)^{1-\gamma} (1-t)^\gamma} dt = M_1 I_1 \quad \dots (3.3.2)$$

The integration I_1 can be carried out numerically or analytically splitting the integration in two parts and using the properties of Beta function. Analytical solution yields

$$I_1 = 2 B_{\frac{1+m}{2}}(1+\gamma, 1-\gamma) - (1+m) B_{\frac{1+m}{2}}(\gamma, 1-\gamma)$$

in which $B_{\frac{1+m}{2}}(1+\gamma, 1-\gamma)$ and $B_{\frac{1+m}{2}}(\gamma, 1-\gamma)$ are incomplete Beta functions.

From eq.(3.3.2) the constant M_1 , is found to be

$$M_1 = \frac{\bar{s} e^{(1-\gamma)ix}}{I_1} \quad \dots (3.3.3)$$

ii) Integration between vertices \bar{D} and \bar{C} ($m \leq t \leq 1$)

For point \bar{D} , $Z_{\bar{D}} = \bar{s} e^{(1-\gamma)i\pi}$ and $t = m$; and for point \bar{C} , $Z_{\bar{C}} = 0$ and $t = 1$.

Applying these conditions in eq.(3.3.1):

$$0 = M_1 \int_m^1 \frac{t-m}{(t+1)^{1-\gamma} (1-t)^\gamma} dt + \bar{s} e^{(1-\gamma)i\pi}$$

$$\text{or } -\bar{s} e^{(1-\gamma)i\pi} = M_1 \int_m^1 \frac{t-m}{(t+1)^{1-\gamma} (1-t)^\gamma} dt = M_1 I_2 \quad \dots(3.3.4)$$

The integration I_2 can be carried out numerically or analytically splitting the integration in two parts and using the properties of Beta function. Analytical integration yields

$$I_2 = 2B(1+\gamma, 1-\gamma) - (1+m) B(\gamma, 1-\gamma)$$

in which $B(1+\gamma, 1-\gamma)$ and $B(\gamma, 1-\gamma)$ are complete Beta functions.

Equating eqs. (3.3.3) and (3.3.4)

$$-[2B(1+\gamma, 1-\gamma) - (1+m) B(\gamma, 1-\gamma)] = 2B_{\frac{1+m}{2}}(1+\gamma, 1-\gamma) - (1+m) B_{\frac{1+m}{2}}(\gamma, 1-\gamma) \dots(3.3.5)$$

For the known value of γ the unknown m can be found using an iteration from eq. (3.3.5). Knowing m , the constant M_1 is found from eq. (3.3.3).

iii) Determination of β_1 :

The parameter β_1 can be found performing the integration between \bar{B} and \bar{E} ($-\beta_1 \leq t \leq -1$)

For point \bar{E} , $Z_{\bar{E}} = 0$ and $t = -1$; and for point \bar{B} , $Z_{\bar{B}} = -\bar{b}_1$ and $t = -\beta_1$.

Applying these conditions

$$0 = M_1 \int_{-\beta_1}^{-1} \frac{t-m}{(t+1)^{1-\gamma} (1-t)^\gamma} dt - \bar{b}_1 \quad \dots(3.3.5 (a))$$

Substituting $t = -\tau$ and $dt = -d\tau$, and accordingly changing the limits

$$0 = -M_1 \int_{\beta_1}^1 \frac{-\tau-m}{(1-\tau)^{1-\gamma} (1+\tau)^\gamma} d\tau - \bar{b}_1 \quad \dots(3.3.5 (b))$$

$$\text{or } \bar{b}_1 = \frac{M_1}{(-1)^{1-\gamma}} \int_1^{\beta_1} \frac{-\tau - m}{(\tau-1)^{1-\gamma} (1+\tau)^\gamma} d\tau = \frac{M_1 I_3}{(-1)^{1-\gamma}} \quad \dots(3.3.5 \text{ (c)})$$

The integration I_3 can be carried out numerically or analytically splitting the integration in two parts and using the method of successive integration by parts. Analytical solution yields

$$I_3 = - \left\{ \left[(1-\beta_1)^\gamma \sum_{n=1}^{\infty} \frac{1}{(\gamma+n-1)(\gamma+n)} \left(\frac{\beta_1-1}{\beta_1+1} \right)^{\gamma+n-1} \right] - (1+m) \sum_{n=1}^{\infty} \left[\frac{1}{\gamma+n-1} \left(\frac{\beta_1-1}{\beta_1+1} \right)^{\gamma+n-1} \right] \right\}$$

Substituting M_1 from equation 3.3.3 in (3.3.5 (c))

$$\bar{b}_1 = \frac{\bar{s} e^{(1-\gamma)ix}}{(-1)^{1-\gamma}} \frac{I_3}{I_1}$$

$$\text{or } \bar{b}_1 = \frac{\bar{s} I_3}{I_1}$$

$$\text{or } \frac{\bar{b}_1}{\bar{s}} = \frac{I_3}{I_1} \quad \dots(3.3.6)$$

Now for known value of \bar{b}_1 the value of β_1 can be found using an iterative procedure.

iv) Determination of β_2 :

The parameter β_2 can be found performing the integration between \bar{C} and \bar{F} ($1 \leq t \leq \beta_2$)

For point \bar{C} , $Z_{\bar{C}} = 0$ and $t = 1$; and for point \bar{F} , $Z_{\bar{F}} = \bar{b}_2$ and $t = \beta_2$.

Now applying these conditions

$$\bar{b}_2 = M_1 \int_1^{\beta_2} \frac{t-m}{(t+1)^{1-\gamma} (1-t)^\gamma} dt \quad \dots(3.3.7 \text{ (a)})$$

$$\text{or } \bar{b}_2 = \frac{M_1}{(-1)^\gamma} \int_1^{\beta_2} \frac{t-m}{(t+1)^{1-\gamma} (t-1)^\gamma} dt = \frac{M_1 I_4}{(-1)^\gamma} \quad \dots(3.3.7 \text{ (b)})$$

The integration I_4 can be carried out numerically or analytically splitting the integration in two parts and using the method of successive integration by parts. Analytical solution yields

$$I_4 = - \left[\left\{ (1 - \beta_2) \gamma \sum_{n=1}^{\infty} \frac{1}{(n-1-\gamma)(n-\gamma)} \left(\frac{\beta_2-1}{\beta_2+1} \right)^{n-1-\gamma} \right\} - (1+m) \sum_{n=1}^{\infty} \left\{ \frac{1}{n-\gamma} \left(\frac{\beta_2-1}{\beta_2+1} \right)^{n-\gamma} \right\} \right]$$

Substituting the value of M_1 from equation (3.3.3) in (3.3.7 (b))

$$\frac{\bar{b}_2}{s} = - \frac{I_4}{I_1} \quad \dots(3.3.8)$$

Now for known values of \bar{b}_2 , the parameter β_2 can be found using an iterative procedure.

Mapping of w plane onto t plane:

The complex potential w is defined as $w = \phi + i\Psi$ in which ϕ = velocity potential and Ψ = stream function. The velocity potential function ϕ is defined as

$$\phi = -k \left(\frac{p}{\gamma_w} - y \right) + C \quad \dots(3.3.9)$$

The w plane corresponding to fictitious flow domain in z plane shown in Fig.3.1 (b) is shown in Fig.3.1(c)

The constant $C = k h_2$, where h_2 is the depth of water in the downstream side which may be taken as zero for convenience. In that case constant $C = 0$.

The mapping of the w plane onto the lower half of the t plane according to the Schwarz-Christoffel transformation is given by

$$w = M_2 \int \frac{dt}{(t+\beta_1)^{1/2} (t-\beta_2)^{1/2}} + N_2 \quad \dots(3.3.10 (a))$$

Integrating

$$w = i M_2 \sin^{-1} \frac{2t + \beta_1 - \beta_2}{\beta_1 + \beta_2} + N_2 \quad \dots(3.3.10 (b))$$

$$\text{or } w = M_3 \sin^{-1} \frac{2t + \beta_1 - \beta_2}{\beta_1 + \beta_2} + N_2 \quad \dots 3.3.10 \text{ (c)}$$

in which M_2 and N_2 are constants.

For point \bar{F} , $t = \beta_2$ and $w = 0$, therefore, $N_2 = -M_3 \pi/2$.

For point \bar{B} , $t = -\beta_1$ and $w = -kH$; hence, $M_3 = kH/\pi$.

Substituting the values of M_3 and N_2 in eq. 3.3.10 (c)

$$w = \frac{kH}{\pi} \sin^{-1} \frac{2t + \beta_1 - \beta_2}{\beta_1 + \beta_2} - \frac{kH}{2} \quad \dots (3.3.11)$$

Along the impervious boundary $\Psi = 0$, therefore $w = \phi$. Equation 3.3.11 yields

$$\frac{\phi}{kH} = \frac{1}{\pi} \sin^{-1} \frac{2t + \beta_1 - \beta_2}{\beta_1 + \beta_2} - \frac{1}{2} \quad \dots (3.3.12)$$

The uplift pressure at any point along the impervious boundary is given by

$$p = \gamma_w \left[\frac{H}{\pi} \cos^{-1} \frac{2t + \beta_1 - \beta_2}{\beta_1 + \beta_2} + y \right] \quad \dots (3.3.13)$$

The pressure at key points can be obtained substituting the corresponding values of t and y co-ordinate in eq. (3.3.13)

For point E, $t = -1$, and $y = 0$.

$$\text{Hence, } P_E = \gamma_w \left[\frac{H}{\pi} \cos^{-1} \frac{-2 + \beta_1 - \beta_2}{\beta_1 + \beta_2} \right] \quad \dots (3.3.14)$$

For point C, $t = 1$, and $y = 0$.

$$\text{Hence, } P_C = \gamma_w \left[\frac{H}{\pi} \cos^{-1} \frac{2 + \beta_1 - \beta_2}{\beta_1 + \beta_2} \right] \quad \dots (3.3.15)$$

And for point D, $t = m$, and $y = \bar{s} \sin \gamma\pi$

$$\text{Hence, } P_D = \gamma_w \left[\frac{H}{\pi} \cos^{-1} \frac{2m + \beta_1 - \beta_2}{\beta_1 + \beta_2} + \bar{s} \sin \gamma\pi \right] \quad \dots (3.3.16)$$

Exit gradient

The exit gradient I_E is given by

$$I_E = \frac{i}{k} \frac{dw}{dt} \frac{dt}{dz}$$

Replacing $\frac{dw}{dt}$ from eq.(3.3.10 (a)) and $\frac{dz}{dt}$ from eq.(3.3.1), and simplifying

$$\bar{I}_E = \frac{H}{\pi} \frac{1}{(t+\beta_1)^{1/2} (t-\beta_2)^{1/2}} \frac{(1+t)^{1-\gamma} (1-t)^\gamma}{|M_1| (t-m)} \quad \dots(3.3.17(a))$$

Substituting the value of M_1 and simplifying, the equation changes into

$$\bar{I}_E \frac{\bar{s}}{H} = \frac{I_1}{\pi} \frac{1}{(t+\beta_1)^{1/2} (t-\beta_2)^{1/2}} \frac{(1+t)^{1-\gamma} (t-1)^\gamma}{(t-m)} \quad \dots(3.3.17(b))$$

For the weir with sheet pile located at downstream end $\beta_2 = 1.0$. Therefore

$$\bar{I}_E \frac{\bar{s}}{H} = \frac{I_1}{\pi} \frac{1}{(t+\beta_1)^{1/2}} \frac{(1+t)^{1-\gamma} (t-1)^{\gamma-0.5}}{(t-m)} \quad \dots(3.3.18)$$

For $\gamma = 0.5$ (i.e. vertical sheet pile case), the above equation can be written as

$$\bar{I}_E \frac{\bar{s}}{H} = \frac{I_1}{\pi} \frac{1}{(t+\beta_1)^{1/2}} \frac{(1+t)^{0.50}}{(t-m)} \quad \dots(3.3.19)$$

3.4 Results and Discussions

Numerical results are presented in the form of curves so that the pressure at key points and magnitude and location of maximum exit gradient for a flat bottomed weir with a vertical sheet pile in anisotropic flow domain can be read off the curves. The curves are prepared for $k_\mu / k_\lambda = 1, 2, 4$ and 10 , $\theta = 0^\circ, 30^\circ, 60^\circ, 120^\circ$ and 150° and b/s ratio = $1, 2, 3, 4, 5, 10$ and 15 . The procedure adopted to arrive at the results presented here, is as follows:

The weir with a vertical sheet pile in the anisotropic flow domain gets transformed into an equivalent weir with an oblique or a vertical sheet pile in the fictitious isotropic flow domain. The governing flow equation, the Laplace equation, is solved satisfying the boundary conditions in the fictitious isotropic flow domain. The

flow characteristics, complex potential under the structure, and exit gradient in the downstream side in the fictitious flow domain, are found and finally these are related to the actual location in flow domain by a reverse co-ordinate transformation.

We define the following ratios to transform the results from fictitious isotropic domain to that at actual anisotropic domain:

$$\frac{\bar{b}}{b} = r_1;$$

$$\frac{\bar{s}}{s} = r_2;$$

$$\frac{\bar{\alpha}}{\alpha} = \frac{\bar{b}}{s} = \frac{r_1}{r_2} = r_3;$$

$$\alpha = \frac{\bar{\alpha}}{r_3};$$

The ratios r_1 and r_2 depend only on degree of anisotropy and orientation of the principle permeability direction. The correspondence between points in the fictitious and actual flow domain is as follows:

$$x = \frac{\bar{x}}{\left(\frac{\bar{b}}{b}\right)},$$

A point on the vertical sheet pile in anisotropic domain is given by :

$$r e^{i\pi} = \frac{\bar{r} e^{(1-\gamma)i\pi}}{r_2}, \text{ where } \bar{r} \text{ is the point on the inclined sheet pile in fictitious}$$

isotropic domain.

Exit gradient at a point in the anisotropic flow domain is given by:

$$\frac{I_{ES}}{H} = \frac{\bar{I}_{ES}}{H r_2} * mf, \text{ where } \bar{I}_E \text{ is the exit gradient at the corresponding point in}$$

the fictitious domain and mf is the magnification factor as depicted in appendix A-II.

ϕ -curves

With known degree of anisotropy and orientation angle (θ) made by the direction of maximum coefficient of permeability with the horizontal, the value of $-\phi/kH$ at key points can be directly obtained from the curves, for known values of α ($= b/s$) and base ratio b_1/b . Dimensionless potential ($\phi/-kH$) at key points of the weir are presented in are in fig.3.2 (a1) through fig. 3.2(f3.3) for various location of the sheet pile and for various ratios of depth of sheet pile to width of the weir for different degree of anisotropy and orientation of the maximum principle permeability direction.. Separate curves for the end sheet pile conditions are also given in fig.3.3 (a1) through fig. 3.3(e3). Using these graph the uplift water pressure can be computed. The results for $k_u/k_v = 1$, which represents the isotropic case, agree with those of khosla's curves.

Pressure head at key points in anisotropic flow domain can be obtained using the following relations:

Pressure head at the junction of sheet pile and the floor,

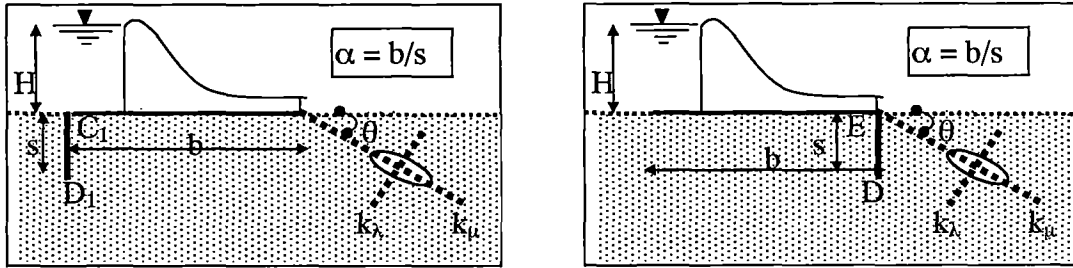
$$P_E / \gamma_w = H (-\phi_E / kH);$$

$$P_C / \gamma_w = H (-\phi_C / kH); \text{ and,}$$

Pressure head at the tip of sheet pile,

$$P_D / \gamma_w = H (-\phi_D / kH) + s.$$

The deviation of potential $\phi/-kH$ in anisotropic flow domain from that, had the domain been isotropic, are presented in the following tables for different degree of anisotropy and orientation of principal permeability direction. The comparison has been made only for key points. (-) minus sign indicates the value higher than that of isotropic flow domain.



Vertical sheet pile at end

α	Isotropic medium		Anisotropic medium (θ = 0°)											
	-φ _{C1} /kh	-φ _{D1} /kh	Kμ/Kλ = 2				Kμ/Kλ = 4				Kμ/Kλ = 10			
			-φ _{C1} /kh	Deviation	-φ _{D1} /kh	Deviation	-φ _{C1} /kh	Deviation	-φ _{D1} /kh	Deviation	-φ _{C1} /kh	Deviation	-φ _{D1} /kh	Deviation
1	0.272	0.555	0.206	24.26	0.532	4.14	0.152	44.12	0.518	6.67	0.099	63.6	0.508	8.47
2	0.424	0.625	0.346	18.4	0.586	6.24	0.272	35.85	0.555	11.2	0.187	55.9	0.527	15.68
3	0.512	0.674	0.437	14.65	0.632	6.23	0.360	29.69	0.592	12.17	0.261	49.02	0.551	18.25
4	0.570	0.709	0.500	12.28	0.667	5.92	0.424	25.61	0.625	11.85	0.322	43.51	0.575	18.9
5	0.612	0.735	0.546	10.78	0.694	5.58	0.473	22.71	0.652	11.29	0.371	39.38	0.598	18.64
10	0.720	0.806	0.670	6.94	0.772	4.22	0.612	15	0.735	8.81	0.523	27.36	0.68	15.63
15	0.770	0.839	0.728	5.45	0.811	3.34	0.679	11.82	0.778	7.27	0.602	21.82	0.729	13.11

Table 3.4.1

α	Isotropic medium		Anisotropic medium (θ = 0°)											
	-φ _E /kh	-φ _D /kh	Kμ/Kλ = 2				Kμ/Kλ = 4				Kμ/Kλ = 10			
			-φ _E /kh	Deviation	-φ _D /kh	Deviation	-φ _E /kh	Deviation	-φ _D /kh	Deviation	-φ _E /kh	Deviation	-φ _D /kh	Deviation
1	0.728	0.445	0.794	-9.07	0.468	-5.17	0.848	-16.48	0.482	-8.31	0.901	-23.76	0.492	-10.56
2	0.576	0.375	0.654	-13.5	0.414	-10.4	0.728	-26.39	0.445	-18.67	0.813	-41.15	0.473	-26.13
3	0.488	0.326	0.563	-15.4	0.368	-12.9	0.640	-31.15	0.408	-25.15	0.739	-51.43	0.449	-37.73
4	0.430	0.291	0.5	-16.3	0.333	-14.4	0.576	-33.95	0.375	-28.87	0.678	-57.67	0.425	-46.05
5	0.388	0.265	0.454	-17	0.306	-15.5	0.527	-35.82	0.348	-31.32	0.629	-62.11	0.402	-51.7
10	0.280	0.194	0.33	-17.9	0.228	-17.5	0.388	-38.57	0.265	-36.6	0.477	-70.36	0.32	-64.95
15	0.230	0.161	0.272	-18.3	0.189	-17.4	0.321	-39.57	0.222	-37.89	0.398	-73.04	0.271	-68.32

Table 3.4.2

Isotropic medium		Anisotropic medium ($\theta = 30^\circ$)												
α	$-\phi_{C1}/kh$	$-\phi_{D1}/kh$	$K_{\mu}/K_{\lambda} = 2$				$K_{\mu}/K_{\lambda} = 4$				$K_{\mu}/K_{\lambda} = 10$			
			$-\phi_{C1}/kh$	Deviation	$-\phi_{D1}/kh$	Deviation	$-\phi_{C1}/kh$	Deviation	$-\phi_{D1}/kh$	Deviation	$-\phi_{C1}/kh$	Deviation	$-\phi_{D1}/kh$	Deviation
1	0.272	0.555	0.275	-1.1	0.607	-9.37	0.286	-5.15	0.661	-19.1	0.286	-5.14	0.729	-31.35
2	0.424	0.625	0.412	2.83	0.661	-5.76	0.412	2.83	0.704	-12.64	0.412	2.80	0.762	-21.92
3	0.512	0.674	0.495	3.32	0.7	-3.86	0.490	4.3	0.735	-9.05	0.490	4.30	0.786	-16.62
4	0.570	0.709	0.551	3.33	0.729	-2.82	0.543	4.74	0.759	-7.05	0.543	4.73	0.804	-13.40
5	0.612	0.735	0.592	3.27	0.751	-2.18	0.583	4.74	0.777	-5.71	0.583	4.74	0.818	-11.29
10	0.720	0.806	0.702	2.5	0.815	-1.12	0.693	3.75	0.832	-3.23	0.693	3.75	0.861	-6.82
15	0.770	0.839	0.754	2.08	0.846	-0.83	0.745	3.25	0.859	-2.38	0.744	3.38	0.883	-5.24

Table 3.4.3

Isotropic medium		Anisotropic medium ($\theta = 30^\circ$)												
α	$-\phi_E/kh$	$-\phi_D/kh$	$K_{\mu}/K_{\lambda} = 2$				$K_{\mu}/K_{\lambda} = 4$				$K_{\mu}/K_{\lambda} = 10$			
			$-\phi_E/kh$	Deviation	$-\phi_D/kh$	Deviation	$-\phi_E/kh$	Deviation	$-\phi_D/kh$	Deviation	$-\phi_E/kh$	Deviation	$-\phi_D/kh$	Deviation
1	0.728	0.445	0.798	-9.62	0.524	-17.8	0.864	-18.68	0.599	-34.61	0.932	-28.02	0.685	-53.93
2	0.576	0.375	0.636	-10.4	0.449	-19.7	0.692	-20.14	0.523	-39.47	0.752	-30.56	0.61	-62.67
3	0.488	0.326	0.536	-9.84	0.39	-19.6	0.579	-18.65	0.452	-38.65	0.616	-26.23	0.52	-59.51
4	0.430	0.291	0.471	-9.53	0.348	-19.6	0.505	-17.44	0.401	-37.8	0.531	-23.49	0.455	-56.36
5	0.388	0.265	0.424	-9.28	0.316	-19.3	0.453	-16.75	0.363	-36.98	0.472	-21.65	0.408	-53.96
10	0.280	0.194	0.304	-8.57	0.231	-19.1	0.321	-14.64	0.262	-35.05	0.33	-17.86	0.289	-48.97
15	0.230	0.161	0.249	-8.26	0.19	-18	0.262	-13.91	0.215	-33.54	0.268	-16.52	0.235	-45.96

Table 3.4.4

Isotropic medium		Anisotropic medium ($\theta = 60^\circ$)												
α	$-\phi_{C1}/kh$	$-\phi_{D1}/kh$	$K_{\mu}/K_{\lambda} = 2$				$K_{\mu}/K_{\lambda} = 4$				$K_{\mu}/K_{\lambda} = 10$			
			$-\phi_{C1}/kh$	Deviation	$-\phi_{D1}/kh$	Deviation	$-\phi_{C1}/kh$	Deviation	$-\phi_{D1}/kh$	Deviation	$-\phi_{C1}/kh$	Deviation	$-\phi_{D1}/kh$	Deviation
1	0.272	0.555	0.339	-24.6	0.63	-13.5	0.398	-46.32	0.698	-25.77	0.457	-68.01	0.772	-39.1
2	0.424	0.625	0.481	-13.4	0.693	-10.9	0.530	-25	0.753	-20.48	0.579	-36.56	0.815	-30.4
3	0.512	0.674	0.560	-9.38	0.734	-8.9	0.602	-17.58	0.786	-16.62	0.644	-25.78	0.841	-24.78
4	0.570	0.709	0.612	-7.37	0.762	-7.48	0.649	-13.86	0.809	-14.1	0.686	-20.35	0.858	-21.02
5	0.612	0.735	0.649	-6.05	0.783	-6.53	0.682	-11.44	0.826	-12.38	0.716	-16.99	0.871	-18.5
10	0.720	0.806	0.746	-3.61	0.841	-4.34	0.770	-6.94	0.872	-8.19	0.794	-10.28	0.906	-12.41
15	0.770	0.839	0.791	-2.73	0.868	-3.46	0.810	-5.19	0.894	-6.56	0.831	-7.92	0.922	-9.89

Table 3.4.5

Isotropic medium		Anisotropic medium ($\theta = 60^\circ$)												
α	$-\phi_E/kh$	$-\phi_D/kh$	$K_\mu/K_\lambda = 2$				$K_\mu/K_\lambda = 4$				$K_\mu/K_\lambda = 10$			
			$-\phi_E/kh$	Deviation	$-\phi_D/kh$	Deviation	$-\phi_E/kh$	Deviation	$-\phi_D/kh$	Deviation	$-\phi_E/kh$	Deviation	$-\phi_D/kh$	Deviation
1	0.728	0.445	0.724	0.55	0.493	-10.8	0.713	2.06	0.534	-20	0.692	4.95	0.573	-28.76
2	0.576	0.375	0.553	3.99	0.401	-6.93	0.523	9.2	0.414	-10.4	0.484	15.97	0.418	-11.47
3	0.488	0.326	0.461	5.53	0.341	-4.6	0.430	11.89	0.346	-6.13	0.392	19.67	0.341	-4.6
4	0.430	0.291	0.402	6.51	0.301	-3.44	0.373	13.26	0.302	-3.78	0.338	21.4	0.296	-1.72
5	0.388	0.265	0.361	6.96	0.272	-2.64	0.333	14.18	0.271	-2.26	0.301	22.42	0.264	0.38
10	0.280	0.194	0.258	7.86	0.196	-1.03	0.236	15.71	0.193	0.52	0.212	24.29	0.186	4.12
15	0.230	0.161	0.211	8.26	0.161	0	0.192	16.52	0.158	1.86	0.172	25.22	0.152	5.59

Table 3.4.6

Isotropic medium		Anisotropic medium ($\theta = 120^\circ$)												
α	$-\phi_{C1}/kh$	$-\phi_{D1}/kh$	$K_\mu/K_\lambda = 2$				$K_\mu/K_\lambda = 4$				$K_\mu/K_\lambda = 10$			
			$-\phi_{C1}/kh$	Deviation	$-\phi_{D1}/kh$	Deviation	$-\phi_{C1}/kh$	Deviation	$-\phi_{D1}/kh$	Deviation	$-\phi_{C1}/kh$	Deviation	$-\phi_{D1}/kh$	Deviation
1	0.272	0.555	0.277	-1.84	0.507	8.65	0.287	-5.51	0.466	16.04	0.308	-13.24	0.427	23.06
2	0.424	0.625	0.447	-5.42	0.599	4.16	0.477	-12.5	0.586	6.24	0.516	-21.7	0.582	6.88
3	0.512	0.674	0.540	-5.47	0.659	2.23	0.570	-11.33	0.654	2.97	0.608	-18.75	0.659	2.23
4	0.570	0.709	0.598	-4.91	0.699	1.41	0.627	-10	0.698	1.55	0.662	-16.14	0.704	0.71
5	0.612	0.735	0.639	-4.41	0.728	0.95	0.667	-8.99	0.729	0.82	0.699	-14.22	0.736	-0.14
10	0.720	0.806	0.742	-3.06	0.803	0.37	0.764	-6.11	0.806	0	0.788	-9.44	0.813	-0.87
15	0.770	0.839	0.789	-2.47	0.838	0.12	0.807	-4.81	0.841	-0.24	0.827	-7.4	0.847	-0.95

Table 3.4.7

Isotropic medium		Anisotropic medium ($\theta = 120^\circ$)												
α	$-\phi_E/kh$	$-\phi_D/kh$	$K_\mu/K_\lambda = 2$				$K_\mu/K_\lambda = 4$				$K_\mu/K_\lambda = 10$			
			$-\phi_E/kh$	Deviation	$-\phi_D/kh$	Deviation	$-\phi_E/kh$	Deviation	$-\phi_D/kh$	Deviation	$-\phi_E/kh$	Deviation	$-\phi_D/kh$	Deviation
1	0.728	0.445	0.661	9.2	0.37	16.85	0.602	17.31	0.302	32.13	0.543	25.41	0.228	48.76
2	0.576	0.375	0.519	9.9	0.307	18.13	0.470	18.4	0.247	34.13	0.421	26.91	0.185	50.67
3	0.488	0.326	0.44	9.84	0.266	18.4	0.398	18.44	0.214	34.36	0.356	27.05	0.159	51.23
4	0.430	0.291	0.388	9.77	0.238	18.21	0.351	18.37	0.191	34.36	0.314	26.98	0.141	51.55
5	0.388	0.265	0.351	9.54	0.217	18.11	0.318	18.11	0.174	34.52	0.2835	26.93	0.129	51.55
10	0.280	0.194	0.254	9.29	0.159	18.04	0.230	17.86	0.127	34.54	0.205	26.79	0.094	51.55
15	0.230	0.161	0.208	9.57	0.131	18.63	0.189	17.83	0.105	34.78	0.168	26.96	0.078	51.55

Table 3.4.8

α	Isotropic medium		Anisotropic medium ($\theta = 150^\circ$)											
	$-\phi_{C1}/kh$	$-\phi_{D1}/kh$	$K\mu/K\lambda = 2$				$K\mu/K\lambda = 4$				$K\mu/K\lambda = 10$			
			$-\phi_{C1}/kh$	Deviation	$-\phi_{D1}/kh$	Deviation	$-\phi_{C1}/kh$	Deviation	$-\phi_{D1}/kh$	Deviation	$-\phi_{C1}/kh$	Deviation	$-\phi_{D1}/kh$	Deviation
1	0.272	0.555	0.202	25.74	0.477	14.05	0.136	50	0.401	27.75	0.068	75	0.315	43.24
2	0.424	0.625	0.364	14.15	0.551	11.84	0.308	27.36	0.477	23.68	0.248	41.51	0.39	37.6
3	0.512	0.674	0.464	9.38	0.61	9.5	0.421	17.77	0.548	18.69	0.384	25	0.48	28.78
4	0.570	0.709	0.529	7.19	0.652	8.04	0.495	13.16	0.599	15.51	0.469	17.72	0.545	23.13
5	0.612	0.735	0.576	5.88	0.684	6.94	0.547	10.62	0.637	13.33	0.528	13.73	0.592	19.46
10	0.720	0.806	0.696	3.33	0.769	4.59	0.679	5.69	0.738	8.44	0.67	6.94	0.711	11.79
15	0.770	0.839	0.751	2.47	0.81	3.46	0.737	4.29	0.785	6.44	0.732	4.94	0.764	8.94

Table 3.4.9

α	Isotropic medium		Anisotropic medium ($\theta = 150^\circ$)											
	$-\phi_E/kh$	$-\phi_D/kh$	$K\mu/K\lambda = 2$				$K\mu/K\lambda = 4$				$K\mu/K\lambda = 10$			
			$-\phi_E/kh$	Deviation	$-\phi_D/kh$	Deviation	$-\phi_E/kh$	Deviation	$-\phi_D/kh$	Deviation	$-\phi_E/kh$	Deviation	$-\phi_D/kh$	Deviation
1	0.728	0.445	0.725	0.41	0.393	11.69	0.714	1.92	0.339	23.82	0.692	4.95	0.271	39.1
2	0.576	0.375	0.588	-2.08	0.339	9.6	0.588	-2.08	0.296	21.07	0.574	0.35	0.238	36.53
3	0.488	0.326	0.505	-3.48	0.3	7.98	0.510	-4.51	0.265	18.71	0.502	-2.87	0.214	34.36
4	0.430	0.291	0.449	-4.42	0.271	6.87	0.457	-6.28	0.241	17.18	0.451	-4.88	0.196	32.65
5	0.388	0.265	0.408	-5.15	0.249	6.04	0.417	-7.47	0.223	15.85	0.413	-6.44	0.182	31.32
10	0.280	0.194	0.298	-6.43	0.185	4.64	0.307	-9.64	0.168	13.4	0.307	-9.64	0.139	28.35
15	0.230	0.161	0.245	-6.52	0.154	4.35	0.254	-10.43	0.141	12.42	0.255	-10.87	0.116	27.95

Table 3.4.10

In most cases the stratification is horizontal. For horizontal stratification, when the sheet pile is located at the middle of the foundation floor, the potential $-\phi_D/kH$ at the tip of the sheet pile is 0.5 irrespective of the degree of anisotropy. If the sheet pile is located nearer to upstream side, with increasing degree of anisotropy, the potential at the tip of the sheet pile decreases. On the other hand, if the sheet pile is located nearer to the downstream side, with increasing degree of anisotropy, the potential increases.

In particular, for $\theta = 0$, $b_1/b = 0.1$, $b/s = 15$, and $N = 1$, $\phi_D/kH = 0.77$ (fig 3.2 (a3)). For $b_1/b = 0.9$, the corresponding value is 0.22. For $N = 4$, the corresponding values are 0.74 and 0.26, respectively.

For $\theta = 0$, $b_1/b = 0.1$, $b/s = 15$, and $N = 1$, $\phi_E/-kH = 0.85$. For $N = 4$, the corresponding value is 0.88. For $b_1/b = 0.9$, for $N = 1$, $\phi_E/-kH = 0.28$. For $N = 4$ the potential is 0.35. Thus with increasing in degree of anisotropy there is increase in the potential $\phi_E/-kH$ irrespective of the position of sheet pile.

Maximum Exit Gradient:

The exit gradient distribution curves for the cases under study are prepared and presented in fig 3.4(a1) through 3.4(c3). With known values of θ , k_μ/k_λ and α , the value of I_E^*s/H at a point downstream of the structure can be directly read off curves. The curves are plotted for I_E^*s/H against x/s , where x is the length measured from downstream sheet pile.

Equation 3.3.18, for $\gamma < 1/2$, the maximum exit gradient at $x = 0$ ($\beta_2 = 1$) becomes infinite. Such condition arises for $0 < \theta < 90^\circ$. A sheet pile of any depth in such case is of no use. An alternate controlling structure needs to be visualized for such condition. Chapter 4 deals with such cases. In this chapter the exit gradient distributions corresponding to $\theta = 0^\circ$, 120° and 150° are analysed and presented.

The values of maximum I_E^*s/H obtained for $k_\mu/k_\lambda = 1$ (which is an isotropic case) tally with those of Khosla.

Sheet piles are provided at the downstream end to control exit gradient. Degree of anisotropy and orientation of the principal permeability direction influence quite strikingly the trend and magnitude of the exit gradient.

For horizontal stratification i.e. $\theta = 0$, and $N > 1$, $I_{E \max}^*s/H$ is higher than that had the domain been isotropic, and the % difference increases as k_μ/k_λ increases. Corresponding to $k_\mu/k_\lambda = 2, 4$ and 10 and $\alpha = 1$, $I_{E \max}^*s/H$ are 4.14%, 6.55% and 8.28% higher than those for isotropic flow domain and for $\alpha = 15$, the corresponding values are 16.81%, 36.28% and 64.60% higher. The location of the maximum exit gradient is at $x = 0$ for all values of k_μ/k_λ and α . With horizontal stratification, the magnitude of exit gradient is increased at all points, however the nature of distribution does not change much. It is maximum near the sheet pile and decreases monotonically with distance from the sheet pile. With increasing degree of anisotropy the exit gradient increases at all

points. Thus if the sheet pile controls the maximum gradient near the sheet pile, the exit gradient at other locations are also under control.

For $\theta = 120^\circ$, $I_{E \max} * s/H$ for anisotropic case is lower than that had the soil been isotropic. The % difference increases as k_μ/k_λ increases. For the same k_μ/k_λ , the % difference increases as b/s ratio increases. Corresponding to $k_\mu/k_\lambda = 2, 4$ and 10 and $\alpha = 1$ the computed values of $I_{E \max} * s/H$ are 25.86%, 41.03% and 54.83% lower than those in isotropic domain. For $\alpha = 15$ the corresponding values are 28.32%, 44.25% and 59.29% lower than those of isotropic flow domain. The location of maximum exit gradient is at $x/s = 0.5, 0.6$ and 0.7 for $k_\mu/k_\lambda = 2, 4$ and 10 , respectively. As k_μ/k_λ increases the position of maximum exit gradient shifts towards downstream, but remains unaltered with change in α .

Similar trend is observed for $\theta = 150^\circ$. Corresponding to $k_\mu/k_\lambda = 2, 4$ and 10 and $\alpha = 1$ the computed values of $I_{E \max} * s/H$ are 24.14%, 43.79% and 62.07% lower than those of values in isotropic domain. For $\alpha = 15$ the corresponding values are 17.70%, 36.28% and 55.75% lower than those of isotropic flow domain. The location of maximum exit gradient is at $x/s = 0.7, 1.10$ and 1.60 for $k_\mu/k_\lambda = 2, 4$ and 10 , respectively. As k_μ/k_λ increases the position of maximum exit gradient shifts towards downstream, but remains unaltered with change in α .

A numerical example is worked out below to show the use of the graphs presented.

Illustrative Example:

Determine the pressure at key points and the minimum factor of safety available to the structure against piping for a flat bottomed weir with a vertical sheet pile at downstream end for the following data:

Width of the horizontal blanket $b = 25$ m

Depth of the vertical sheet pile $s = 5$ m.

Upstream head of the water $H = 5$ m. and there is no water in downstream side.

Critical exit gradient = 1.

The cases to be considered are:

For $k_{\mu}/k_{\lambda} = 1$ (isotropic case)

For $k_{\mu}/k_{\lambda} = 10$ and $\theta = 0^{\circ}, 30^{\circ}, 60^{\circ}, 120^{\circ}$ and 150°

Solution:

$$\alpha = b/s = 25/5 = 5$$

i) $\theta = 0^{\circ}$, $k_{\mu}/k_{\lambda} = 10$, $\alpha = 5$

From Fig.3.3(a3), $-\phi_E/kH = 0.629$

From Fig.3.3(a4), $-\phi_D/kH = 0.402$

From Fig.3.4(a3), $I_{E_{\max}} * s/H = 0.2657$ at $x/s = 0$

Pressure at the junction of sheet pile and floor = $0.629 * H * \gamma_w = 0.629 * 5 * \gamma_w = 3.145 \gamma_w$

Pressure at the tip of sheet pile = $(0.402 * H + s) * \gamma_w = (0.402 * 5 + 5) * \gamma_w = 7.01 \gamma_w$

Maximum exit gradient $I_{E_{\max}} = 0.2657 * H/s = 0.2657 * 5/5 = 0.2657$

Minimum factor of safety available against piping = $I_{\text{critical}} / I_{E_{\max}} = 1/0.2657 = 3.76$

ii) $\theta = 30^{\circ}$, $k_{\mu}/k_{\lambda} = 10$, $\alpha = 5$

From Fig.3.3(b3), $-\phi_E/kH = 0.472$

From Fig.3.3(b4), $-\phi_D/kH = 0.408$

$$I_{E_{\max}} = \infty$$

Pressure at the junction of sheet pile and floor = $0.472 * H * \gamma_w = 0.472 * 5 * \gamma_w = 2.36 \gamma_w$

Pressure at the tip of sheet pile = $(0.408 * H + s) * \gamma_w = (0.408 * 5 + 5) * \gamma_w = 7.04 \gamma_w$

Minimum factor of safety available against piping = $I_{\text{critical}} / I_{E_{\max}} = 1 / \infty = 0$

iii) $\theta = 60^{\circ}$, $k_{\mu}/k_{\lambda} = 10$, $\alpha = 5$

From Fig.3.3(c3), $-\phi_E/kH = 0.301$

From Fig.3.3(c4), $-\phi_D/kH = 0.271$

$$I_{E_{\max}} = \infty$$

Pressure at the junction of sheet pile and floor = $0.301 * H * \gamma_w = 0.301 * 5 * \gamma_w = 1.505 \gamma_w$

Pressure at the tip of sheet pile = $(0.271 * H + s) * \gamma_w = (0.271 * 5 + 5) * \gamma_w = 6.355 \gamma_w$

Minimum factor of safety available against piping = $I_{\text{critical}} / I_{\text{E}_{\text{max}}} = 1/\infty = 0$

iv) $\theta = 120^\circ$, $k_\mu/k_\lambda = 10$, $\alpha = 5$

From Fig.3.3(d3), $-\phi_E/kH = 0.284$

From Fig.3.3(d4), $-\phi_D/kH = 0.129$

From Fig.3.4(b3), $I_{\text{E}_{\text{max}}} * s/H = 0.076$ at $x/s = 0.7$

Pressure at the junction of sheet pile and floor = $0.284 * H * \gamma_w = 0.284 * 5 * \gamma_w = 1.42\gamma_w$

Pressure at the tip of sheet pile = $(0.129 * H + s) * \gamma_w = (0.129 * 5 + 5) * \gamma_w = 6.45\gamma_w$

Maximum exit gradient $I_{\text{E}_{\text{max}}} = 0.076 * H/s = 0.076 * 5/5 = 0.076$

Minimum factor of safety available against piping = $I_{\text{critical}} / I_{\text{E}_{\text{max}}} = 1/0.076 = 13.16$

v) $\theta = 150^\circ$, $k_\mu/k_\lambda = 10$, $\alpha = 5$

From Fig.3.3(e3), $-\phi_E/kH = 0.413$

From Fig.3.3(e4), $-\phi_D/kH = 0.182$

From Fig.3.4(c3), $I_{\text{E}_{\text{max}}} * s/H = 0.076$ at $x/s = 1.6$

Pressure at the junction of sheet pile and floor = $0.413 * H * \gamma_w = 0.413 * 5 * \gamma_w = 2.065\gamma_w$

Pressure at the tip of sheet pile = $(0.182 * H + s) * \gamma_w = (0.182 * 5 + 5) * \gamma_w = 5.91\gamma_w$

Maximum exit gradient $I_{\text{E}_{\text{max}}} = 0.076 * H/s = 0.076 * 5/5 = 0.076$

Minimum factor of safety available against piping = $I_{\text{critical}} / I_{\text{E}_{\text{max}}} = 1/0.076 = 13.16$

v) $k_\mu/k_\lambda = 1$ (isotropic case), $\alpha = 5$ and $1/\alpha = 0.2$

$-\phi_E/kH = 0.388$

$-\phi_D/kH = 0.265$

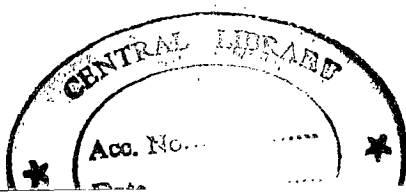
$I_{\text{E}_{\text{max}}} * s/H = 0.1823$ at $x/s = 0$

Pressure at the junction of sheet pile and floor = $0.388 * H * \gamma_w = 0.388 * 5 * \gamma_w = 1.94\gamma_w$

Pressure at the tip of sheet pile = $(0.265 * H + s) * \gamma_w = (0.265 * 5 + 5) * \gamma_w = 6.325\gamma_w$

Maximum exit gradient $I_{\text{E}_{\text{max}}} = 0.1823 * H/s = 0.1823 * 5/5 = 0.1823$

Minimum factor of safety available against piping = $I_{\text{critical}} / I_{\text{E}_{\text{max}}} = 1/0.1823 = 5.49$



Compared to the isotropic flow domain, from the above examples, it is seen that for $0 < \theta < 90^\circ$ an upstream blanket becomes less effective in dissipating the total head along its width. In such cases of stratification a vertical sheet pile is more effective in dissipating the total head along its length. For $90^\circ < \theta < 180^\circ$ an upstream blanket becomes more effective in dissipating the total head along its width. In general, it is seen that as θ approaches to either 0 or π , an horizontal floor becomes less effective while a vertical sheet pile becomes more effective in dissipating the total head. As θ approaches to $\pi/2$ the horizontal floor becomes more effective in dissipating the total head.

In the above illustrated example, if the flow domain is anisotropic with $\theta = 0$ and $k_\mu/k_\lambda = 10$, then design based on isotropic condition gives the lesser thickness of the apron than the required. At the junction of the down stream sheet pile and floor, uplift force equal to $(0.629-0.388) * H * \gamma_w = 0.241 * H * \gamma_w$ remains unbalanced and the apron may be susceptible to the floating. In addition, the minimum factor of safety provided against piping is reduced from 5.49 to 3.65.

Similarly, if the flow domain is anisotropic with $\theta = 120^\circ$ and $k_\mu/k_\lambda = 10$, then the design based on isotropic condition gives a larger thickness of the apron at the junction of the downstream sheet pile than the required and the thickness for uplift force equal to $(0.388-0.284) * H * \gamma_w = 0.104 * H * \gamma_w$ remains unused. In addition, the minimum factor of safety provided against piping is increased from 5.49 to 13.16 which indicates an over estimate of length of blanket and/or the depth of sheet pile.

3.5 Conclusion

Based on the results presented in this chapter the following conclusions are drawn:

Depending upon the degree of anisotropy, the value of $-\phi/kh$ underneath the structure and the maximum exit gradient, may be significantly different in two identical structures of same shape and size but constructed on isotropic and anisotropic porous medium. For the same inclination of the maximum coefficient of permeability, the exit gradient increases as the degree of anisotropy increases.

Compared to the isotropic flow domain, as θ approaches to either 0 or π the horizontal floor becomes less effective while vertical sheet pile becomes more effective

in dissipating the total head and as θ approaches to $\pi/2$ an horizontal floor is more effective in dissipating the total head.

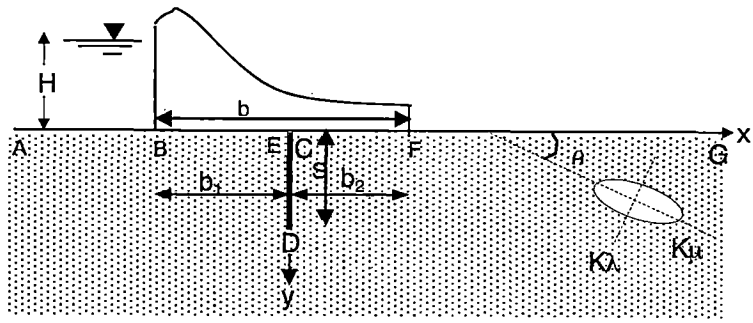
For $\theta = 0$, the position of maximum exit gradient is at the downstream end of the structure, and for all $k_\mu/k_\lambda > 1$, the value of maximum exit gradient is always more than that of isotropic flow domain.

For $\pi/2 < \theta < \pi$, the maximum exit gradient is finite but occurs somewhere downstream of the structure. As θ increases the position of maximum exit gradient shifts away from the structure. In this case, the value of maximum exit gradient is always less than that of isotropic medium.

For $0 < \theta < \pi/2$, the exit gradient becomes infinite at the downstream end of the structure, therefore, the structure becomes vulnerable to the piping. Care should be taken to bring the maximum exit gradient within the safe limit.

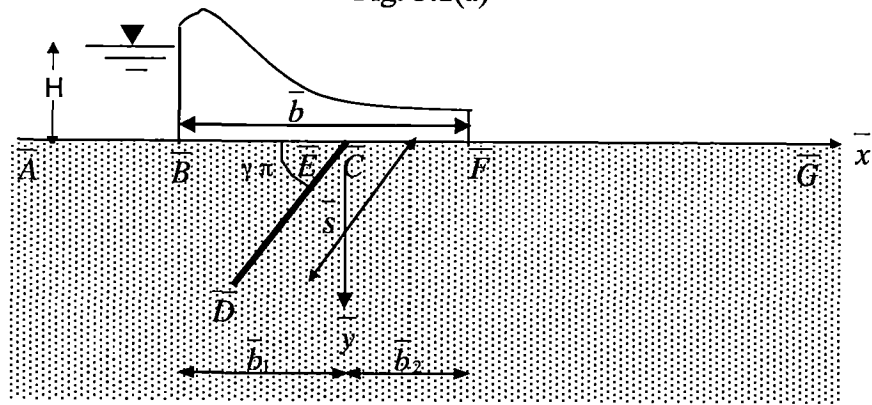
Design of a weir based on isotropic flow medium may be over or under designed for anisotropic flow medium depending upon θ and k_μ/k_λ .

The results obtained for $k_\mu/k_\lambda = 1$ tally with the results given by Khosla et al.



Structure in actual Anisotropic flow domain

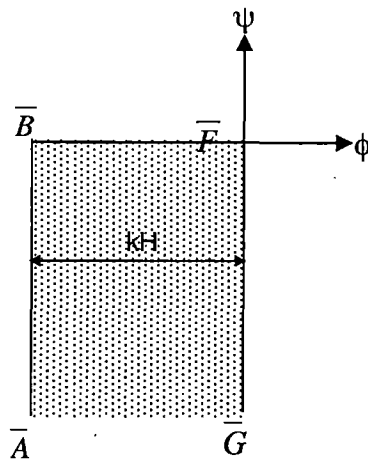
Fig. 3.1(a)



z-Plane

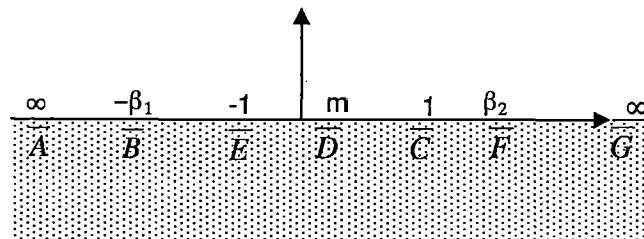
Structure in Transformed fictitious isotropic flow domain

Fig. 3.1(b)



w-Plane

Fig 3.1 (c)



t-Plane

Fig. 3.1(d)

FIG.3.1, STEPS FOR FLOW DOMAIN TRANSFORMATION & CONFORMAL MAPPING

ϕ curves for $K_\mu/K_\lambda = 1$ for all values of θ
 (isotropic case)

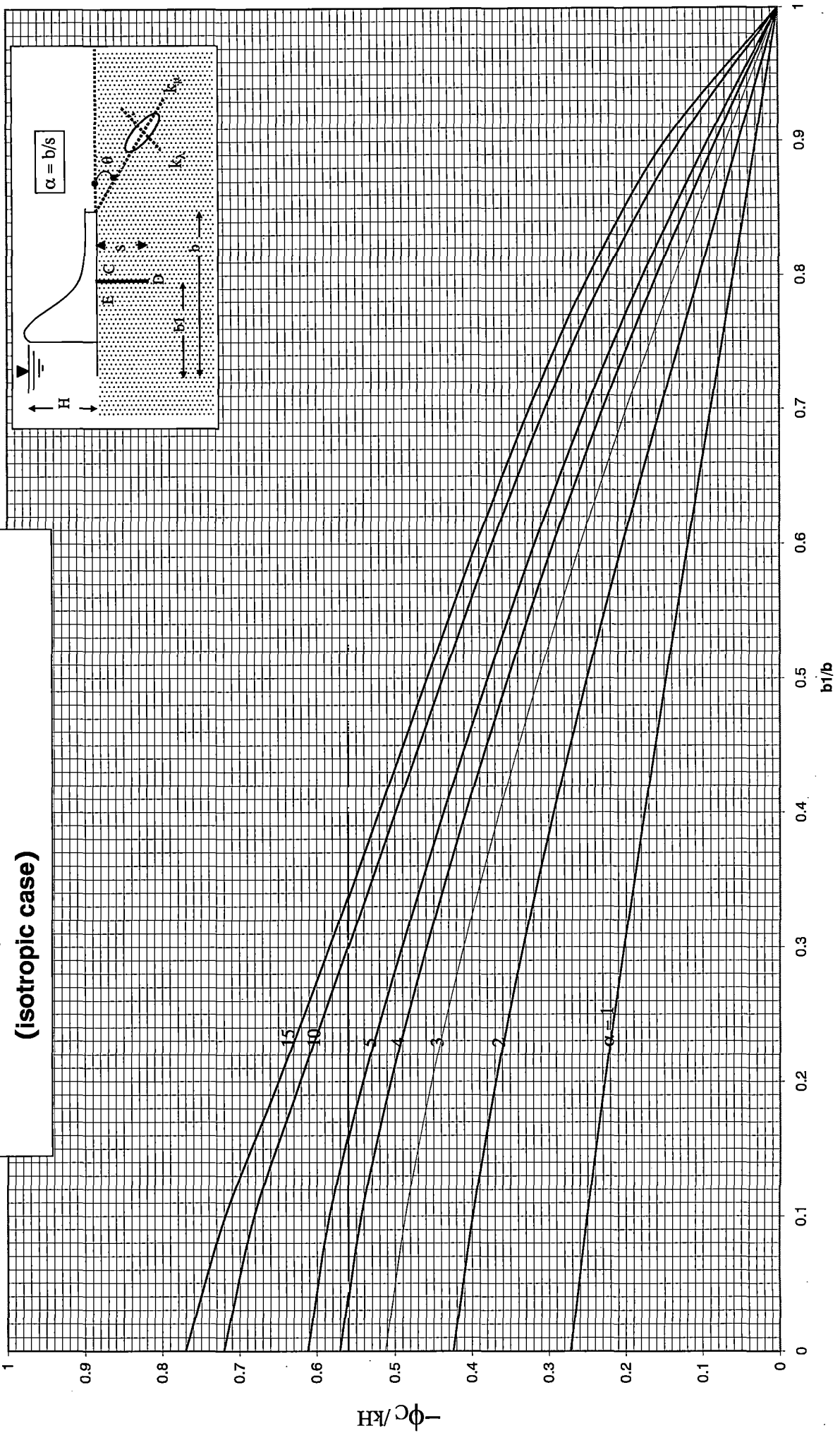


Fig.3.2(a1)

ϕ curves for $K_\mu/K_\lambda = 1$ for all values of θ
 (isotropic case)

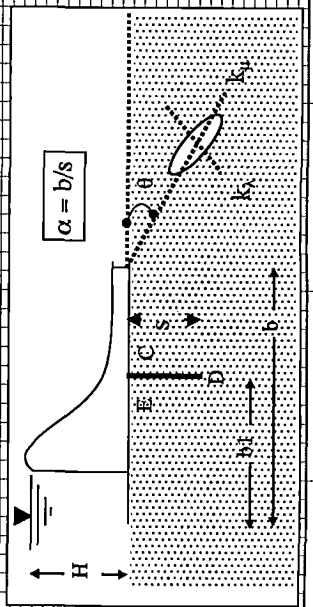
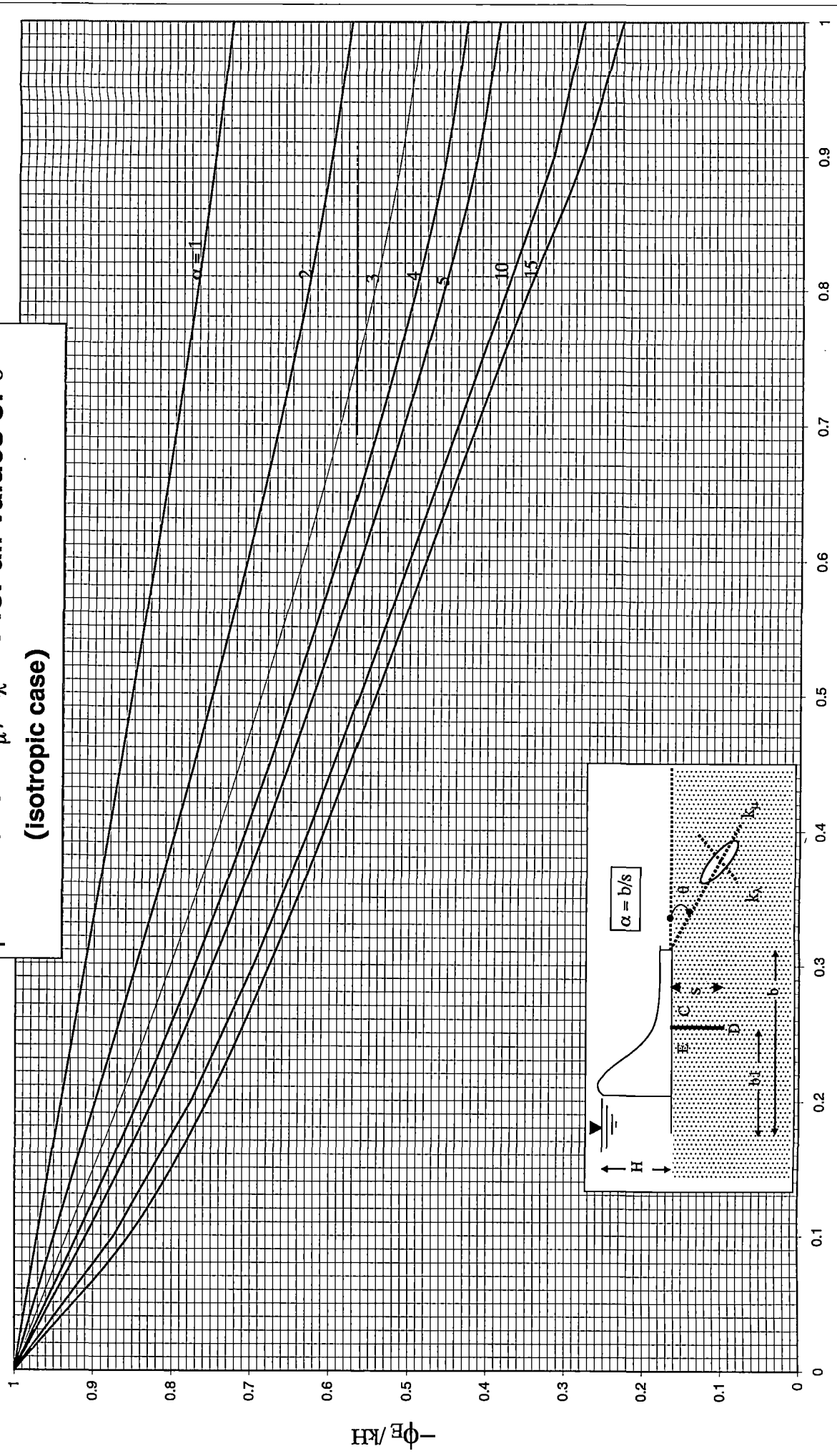


Fig.3.2(a2)

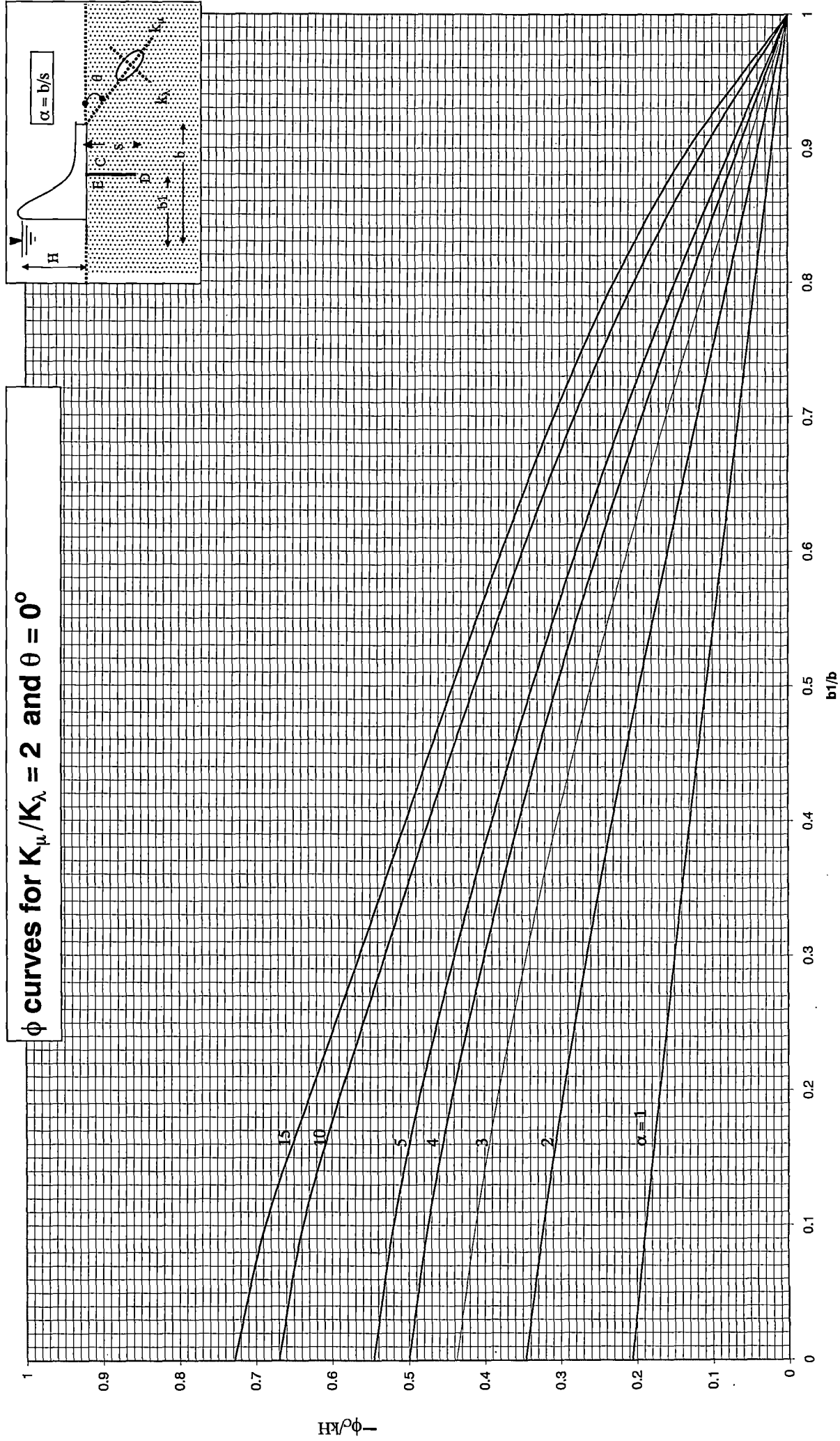


Fig.3.2(b1.1)

ϕ curves for $K_\mu/K_\lambda = 2$ and $\theta = 0^\circ$

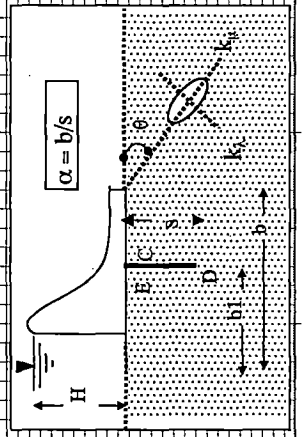
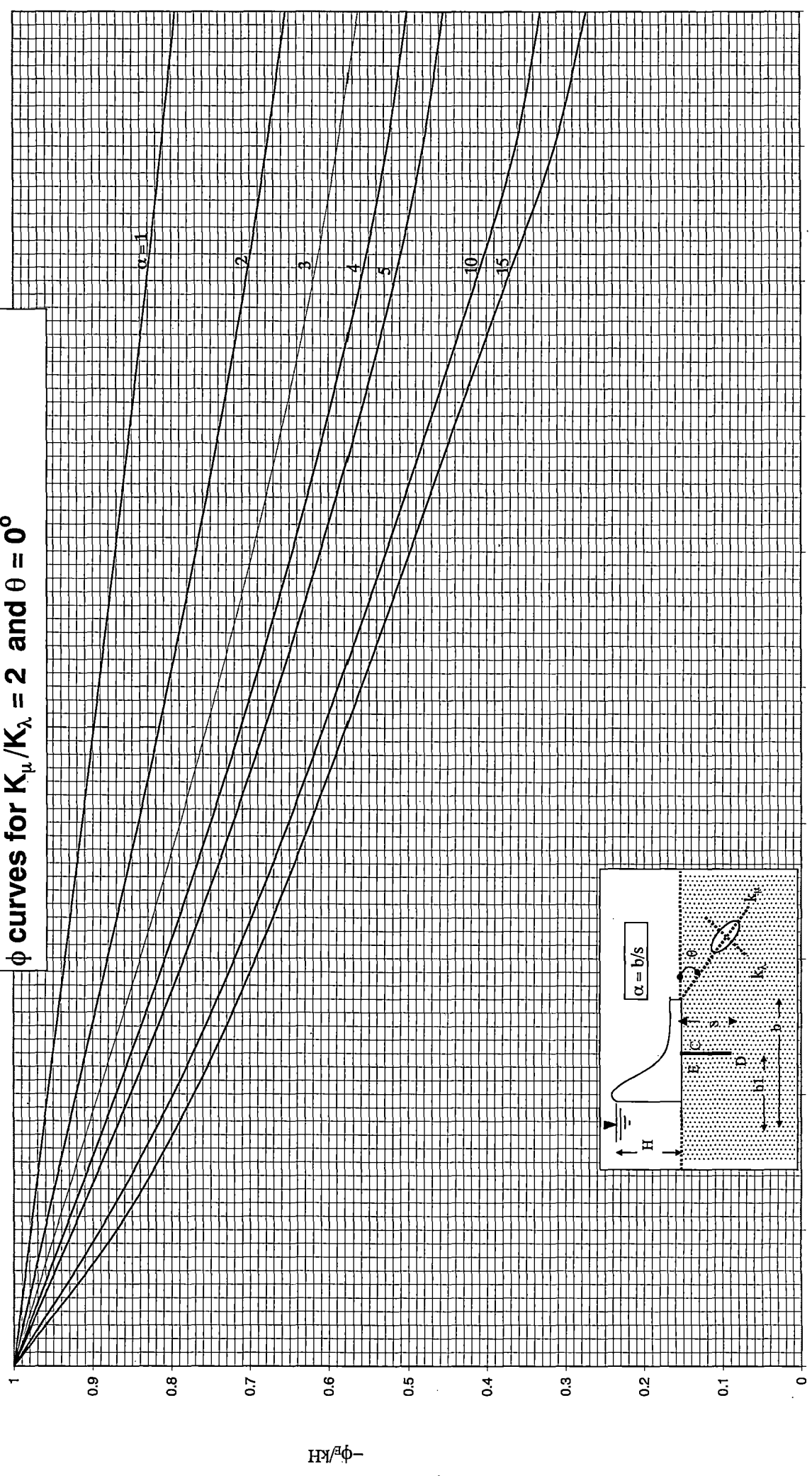


Fig.3.2(b1.2)

ϕ curves for $K_\mu/K_\lambda = 2$ and $\theta = 0^\circ$

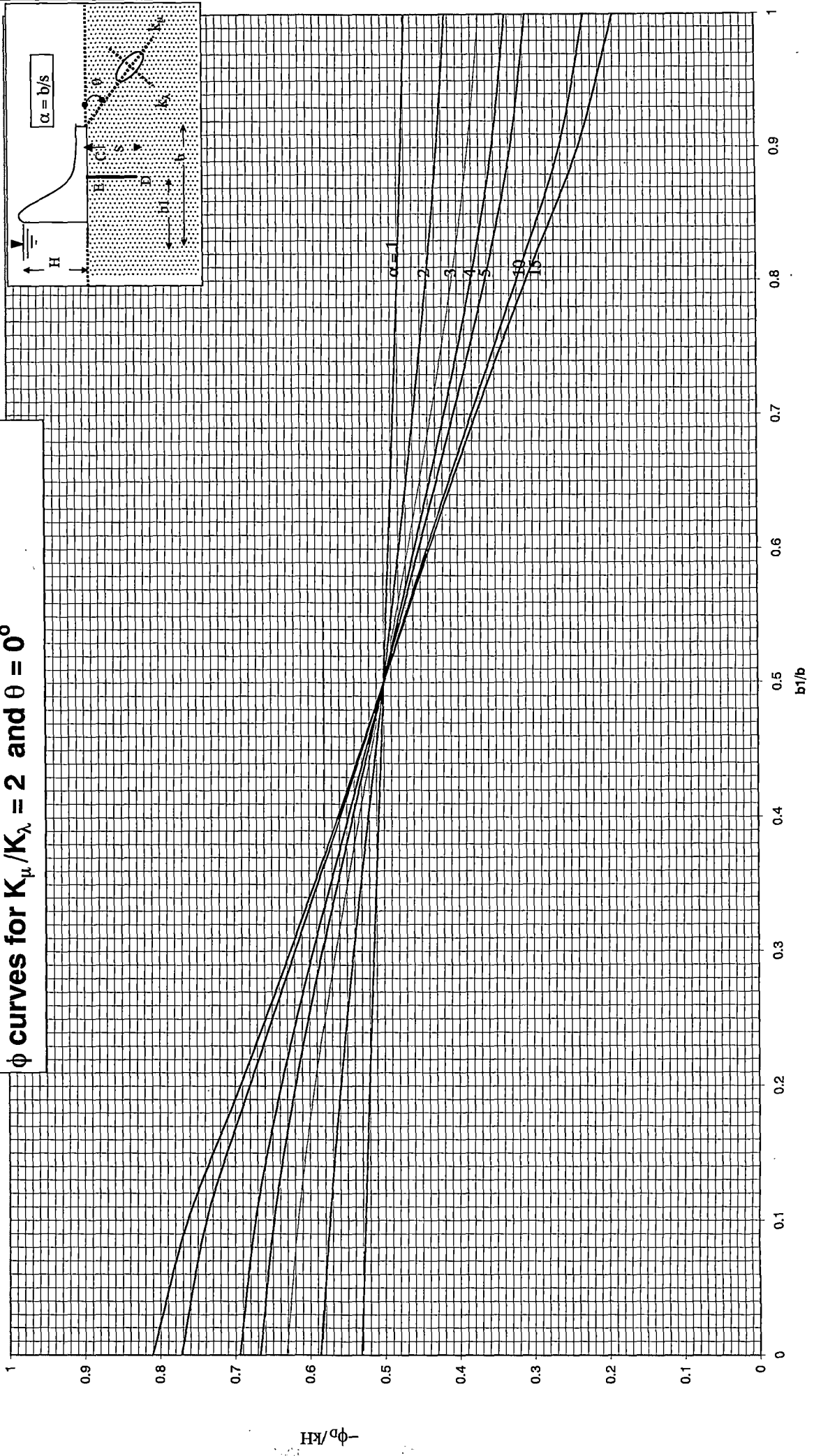


Fig.3.2(b1.3)

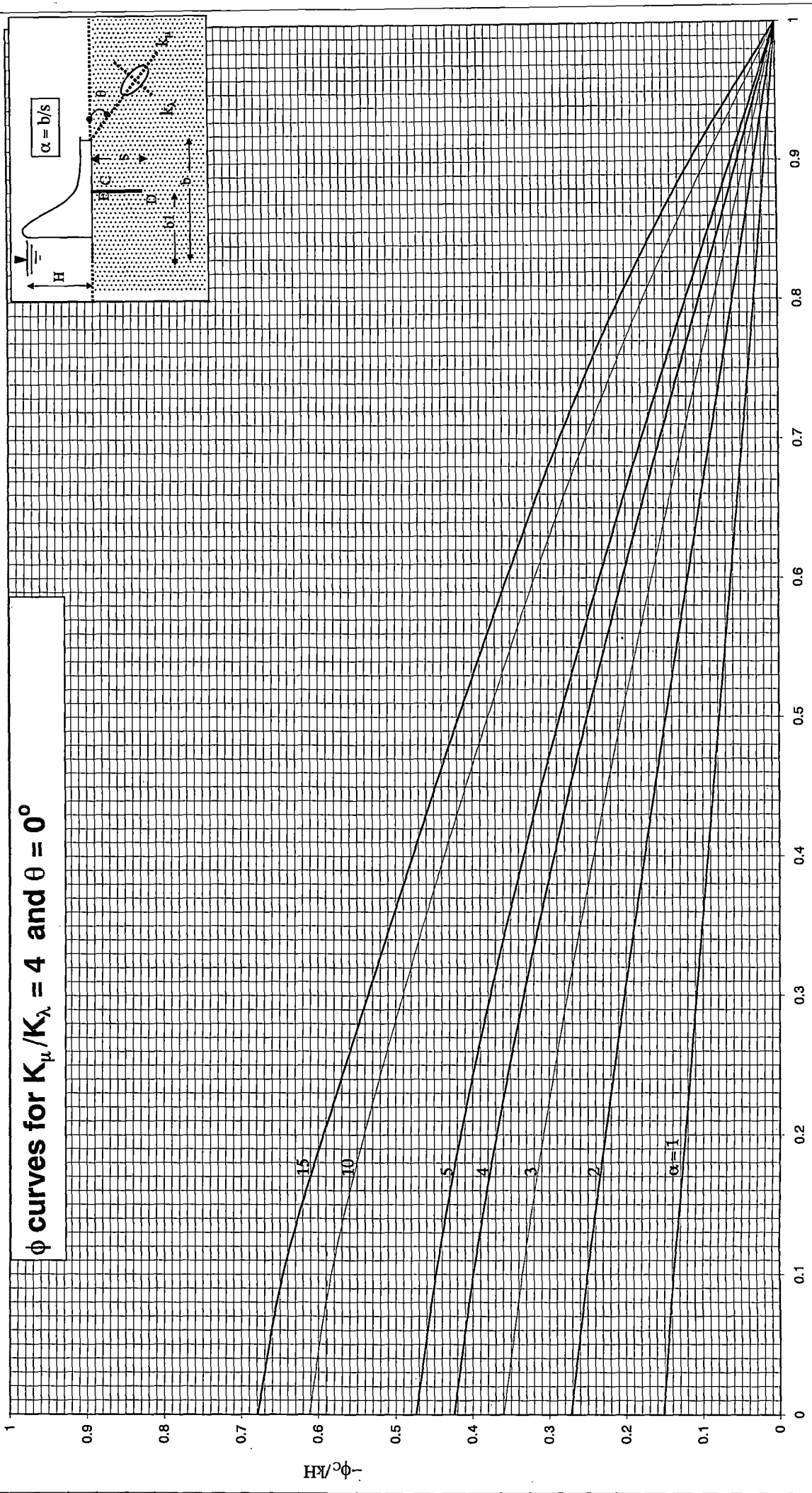


Fig. 3.2(b2.1)

ϕ curves for $K_{\mu}/K_{\lambda} = 4$ and $\theta = 0^{\circ}$

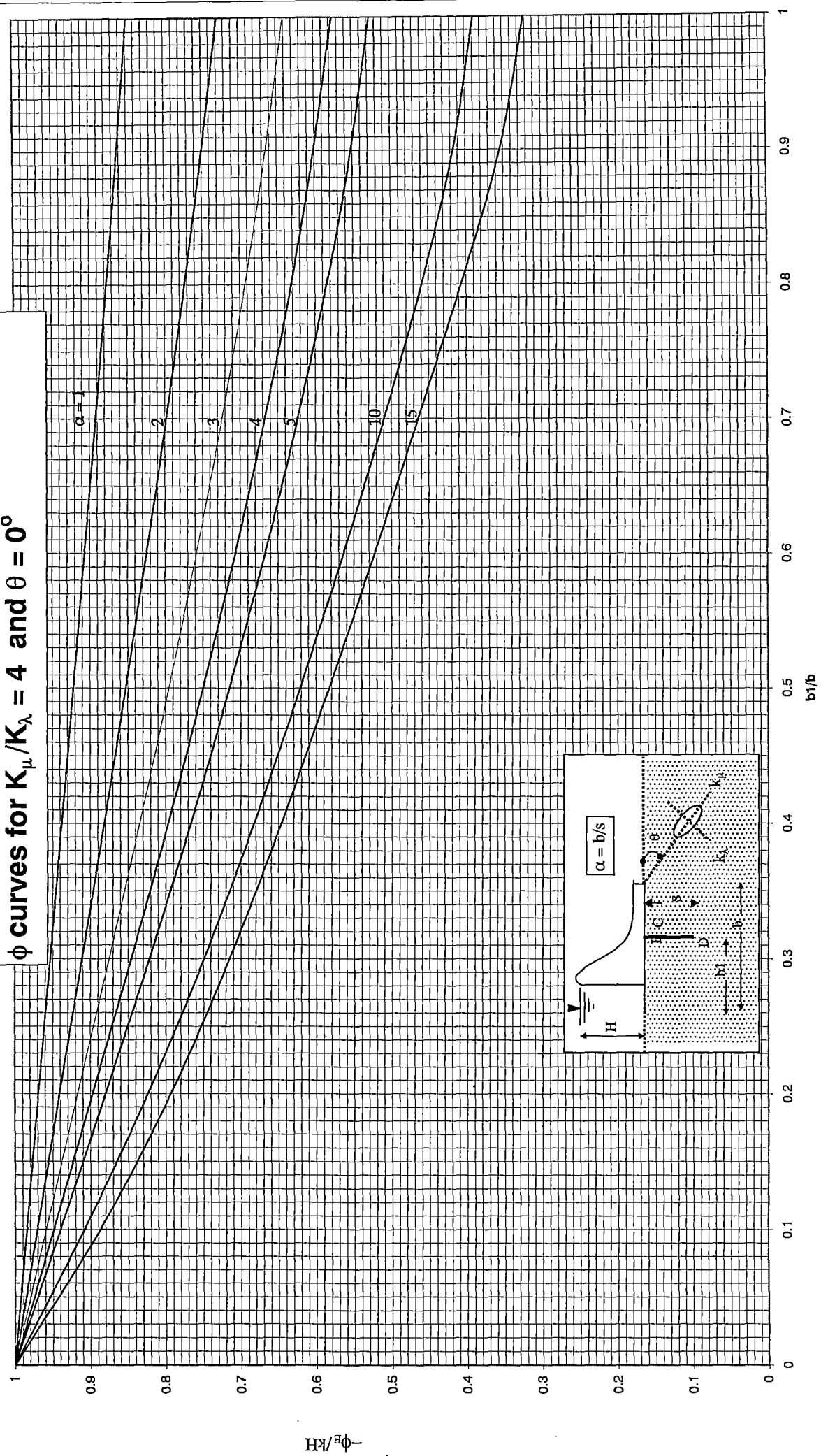


Fig.3.2(b2.2)

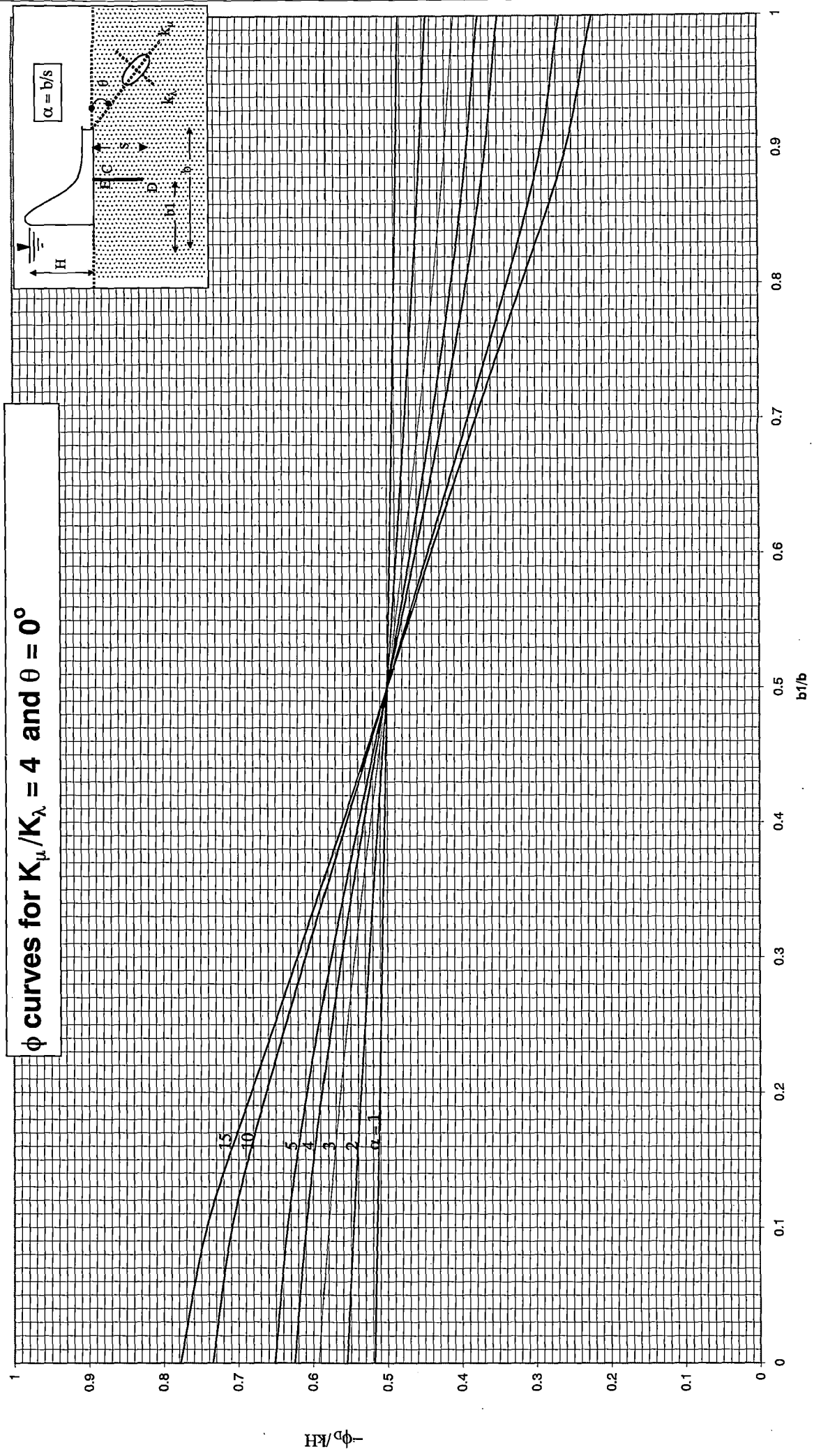


Fig.3.2(b2.3)

ϕ curves for $K_\mu/K_\lambda = 10$ and $\theta = 0^\circ$

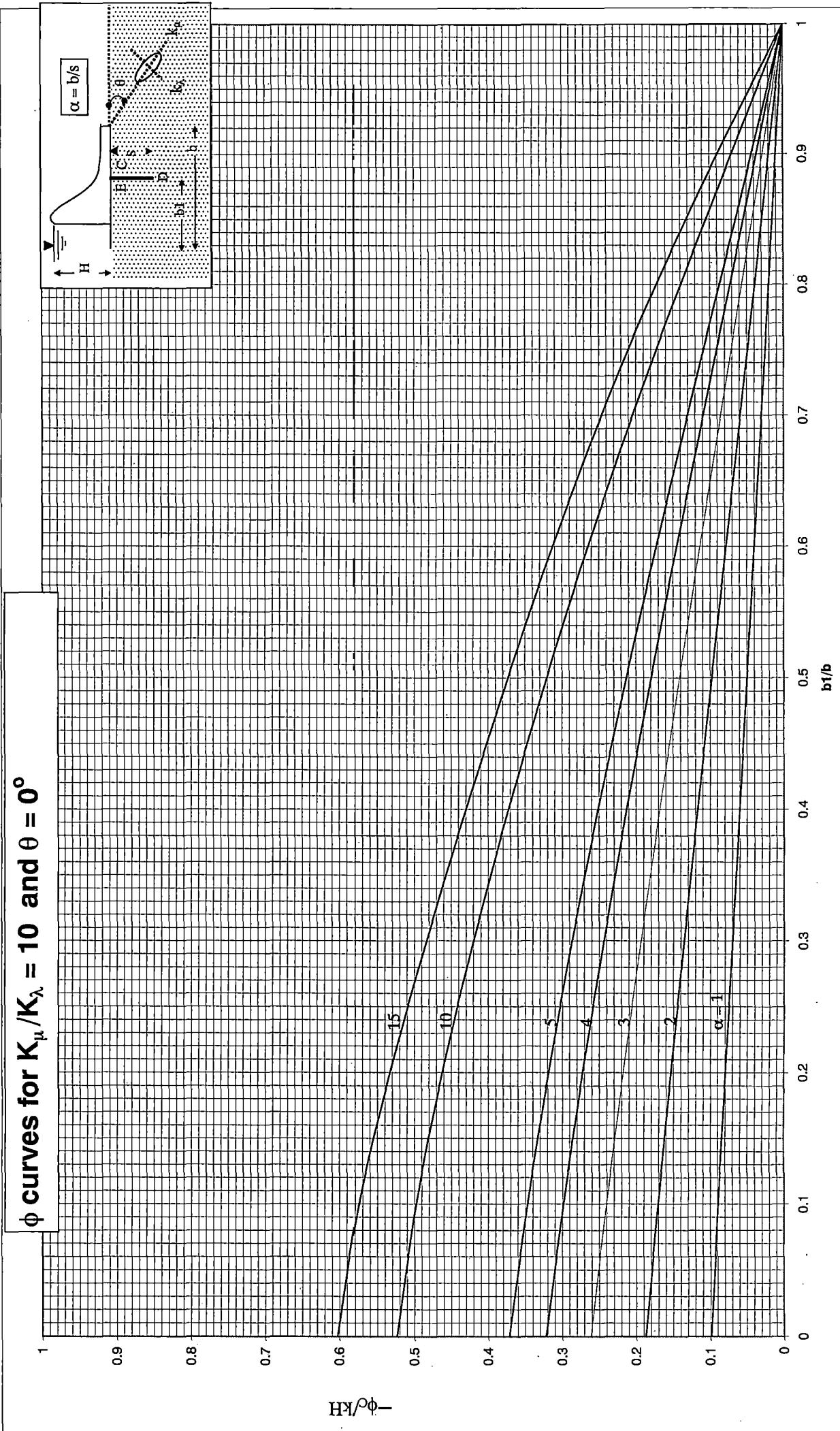


Fig.3.2(b3.1)

ϕ curves for $K_\mu/K_\lambda = 10$ and $\theta = 0^\circ$

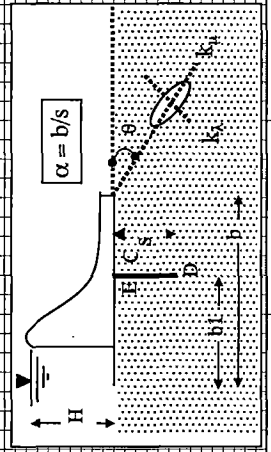
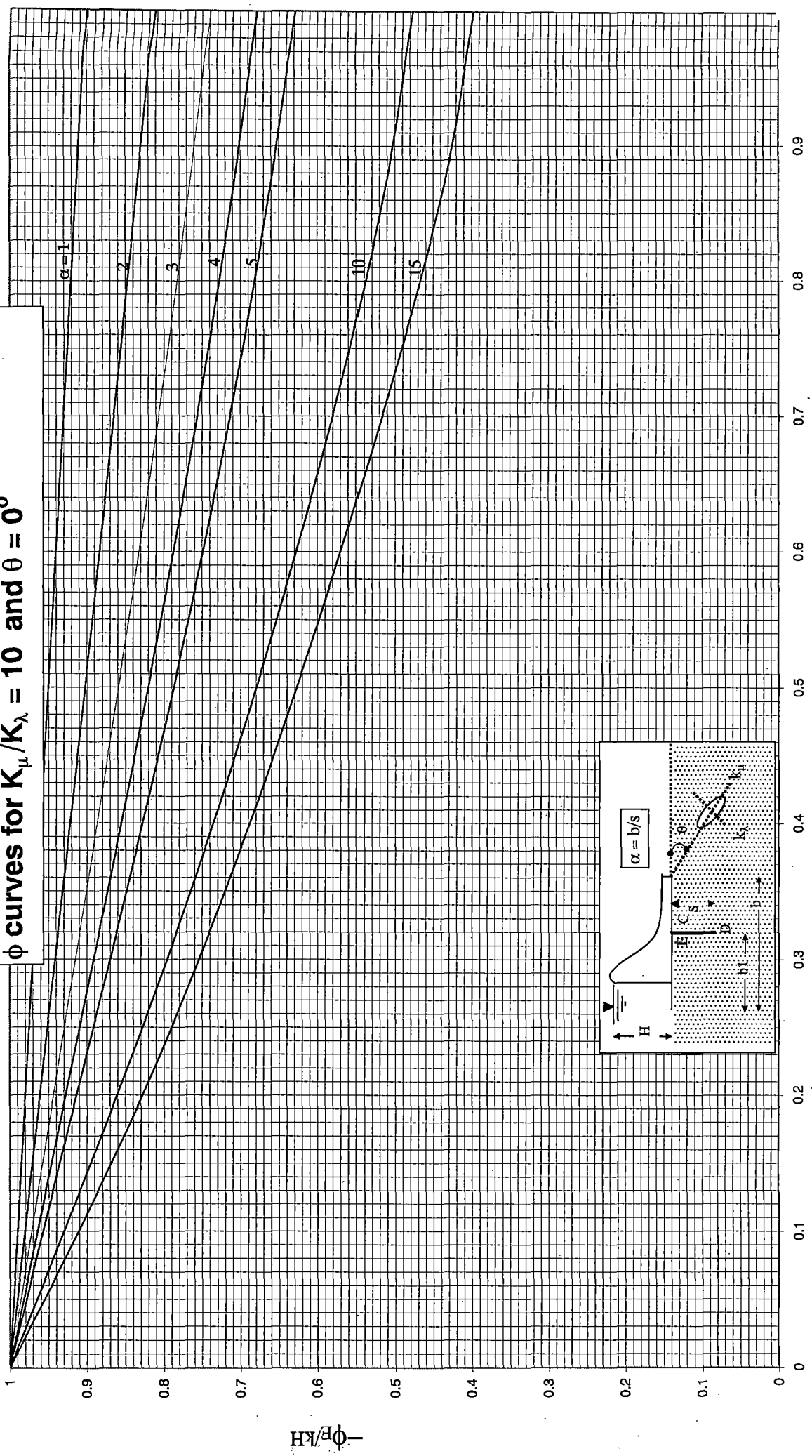


Fig.3.2(b3.2)

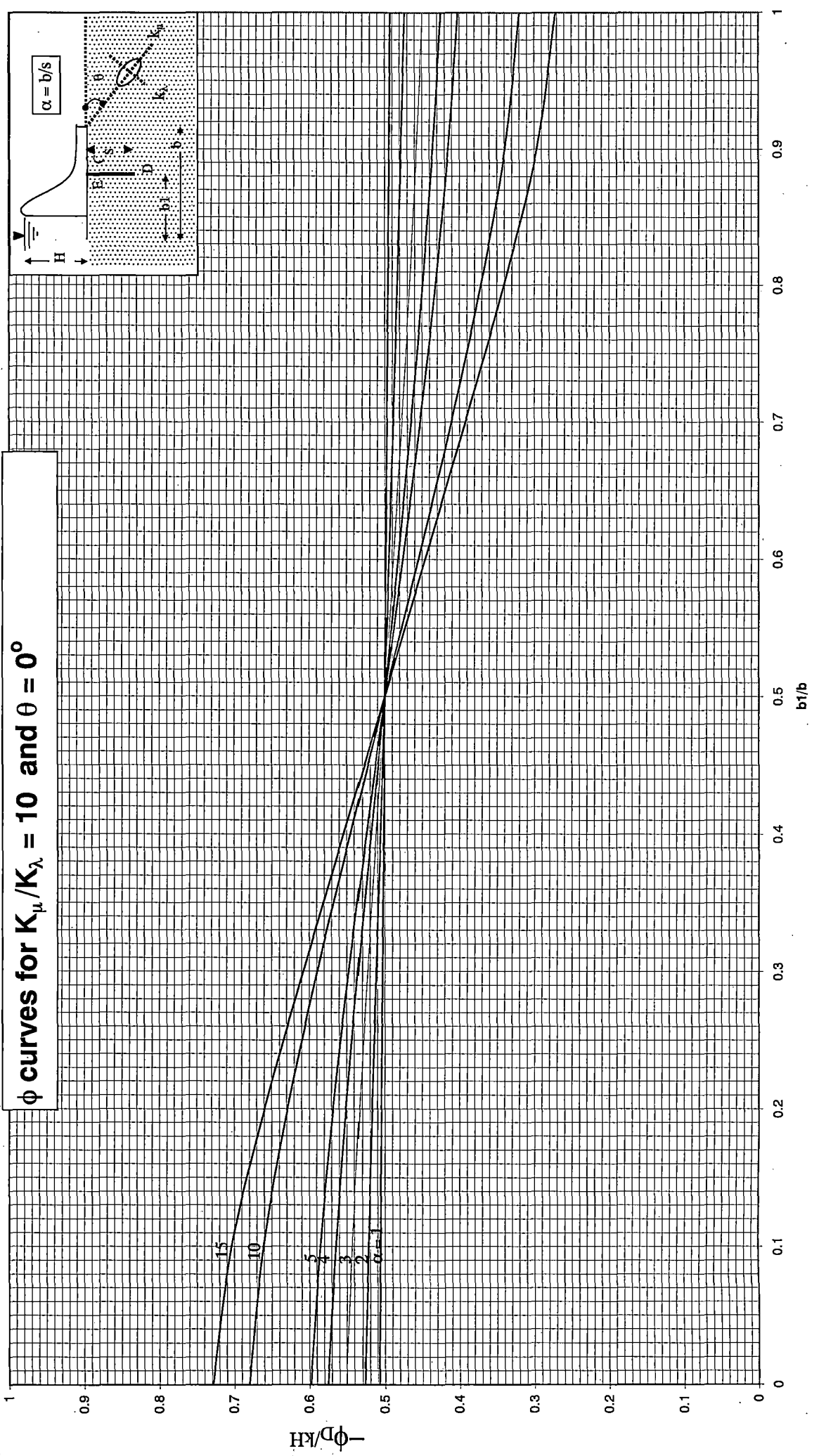


Fig.3.2(b3.3)

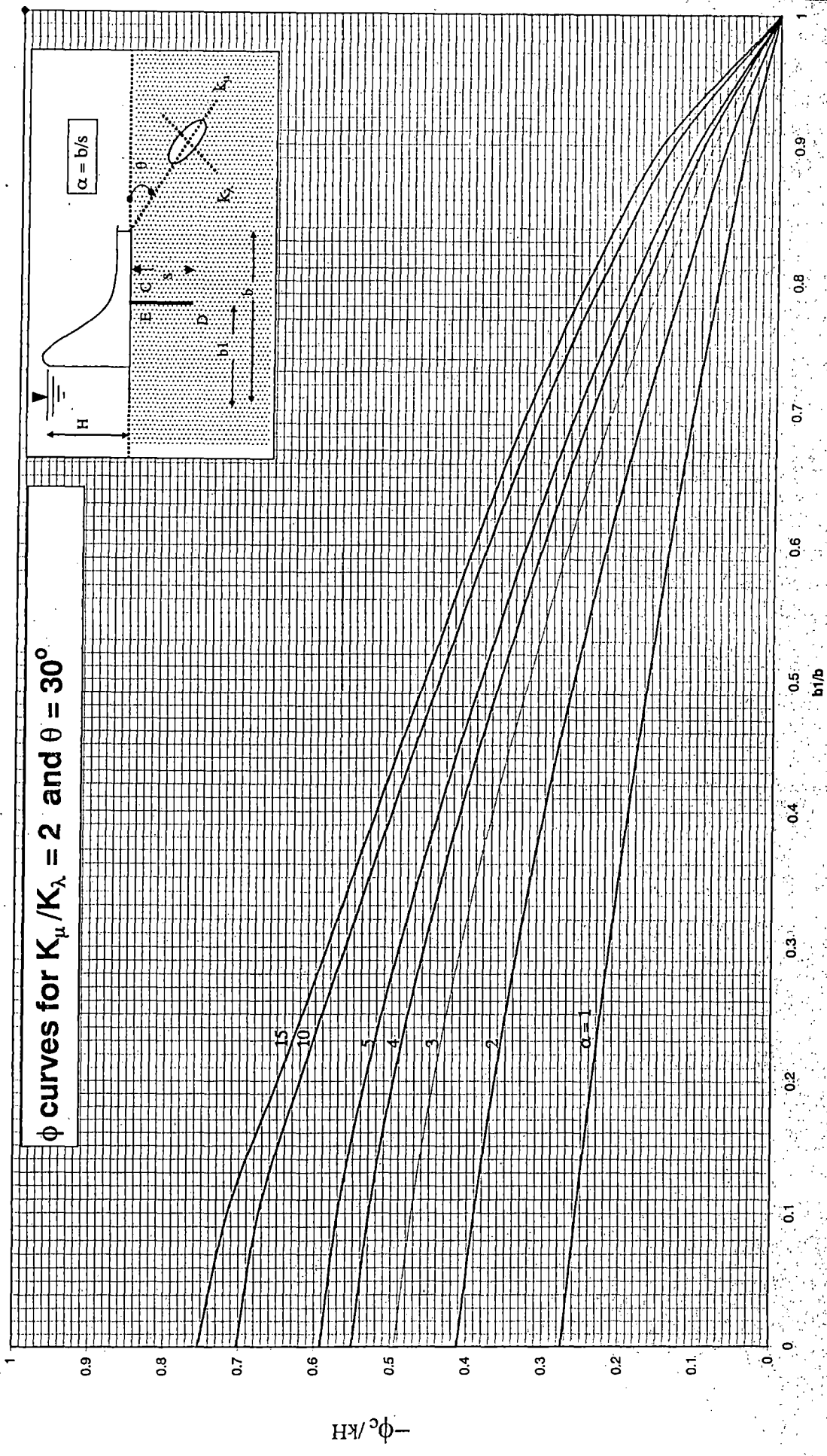


Fig.3.2(c1.1)

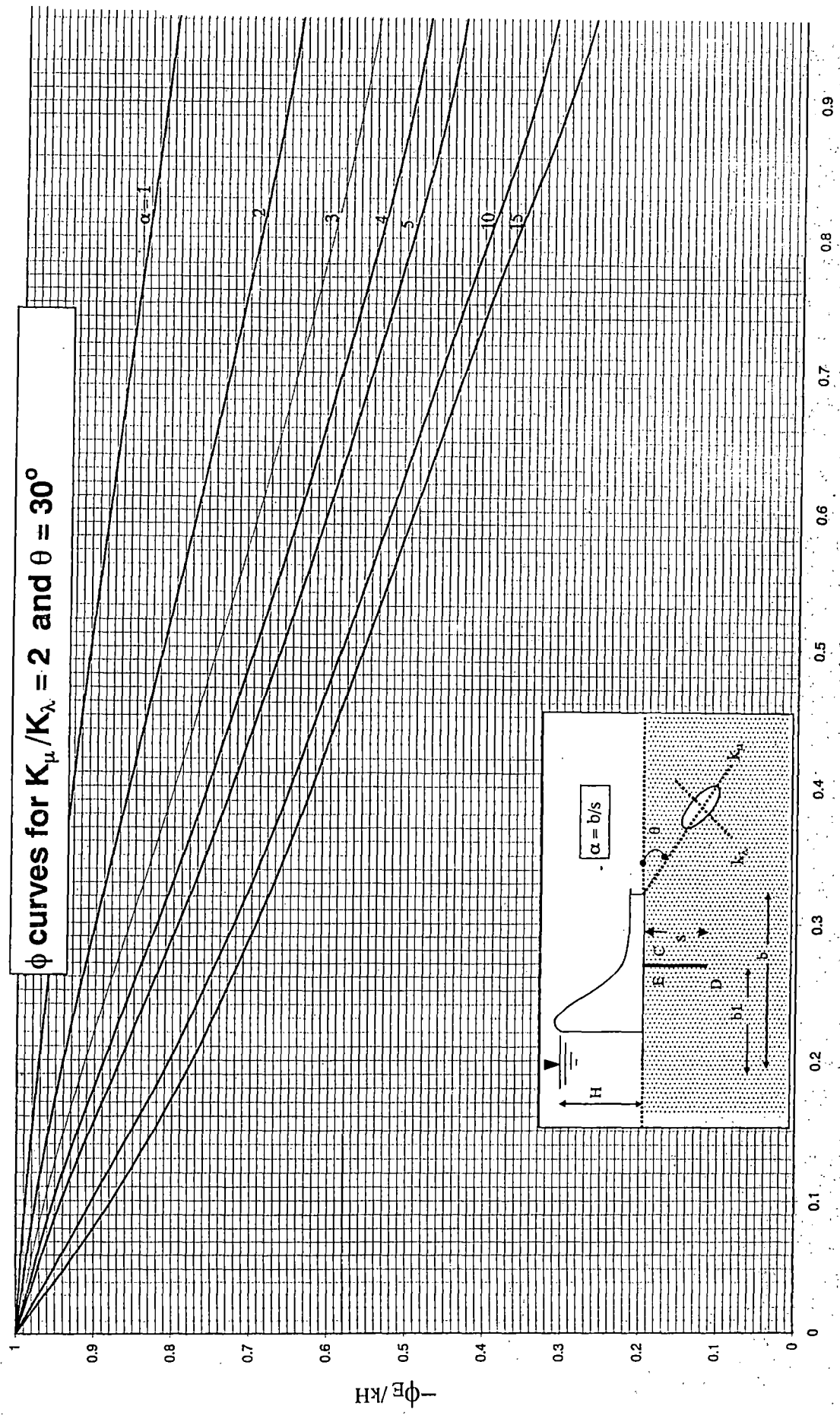


Fig.3.2(c1.2)

ϕ curves for $K_{\mu}/K_{\lambda} = 2$ and $\theta = 30^{\circ}$

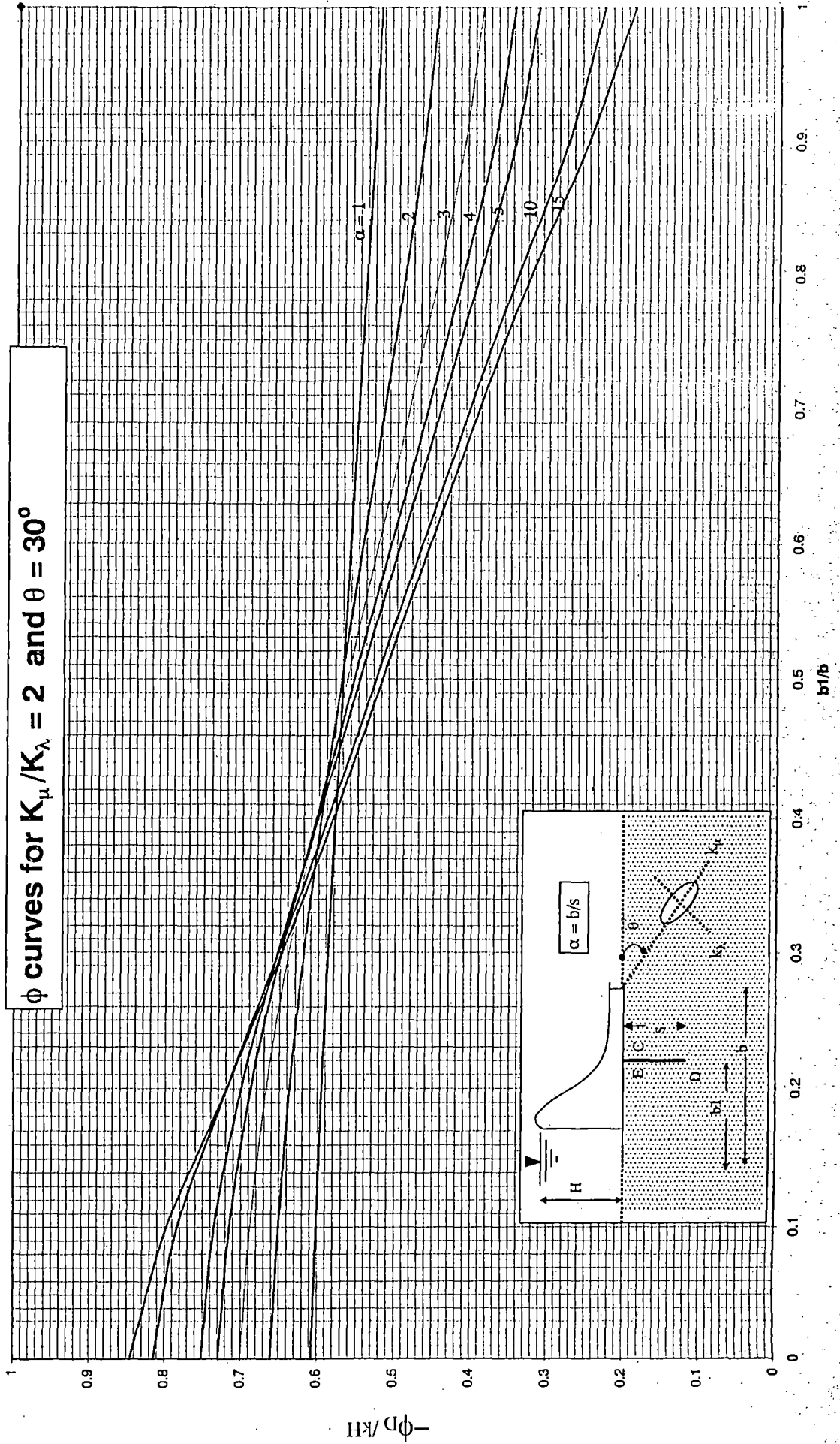


Fig.3.2(c1.3)

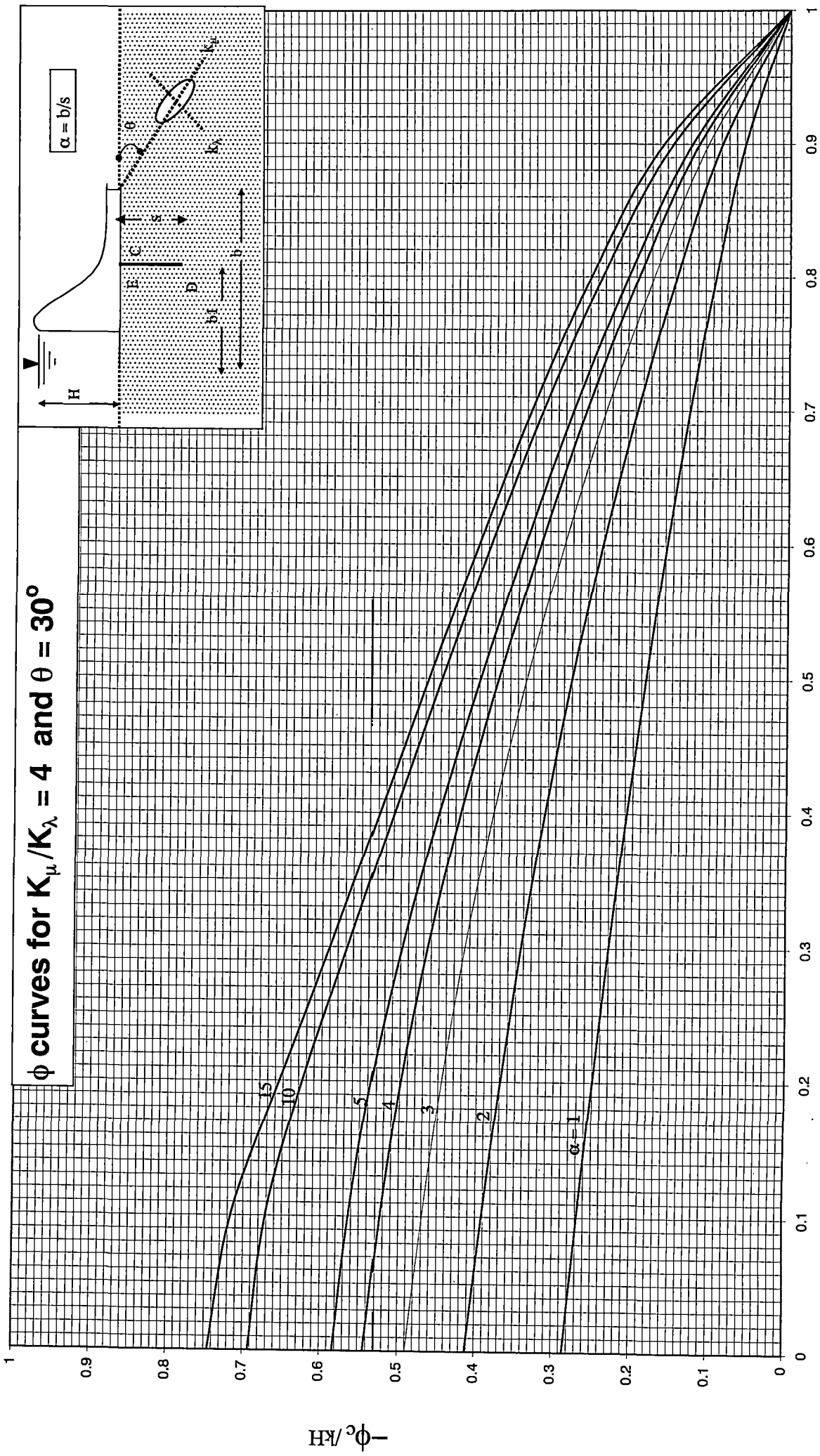


Fig.3.2(c2.1)

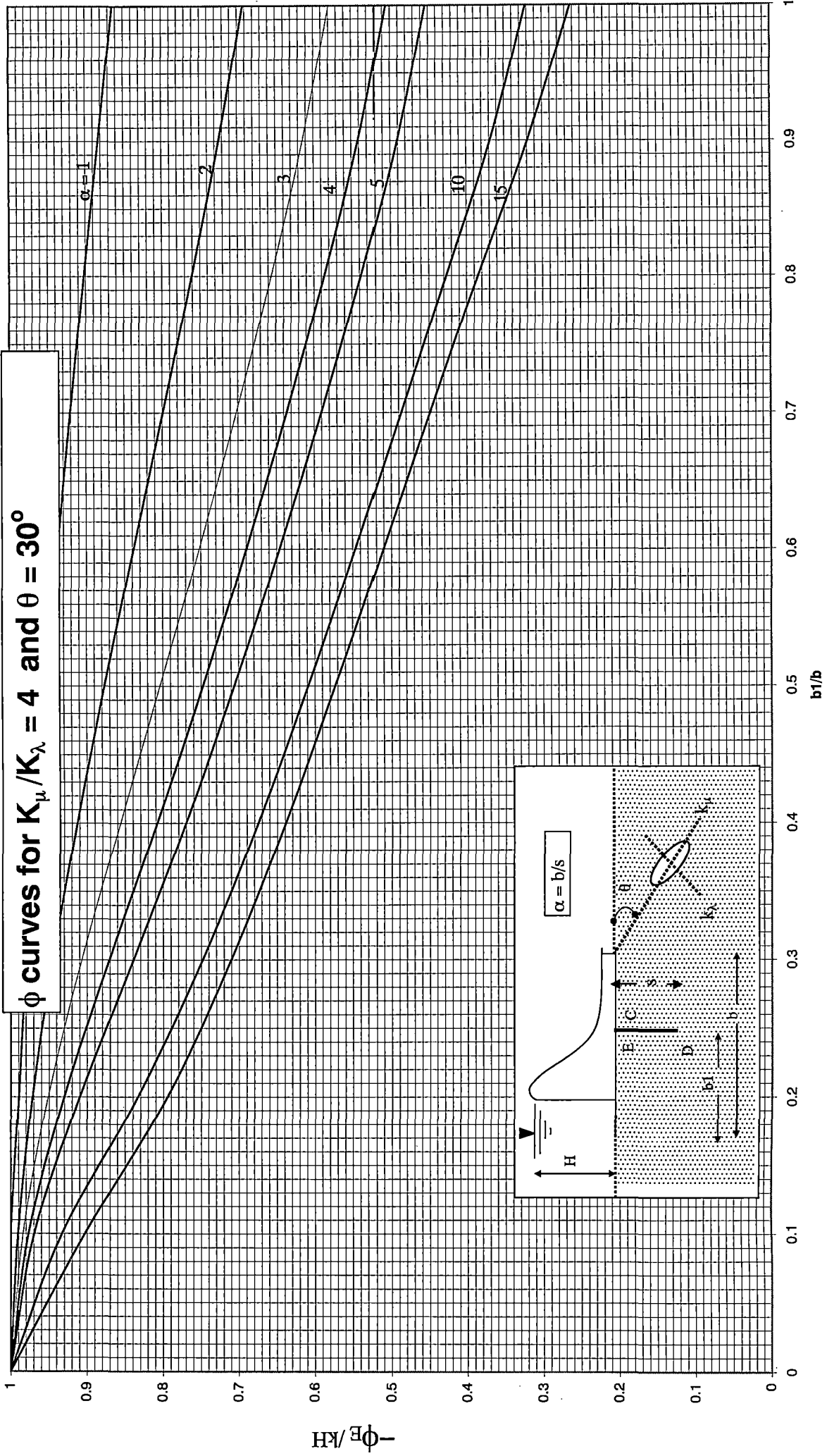
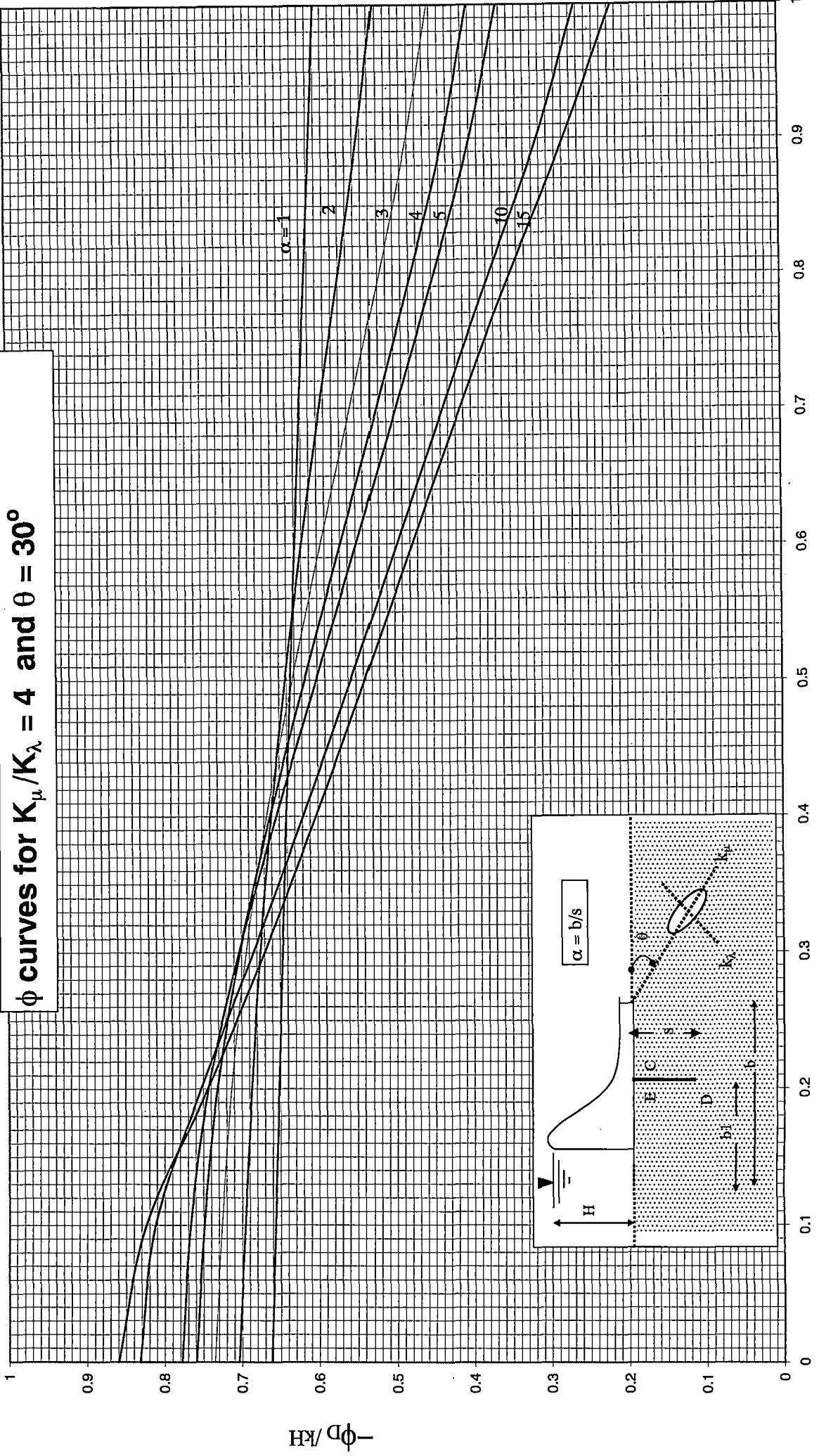
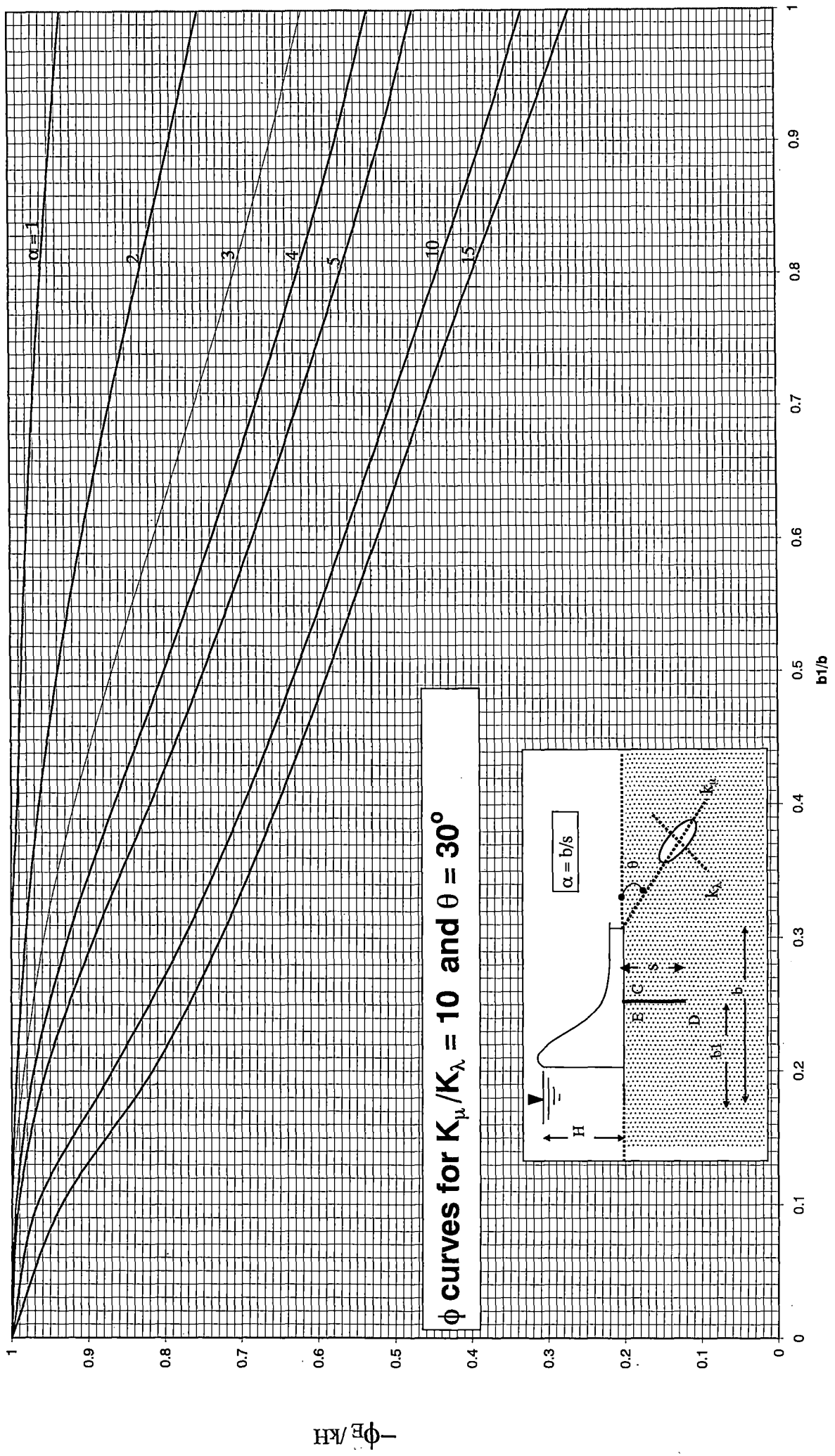


Fig.3.2(c2.2)



ϕ curves for $K_\mu/K_\lambda = 4$ and $\theta = 30^\circ$

Fig.3.2(c2.3)



ϕ curves for $K_\mu/K_\lambda = 10$ and $\theta = 30^\circ$

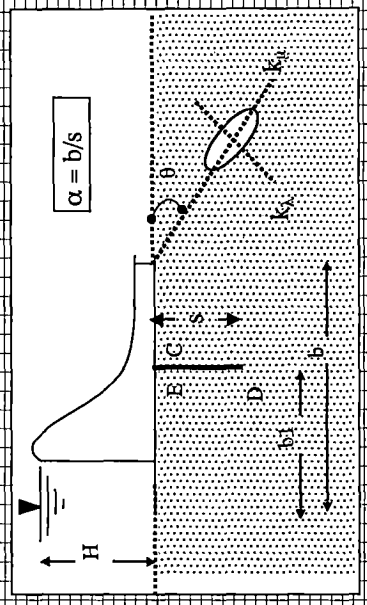


Fig.3.2(c3.2)

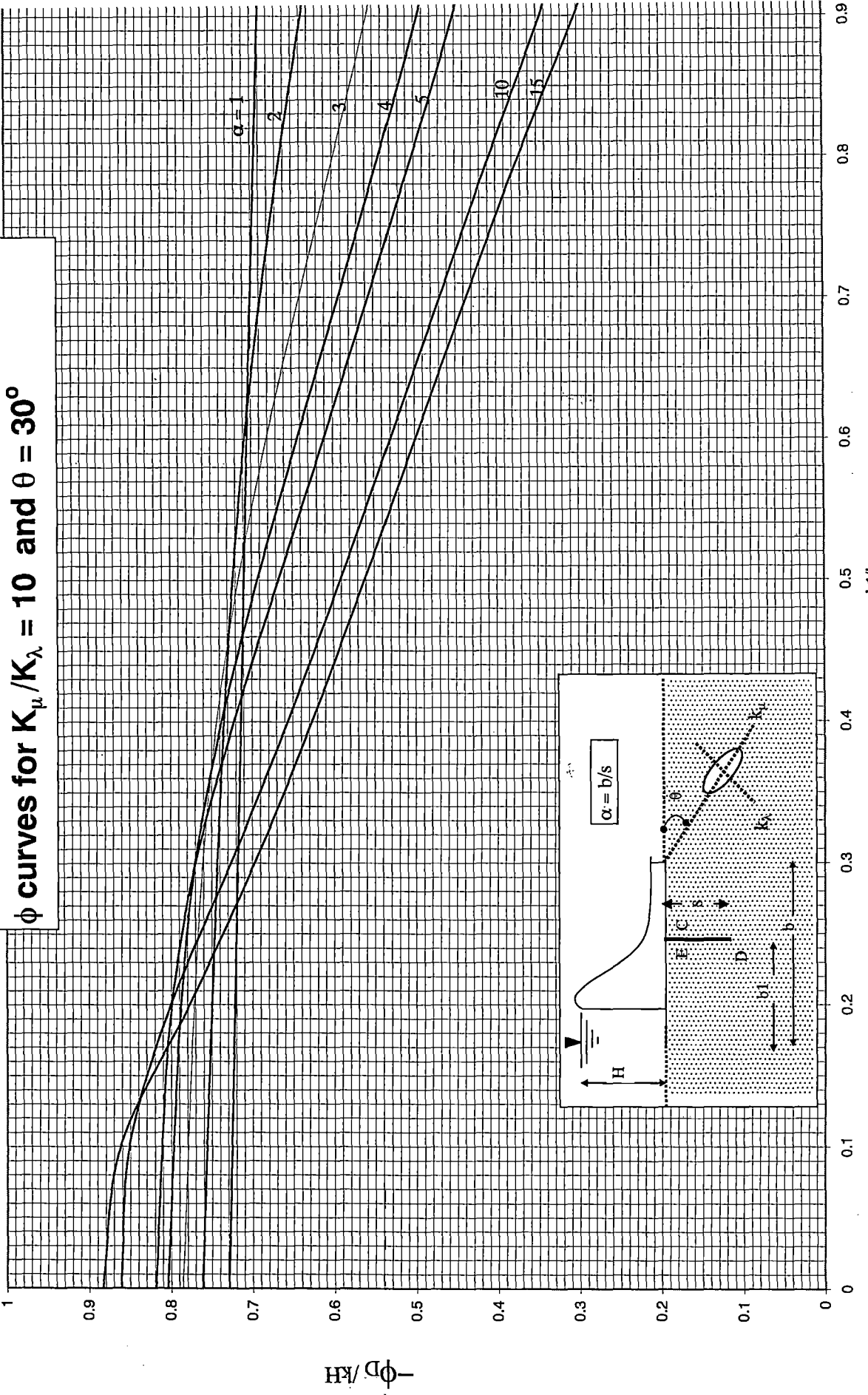


Fig.3.2(c3.3)

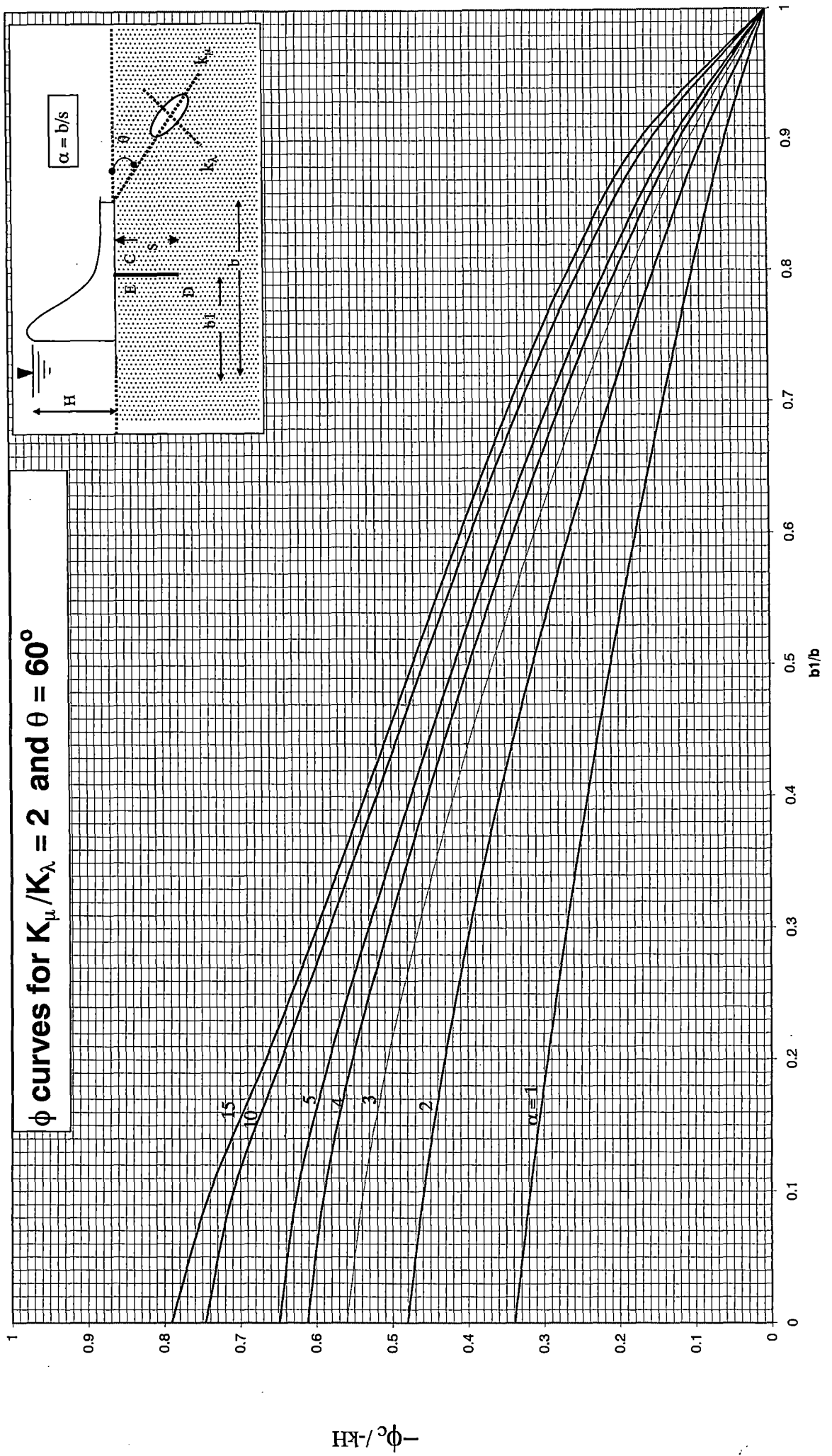


Fig.3.2(d1.1)

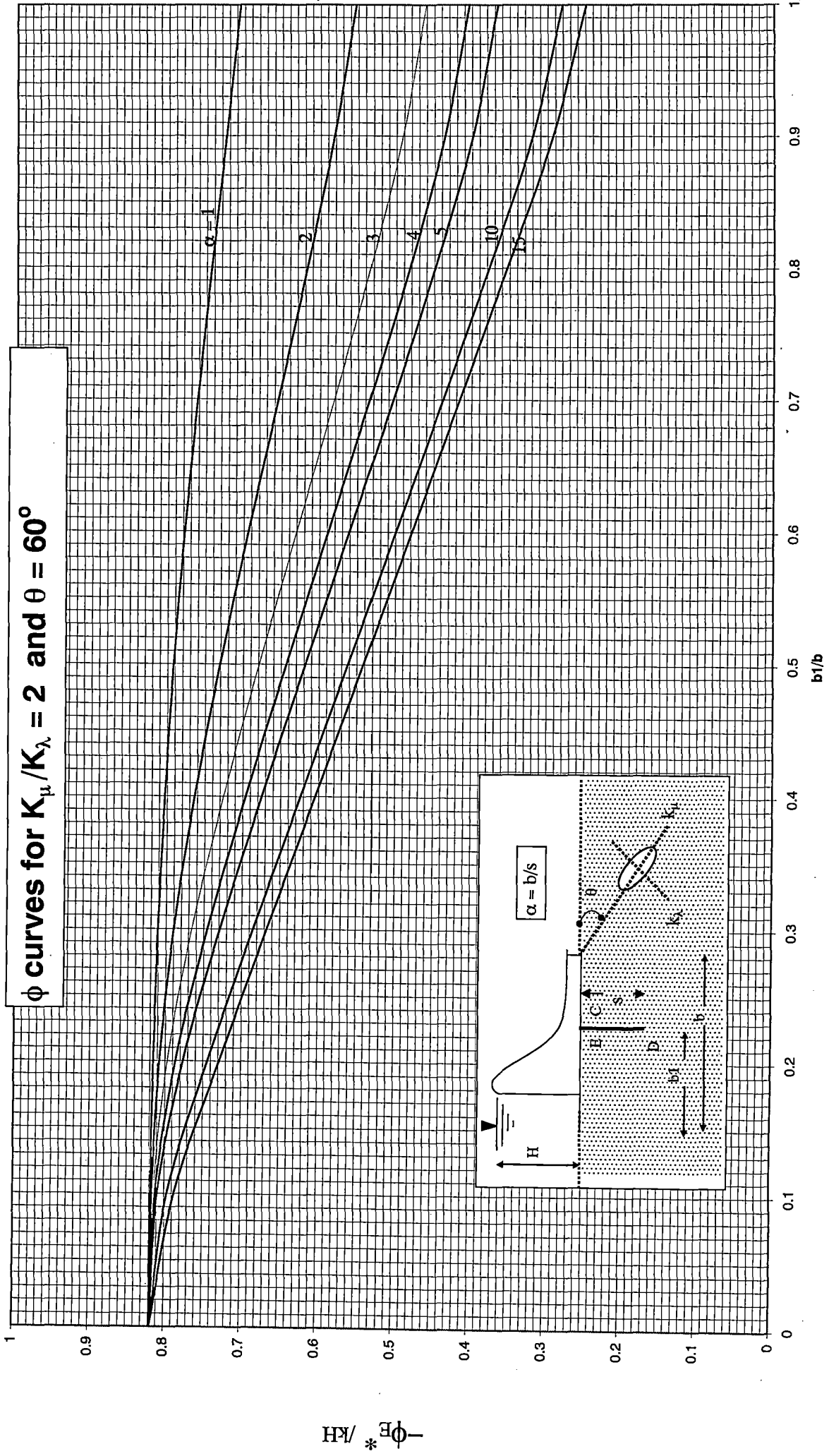
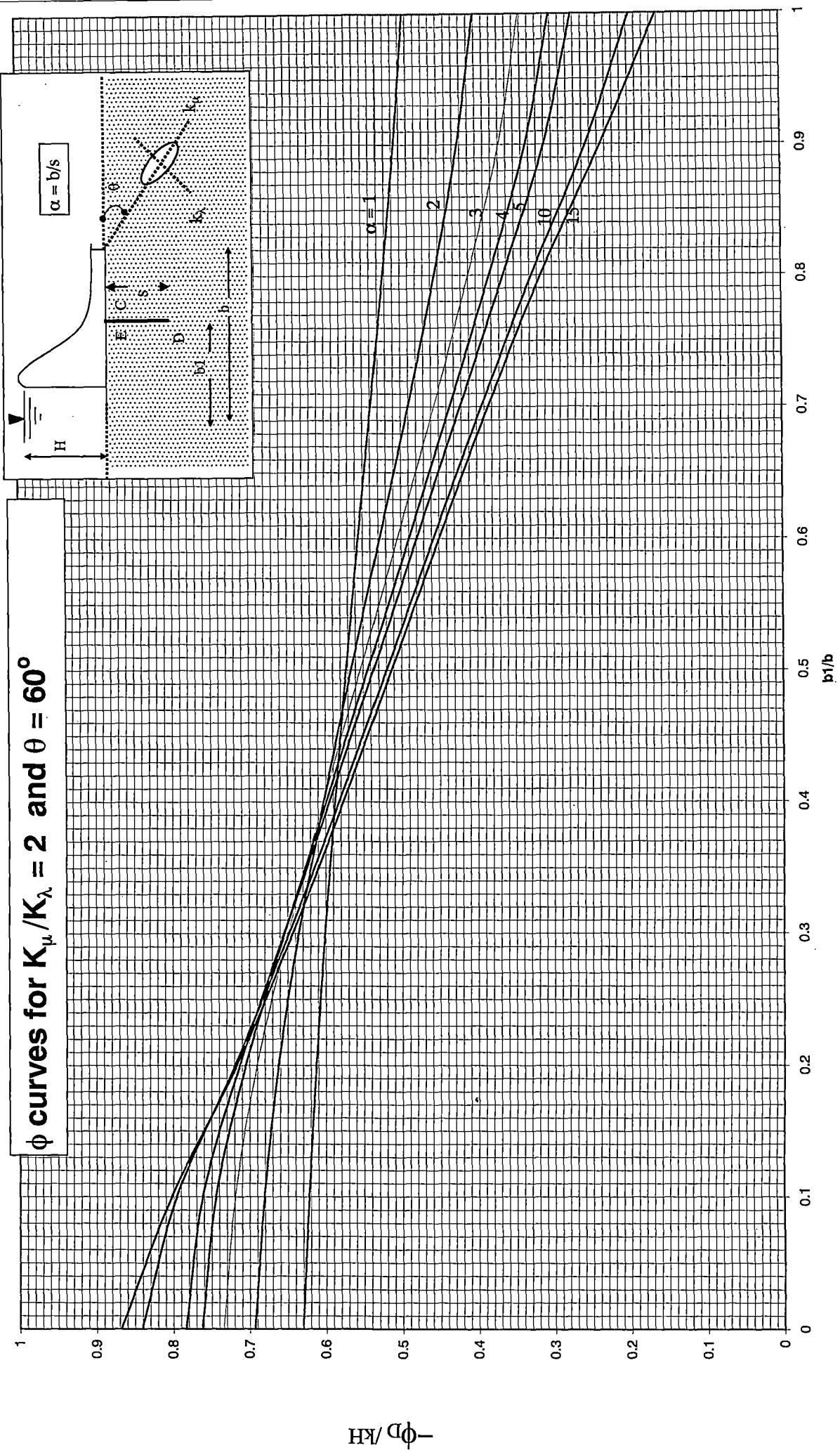


Fig.3.2(d1.2)



ϕ curves for $K_\mu/K_\lambda = 2$ and $\theta = 60^\circ$

Fig.3.2(d1.3)

ϕ curves for $K_\mu/K_\lambda = 4$ and $\theta = 60^\circ$

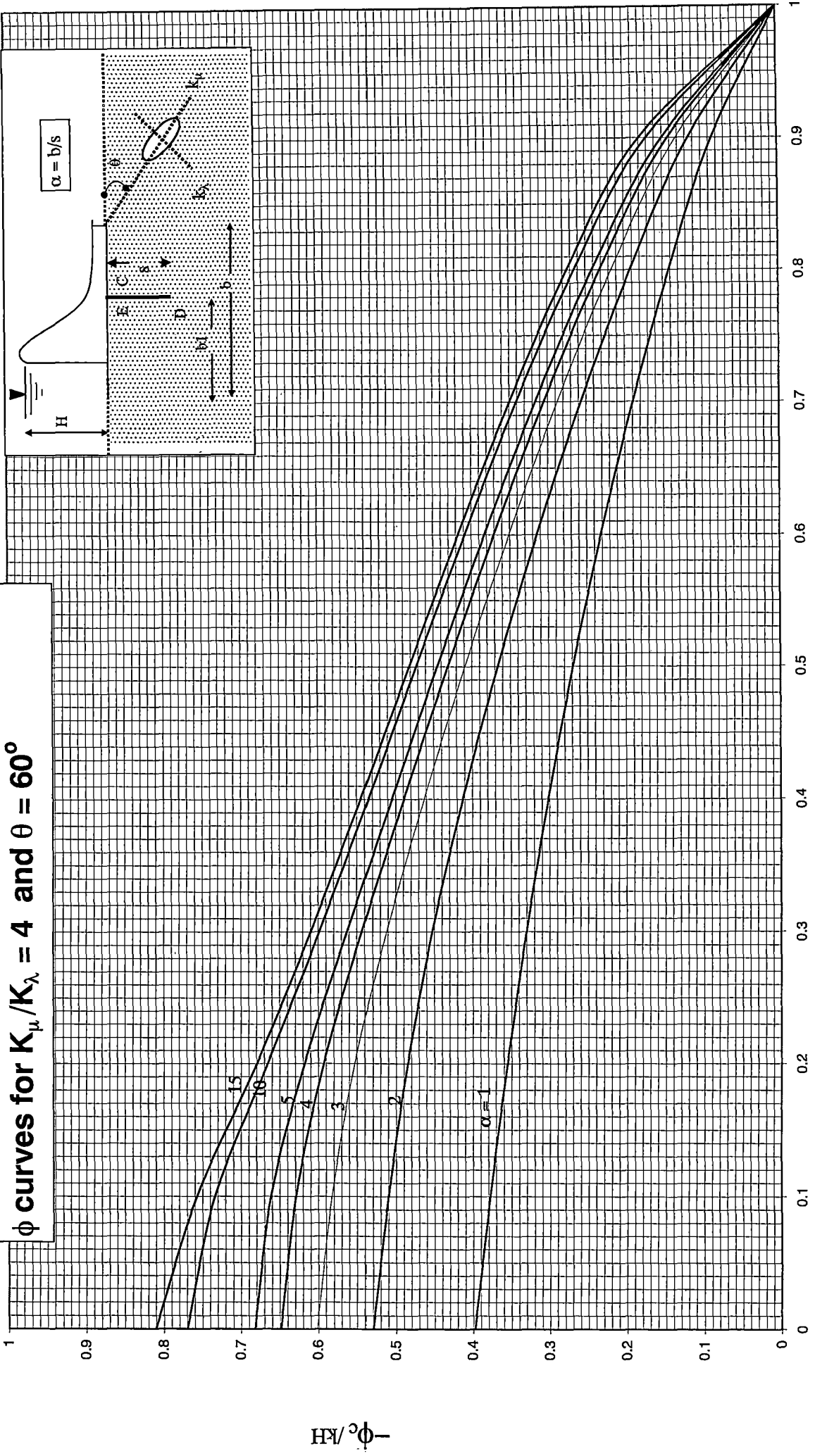


Fig.3.2(d2.1)

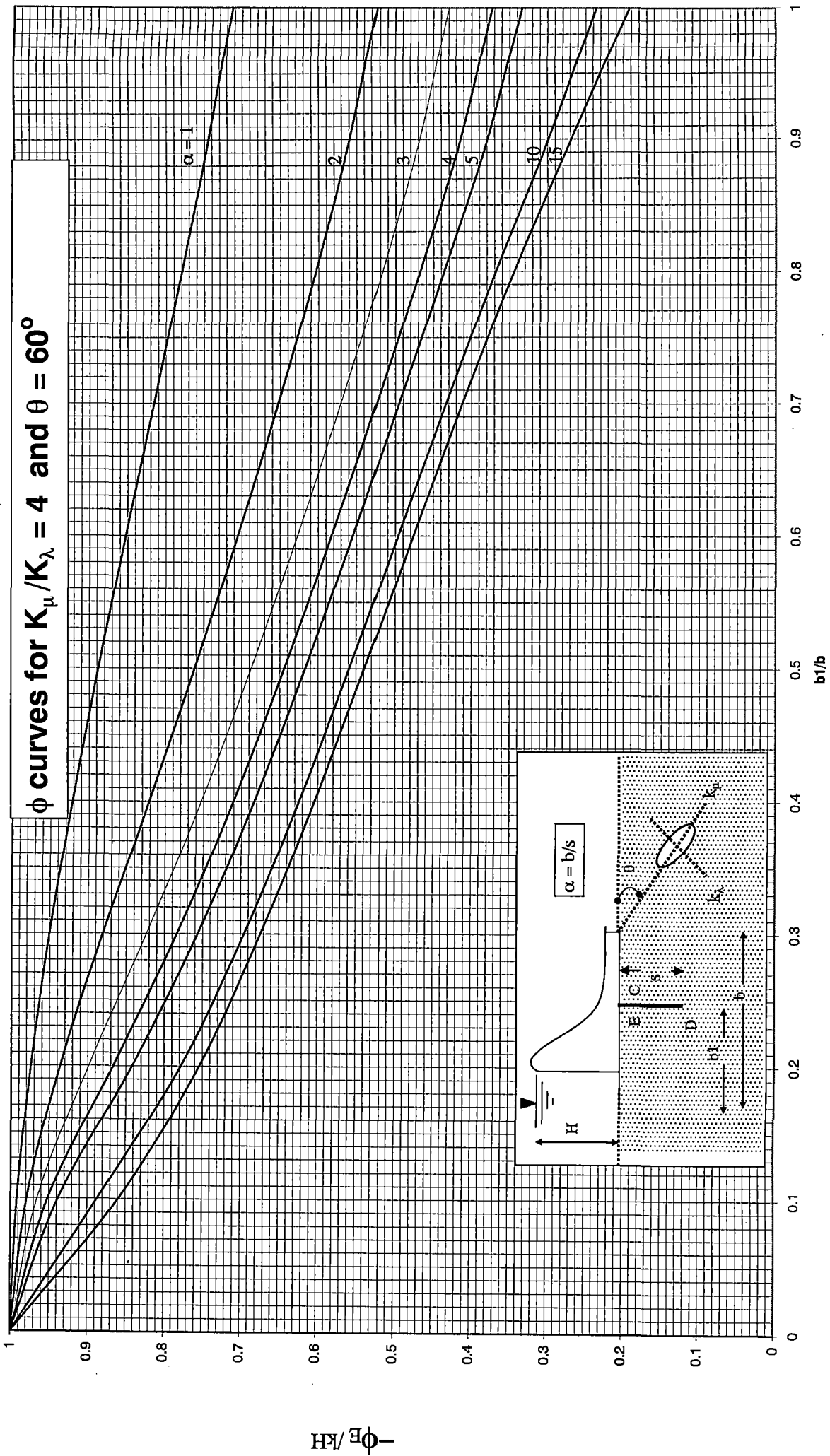


Fig.3.2(d2.2)

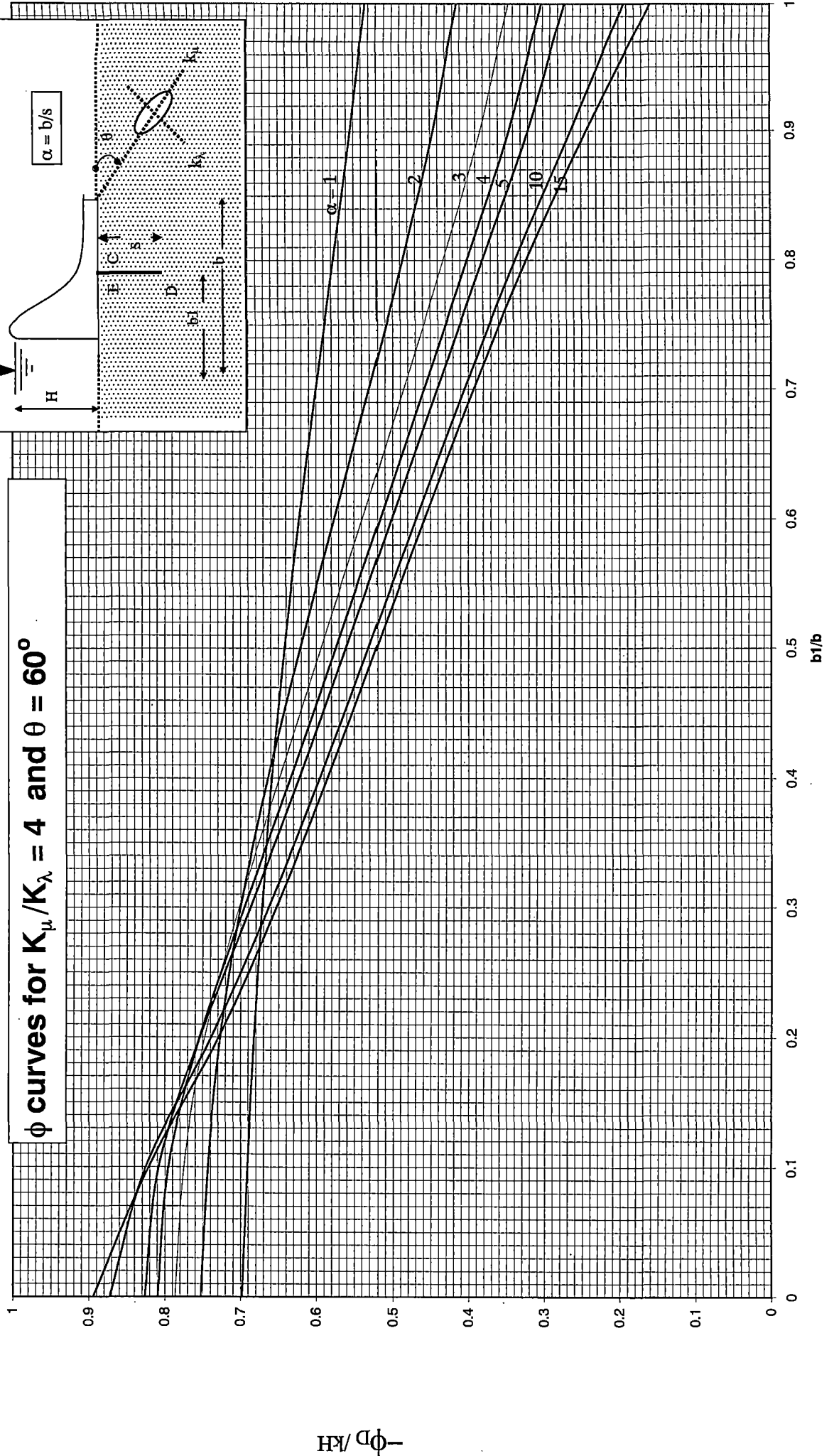


Fig.3.2(d2.3)

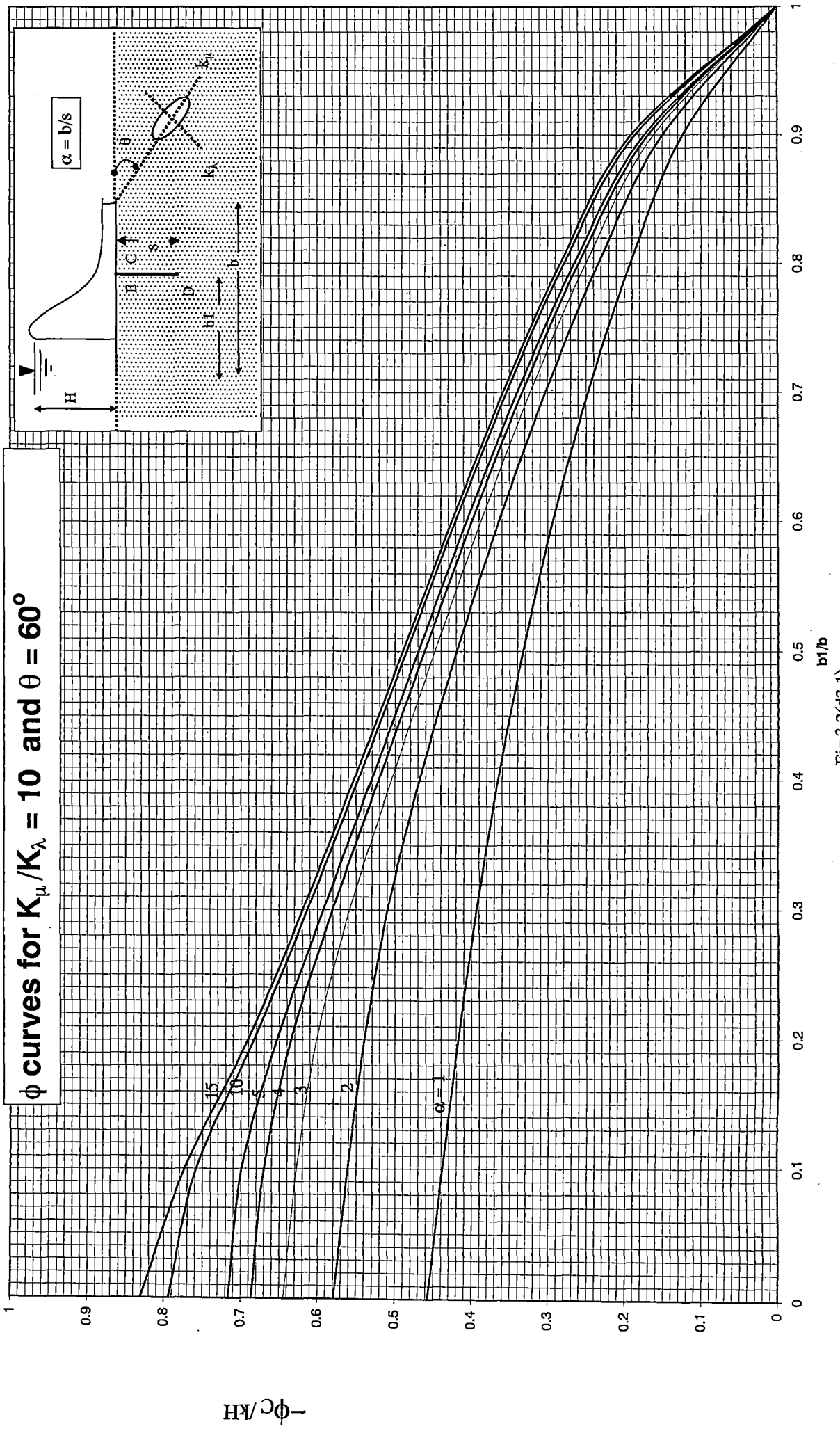


Fig.3.2(d3.1)

ϕ curves for $K_{\mu}/K_{\lambda} = 10$ and $\theta = 60^{\circ}$

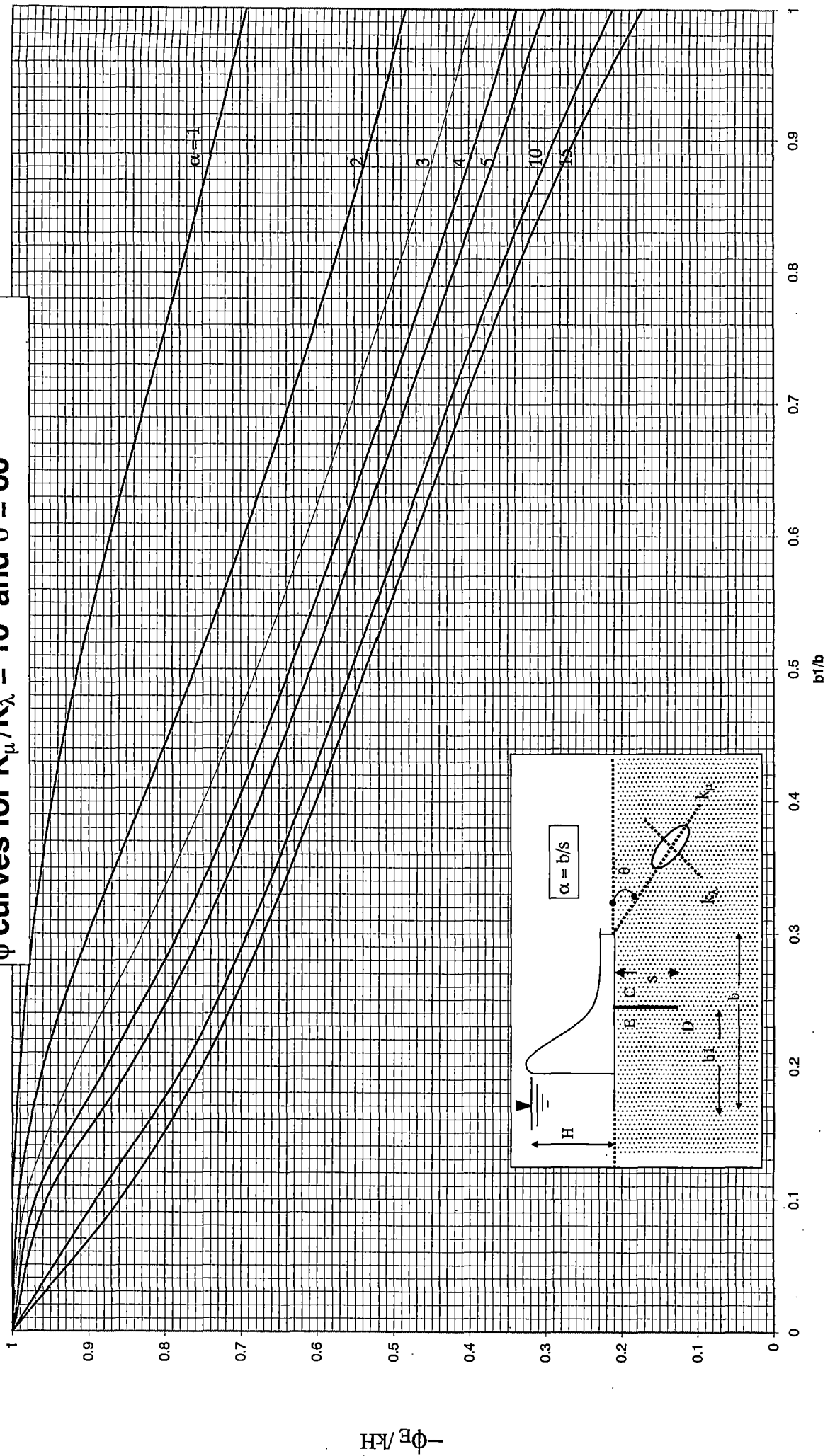


Fig.3.2(d3.2)

ϕ curves for $K_{\mu}/K_{\lambda} = 10$ and $\theta = 60^{\circ}$

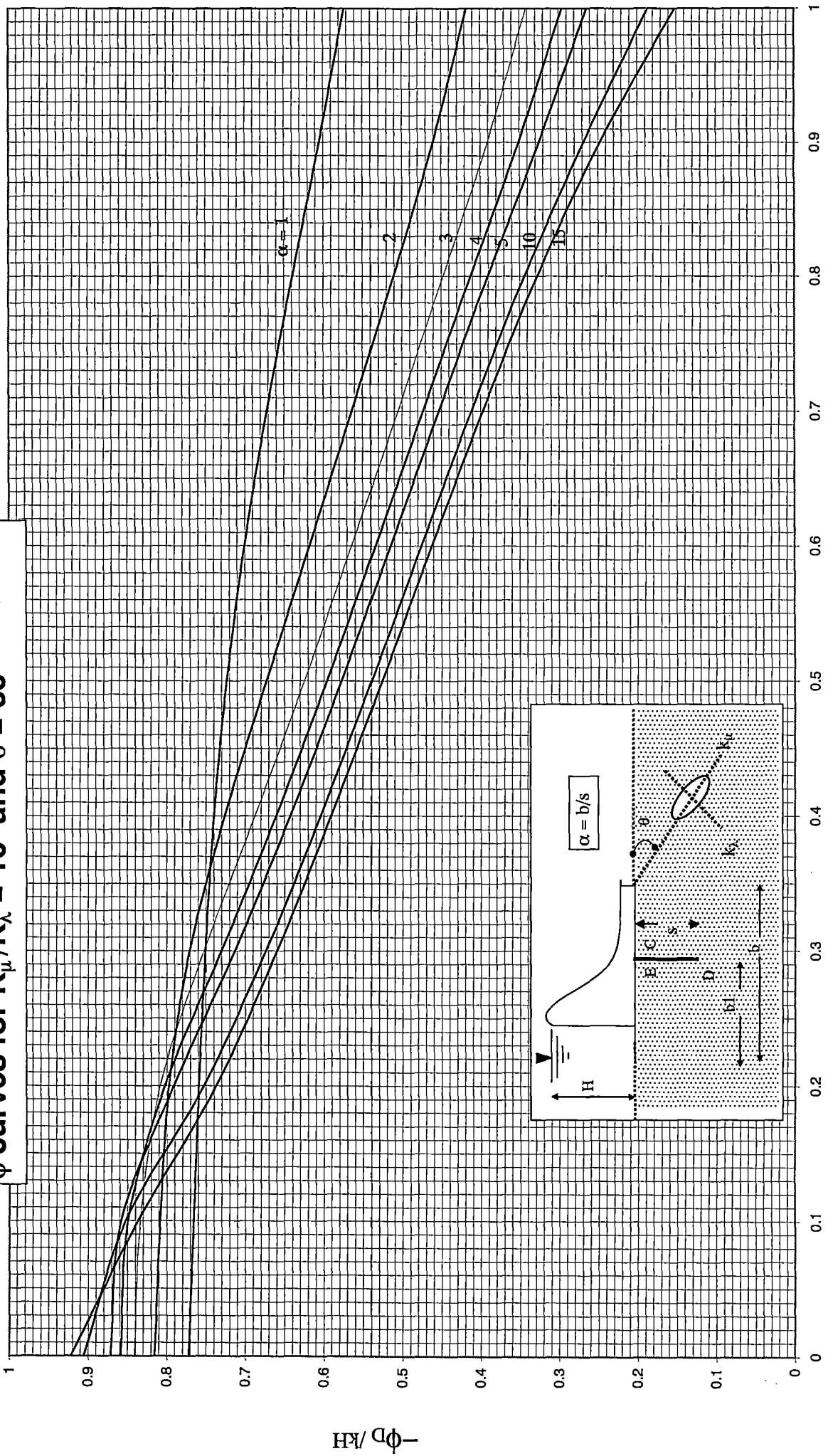


Fig.3.2(d3.3)

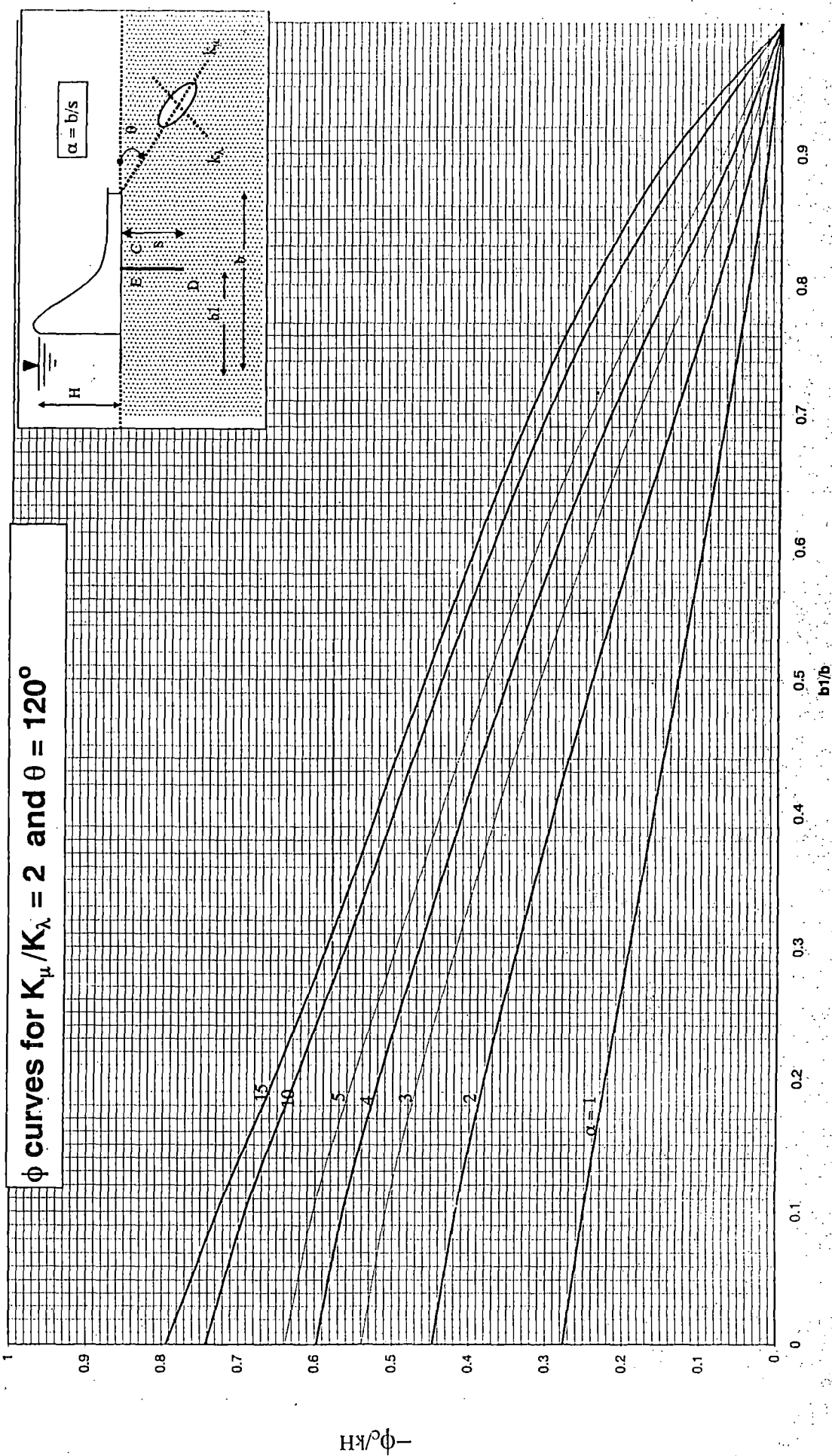


Fig.3.2(c1.1)

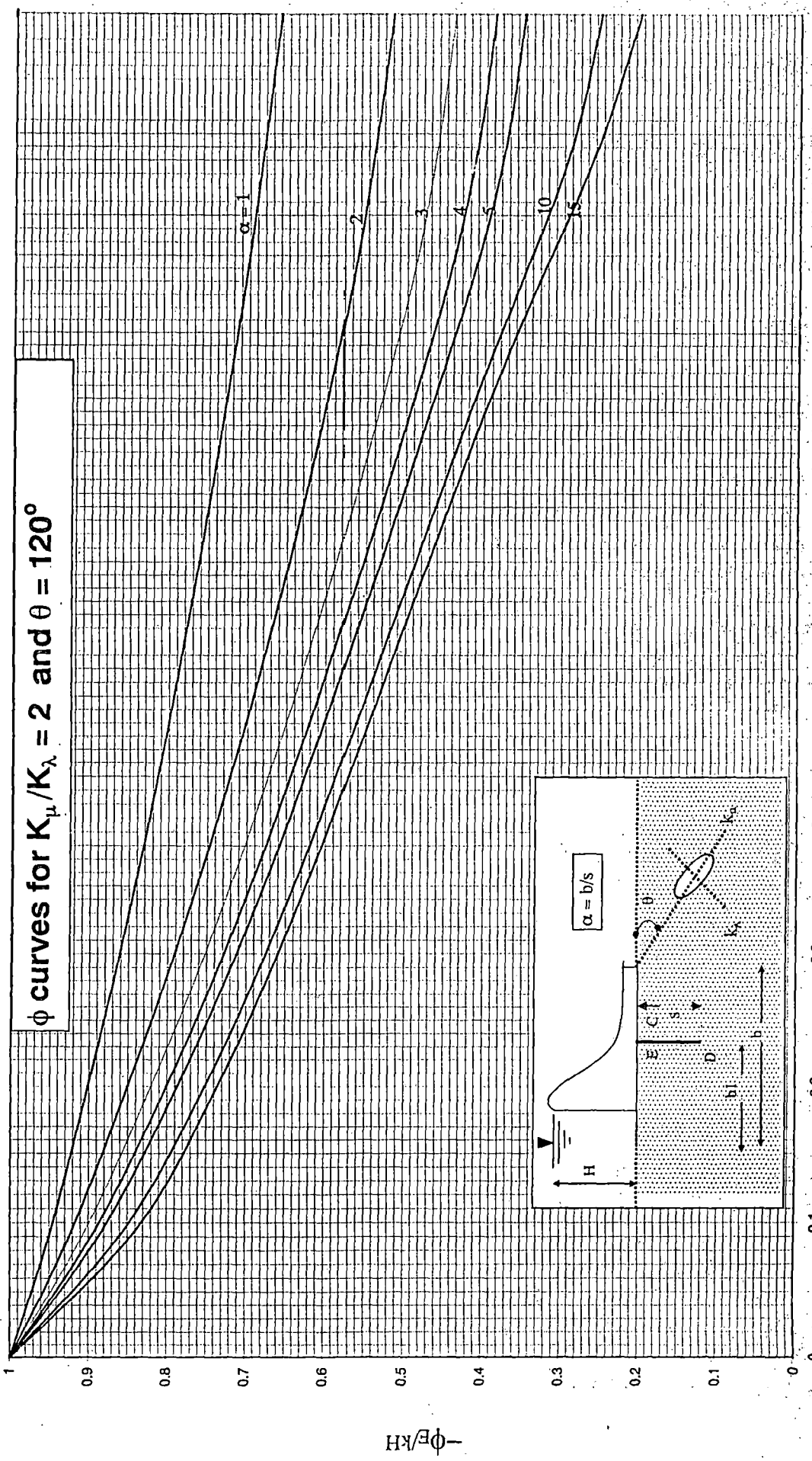


Fig.3.2(e1.2)

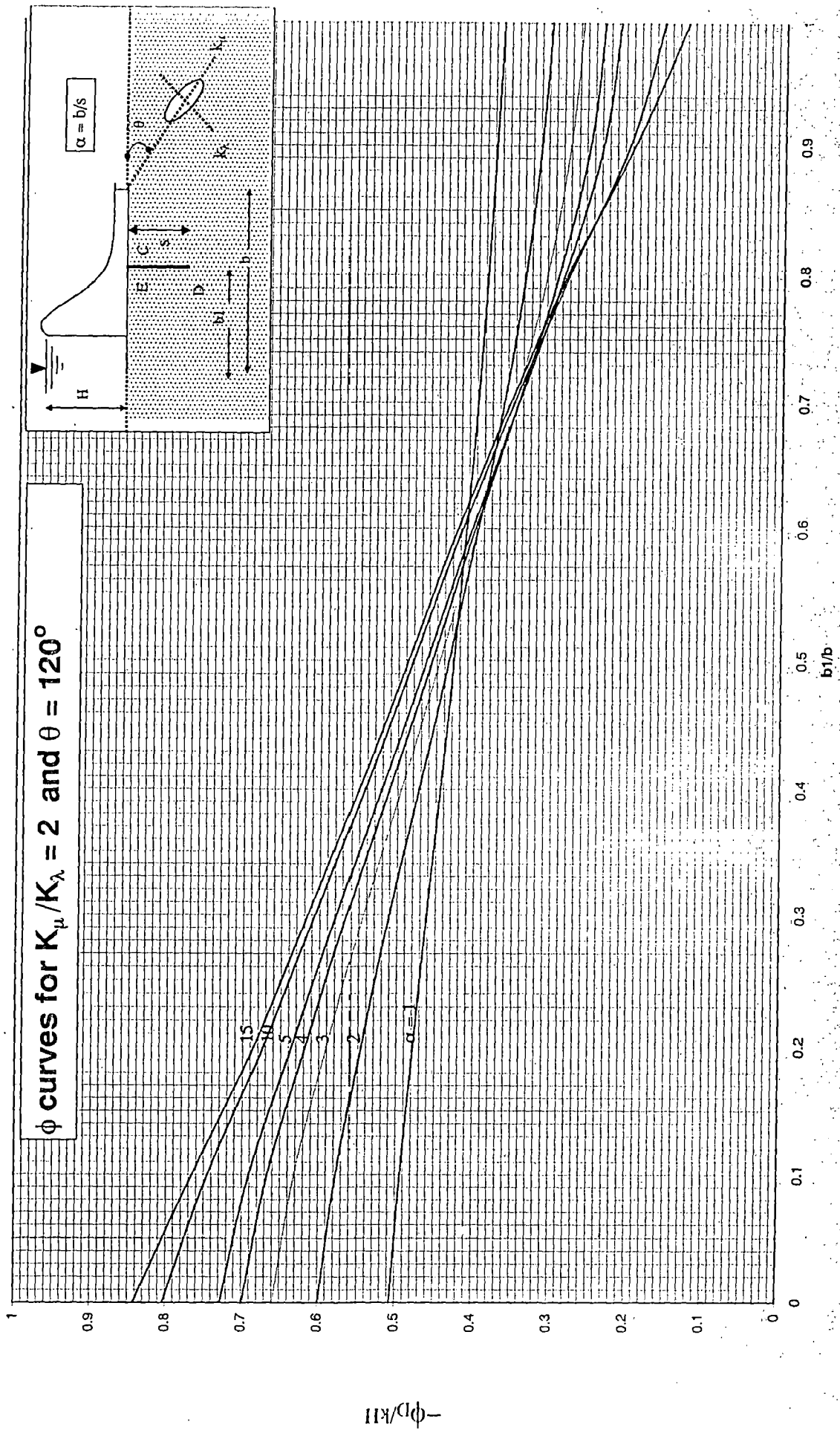


Fig.3.2(e1.3)

ϕ curves for $K_H/K_x = 4$ and $\theta = 120^\circ$

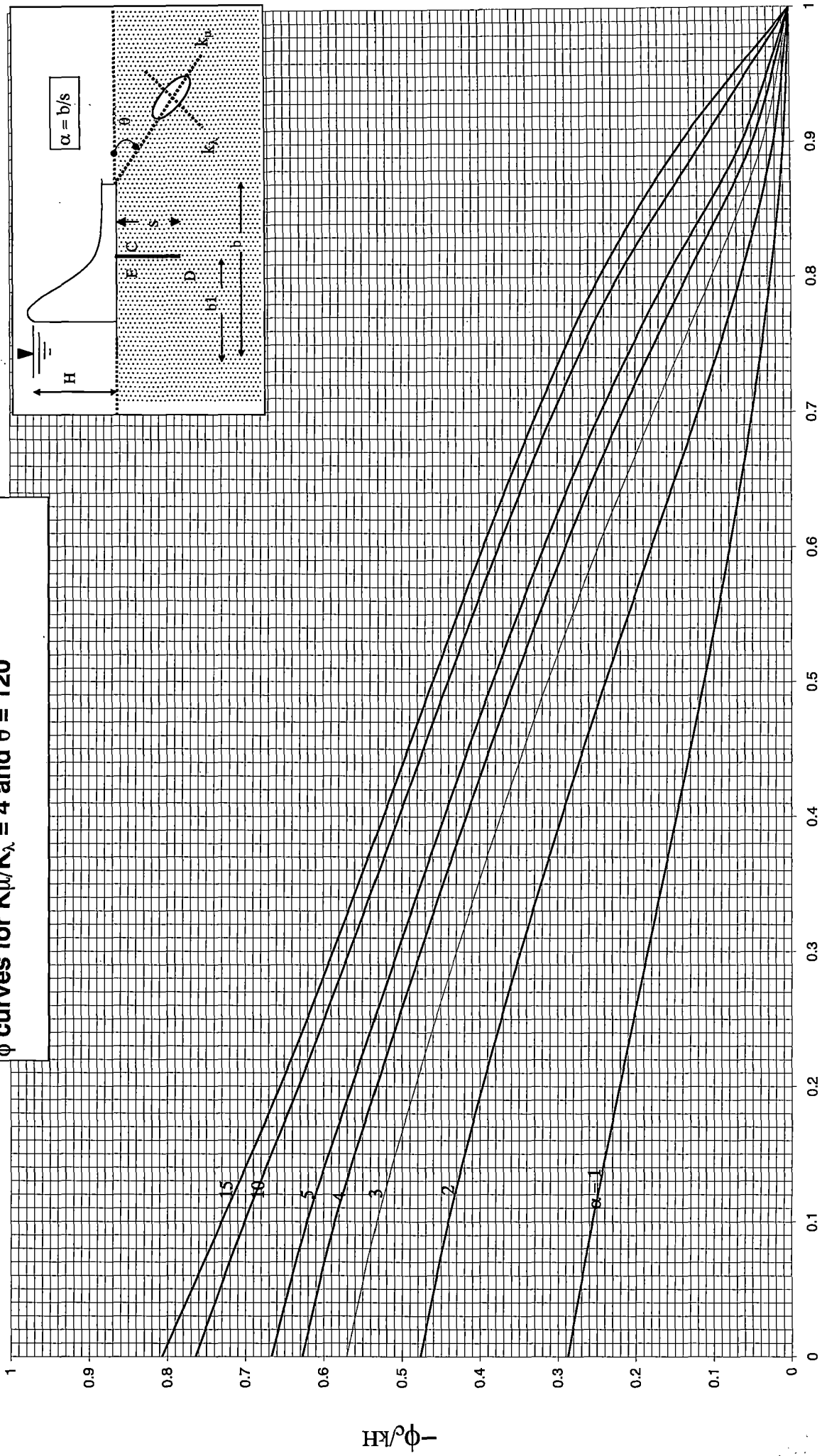


Fig.3.2(e2.1)

ϕ curves for $K_{\mu}/K_{\lambda} = 4$ and $\theta = 120^{\circ}$

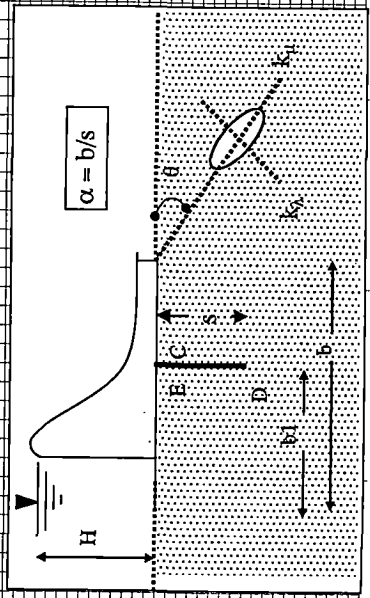
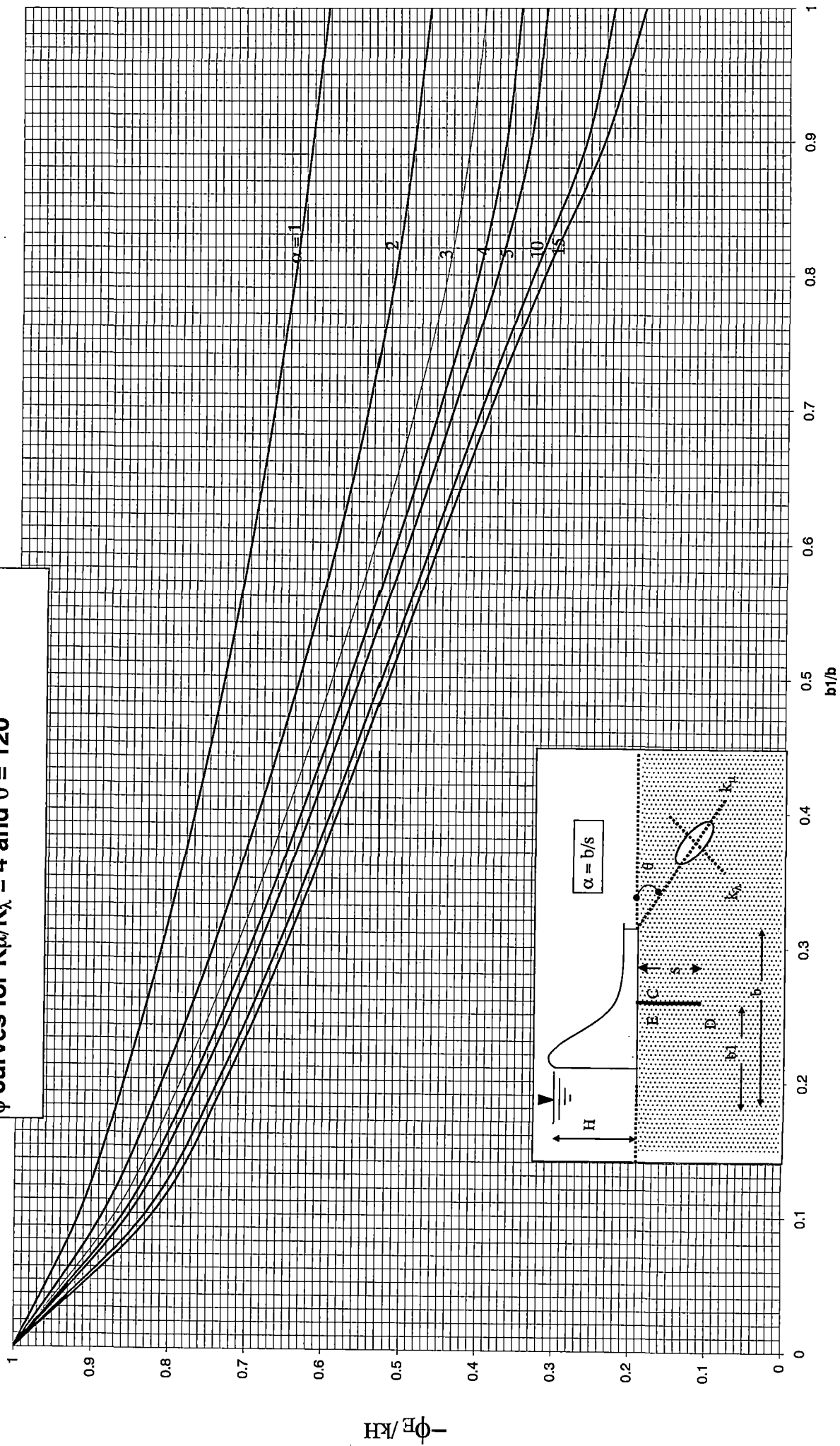


Fig.3.2(e2.2)

ϕ curves for $K_{\mu}/K_{\lambda} = 4$ and $\theta = 120^{\circ}$

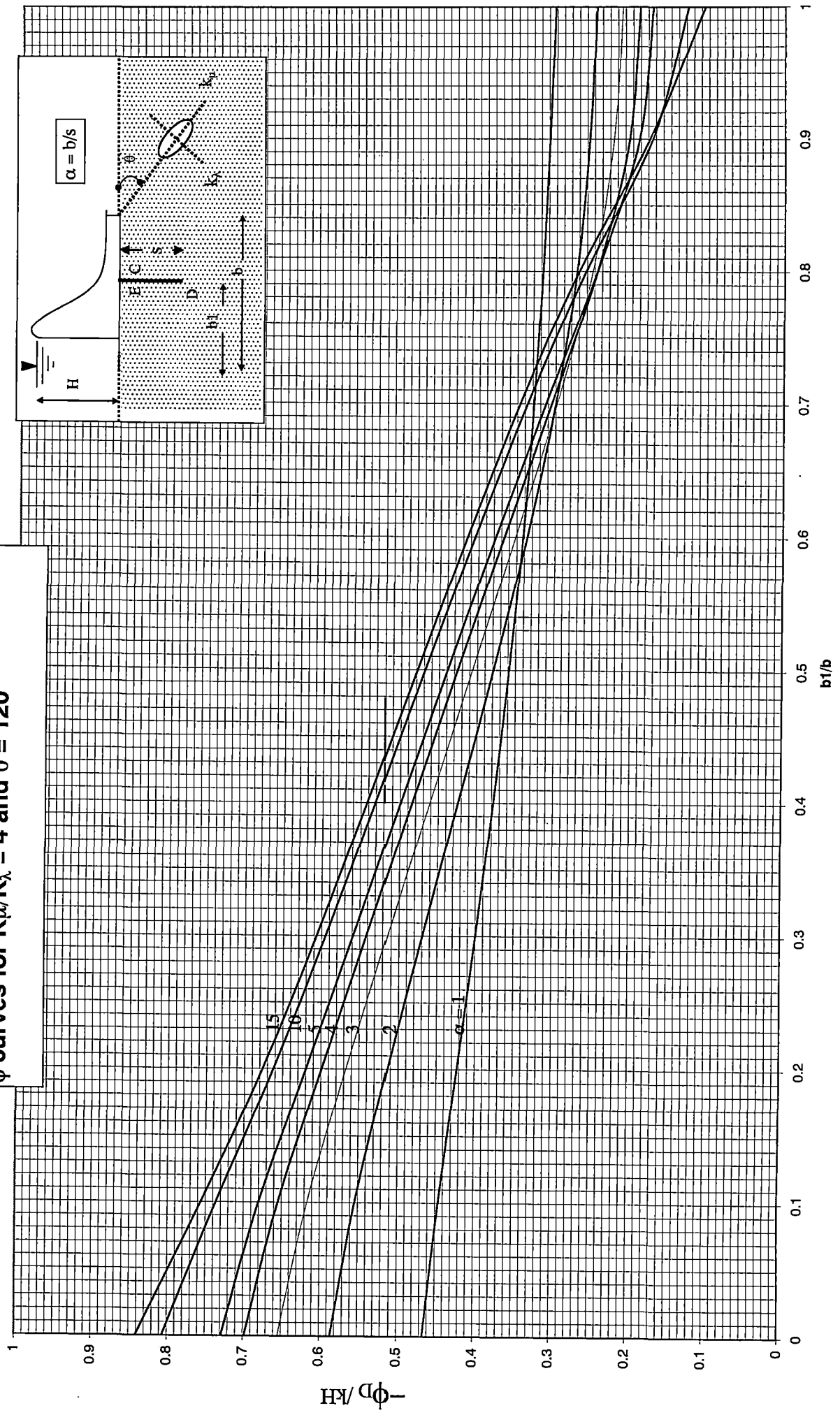


Fig.3.2(e2.3)

ϕ curves for $K_{\mu}/K_{\lambda} = 10$ and $\theta = 120^{\circ}$

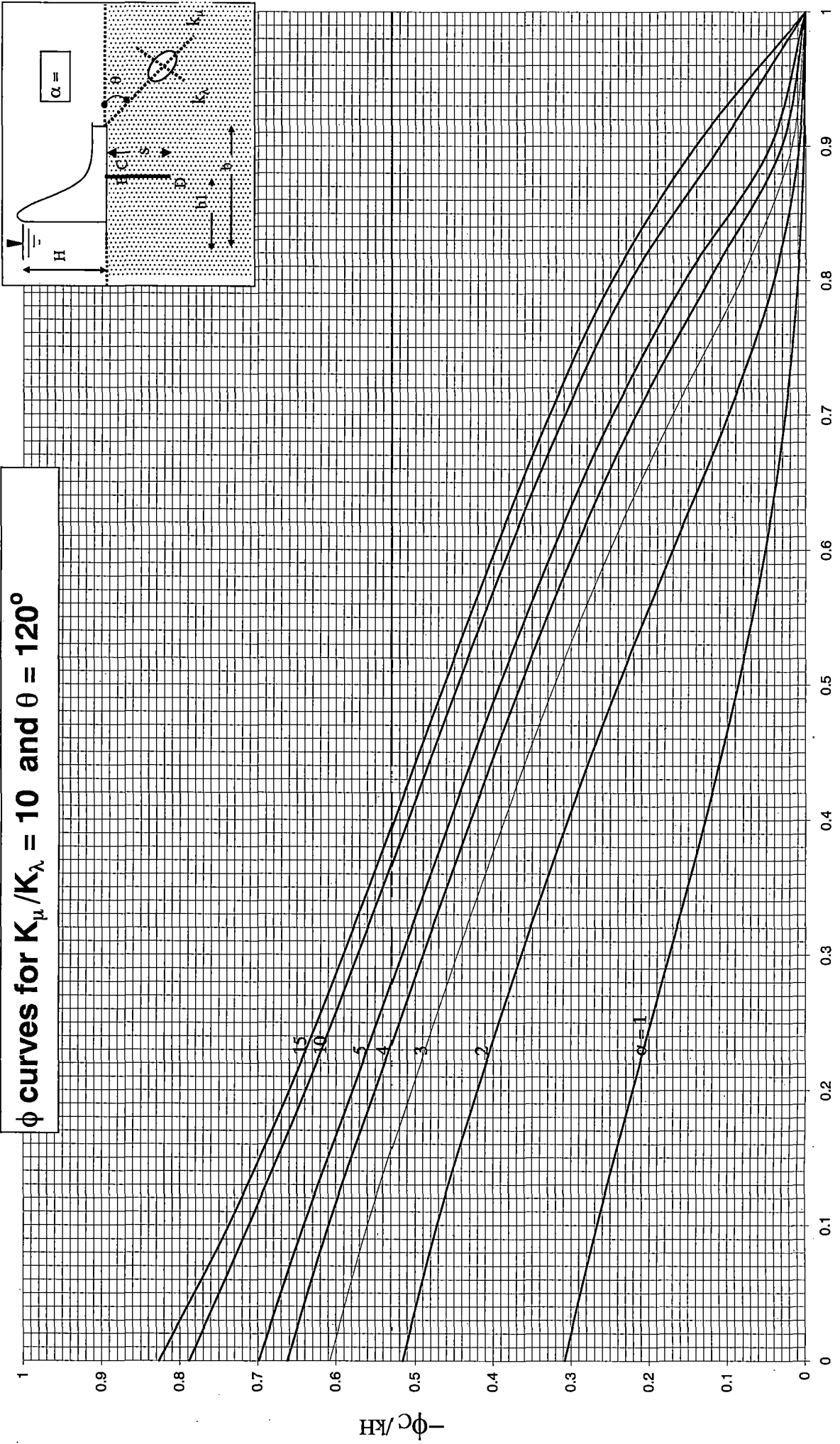


Fig.3.2(e3.1)

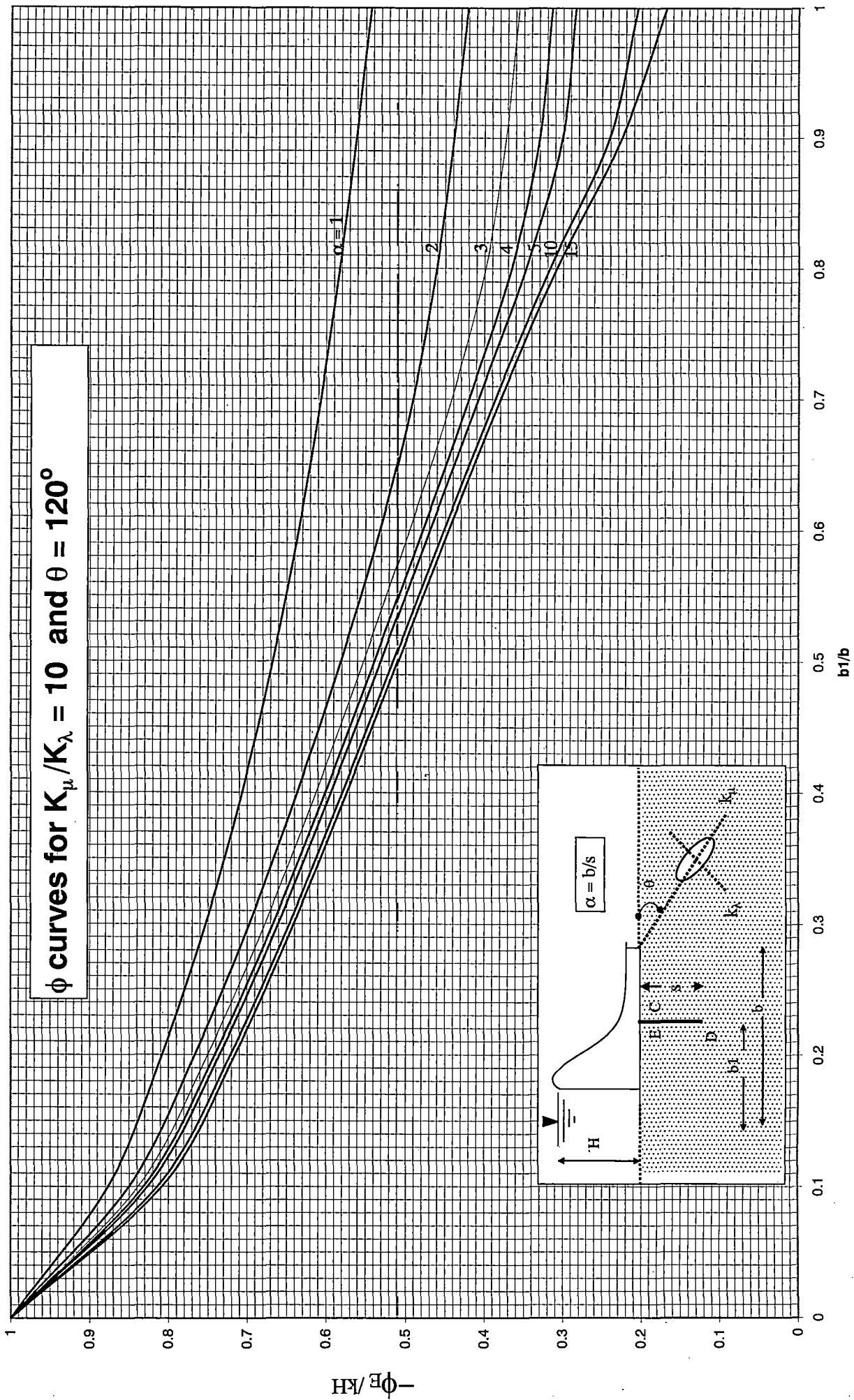


Fig.3.2(e3.2)

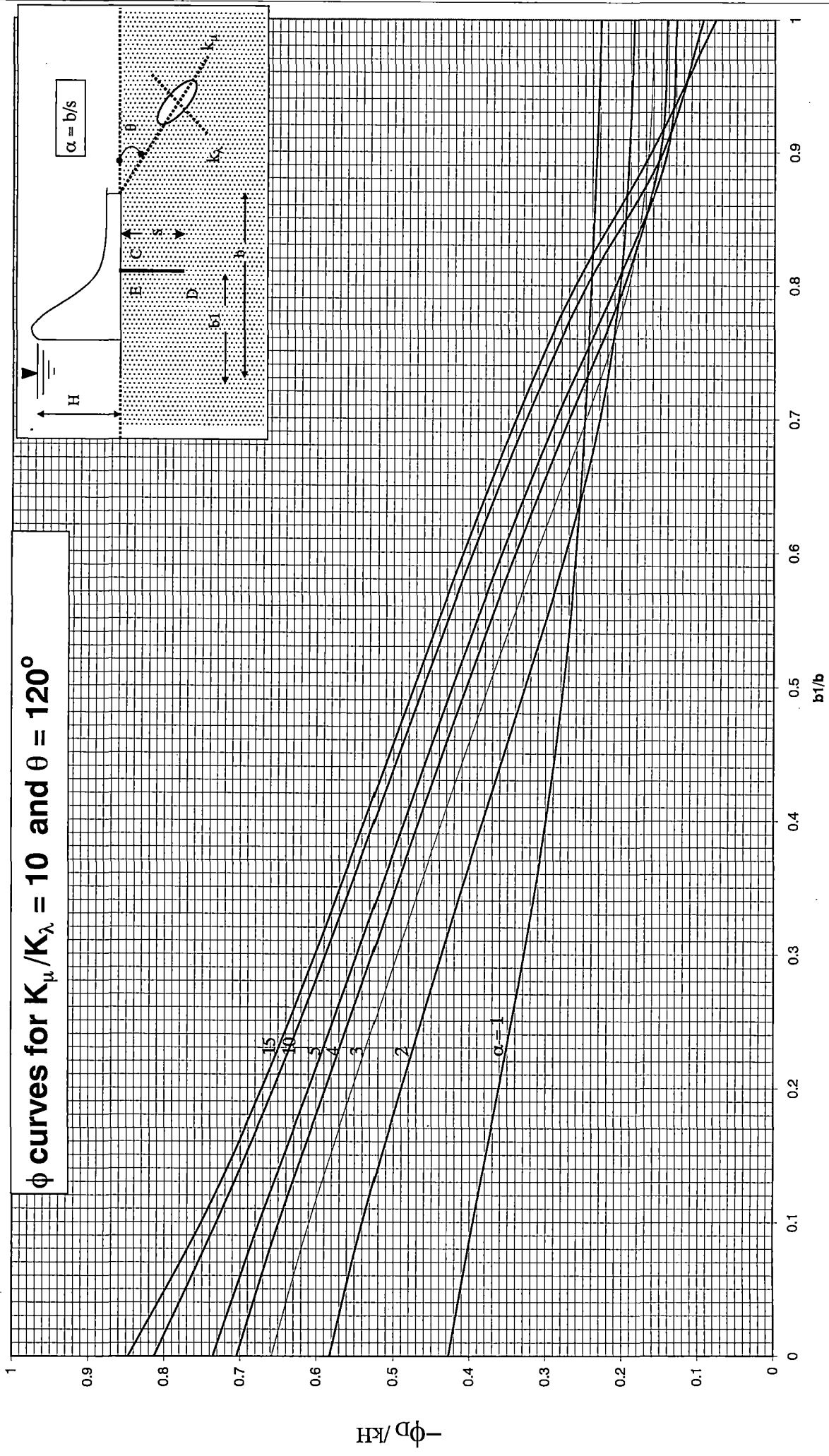


Fig.3.2(e3.3)

ϕ curves for $K_\mu/K_\lambda = 2$ and $\theta = 150^\circ$

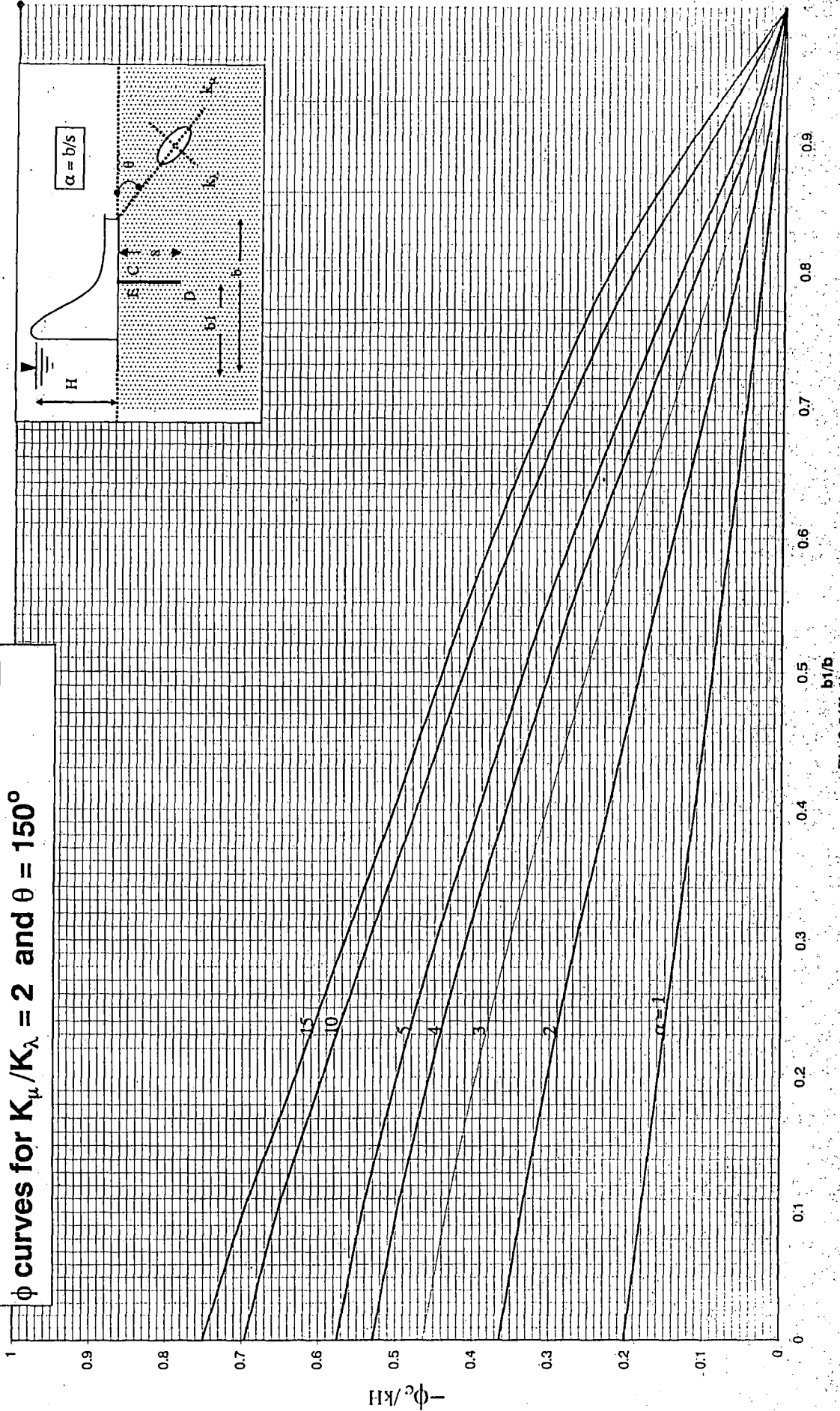


Fig.3.2(f1.1)

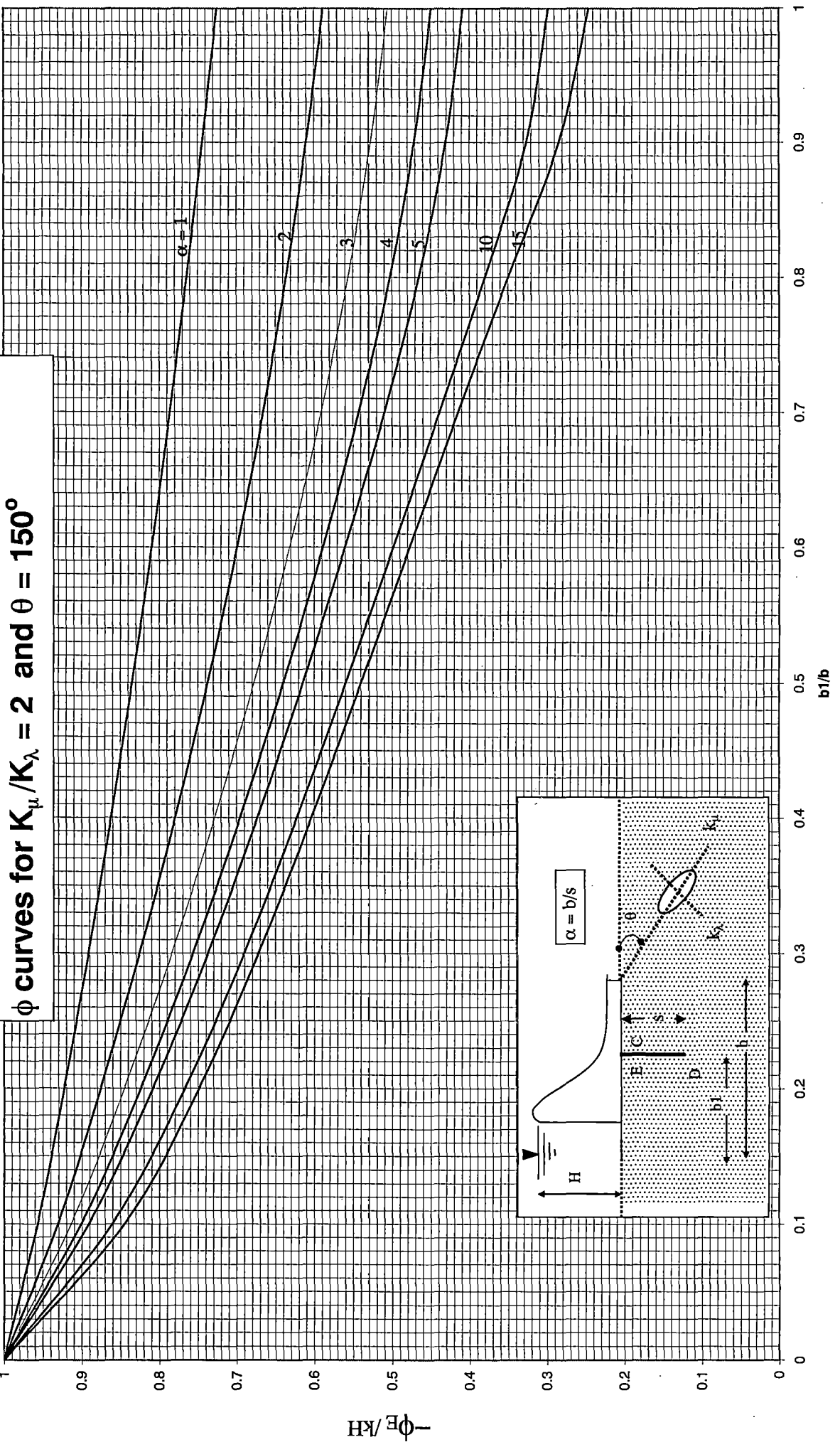


Fig.3.2(f1.2)

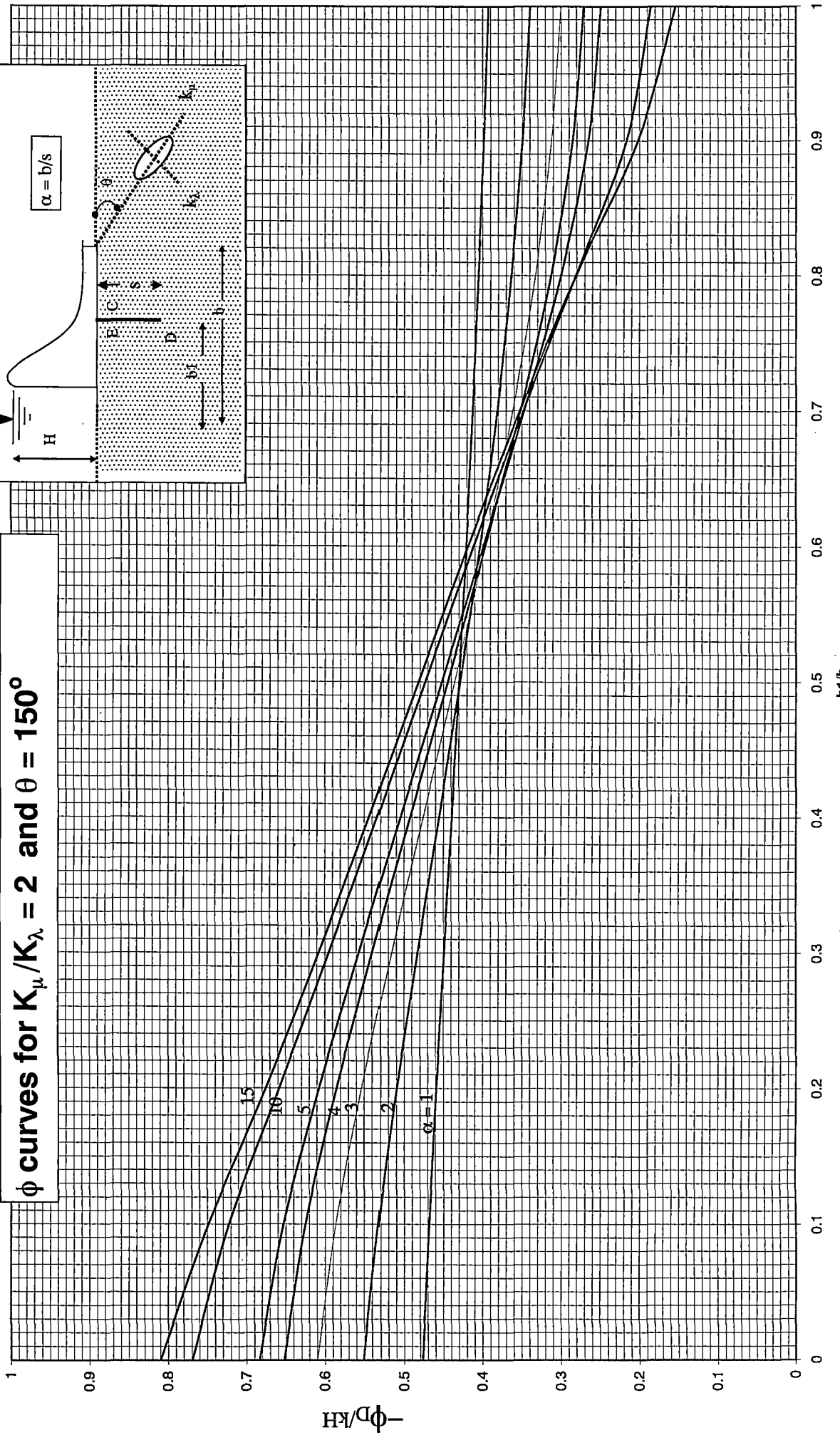
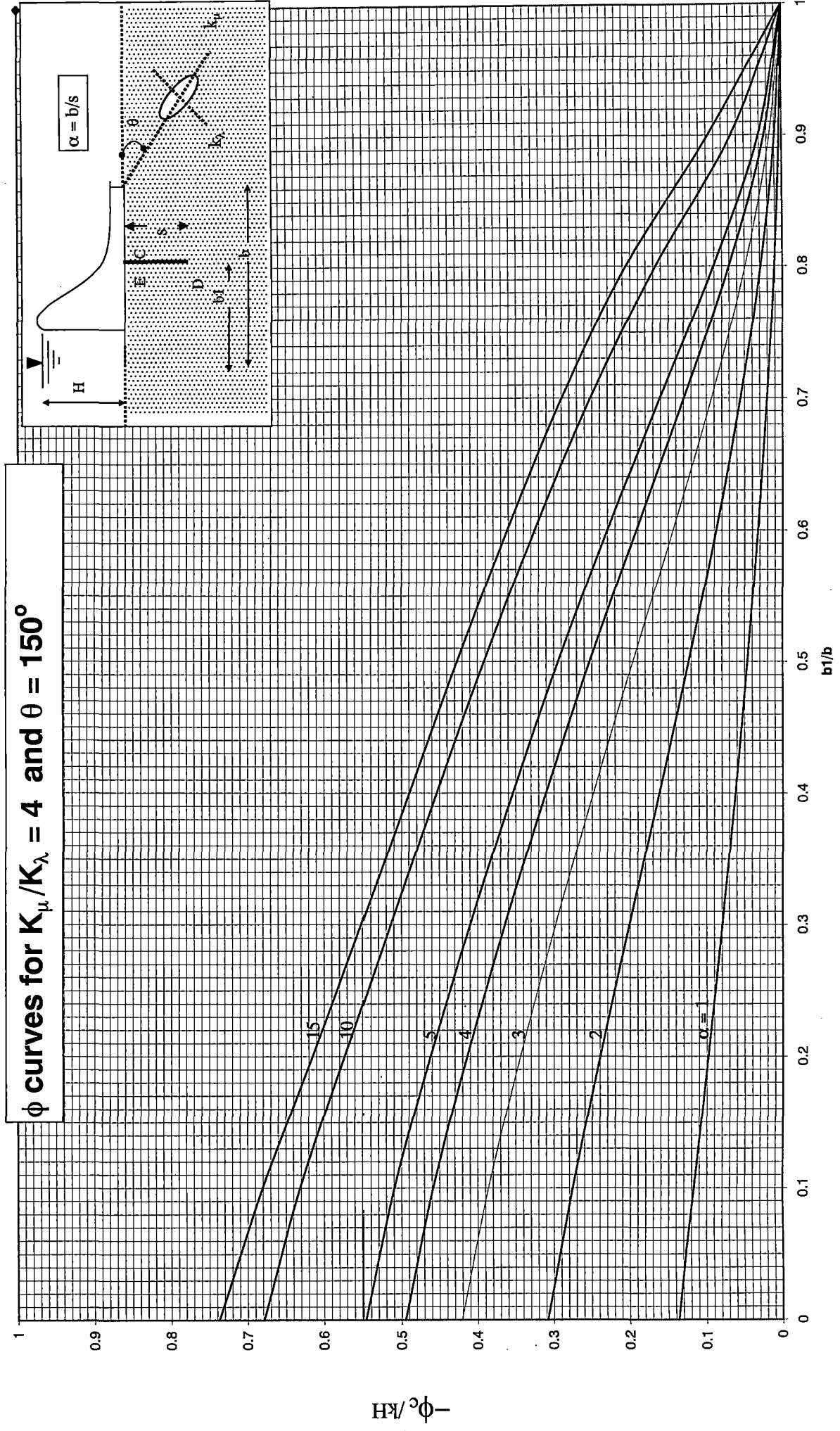


Fig.3.2(f1.3)



ϕ curves for $K_u/K_\lambda = 4$ and $\theta = 150^\circ$

Fig.3.2(f2.1)

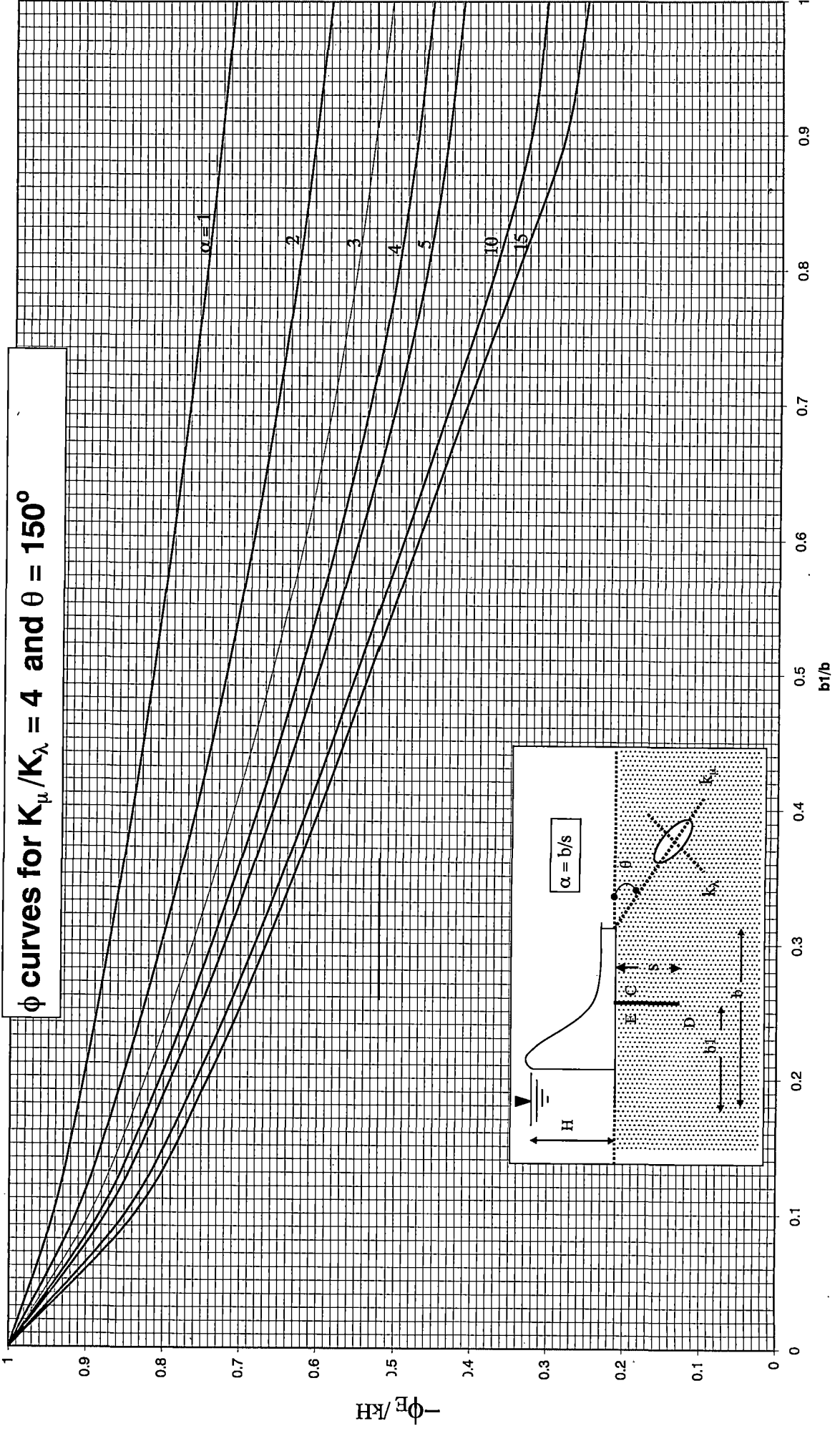


Fig.3.2((2.2))

ϕ curves for $K_{\mu}/K_{\lambda} = 4$ and $\theta = 150^{\circ}$

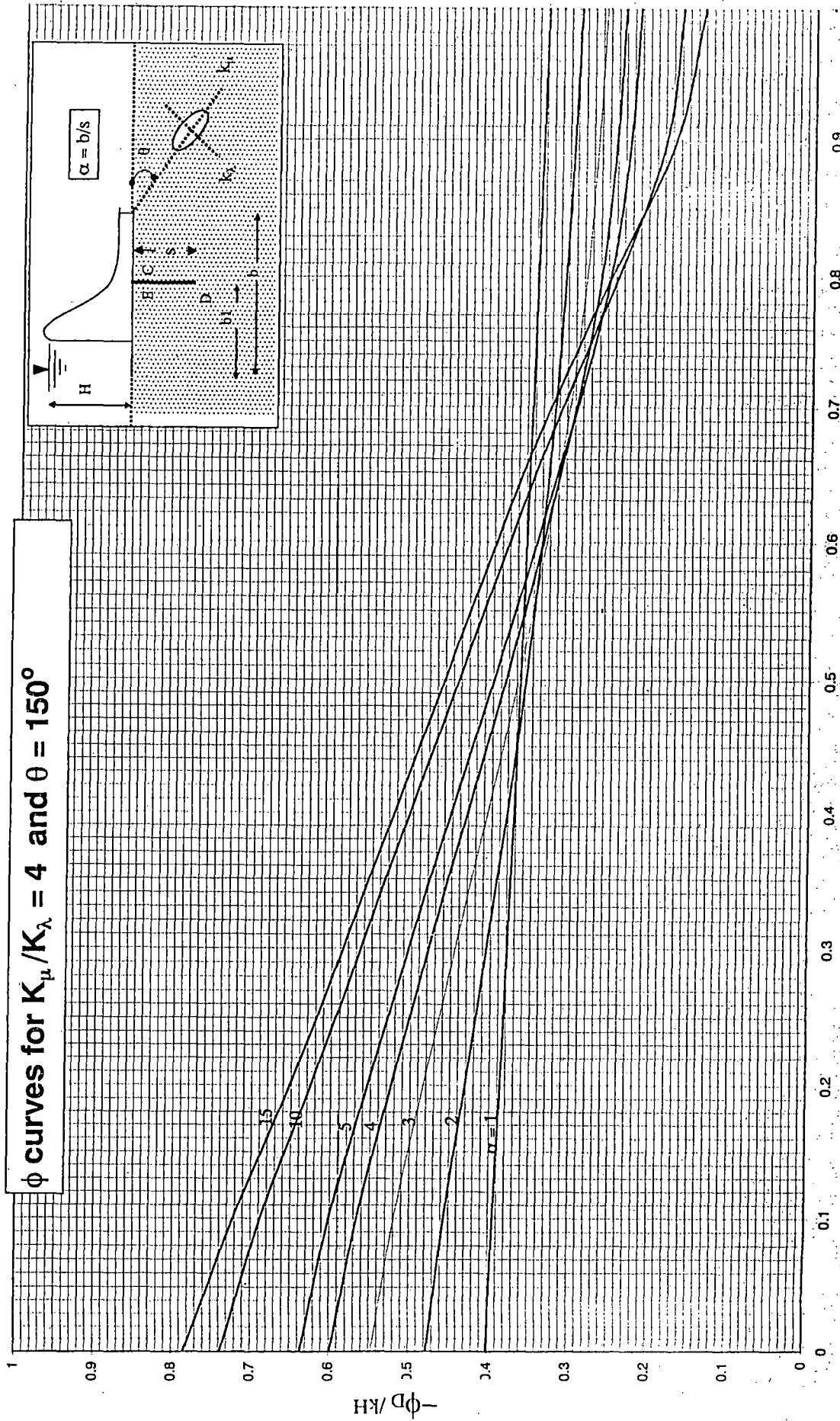


Fig. 3.2(f2.3)

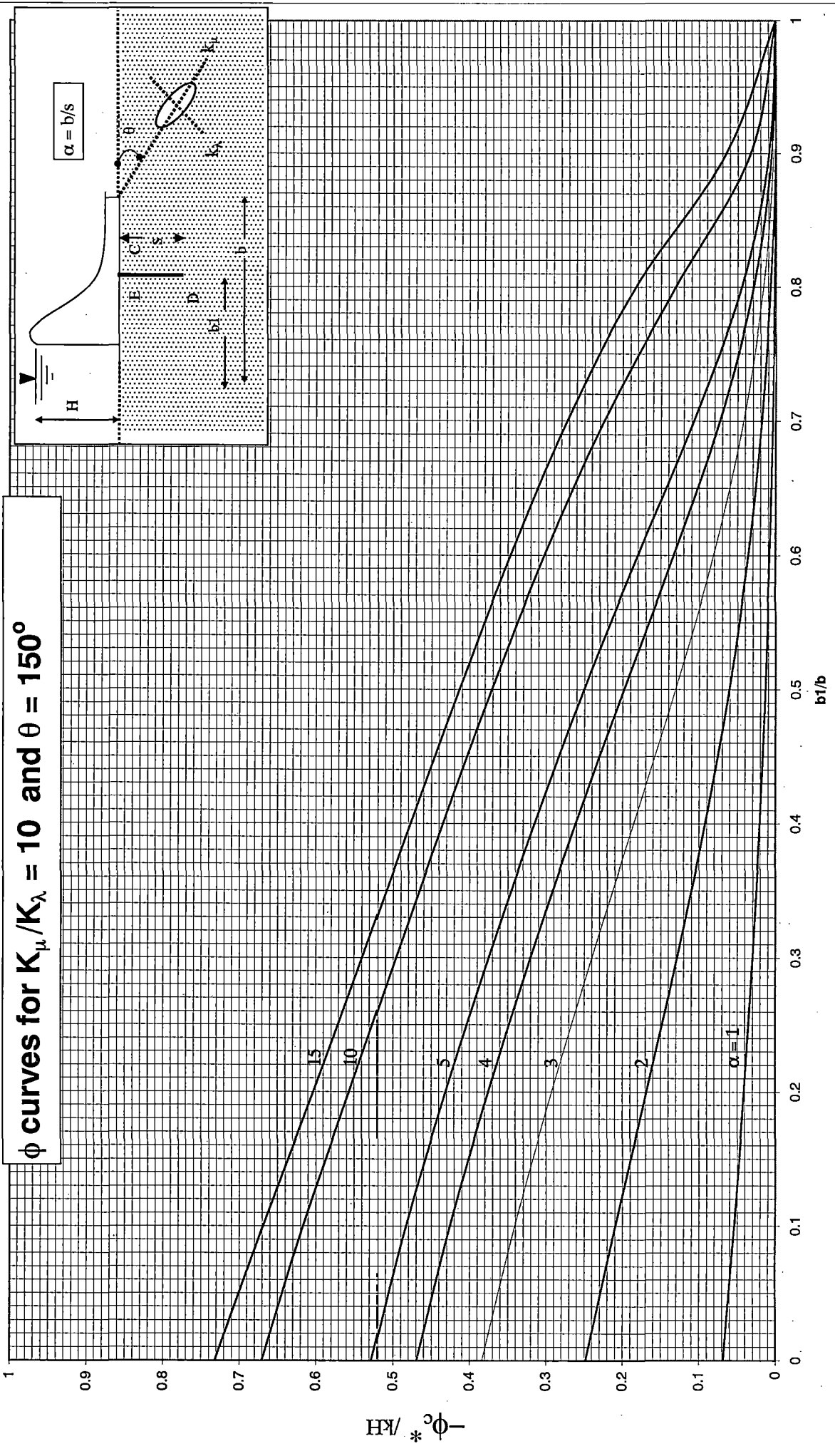


Fig.3.2((3.1)

ϕ curves for $K_\mu/K_\lambda = 10$ and $\theta = 150^\circ$

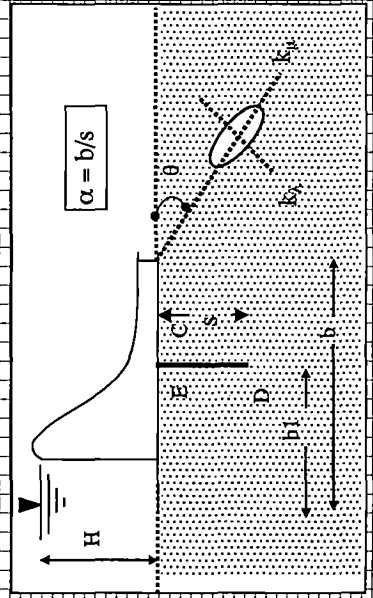
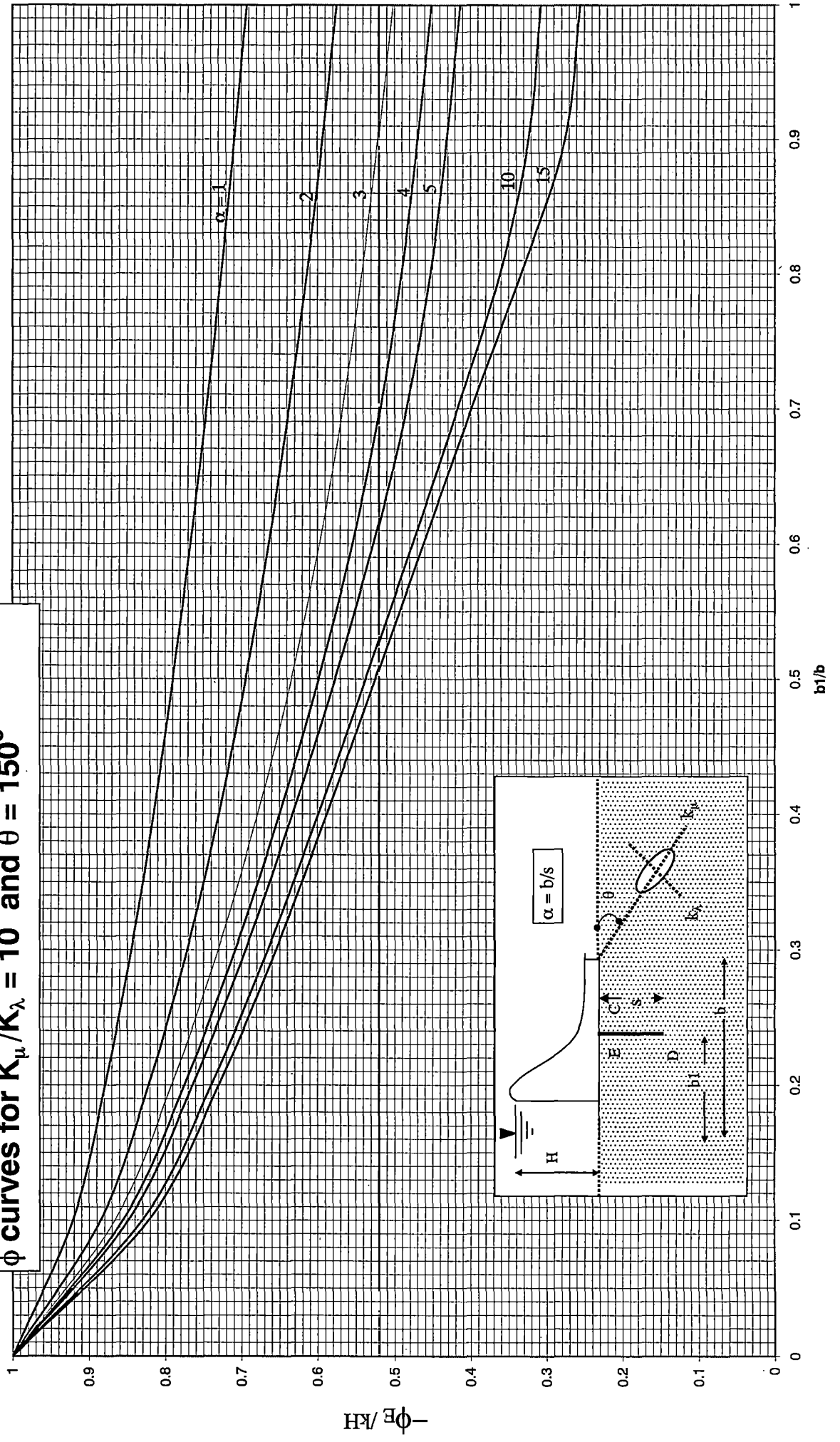


Fig.3.2(f3.2)

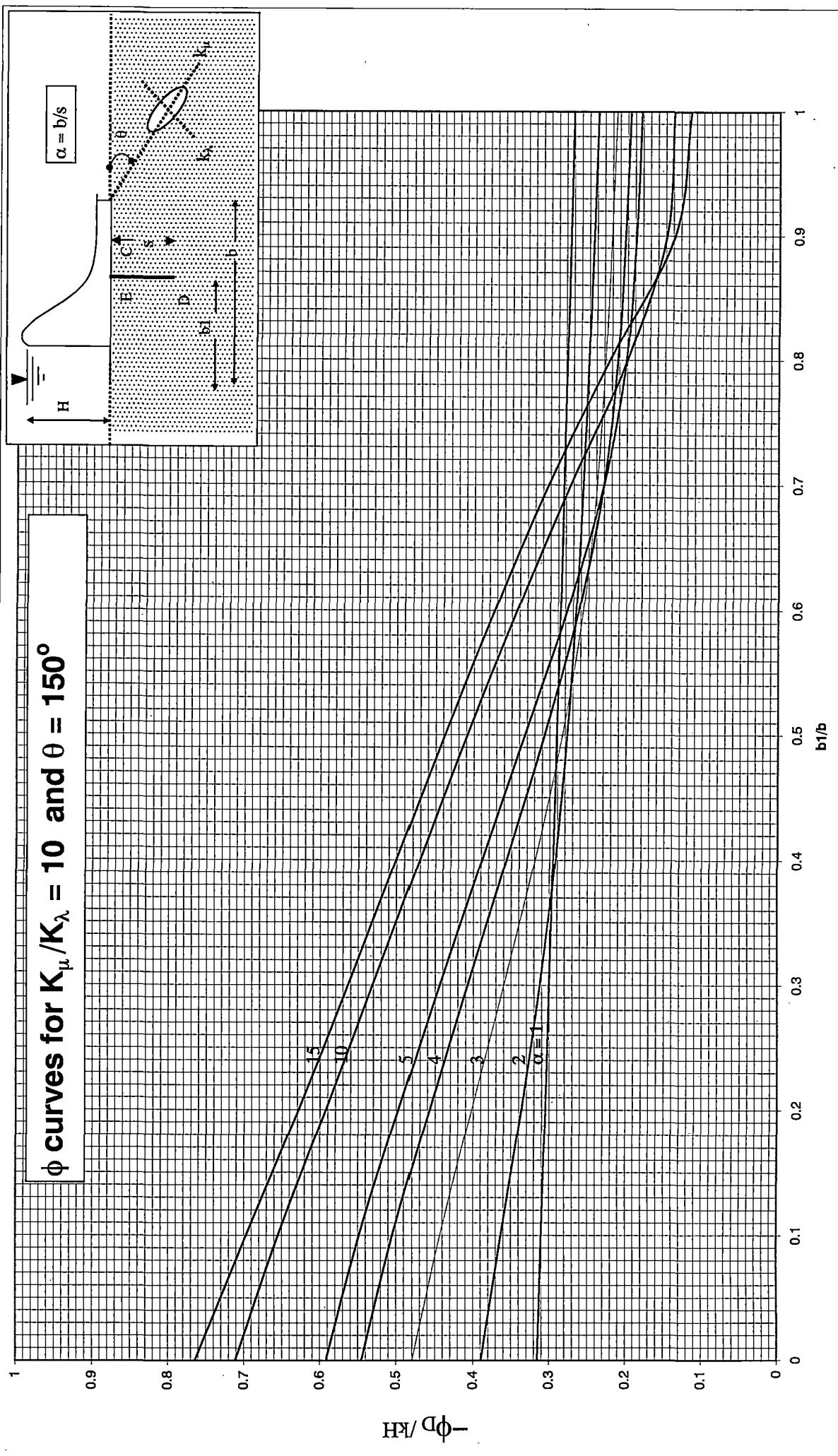


Fig.3.2(3.3)

ϕ curves for $\theta = 0$ with end sheet pile

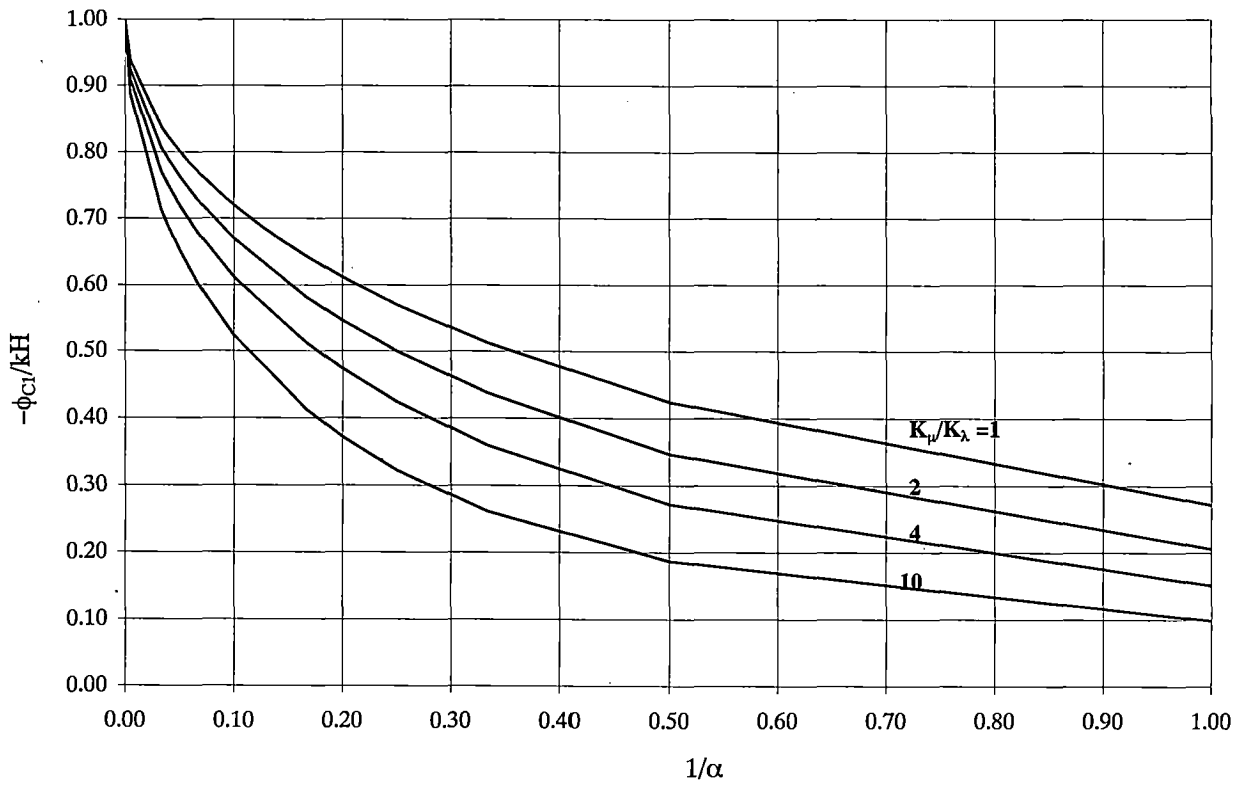


Fig. 3.3(a1)

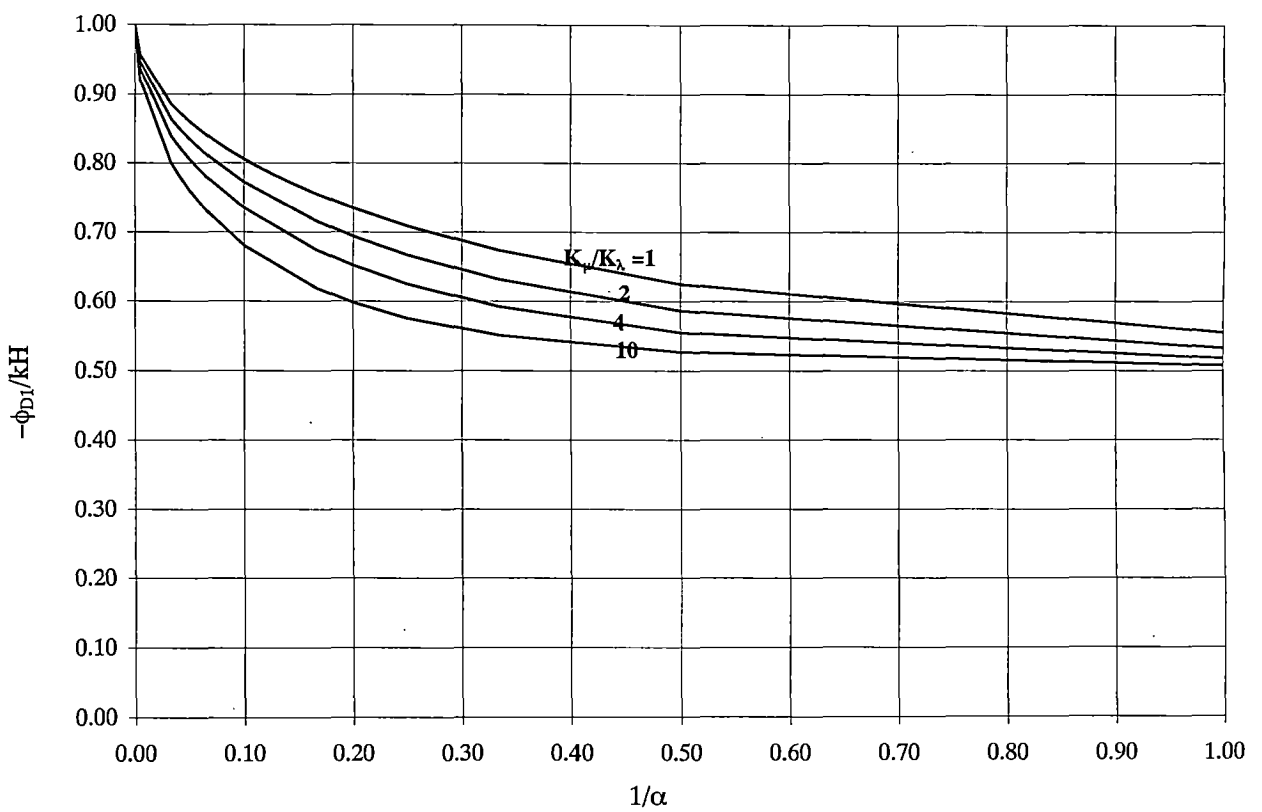
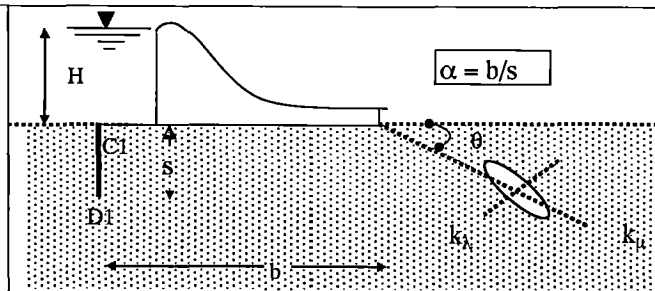
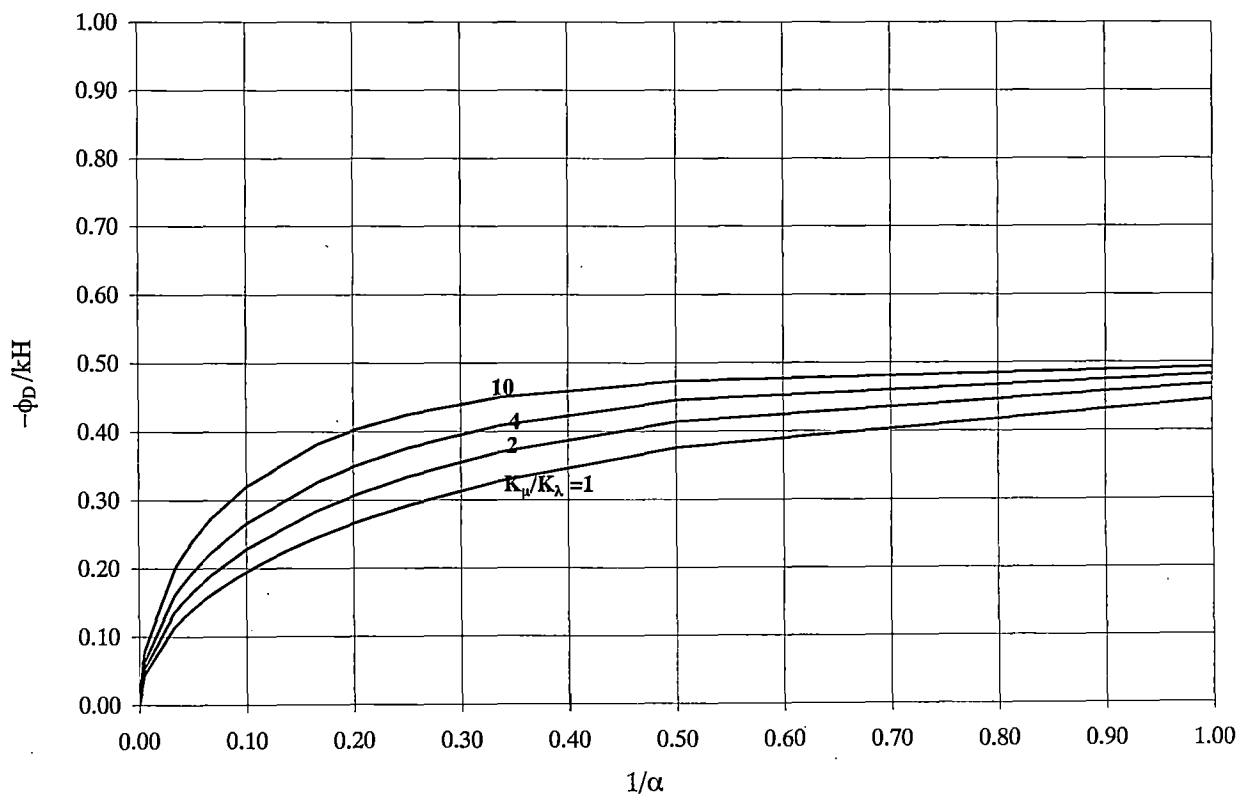
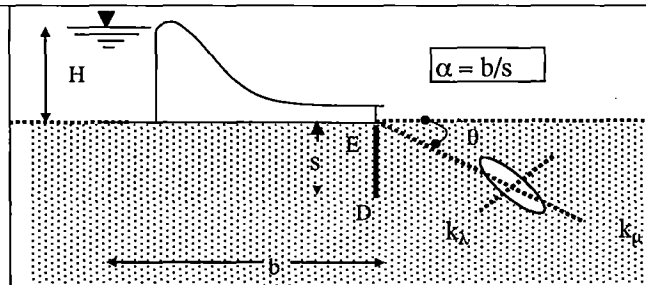
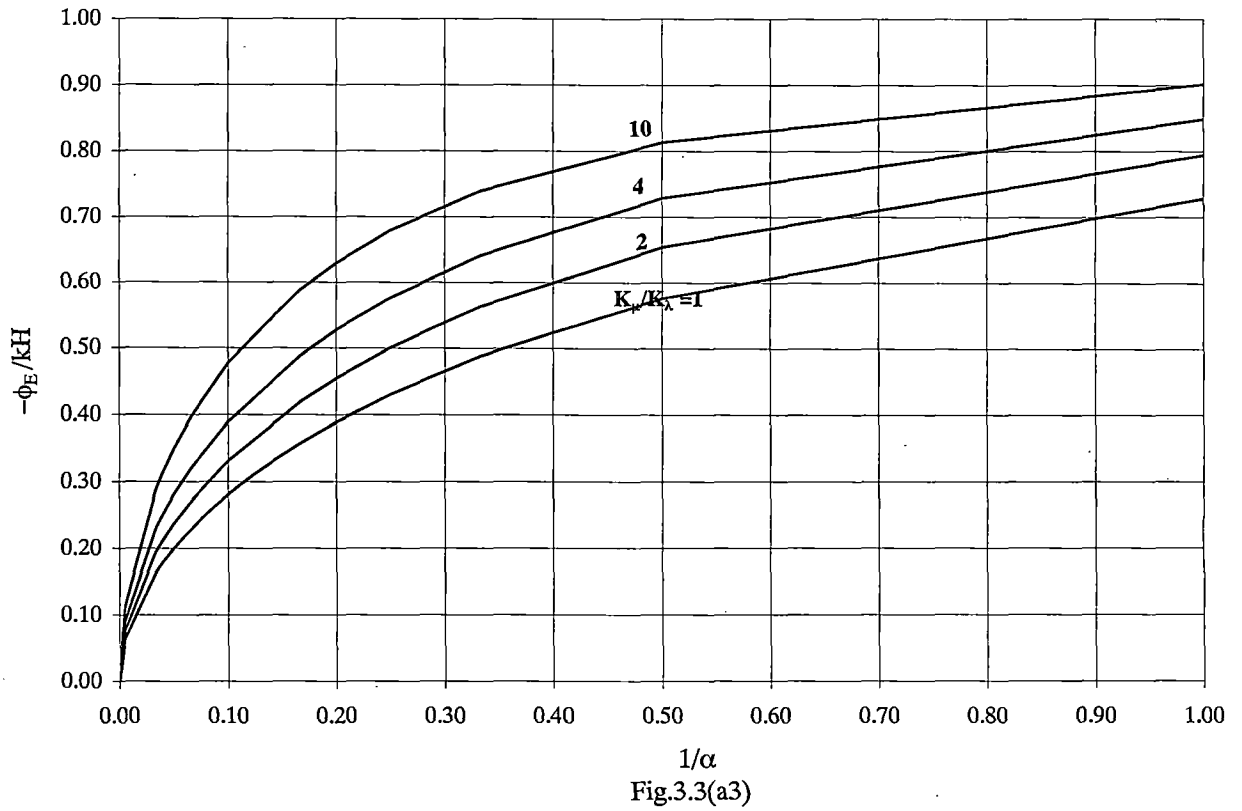
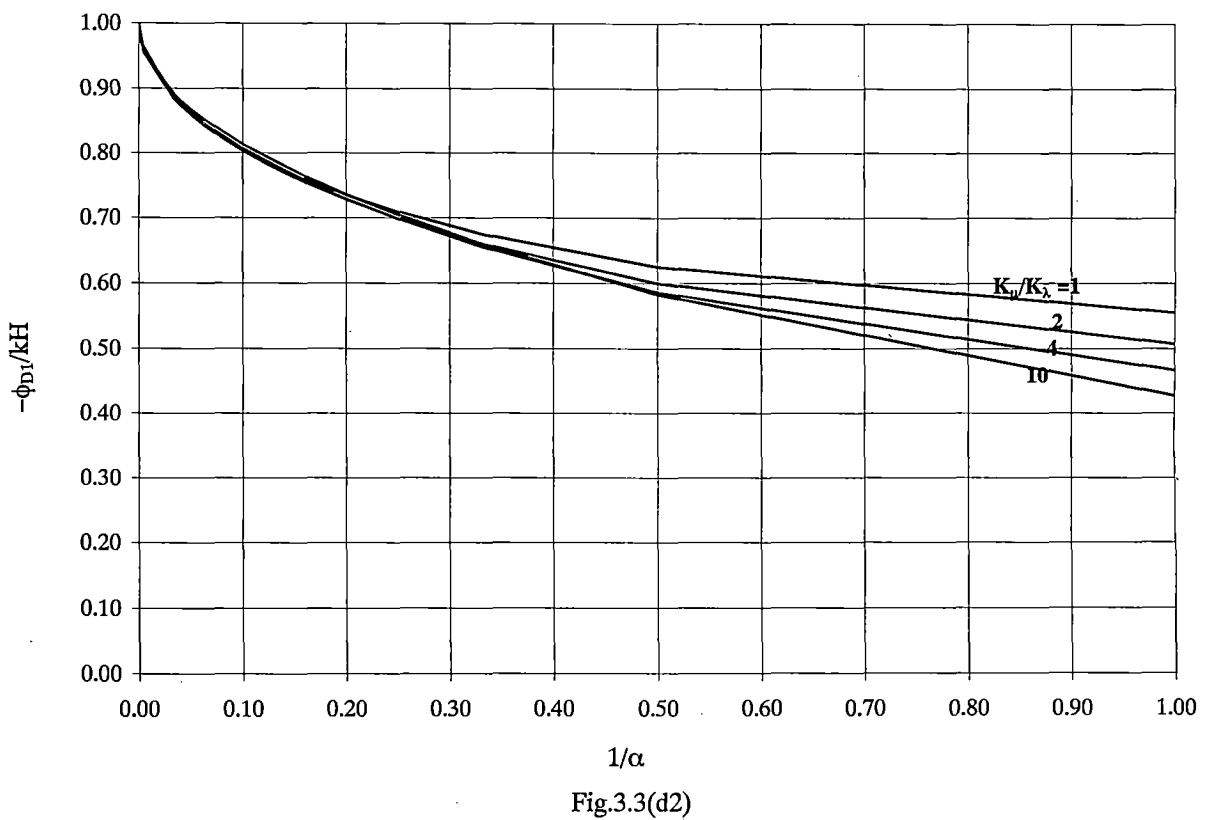
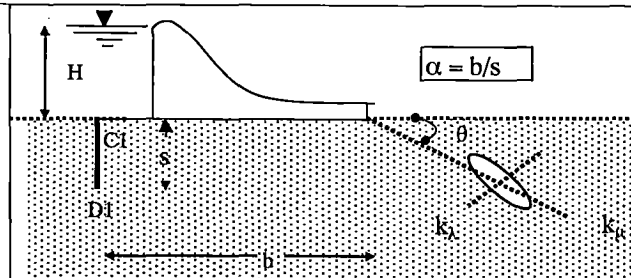
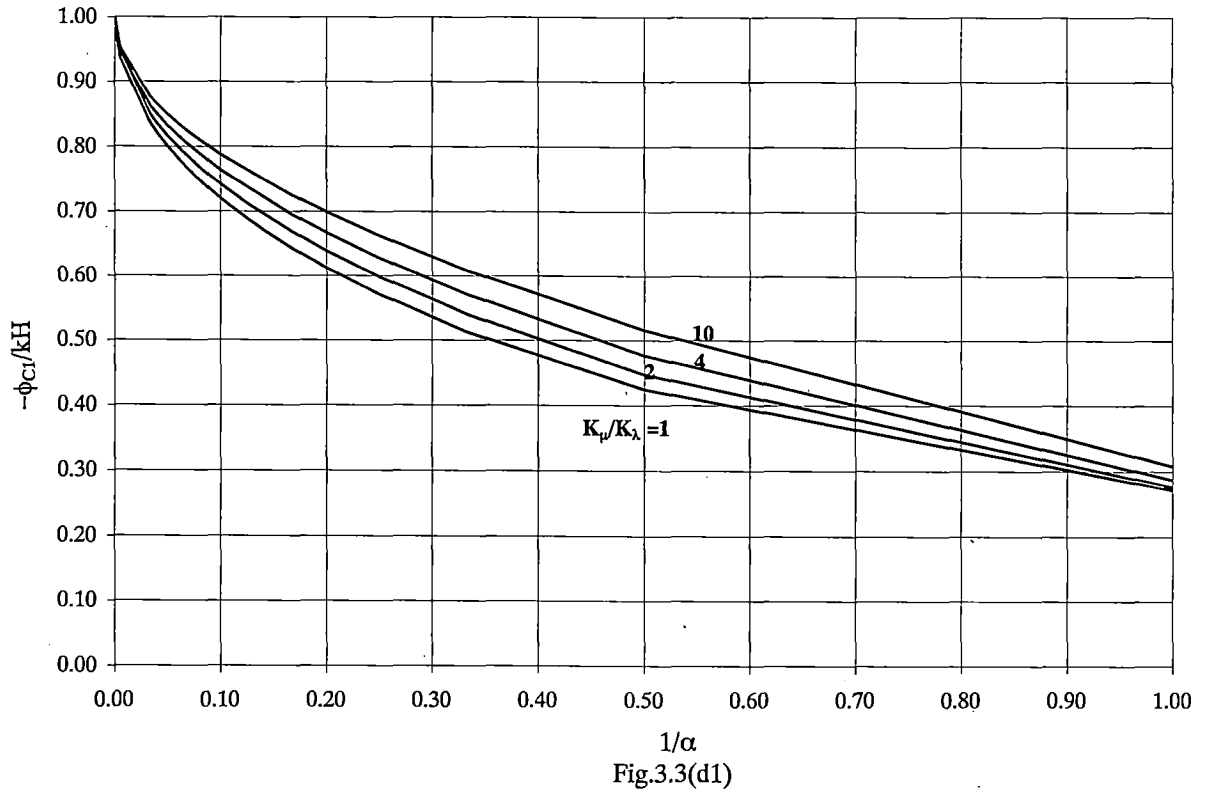


Fig. 3.3(b)

ϕ curves for $\theta = 0$ with end sheet pile



ϕ curves for $\theta = 120^\circ$ with end sheet pile



ϕ curves for $\theta = 120^\circ$ with end sheet pile

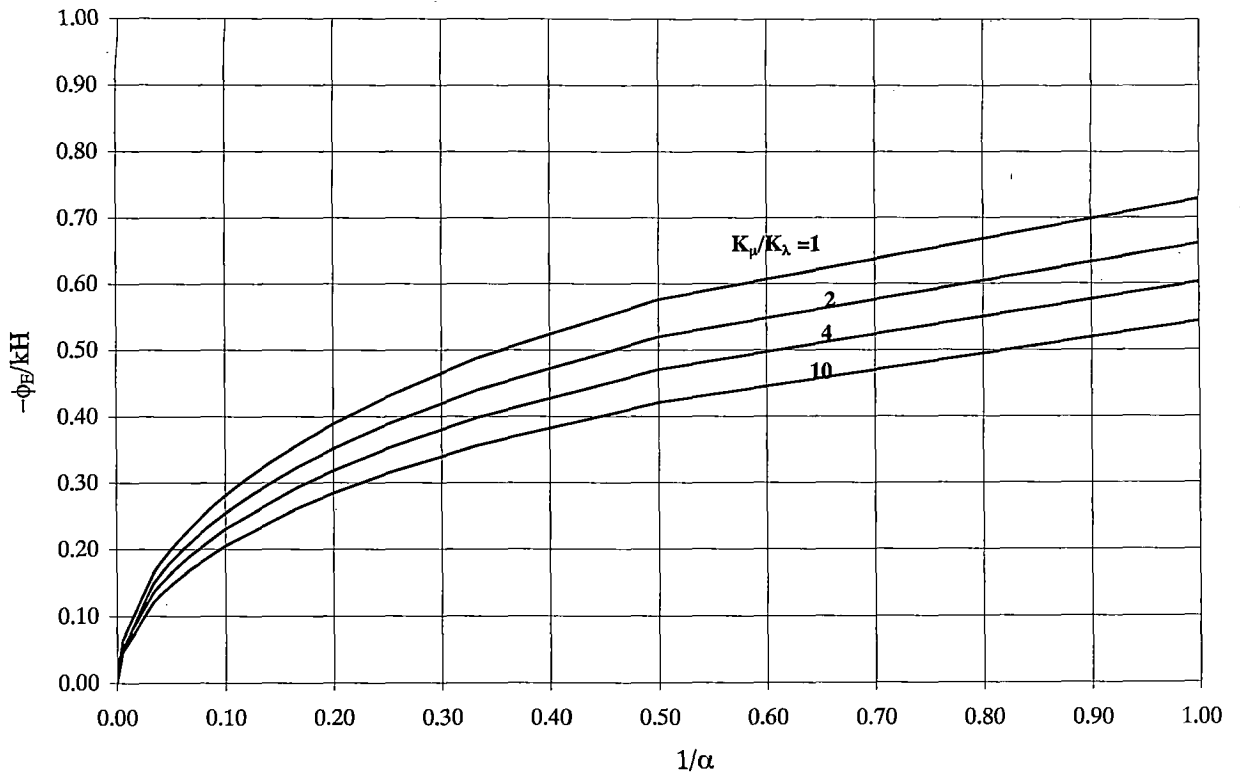


Fig.3.3(d3)

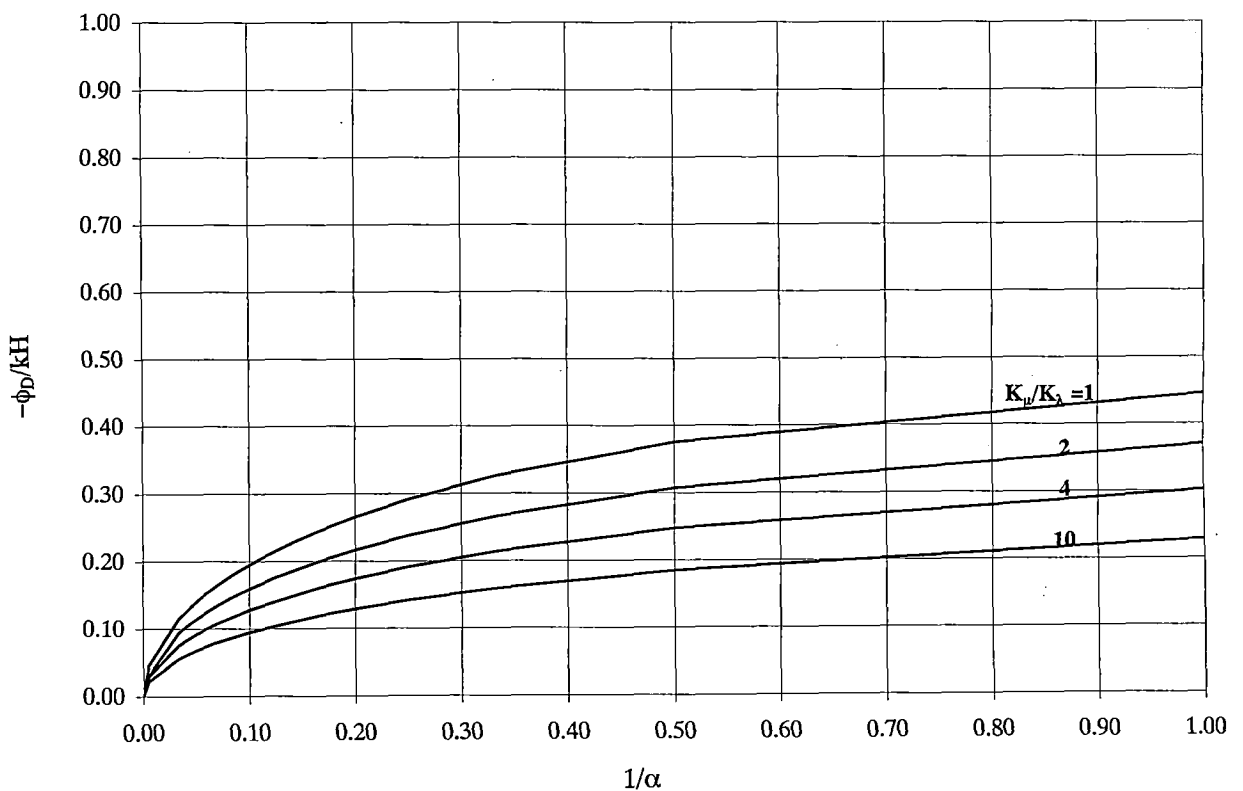
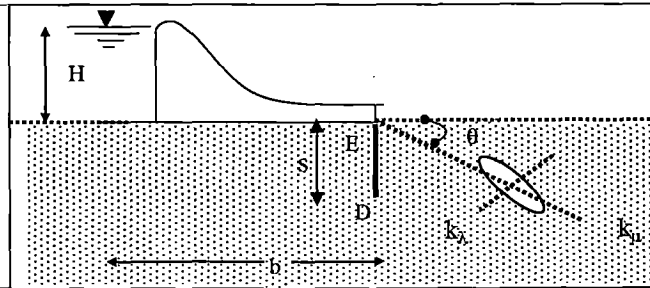
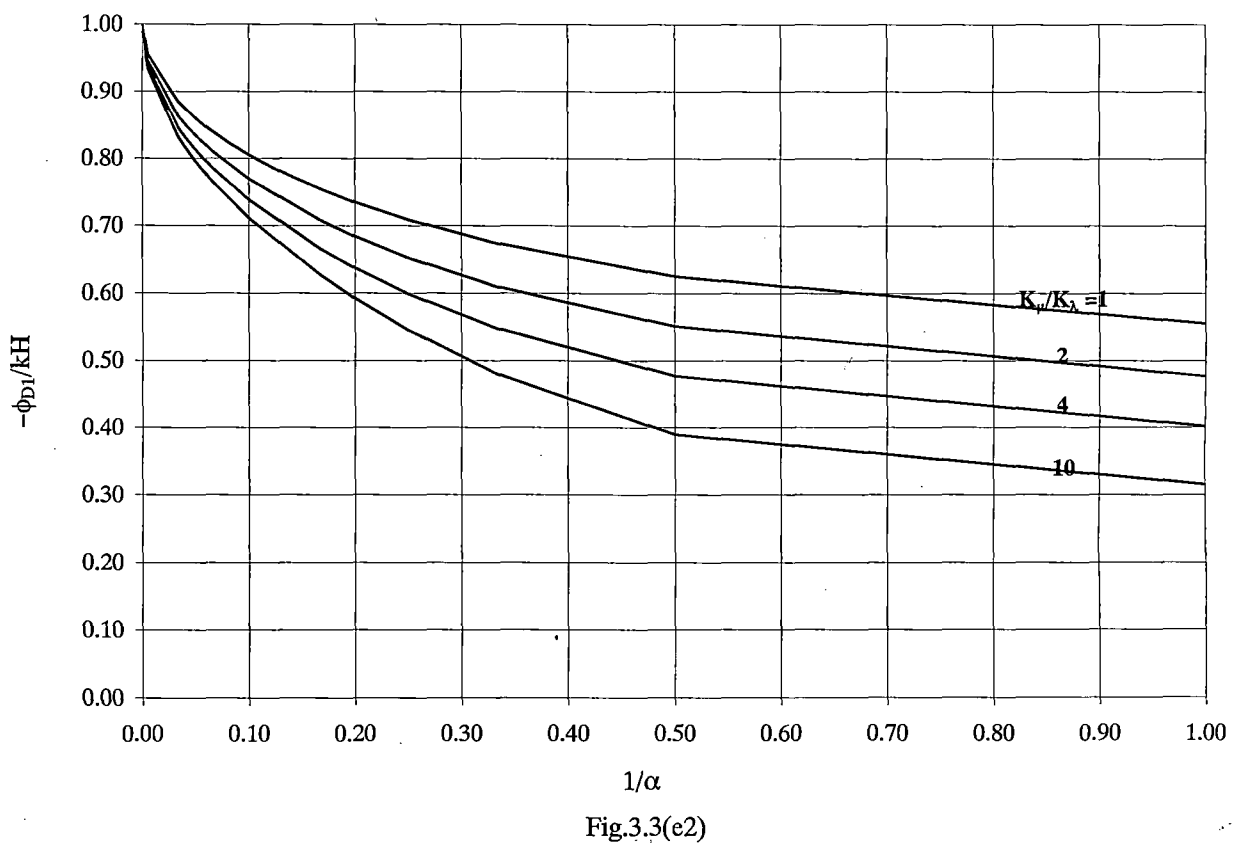
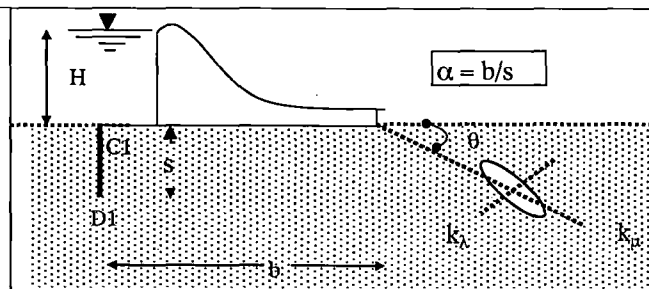
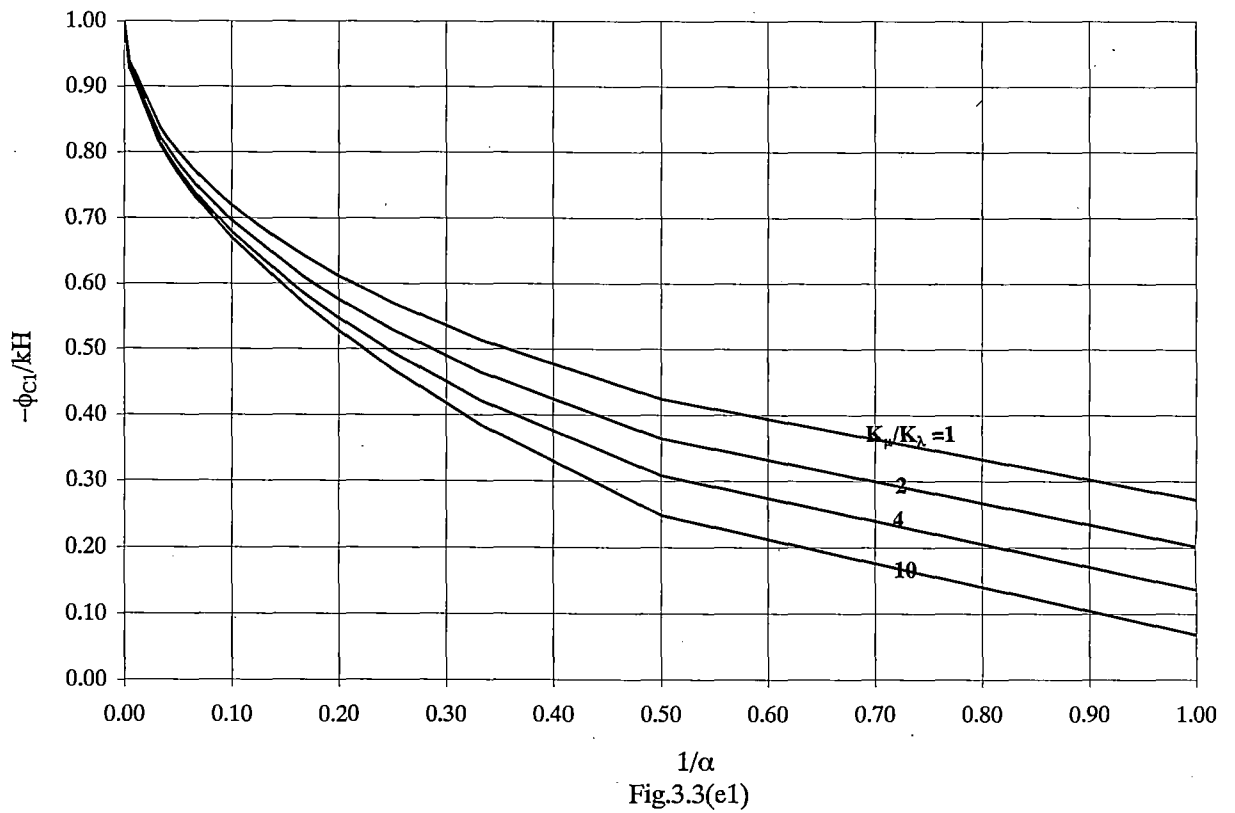


Fig.3.3(d4)

ϕ curves for $\theta = 150^\circ$ with end sheet pile



ϕ curves for $\theta = 150^\circ$ with end sheet pile

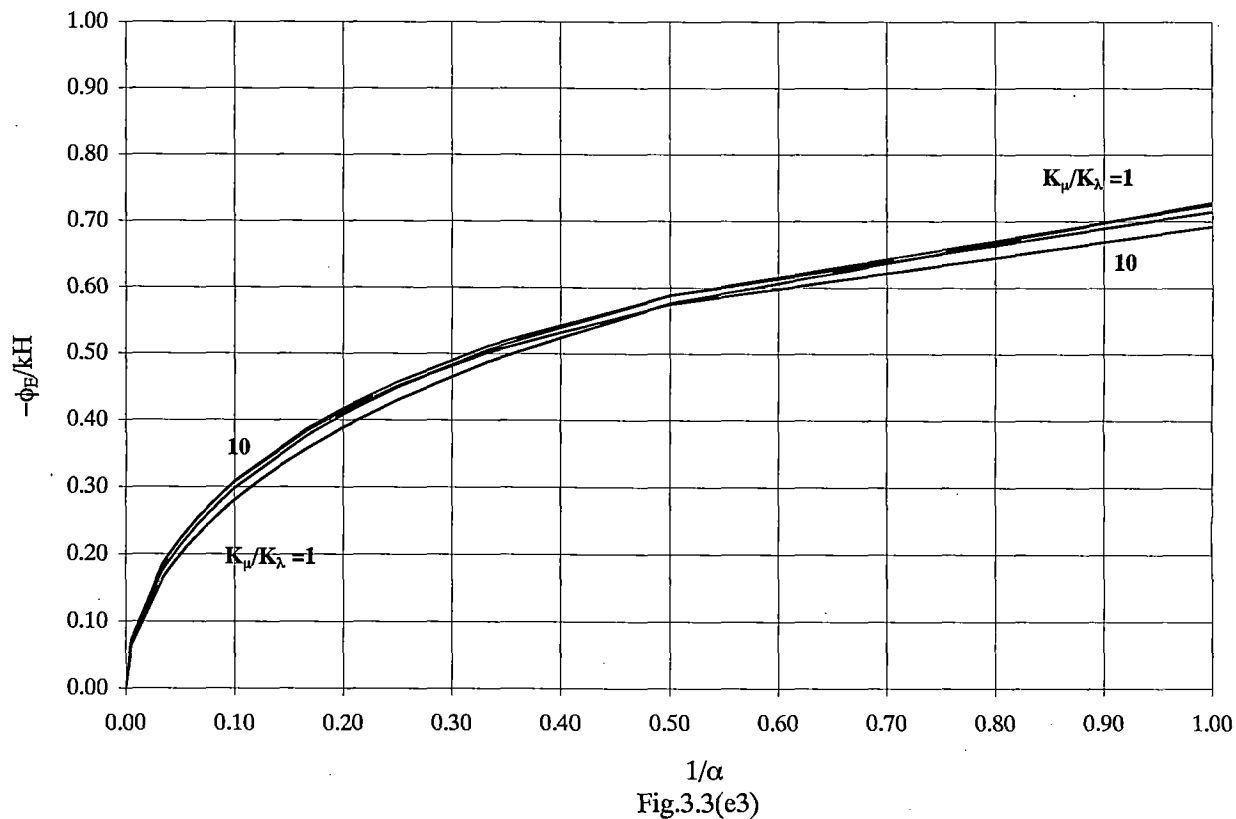
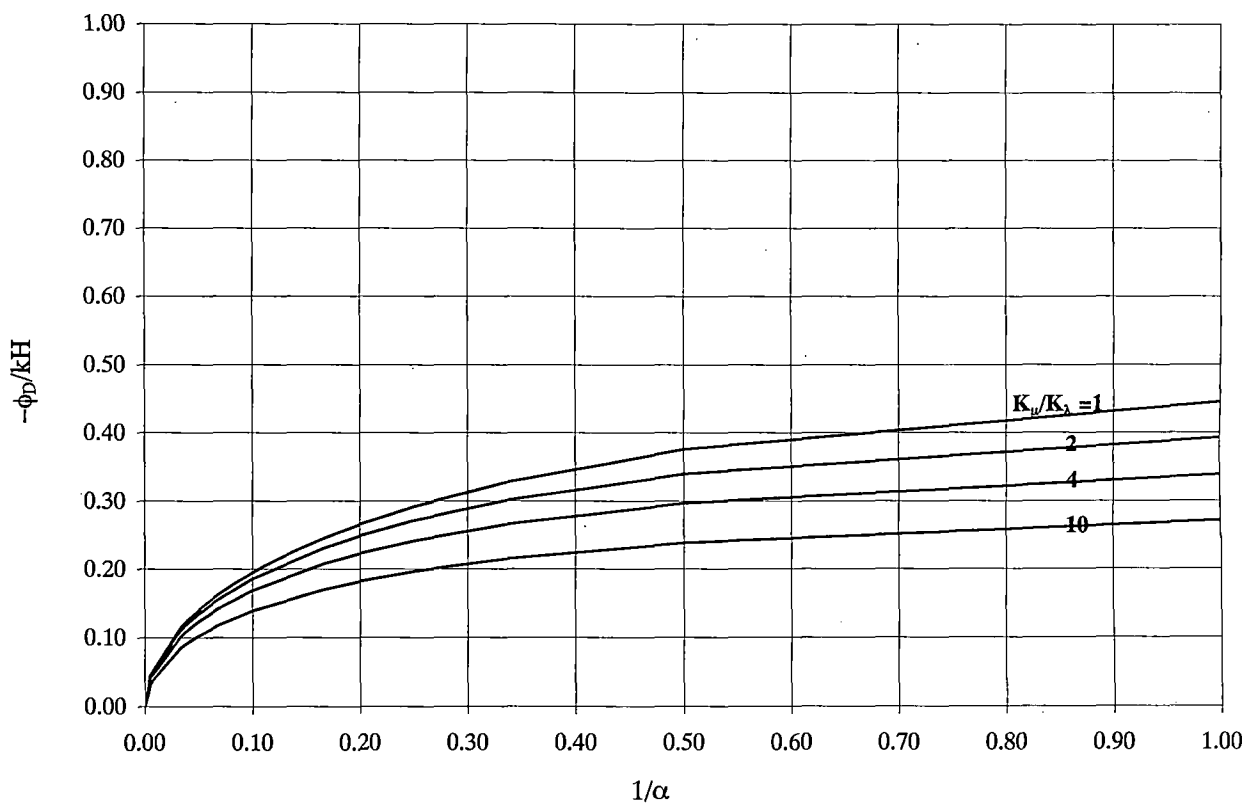
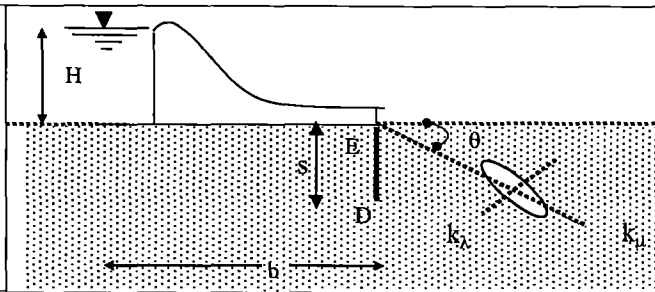


Fig.3.3(e3)



ϕ curves for $\theta = 30^\circ$ with end sheet pile

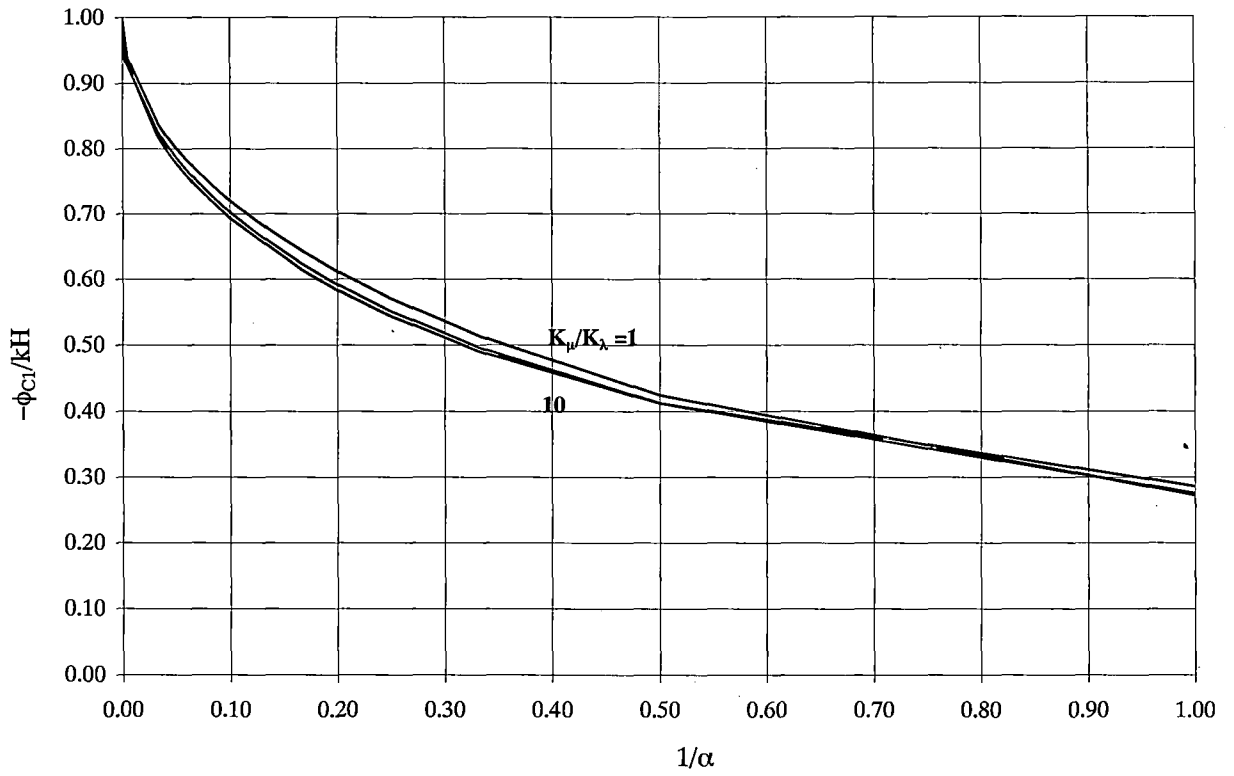


Fig.3.3(b1)

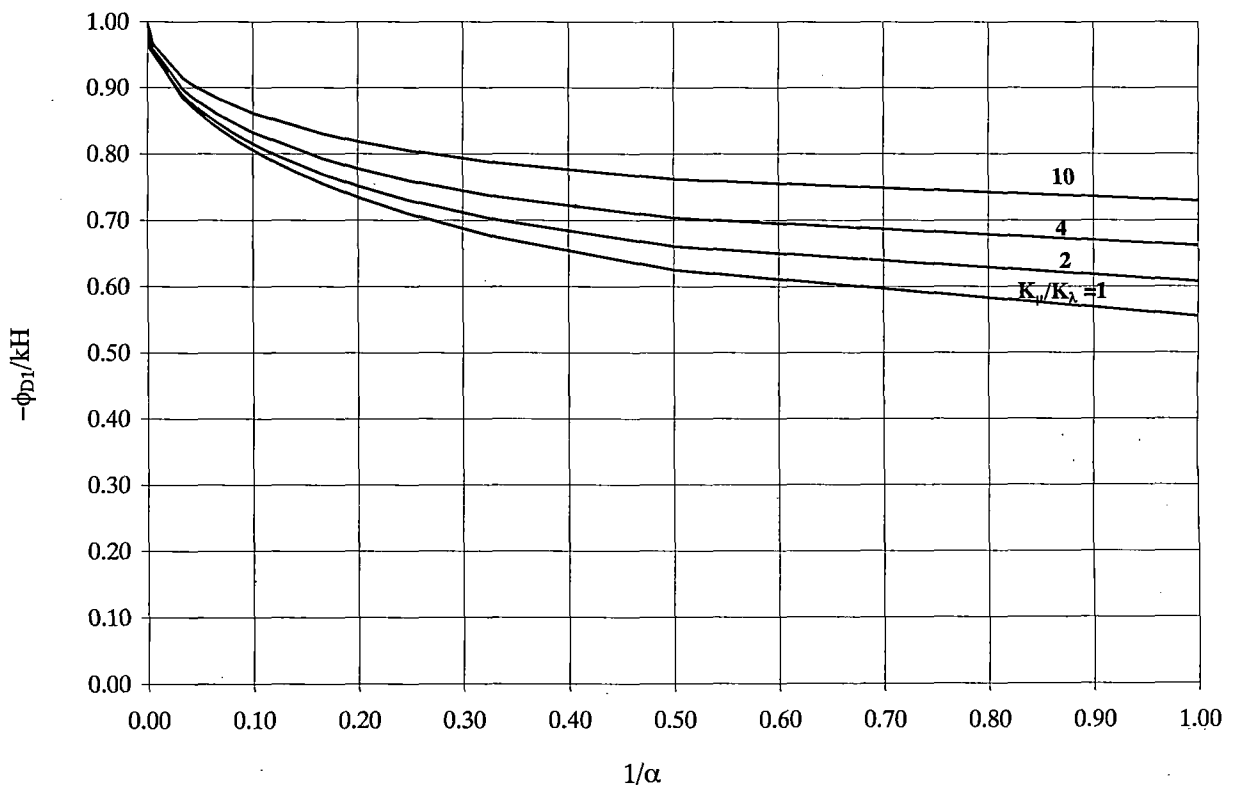
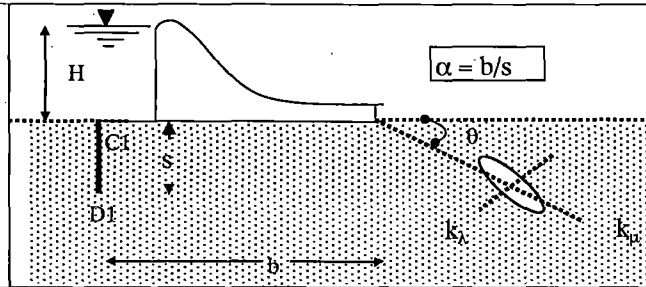
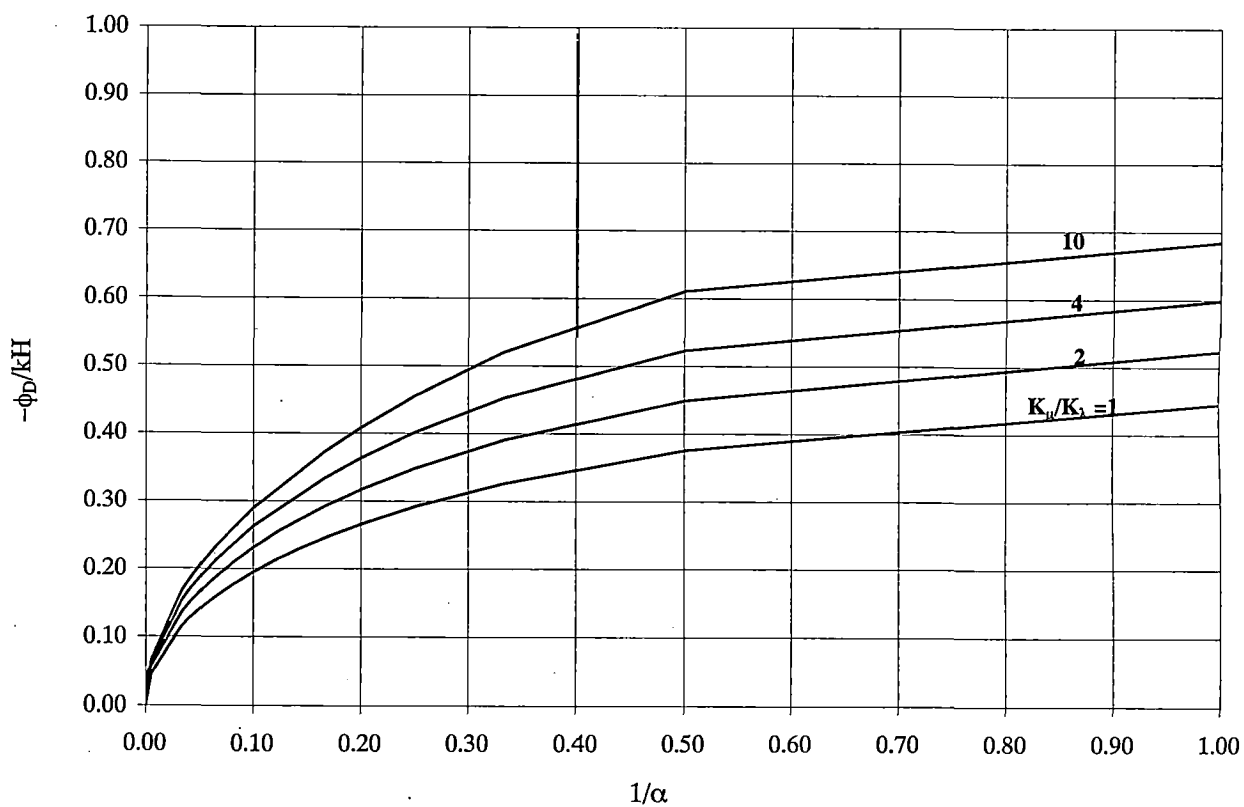
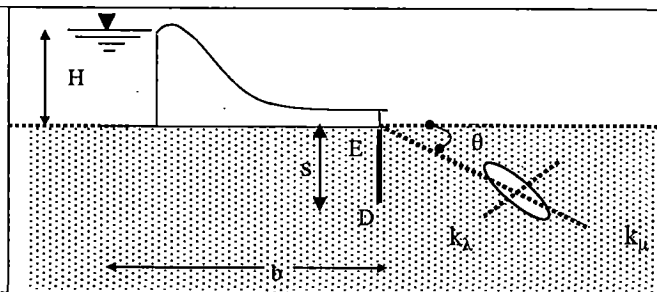
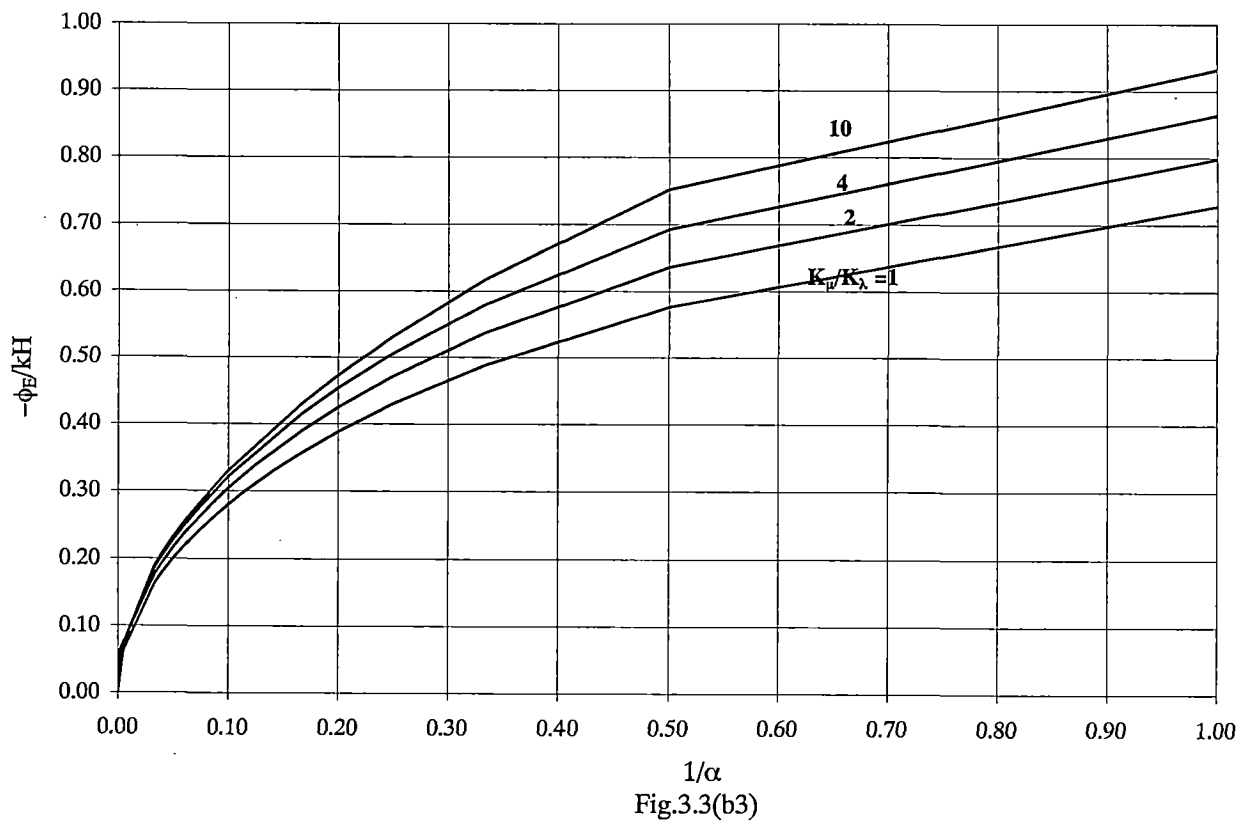


Fig.3.3(b2)

ϕ curves for $\theta = 30^\circ$ with end sheet pile



ϕ curves for $\theta = 60^\circ$ with end sheet pile

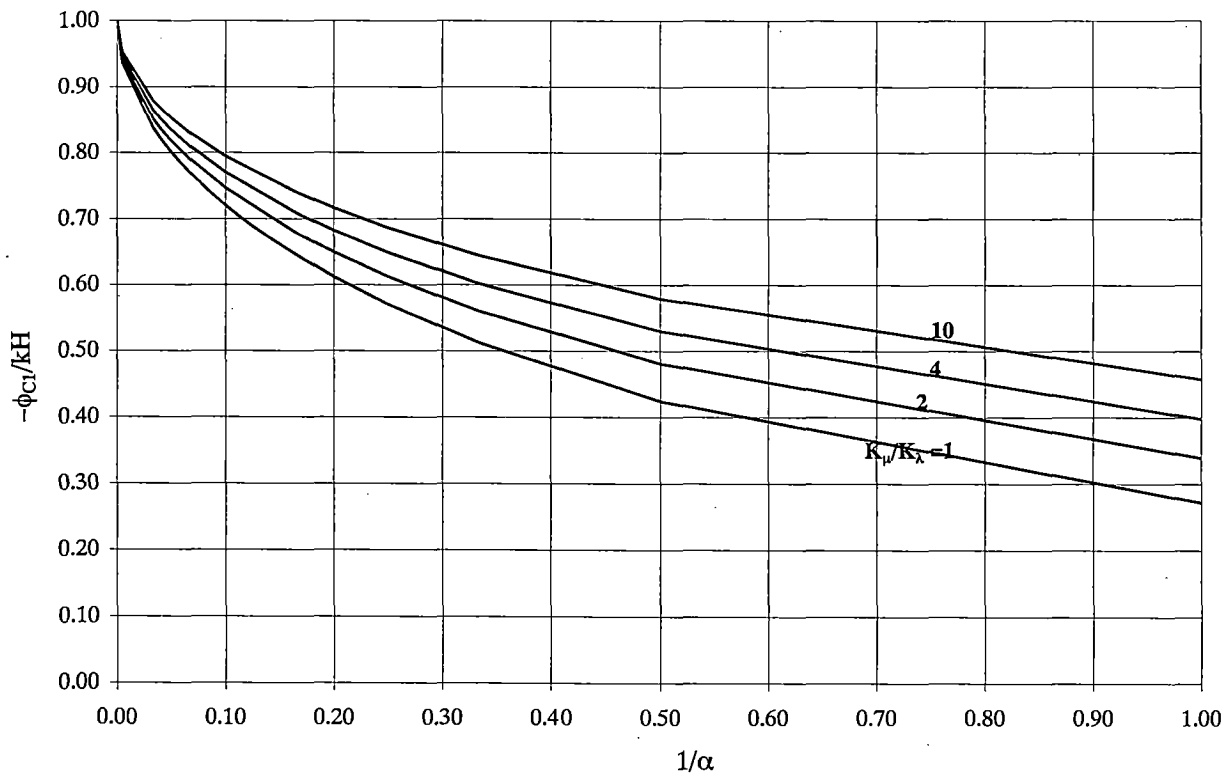


Fig.3.3(c1)

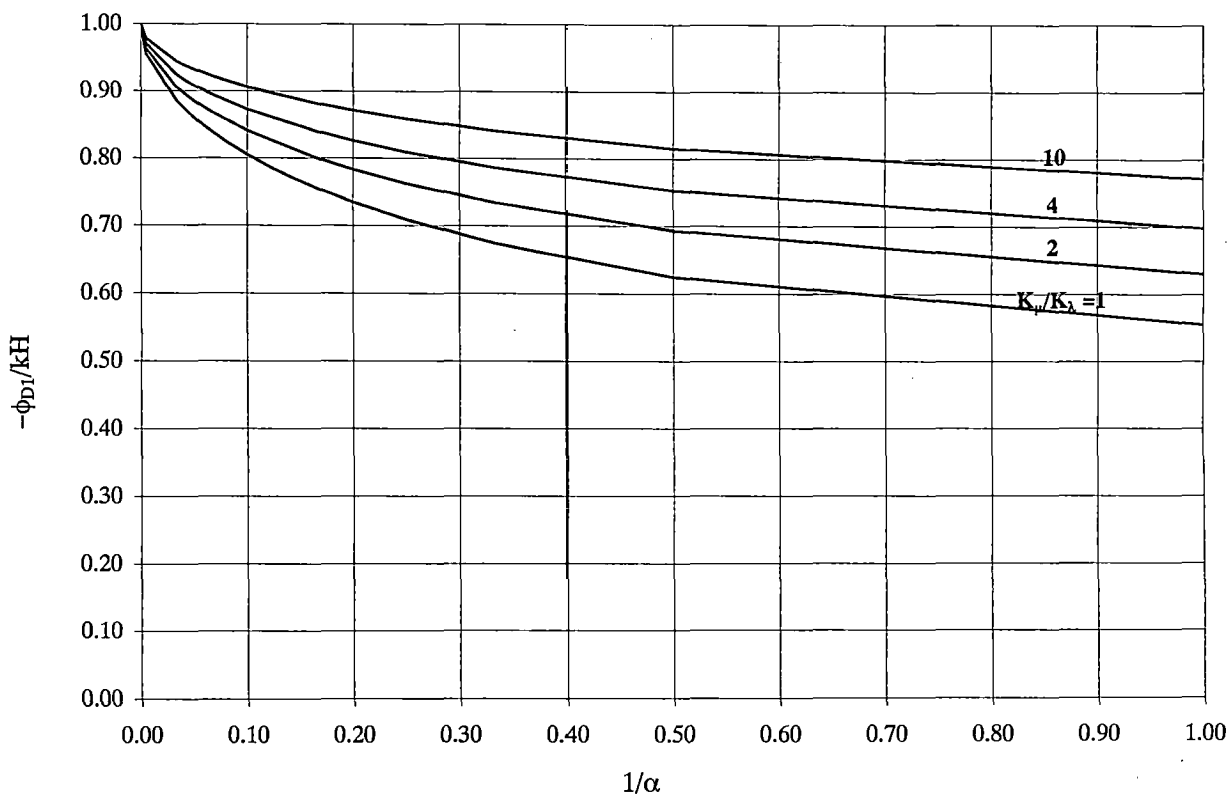
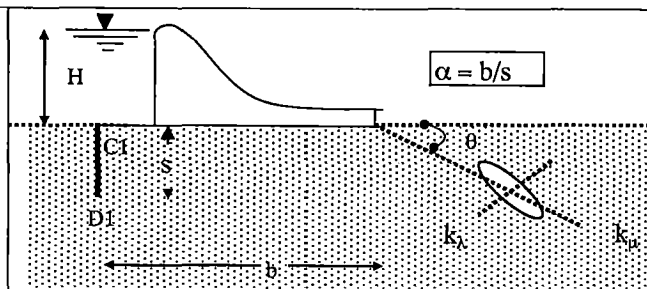


Fig.3.3(c2)

ϕ curves for $\theta = 60^\circ$ with end sheet pile

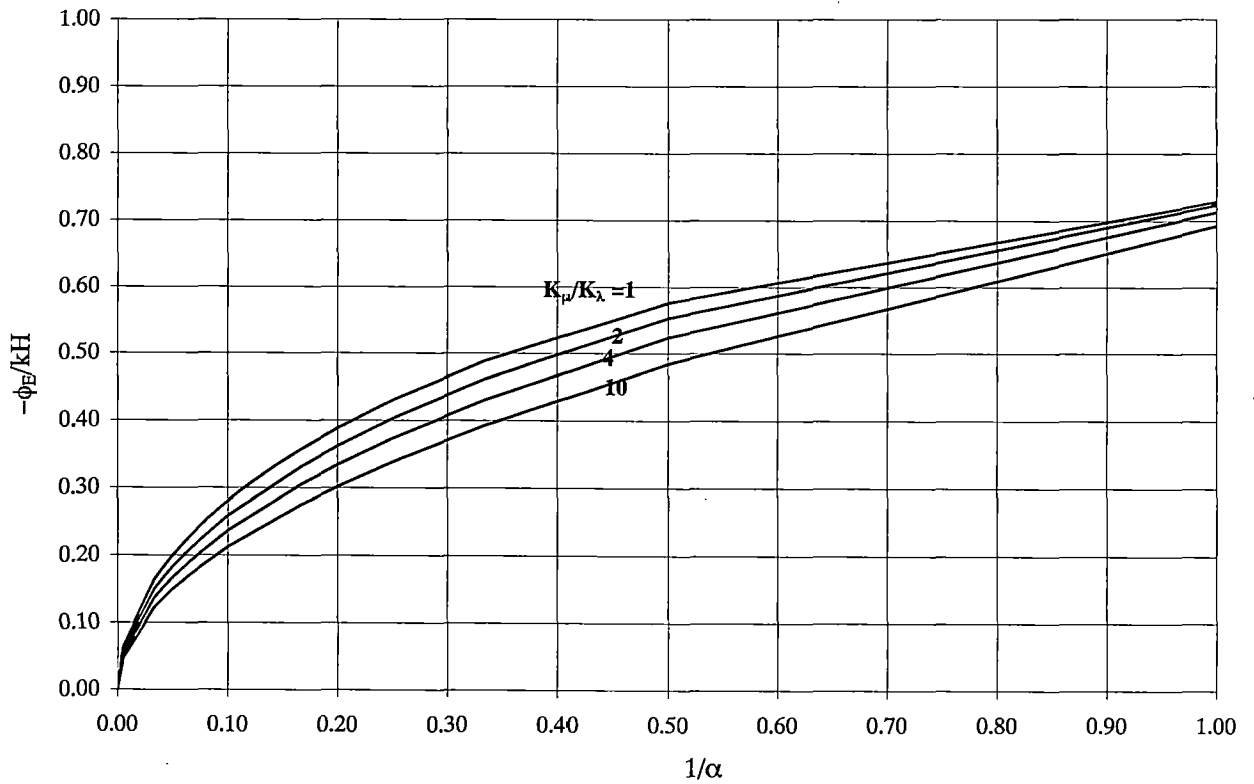


Fig.3.3(c3)

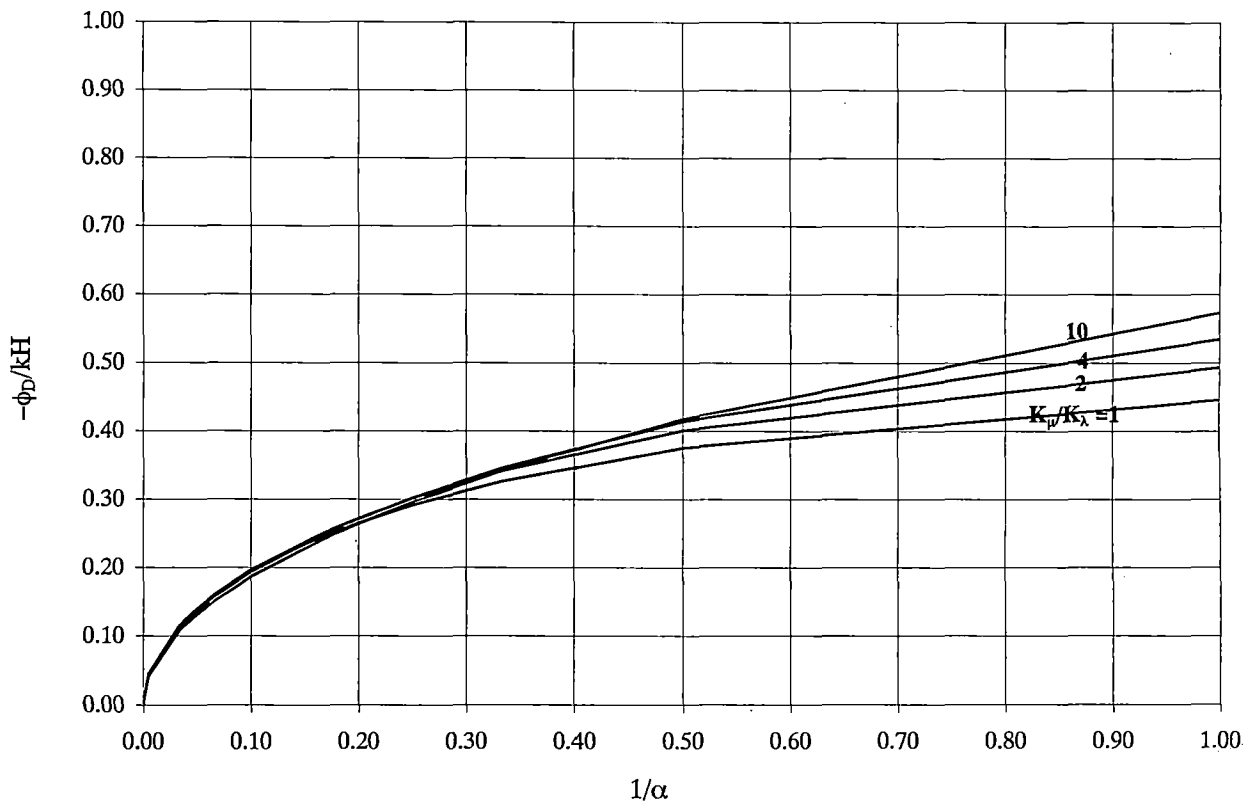
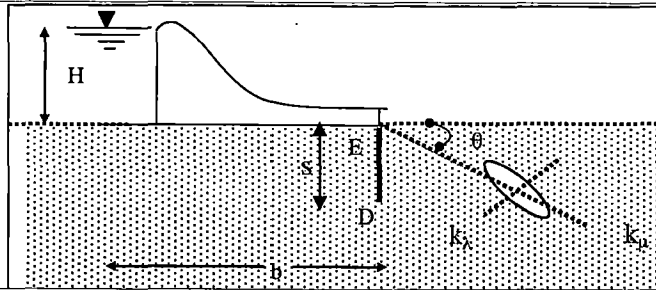


Fig.3.3(c4)

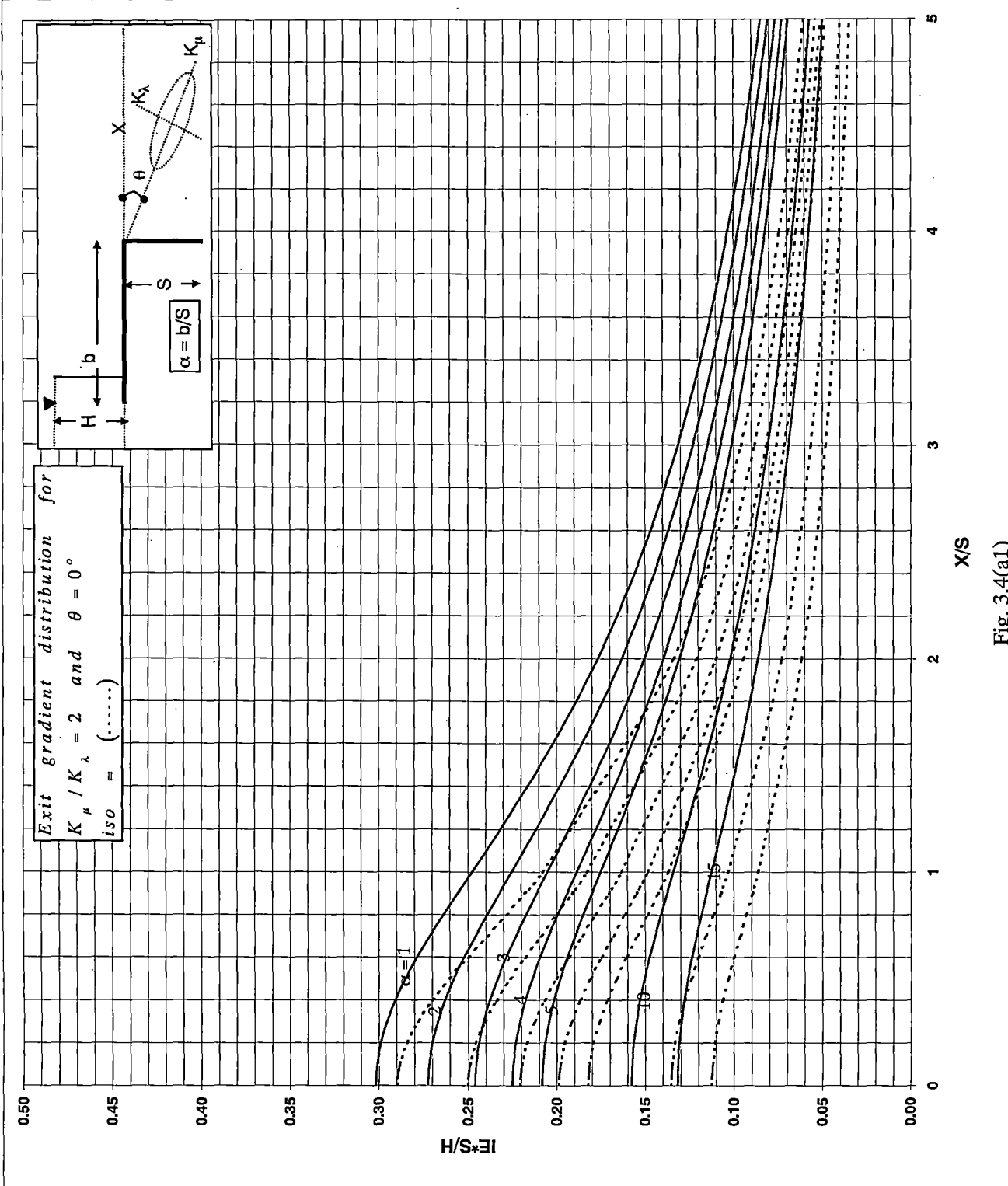


Fig. 3.4(a1)

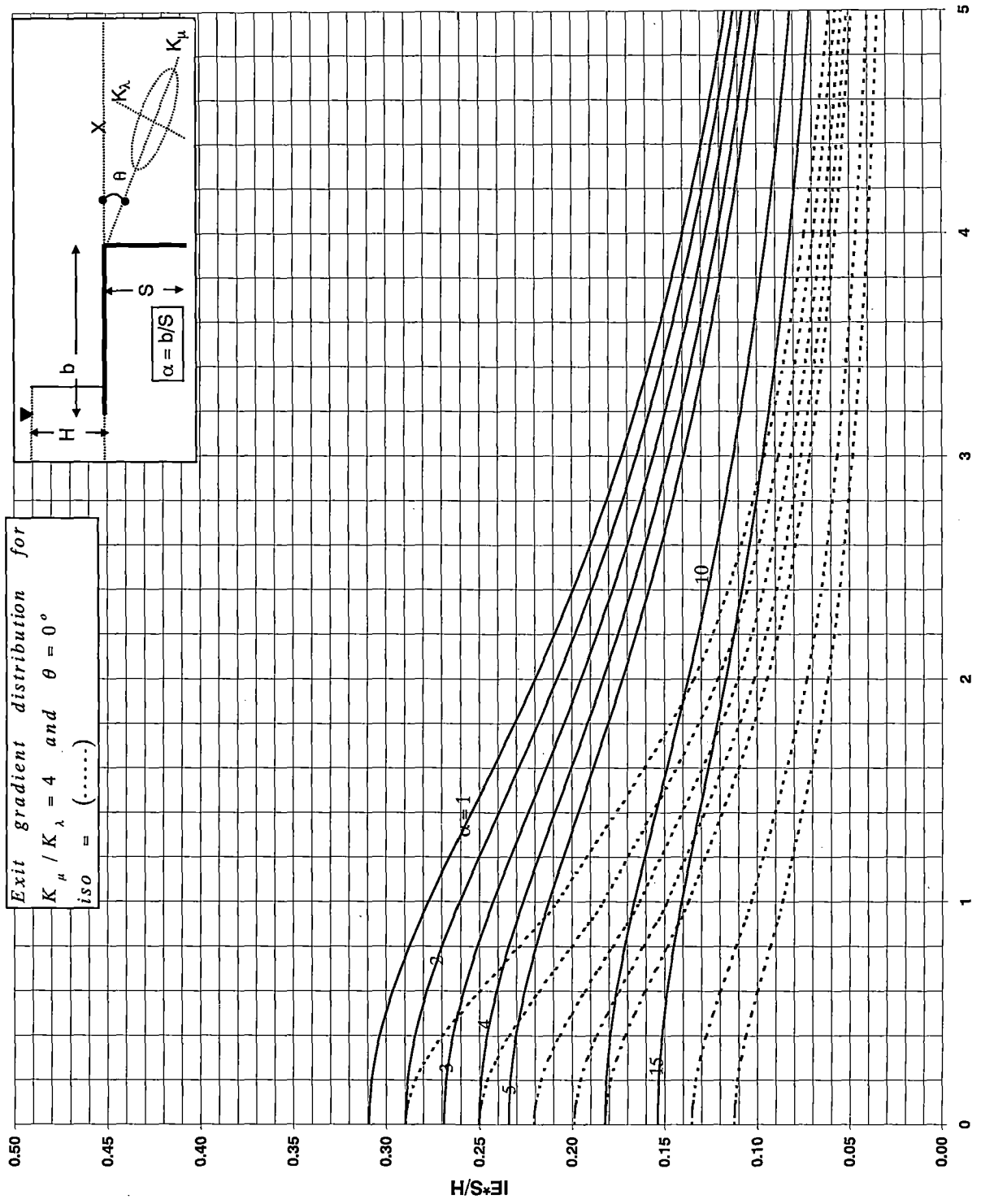


Fig.3.4(a2)

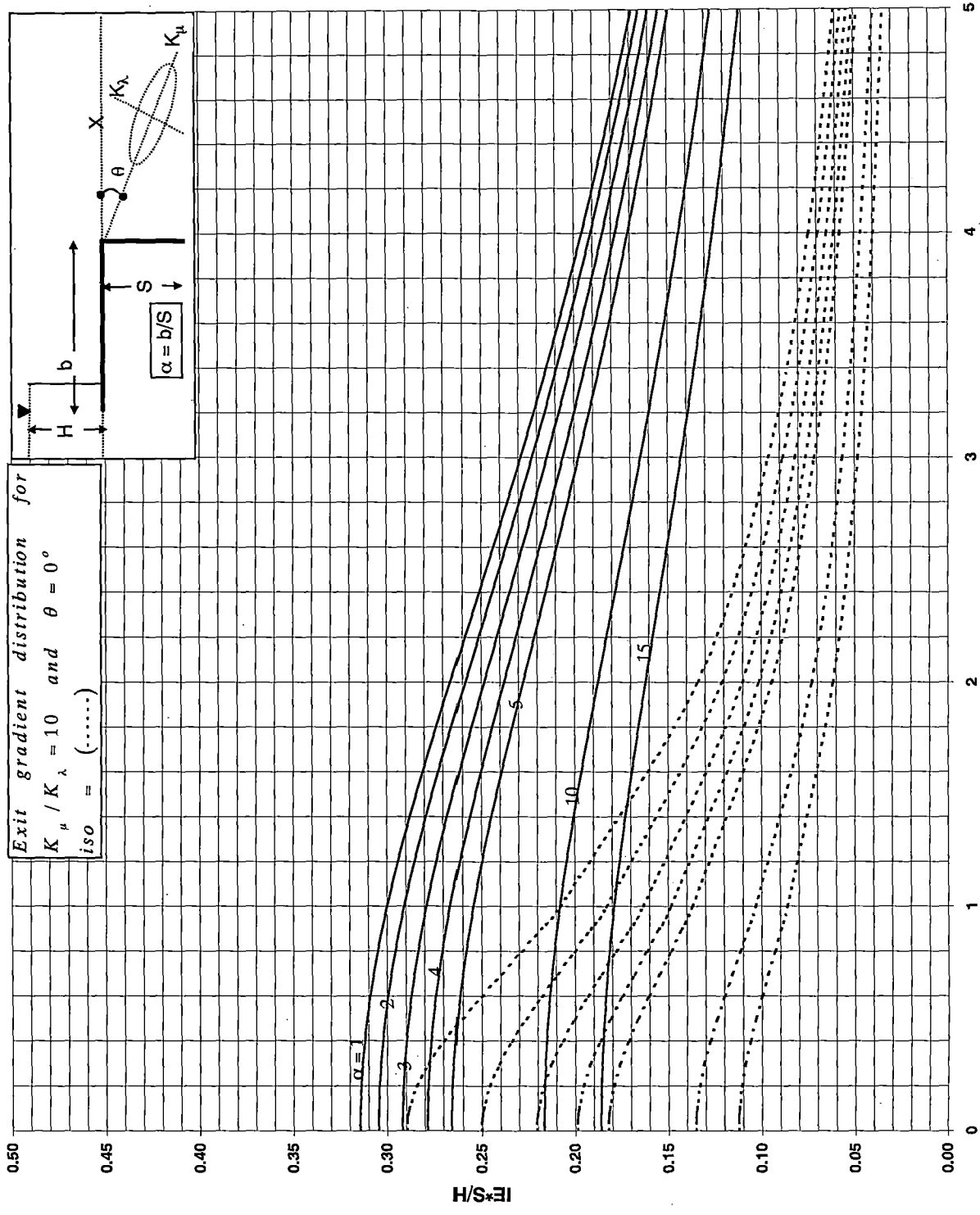


Fig.3.4(a3)

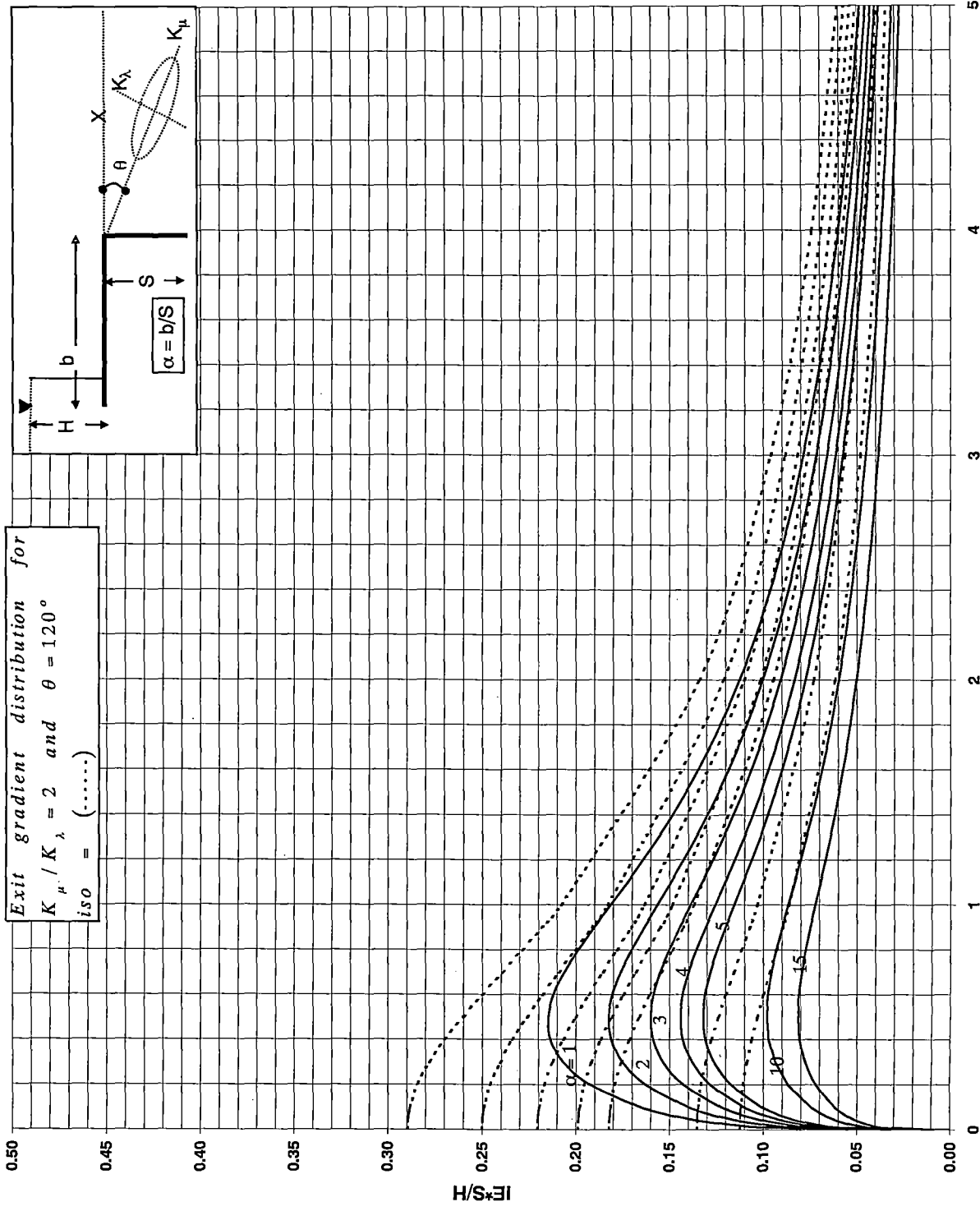
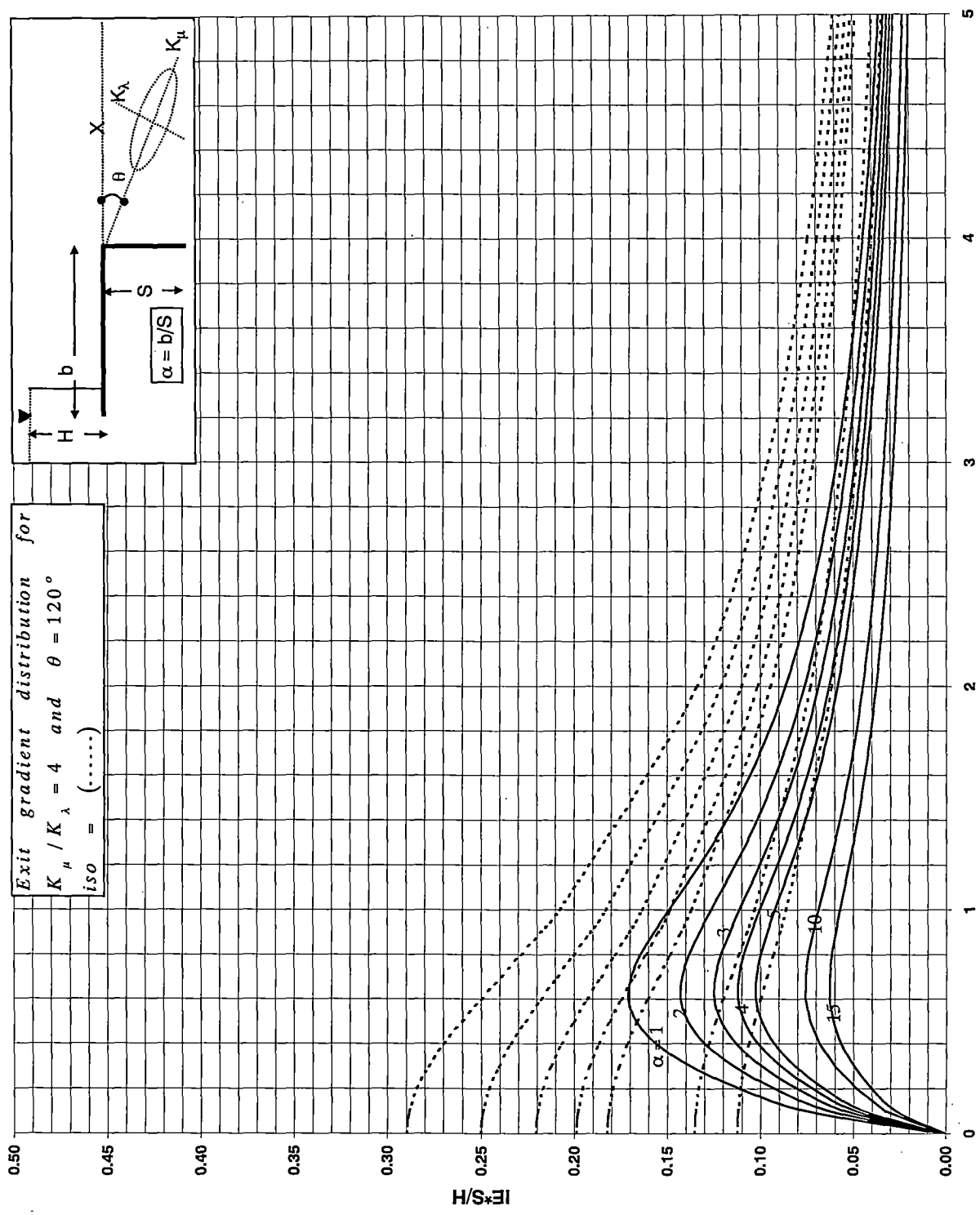
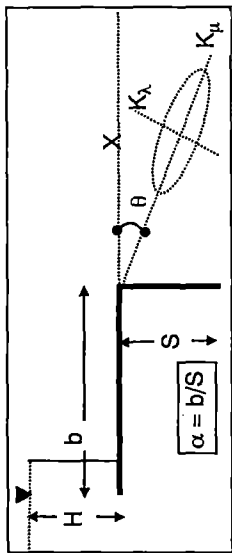


Fig.3.4(b1)

Exit gradient distribution for
 $K_\mu / K_\lambda = 4$ and $\theta = 120^\circ$
 $iso = (\dots\dots)$



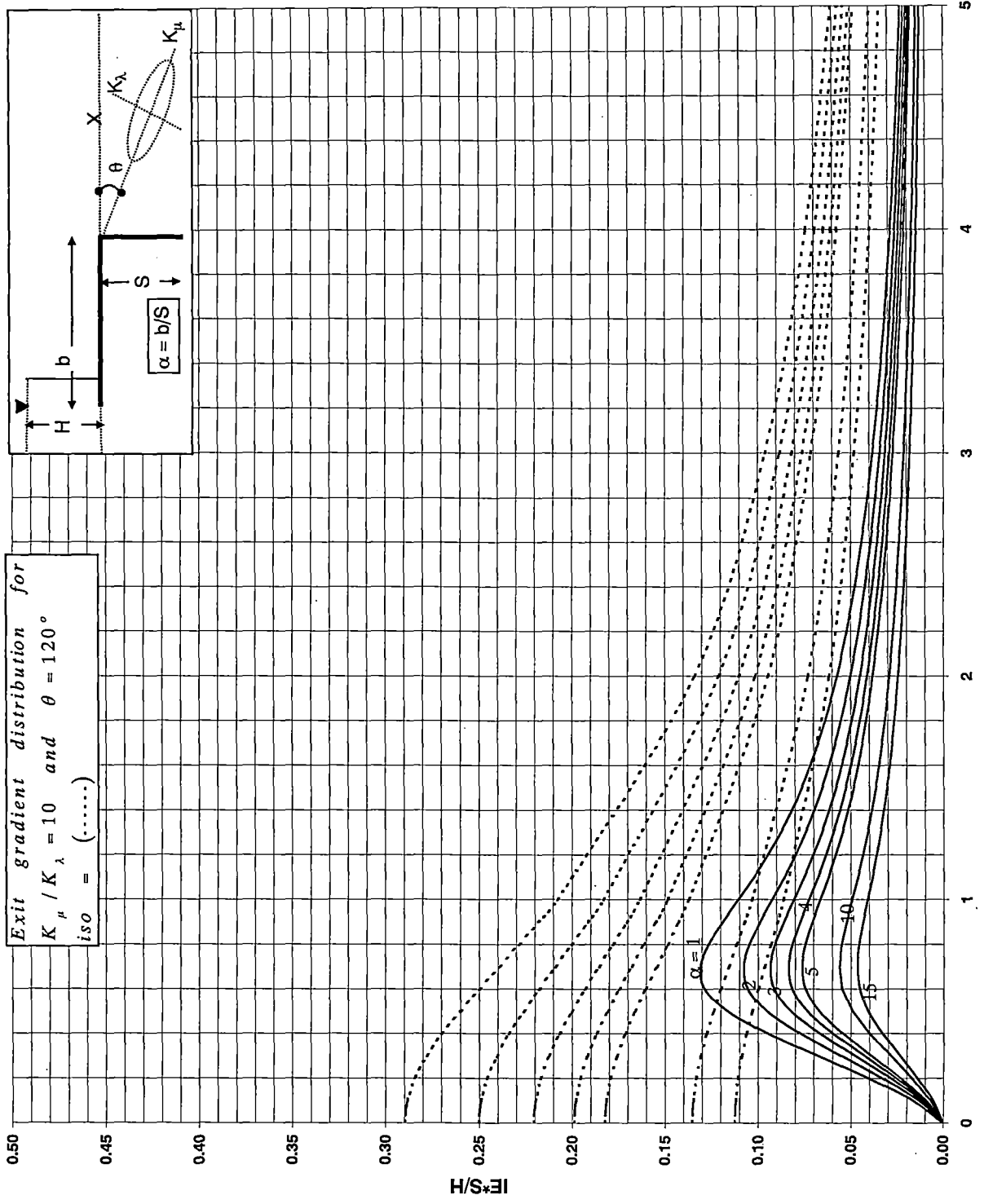


Fig.3.4(b3)

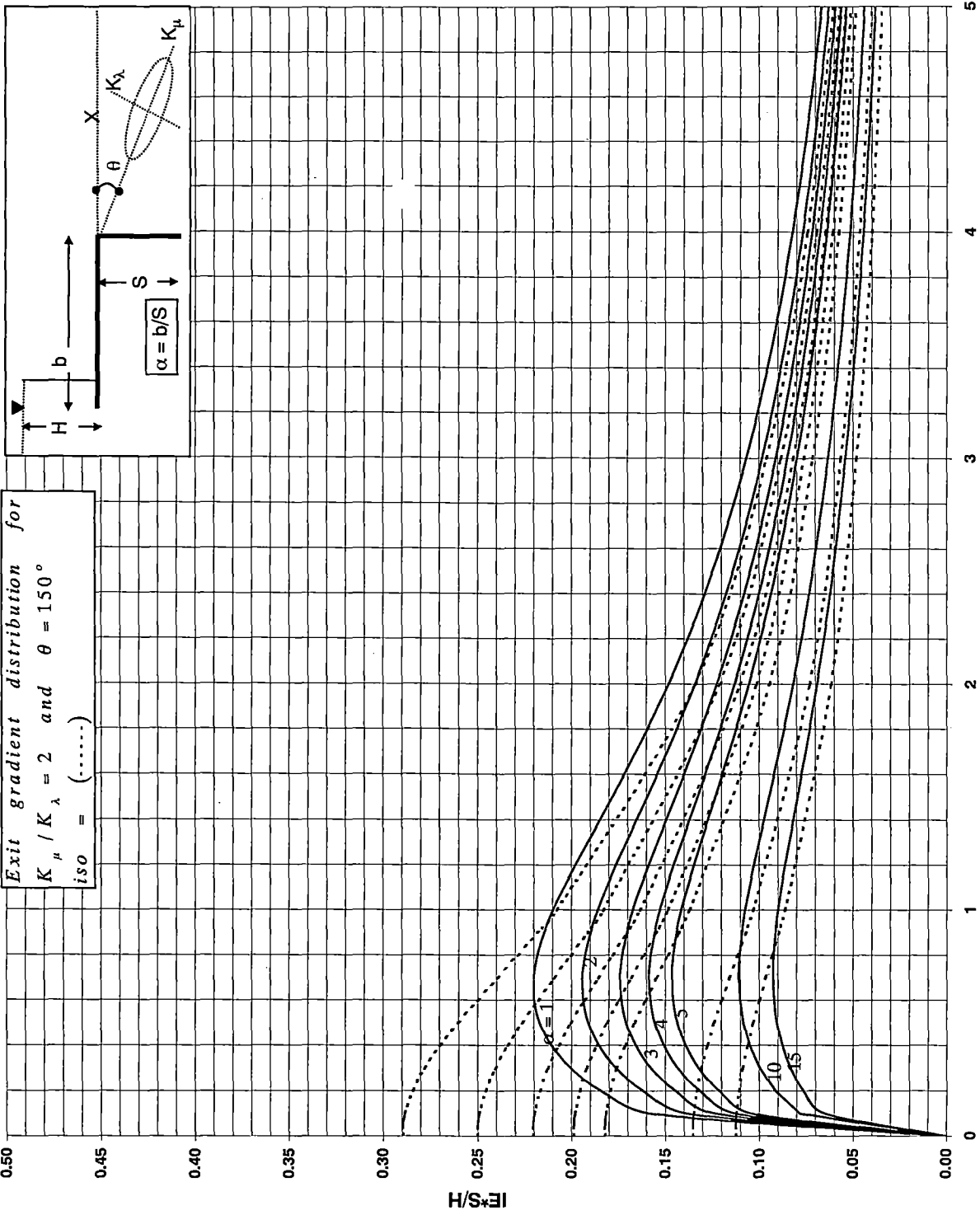


Fig.3.4(c1)

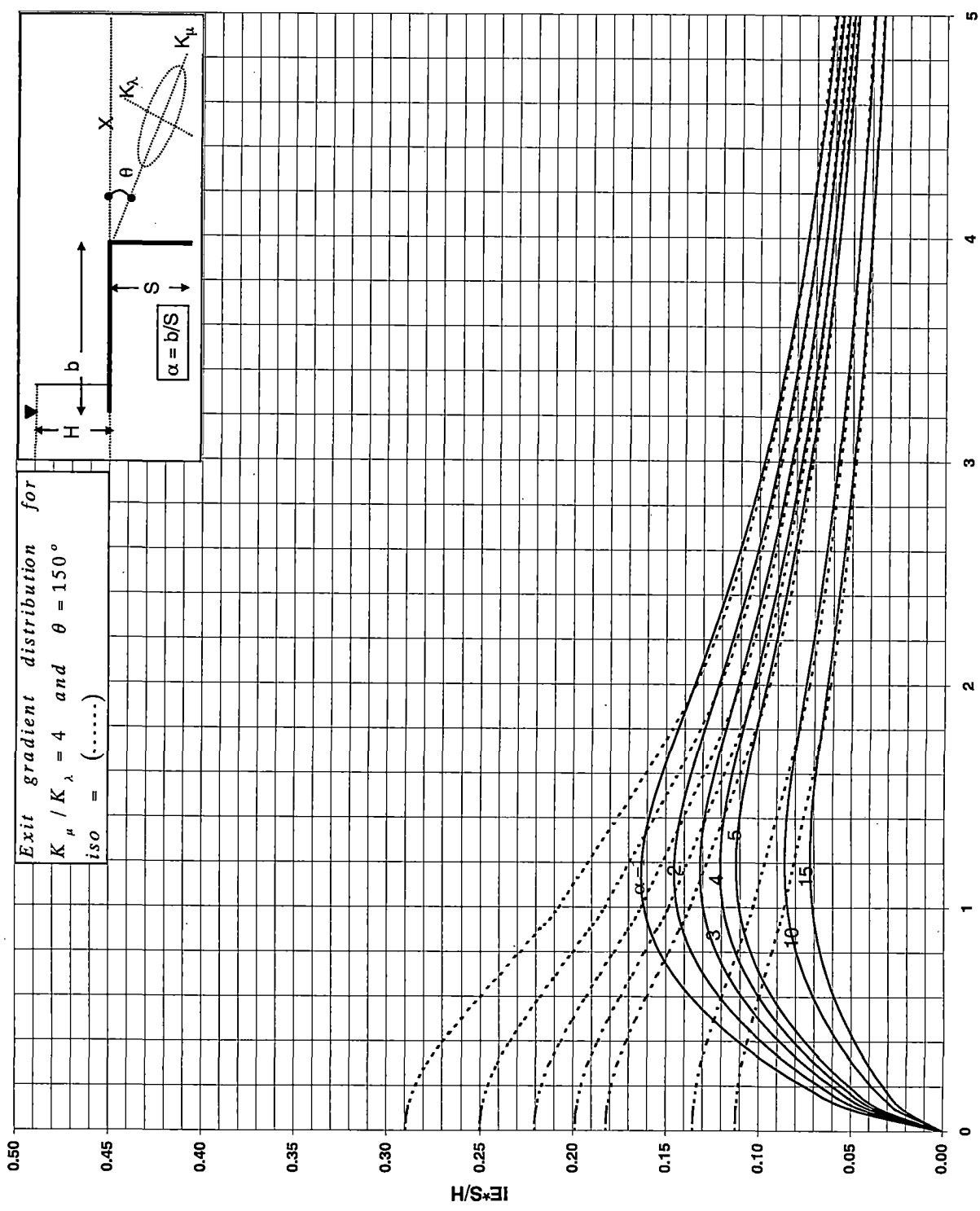


Fig. 3.4(c2)

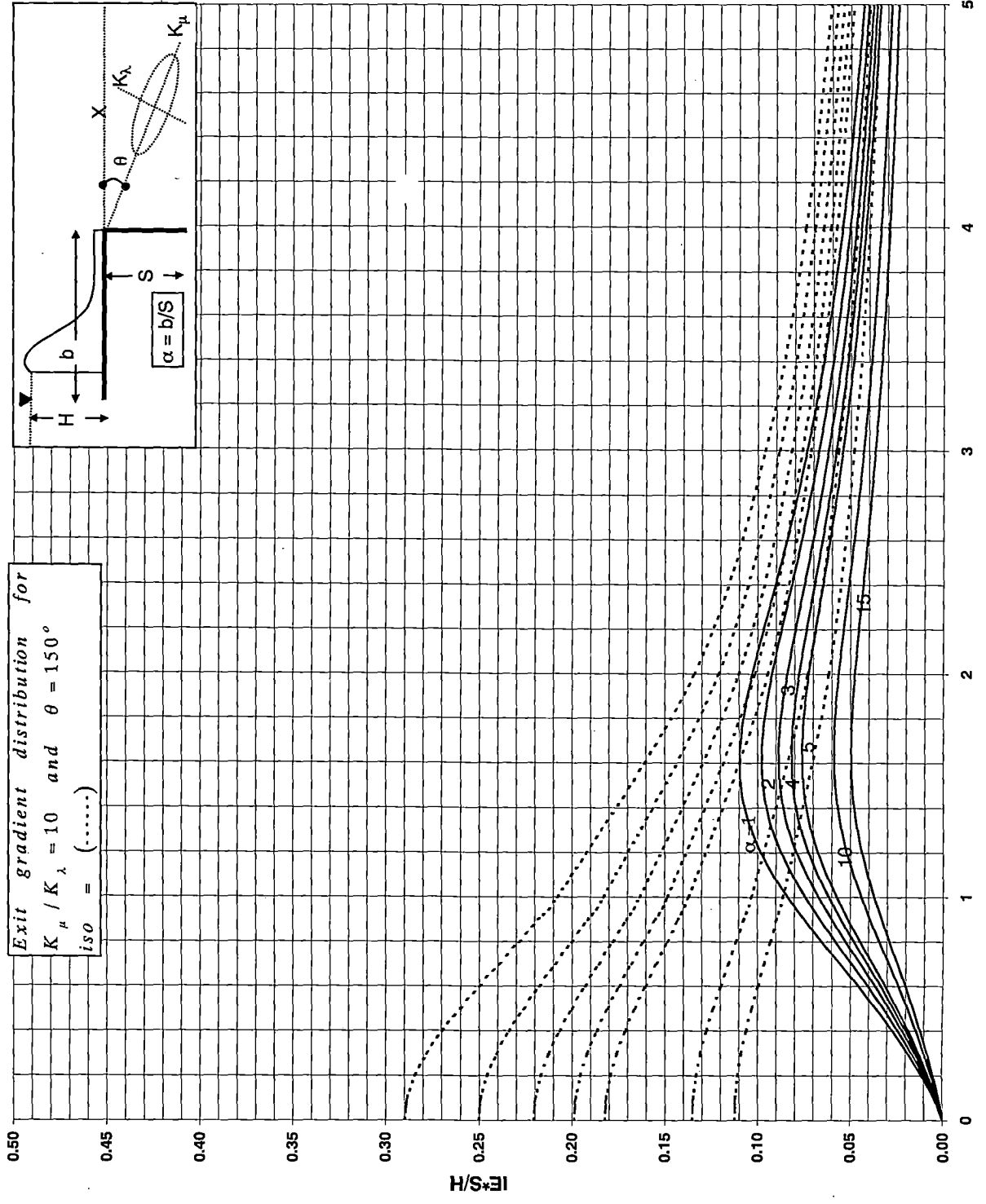


Fig.3.4(c3)

CHAPTER 4

DESIGN OF TOE STRUCTURE FOR CONTROLLING THE EXIT GRADIENT

4.1 General

The study of flow under a flat bottomed weir with a vertical sheet pile at the downstream end in an anisotropic porous medium reveals that in cases where inclination of maximum coefficient of permeability makes an angle $0 < \theta < \pi/2$ with the horizontal, the exit gradient becomes infinite near the downstream sheet pile, and therefore, the structure vulnerable to piping. In such cases, undermining would start at the downstream point of the sheet pile. Though the infinite gradient rapidly falls to a safe figure within a finite distance from the sheet pile, even then, a certain zone is subjected to gradient in excess of the critical, and piping is likely to start in this zone.

Flow under a controlling structure (other than sheet pile) that can govern the exit gradient in anisotropic domain has been analysed in this chapter.

4.2 Statement of the Problem

Fig.4.1 (a) shows a flat bottomed weir with a vertical sheet pile embedding a toe structure. The direction of maximum coefficient of permeability makes an angle θ , $0 < \theta < \pi/2$, with the horizontal axis ox , measured in clockwise direction. k_μ and k_λ are the magnitude of the maximum and minimum coefficients of permeability, respectively. The width of the apron is b and s is the length of the vertical sheet pile. An impervious toe structure is constructed flushed with the sheet pile downstream, x_2 and s_1 being the top width and the depth of the toe structure, respectively. The downstream face of the toe structure makes an angle ϕ with the horizontal as shown in the figure. It is required to find the shape (angle ϕ) and size of the toe structure so that the maximum exit gradient is finite.

4.3 Analysis

The actual anisotropic flow domain is transformed into fictitious isotropic flow domain using the co-ordinate transform equations given in appendix - I. The shape of the

toe structure should be such that the angle ϕ' gets transformed into $\pi/2$ with the horizontal in isotropic fictitious domain. Value of ϕ' can be obtained using the equation given in appendix II.

Let the x axis be transformed into \bar{x} axis and a vertical sheet pile in the anisotropic domain makes an angle $\gamma\pi$ with \bar{x} axis measured from upstream side in anti clockwise direction. Let in the fictitious flow domain the length of the oblique sheet pile be \bar{s} and the width of the structure be \bar{b} . The top width x_2 and the depth of the toe structure s_1 are converted to \bar{x}_2 and \bar{s}_1 , respectively. The equivalent section of the weir in the fictitious isotropic flow domain is shown in fig.4.1 (b).

The two dimensional flow under the weir in isotropic fictitious flow domain is analysed using the Schwarz-Christoffel transformation. The results obtained are then transferred to the corresponding points in the actual anisotropic flow domain. The values of exit gradient at a point in fictitious flow domain is multiplied by the magnification factor given in appendix - II to get the value of the exit gradient in the actual flow domain at the corresponding point.

First, the fictitious isotropic flow region in z plane is mapped onto the lower half of an auxiliary t plane and then the complex potential plane is mapped onto the lower half of the auxiliary t plane. From these two conformal mappings, the relationship between w and z plane is obtained. The Schwarz-Christoffel transformation for mapping the polygon $\overline{ACDEFGI}$ onto the lower half of the auxiliary t plane shown in fig.4.1 (d) is given by

$$z = M \int \frac{(t-m)(v-t)^{1/2}}{(1+t)^{1-\gamma}(1-t)^{\gamma}(\beta-t)^{1/2}} dt + N \quad \dots(4.3.1)$$

The vertices $\overline{A}, \overline{C}, \overline{D}, \overline{E}, \overline{F}, \overline{G}, \overline{I}$ being mapped onto $-\infty, -1, m, 1, v, \beta, \infty$, respectively. In eq. 4.3.1, M and N are constants to be determined. Let the point \overline{B} be mapped onto the points $t = -\beta_1$.

The correspondences between z and t are:

Vertex	t	z
C	-1	$Z_{\bar{C}} = 0$
D	m	$Z_{\bar{D}} = \bar{s} e^{(1-\gamma)i\pi}$
E	1	$Z_{\bar{E}} = \bar{s}_1 e^{(1-\gamma)i\pi} = -\bar{x}_1 + i\bar{d}$
		$\bar{x}_1 = \bar{s}_1 \cos \gamma\pi; \bar{d} = \bar{s}_1 \sin \gamma\pi.$
F	γ	$Z_{\bar{F}} = \bar{x}_2 + i\bar{d}$
G	β_2	$Z_{\bar{G}} = \bar{x}_2$

Integration between consecutive vertices are carried out to relate the geometrical dimension of the flow domain and the transformation parameter. Using the relations the constant M, and the unknown parameters m, v, β are found. The constant N is governed by the lower limit of integration.

i) Integration between vertices \bar{C} and \bar{D} ($-1 \leq t \leq m$)

$$Z_{\bar{D}} = M \int_{-1}^m \frac{(-t+m)(v-t)^{1/2}}{(1+t)^{1-\gamma}(1-t)^\gamma(\beta-t)^{1/2}} dt \quad \dots 4.3.2(a)$$

$$\text{or } \bar{s} e^{(1-\gamma)i\pi} = M I_1 \quad \dots 4.3.2(b)$$

$$\text{where } I_1 = \int_{-1}^m \frac{(-t+m)(v-t)^{1/2}}{(1+t)^{1-\gamma}(1-t)^\gamma(\beta-t)^{1/2}} dt$$

From 4.3.2(b)

$$M = \frac{\bar{s} e^{(1-\gamma)i\pi}}{I_1} \quad 4.3.2(c)$$

ii) Integration between vertices \bar{D} and \bar{E} ($m \leq t \leq 1$)

$$\begin{aligned} \bar{s}_1 e^{(1-\gamma)i\pi} &= -M \int_m^1 \frac{(t-m)(v-t)^{1/2}}{(t+1)^{1-\gamma}(1-t)^\gamma(\beta-t)^{1/2}} dt + \bar{s} e^{(1-\gamma)i\pi} \\ &= -\frac{\bar{s} e^{(1-\gamma)i\pi}}{I_1} I_2 + \bar{s} e^{(1-\gamma)i\pi} \end{aligned} \quad 4.3.3(a)$$

$$\text{where } I_2 = \int_m^1 \frac{(t-m)(\nu-t)^{1/2}}{(t+1)^{1-\gamma}(1-t)^\gamma(\beta-t)^{1/2}} dt$$

Simplifying

$$\bar{s} - \bar{s}_1 = \bar{s} \frac{I_2}{I_1} \quad 4.3.3(\text{b})$$

$$\text{or } \frac{\bar{s} - \bar{s}_1}{\bar{s}} = \frac{I_2}{I_1}$$

$$1 - \frac{\bar{s}_1}{\bar{s}} - \frac{I_2}{I_1} = 0 \quad 4.3.3(\text{c})$$

iii) Integration between vertices \bar{E} and \bar{F} ($1 \leq t \leq \nu$) leads to

$$\bar{x}_2 + i\bar{d} = \frac{\bar{s} e^{(1-\gamma)i\pi}}{I_1} \int_1^\nu \frac{(m-t)(\nu-t)^{1/2}}{(1+t)^{1-\gamma}(1-t)^\gamma(\beta-t)^{1/2}} dt - \bar{x}_1 + i\bar{d} \quad (4.3.4(\text{a}))$$

$$\text{or } \bar{x}_2 + \bar{x}_1 = \frac{\bar{s} e^{(1-\gamma)i\pi}}{I_1} \int_1^\nu \frac{(-1)(t-m)(\nu-t)^{1/2}}{(1+t)^{1-\gamma}(1-t)^\gamma(\beta-t)^{1/2}} dt \quad 4.3.4(\text{b})$$

considering $-1 = e^{-i\pi}$, Eq. (4.3.4(b)) reduces to

$$\frac{\bar{x}_2}{\bar{s}} + \frac{\bar{x}_1}{\bar{s}} - \frac{I_3}{I_1} = 0 \quad 4.3.4(\text{c})$$

$$\text{or } \frac{\bar{x}_2}{\bar{s}} + \frac{\bar{x}_1}{\bar{s}} \cos \gamma\pi - \frac{I_3}{I_1} = 0$$

$$\text{where } I_3 = \int_1^\gamma \frac{(t-m)(\gamma-t)^{\frac{1}{2}} dt}{(1+t)^{1-\gamma}(t-1)^\gamma(\beta-t)^{\frac{1}{2}}}$$

iv) Integration between vertices \bar{F} and \bar{G} ($\gamma \leq t \leq \beta$) leads to

$$x_2 = \frac{se^{i(1-\gamma)\pi} \int_{\gamma}^{\beta} \frac{(m-t)(\gamma-t)^{\frac{1}{2}}}{(1+t)^{1-\gamma} (1-t)^{\gamma} (\beta-t)^{\frac{1}{2}}} dt + x_2 + id}{I_1} \quad [4.3.5(a)]$$

$$= \frac{se^{i(1-\gamma)\pi} \int_{\gamma}^{\beta} \frac{(-)(t-m)(-1)^{\frac{1}{2}}(t-\gamma)^{\frac{1}{2}}}{(-1)^{\gamma} (1+t)^{1-\gamma} (t-1)^{\gamma} (\beta-t)^{\frac{1}{2}}} dt + x_2 + id}{I_1} \quad [4.3.5(b)]$$

simplifying

$$\frac{d}{s} - \frac{I_4}{I_1} = 0$$

$$\text{or } \frac{S_1}{S} \sin \gamma\pi - \frac{I_4}{I_1} = 0 \quad [4.3.5(c)]$$

$$\text{where } I_4 = \int_{\gamma}^{\beta} \frac{(t-m)(t-\gamma)^{\frac{1}{2}}}{(1+t)^{1-\gamma} (t-1)^{\gamma} (\beta-t)^{\frac{1}{2}}} dt$$

The parameter m, γ and β can be solved from equations 4.3.3 (c), 4.3.4 (c) and 4.3.5 (c),

$$\text{for known values of } \gamma, \frac{d}{s}, \frac{S_1}{s} \text{ and } \frac{x_2}{s}$$

Determination of β_1

For point \bar{B} , $z_{\bar{B}} = -\bar{b}$ and $t = -\beta_1$

Integration between \bar{B} and \bar{C} ($-\beta_1 \leq t \leq -1$) leads to

$$-\bar{b} = \frac{se^{i(1-\gamma)\pi} \int_{-1}^{-\beta_1} \frac{(m-t)(\gamma-t)^{\frac{1}{2}}}{(1+t)^{1-\gamma} (1-t)^{\gamma} (\beta-t)^{\frac{1}{2}}} dt}{I_1}$$

$$= \frac{se^{i(1-\gamma)\pi} \int_{-1}^{-\beta_1} \frac{(m-t)(\gamma-t)^{\frac{1}{2}}}{(-1)^{1-\gamma} (-1-t)^{1-\gamma} (1-t)^{\gamma} (\beta-t)^{\frac{1}{2}}} dt}{I_1}$$

Let $t = -\tau$

$$\bar{b} = \frac{\bar{s} e^{i(1-\gamma)\pi} \int_1^{\beta_1} \frac{(m+\tau)(\gamma+\tau)^{\frac{1}{2}}}{(\tau-1)^{1-\gamma} (1+\tau)^\gamma (\beta+\tau)^{\frac{1}{2}}} d\tau}{I_1 - (1)^{1-\gamma}}$$

or $\frac{\bar{b}}{\bar{s}} = \frac{I_5}{I_1}$ (4.3.6)

in which
$$I_5 = \int_1^{\beta_1} \frac{(m+\tau)(\gamma+\tau)^{\frac{1}{2}}}{(\tau-1)^{1-\gamma} (1+\tau)^\gamma (\beta+\tau)^{\frac{1}{2}}} d\tau$$

β_1 can be found using an iteration procedure for known $\frac{\bar{b}}{\bar{s}}$

Determination β_2

For point \bar{H} , $z_{\bar{H}} = \bar{L}$ and $t = \beta_2$

Integrating between \bar{G} and \bar{H} ($1 \leq t \leq \beta_2$)

$$\bar{L} - \bar{x}_2 = \frac{\bar{s} e^{i(1-\gamma)\pi} \int_{\beta}^{\beta_2} \frac{(m-t)(\gamma-t)^{\frac{1}{2}}}{(1+t)^{1-\gamma} (1-t)^\gamma (\beta-t)^{\frac{1}{2}}} dt}{I_1}$$

$$\frac{\bar{L}}{\bar{s}} - \frac{\bar{x}_2}{\bar{s}} = \frac{e^{i(1-\gamma)\pi} \int_{\beta}^{\beta_2} \frac{(-)(-1)^{\frac{1}{2}} (t-m)(t-\gamma)^{\frac{1}{2}}}{(-1)^{\gamma+1} (1+t)^{1-\gamma} (t-1)^\gamma (t-\beta)^{\frac{1}{2}}} dt}{I_1}$$

$$\frac{\bar{L}}{\bar{s}} - \frac{\bar{x}_2}{\bar{s}} = \frac{I_6}{I_1}$$
 (4.3.7)

where
$$I_6 = \int_{\beta}^{\beta_2} \frac{(t-m)(t-\gamma)^{\frac{1}{2}}}{(1+t)^{1-\gamma} (t-1)^\gamma (t-\beta)^{\frac{1}{2}}} dt$$

Mapping of w plane onto t plane:

The complex potential w is defined as $w = \phi + i\Psi$ in which ϕ = velocity potential and Ψ = stream function. The velocity potential function ϕ is defined as

$$\phi = -k \left(\frac{P}{\gamma_w} - y \right) + C \quad \dots(4.3.8)$$

in which $C = kh_2$

The w plane for the flow domain is shown in fig.4.1(c)

The mapping of the w plane onto the lower half of the t plane according to the Schwarz-Christoffel transformation is given by

$$w = M_2 \int \frac{dt}{(t+\beta_1)^{1/2} (t-\beta)^{1/2}} + N_2 \quad \dots(4.3.9)$$

$$\text{or } w = M_2 \sin^{-1} \frac{2t + \beta_1 - \beta}{\beta_1 + \beta} + N_2 \quad \dots(4.3.10)$$

in which M_2 and N_2 are constants.

For point \bar{G} , $t = \beta$ and $w = 0$, therefore, $N_2 = -M_2 \pi/2$

For point \bar{B} , $t = -\beta_1$ and $w = -kh$ gives

$$M_2 = kh/\pi$$

Substituting the values of M_2 and N_2 in eq. 4.3.10

$$w = \frac{kh}{\pi} \sin^{-1} \frac{2t + \beta_1 - \beta}{\beta_1 + \beta} - \frac{kh}{2} \quad \dots(4.3.11)$$

Exit gradient

The exit gradient I_E is given by

$$I_E = \frac{i}{k} \frac{dw}{dt} \frac{dt}{dz}$$

Replacing $\frac{dw}{dt}$ from eq.4.3.9 and $\frac{dz}{dt}$ from eq.4.3.1, and simplifying,

$$\bar{I}_E \frac{\bar{s}}{H} = \frac{I_1}{\pi} \frac{1}{(t + \beta_1)^{1/2} (t - \nu)^{1/2}} \frac{(1+t)^{1-\gamma} (t-1)^\gamma}{(t-m)} \quad (4.3.12)$$

Substituting the value of $t \geq \beta$, the exit gradient at a point along the reservoir boundary \overline{GH} can be found.

The maximum exit gradient occurs at point \bar{G} , thus, putting the value of $t = \beta$, the maximum exit gradient is given by,

$$\bar{I}_{E \max} \frac{\bar{s}}{H} = \frac{I_1}{\pi} \frac{1}{(\beta + \beta_1)^{1/2} (\beta - \nu)^{1/2}} \frac{(1+\beta)^{1-\gamma} (\beta-1)^\gamma}{(\beta-m)} \quad \dots(4.3.13)$$

4.4 Results and Discussion

Numerical results are presented so that the shape and size of the toe structure for a weir with a vertical sheet pile constructed in an anisotropic flow domain with can be readily obtained corresponding to desired (safe) maximum exit gradient. Only inclinations $\theta = 30^\circ$ and 60° been considered.

The procedure adopted to arrive at the results presented in this chapter, is as follows:

We define the following ratios to transform the results from fictitious isotropic domain to that at actual anisotropic domain:

$$\frac{\bar{b}}{b} = r_1;$$

$$\frac{\bar{s}}{s} = r_2;$$

$$\alpha = \frac{\bar{b}}{s} = \frac{r_1}{r_2} = r_3;$$

$$\alpha = \frac{\bar{\alpha}}{r_3};$$

The ratios r_1 and r_2 depend only on degree of anisotropy and orientation of the principle permeability direction. The correspondence between points in the fictitious and actual flow domain is as follows:

$$x = \frac{\bar{x}}{\left(\frac{\bar{b}}{b}\right)},$$

A point on the vertical sheet pile in anisotropic domain is given by :

$$r e^{i\pi} = \frac{\bar{r} e^{(1-\gamma)i\pi}}{r_2}, \text{ where } \bar{r} \text{ is the point on the inclined sheet pile in fictitious}$$

isotropic domain.

Exit gradient at a point in the anisotropic flow domain is given by:

$$\frac{I_{E S}}{H} = \frac{\bar{I}_{E S}}{H r_2} * mf, \text{ where } \bar{I}_E \text{ is the exit gradient at the corresponding point in}$$

the fictitious domain and mf is the magnification factor as depicted in appendix A-II.

The variations of maximum exit gradient with s_1/s , has been obtained for different values of α with top width of the toe as 0 and 0.1s for the inclination of downstream face of the toe structure with the horizontal (ϕ') and are shown in fig. 4.2(a1.1) through fig. 4.2(b3.2).

From the curves, it is seen that the exit gradient decreases as α increases. Initially, the rate of decrease is slow, then the gradient decreases when $\alpha > 1$. The decrease at higher value of α is monotonic. For example, for $\theta = 30^\circ$, $k_\mu/k_\lambda = 10$, $s_1/s = 0.1$ and $x_2/s = 0.1$, from the figure 4.2(a3.2), it is seen that as α increases from 0 to 1.4, $I_{E \max} * s/H$ decreases from 0.417 to 0.408; as α increases from 1.4 to 2.8, $I_{E \max} * s/H$ decreases from 0.408 to 0.35; and as α increases from 10.2 to 11.6, $I_{E \max} * s/H$ decreases from 0.208 to 0.197. For an increment in α by 1.4, initially $I_{E \max}$ decreases by 2.16%, then it decreases by 14.20% and afterwards it decreases by about 5%. As the depth of toe structure increases exit gradient decreases but the rate of decrease decreases. For example, for $\theta = 30^\circ$, $k_\mu/k_\lambda = 10$, $s_1/s = 0.1$ and $x_2/s = 0.1$, from the figure 4.2(a3.2), it is seen that as s_1/s increases from 0.1 to 0.2, $I_{E \max} * s/H$ decreases from 0.417 to 0.3096 and as s_1/s increases from 0.1 to 0.2, $I_{E \max} * s/H$ decreases from 0.3096 to 0.259. For an increment of s_1/s by 0.1, initially $I_{E \max}$ decreases by 25.75%, and then it decreases by 16.34% and so on. In addition, it is seen that for small value of s_1/s , the effect of top width of the toe structure

is negative, i.e. it increases the exit gradient while for large value of s_1/s , it decreases the exit gradient but the amount decrease is insignificant.

A numerical example is worked out below to show the use of the results obtained.

Illustrative Example:

For the data given for example in chapter 3, design a suitable toe structure so that minimum factor of safety against piping should not be less than 5. Take $\theta = 30^\circ$

Solution.

$$\alpha = 5, s = 5, H = 5, k_\mu / k_\lambda = 10$$

For a factor of safety ≥ 5

$$I_{E_{\max}} * s / H \leq (1/5) * s / H$$

$$I_{E_{\max}} * s / H \leq 0.20$$

Take top width of the toe structure $x_2 = 0$

From the fig.4.2 (a3.1), the angle $\phi' = 39.82^\circ$

For $\alpha = 5$ and $I_{E_{\max}} * s / H = 0.2$, $s_1/s = 0.25$

Let us take $s_1/s = 0.30$, the corresponding $I_{E_{\max}} * s / H = 0.1823$.

Available factor of safety against piping = $1/0.1823 = 5.49 > 5$

The section of the toe structure is as follows:

Top width of the structure = 0 (triangular section)

Depth of the structure $s_1 = 0.3 * s = 0.3 * 5 = 1.50$ m.

Bottom width of the structure = $s_1 / \tan \phi = 1.50 / \tan 39.82^\circ = 1.80$ m.

4.5 Conclusion

Based on the results presented in this chapter the following conclusions are drawn:

For $0 < \theta < \pi/2$, the maximum exit gradient, just down stream of the structure becomes infinite, which makes the structure unstable against piping, in such cases the exit gradient can be controlled by providing a suitable toe structure. The inclination of the

down stream face of the toe structure with the horizontal should be such that, in transformed fictitious isotropic flow domain, the face makes an angle $\leq \pi/2$ with the transformed x axis. If the inclination of the toe structure is placed in such a way that in transformed fictitious flow domain, it makes an angle $\pi/2$ with the transformed x axis, then the maximum exit gradient is finite and occurs just downstream of the structure.

The value of the maximum exit gradient can be decreased by increasing the depth of toe structure. The effect of increasing the depth of toe structure is more effective for decreasing the exit gradient for small value of α as compared to large value of α .

For small depth of the toe structure, the effect of top width of the toe structure is not preferable, i.e. it increases the exit gradient while for large depth of toe structure, it decreases the exit gradient. Therefore, minimum possible top width of toe structure, feasible from practical point of view, will be appropriate one.

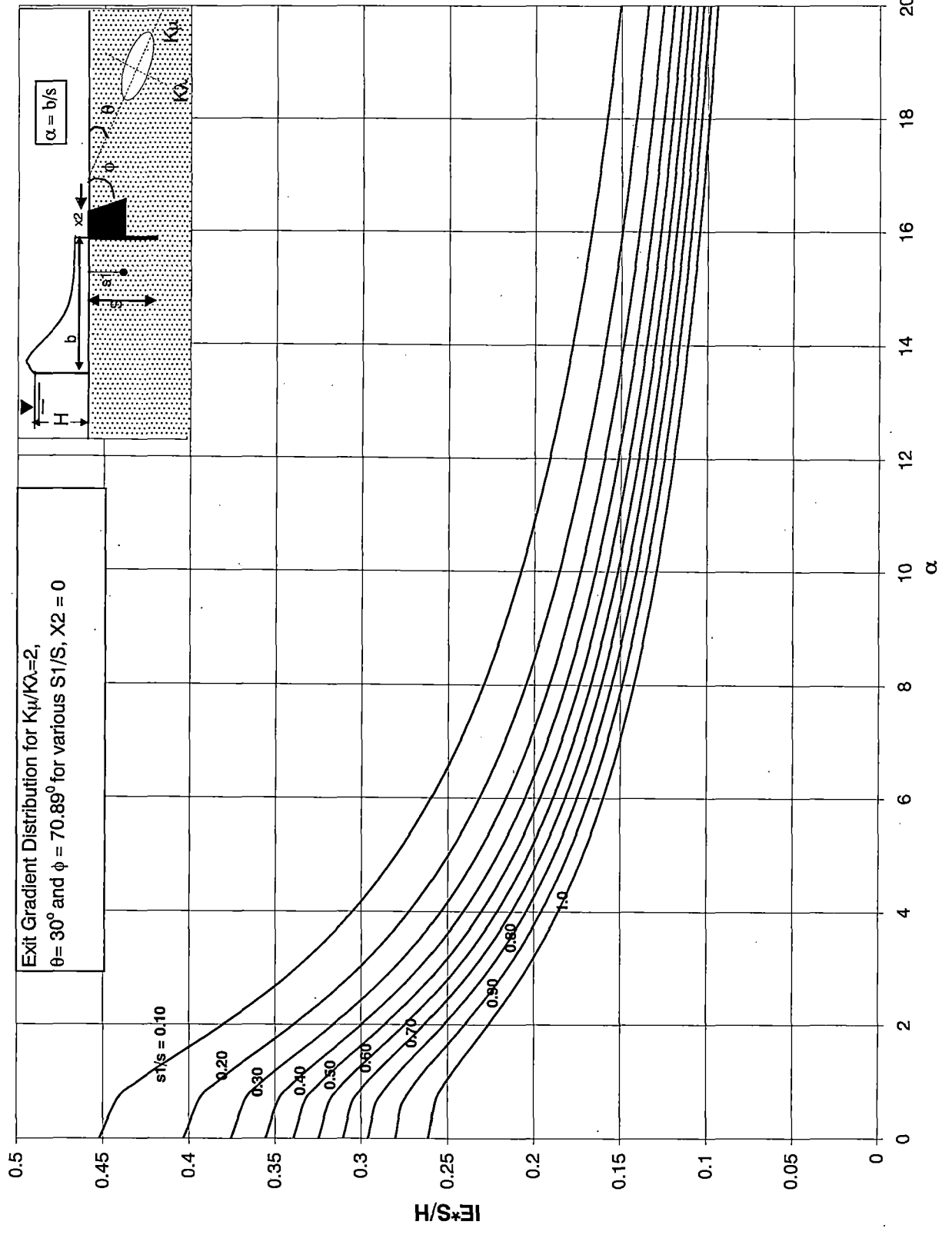


Fig.4.2(a1.1)

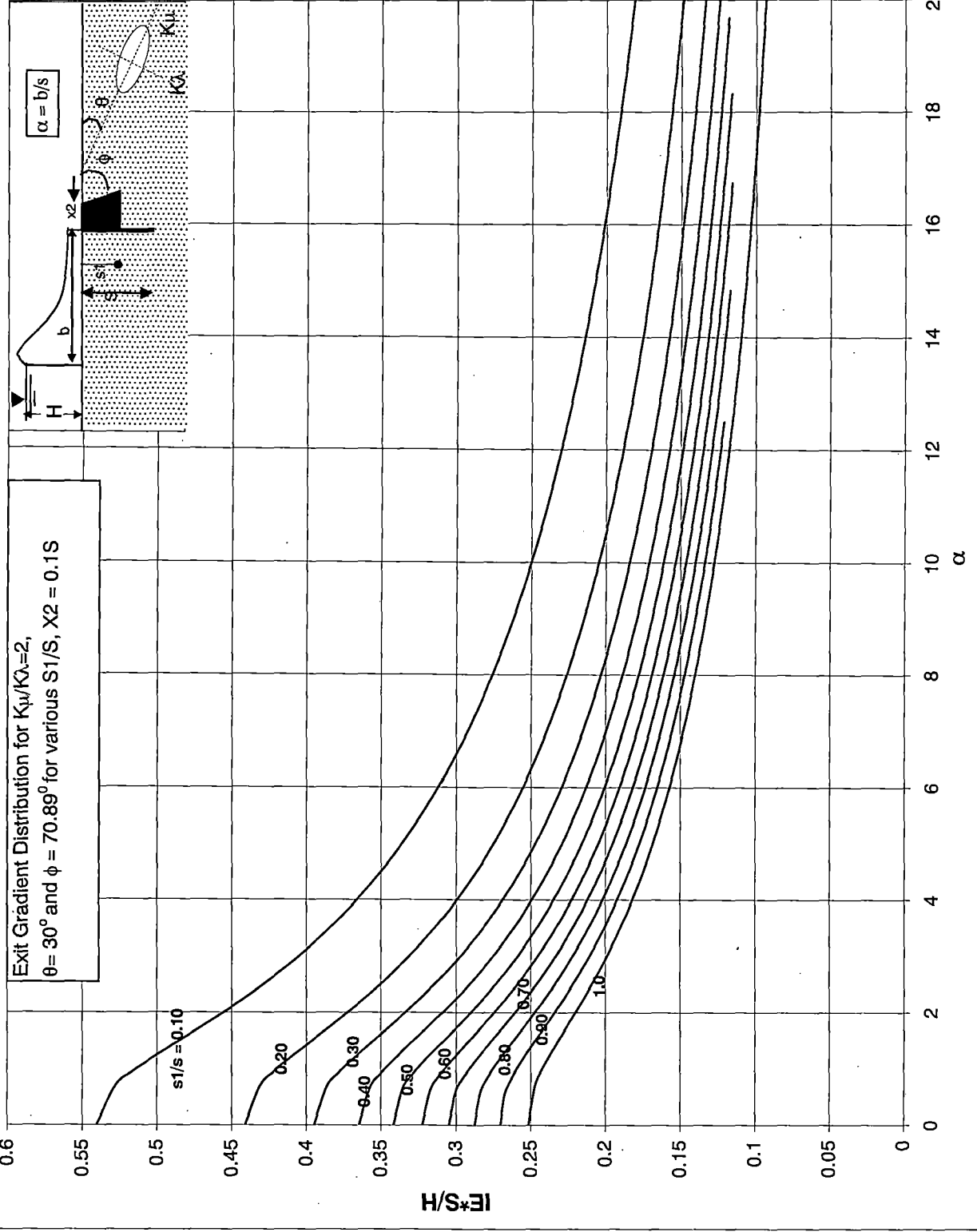


Fig.4.2(a1.2)

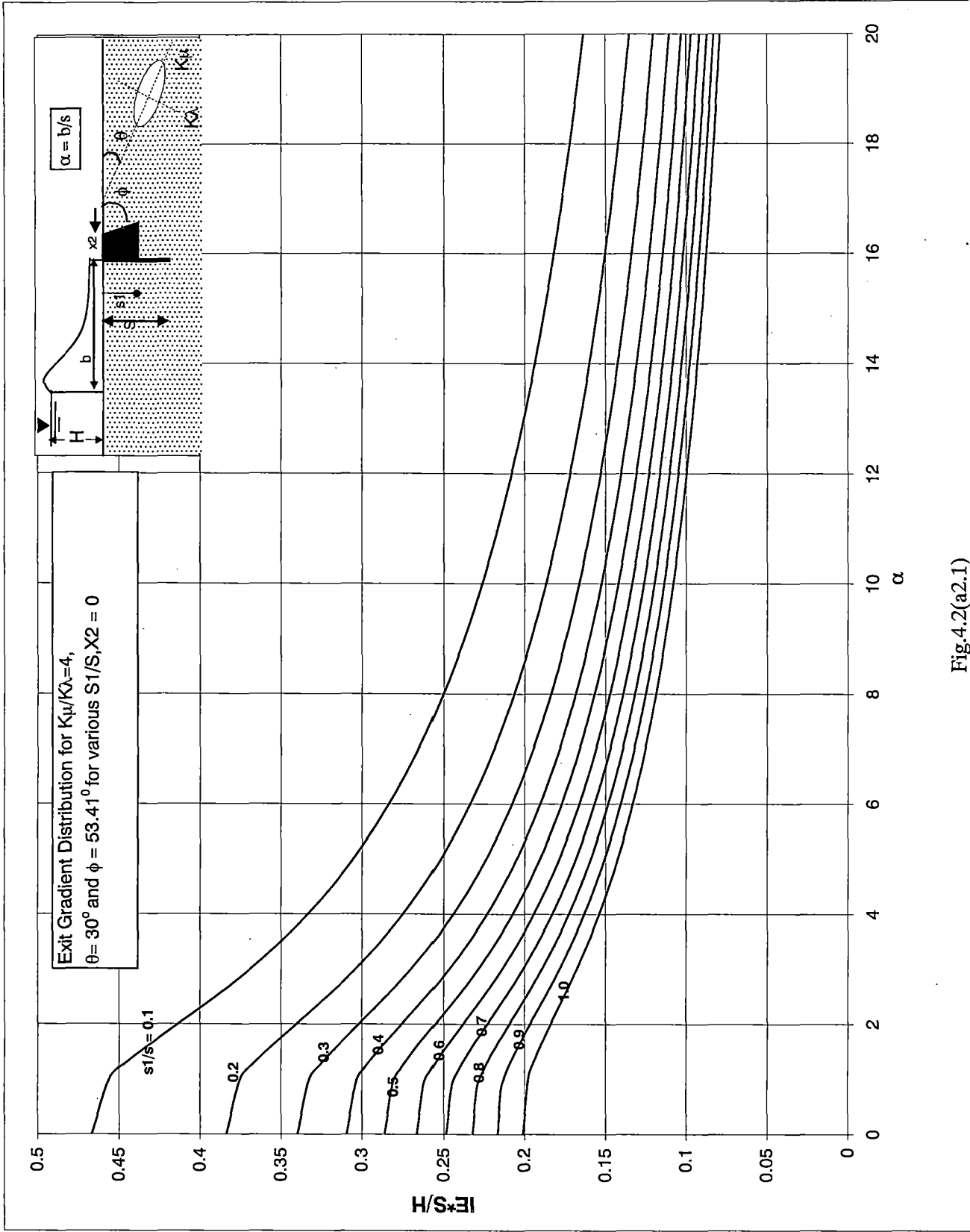


Fig.4.2(a2.1)

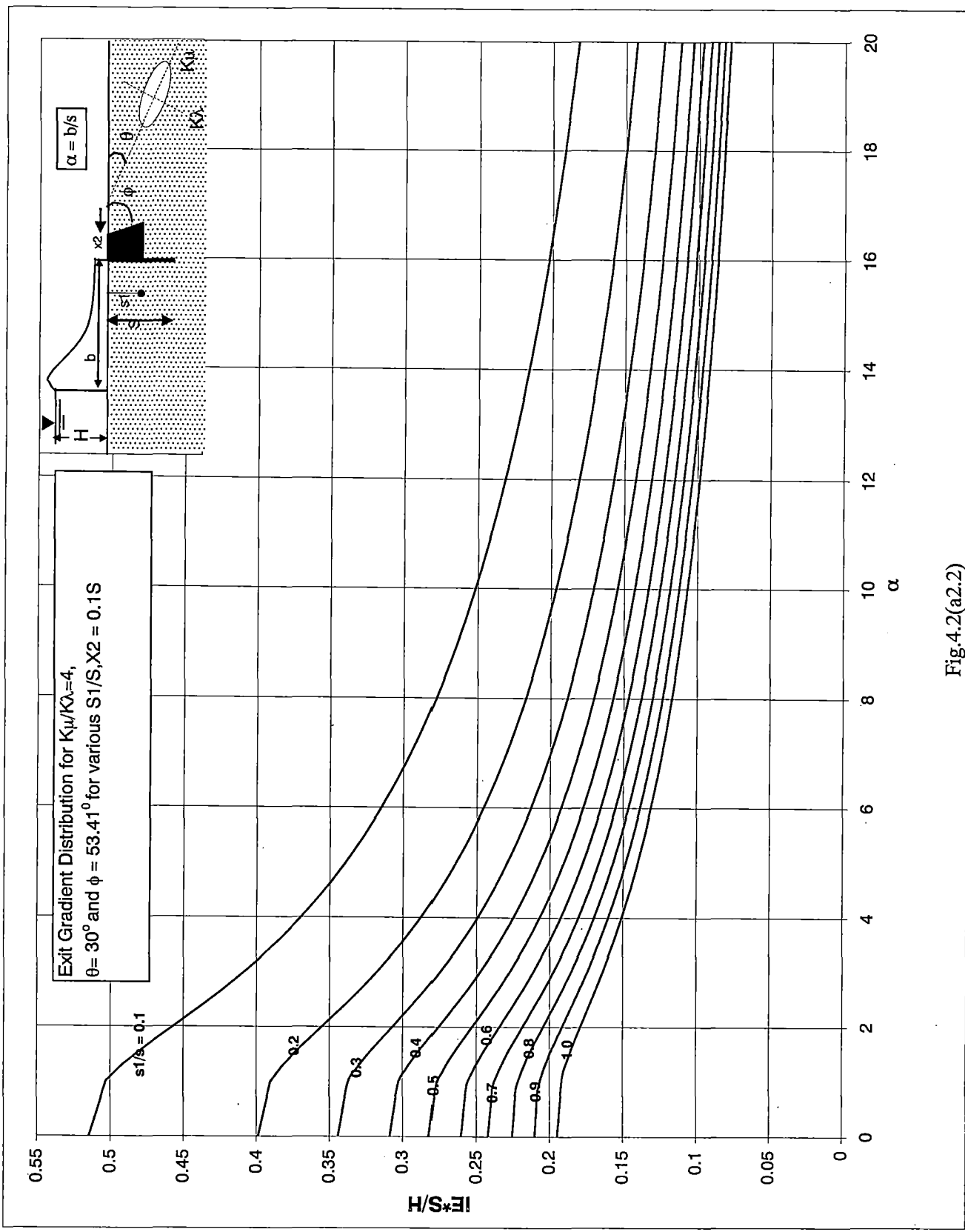


Fig.4.2(a2.2)

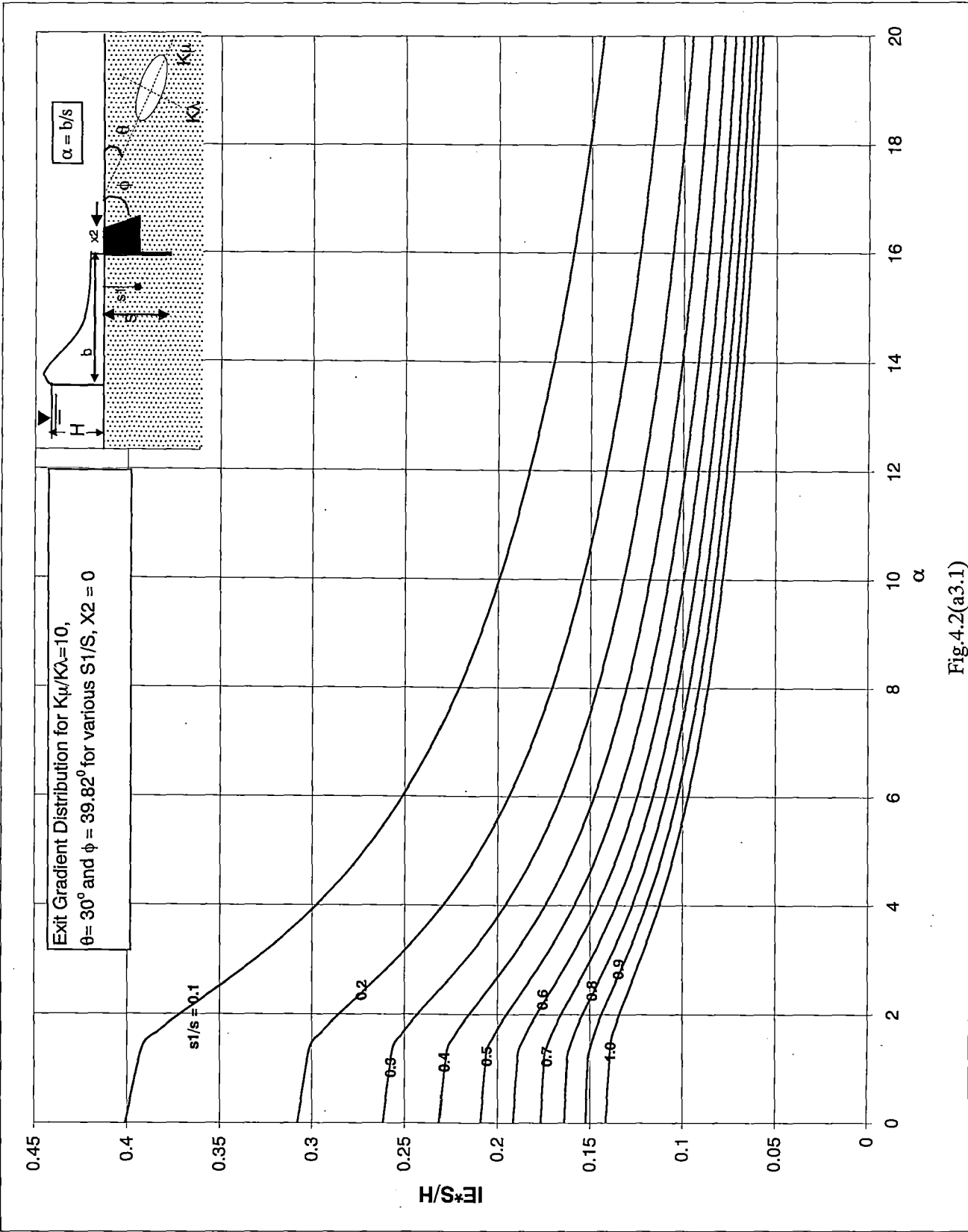


Fig.4.2(a3.1)

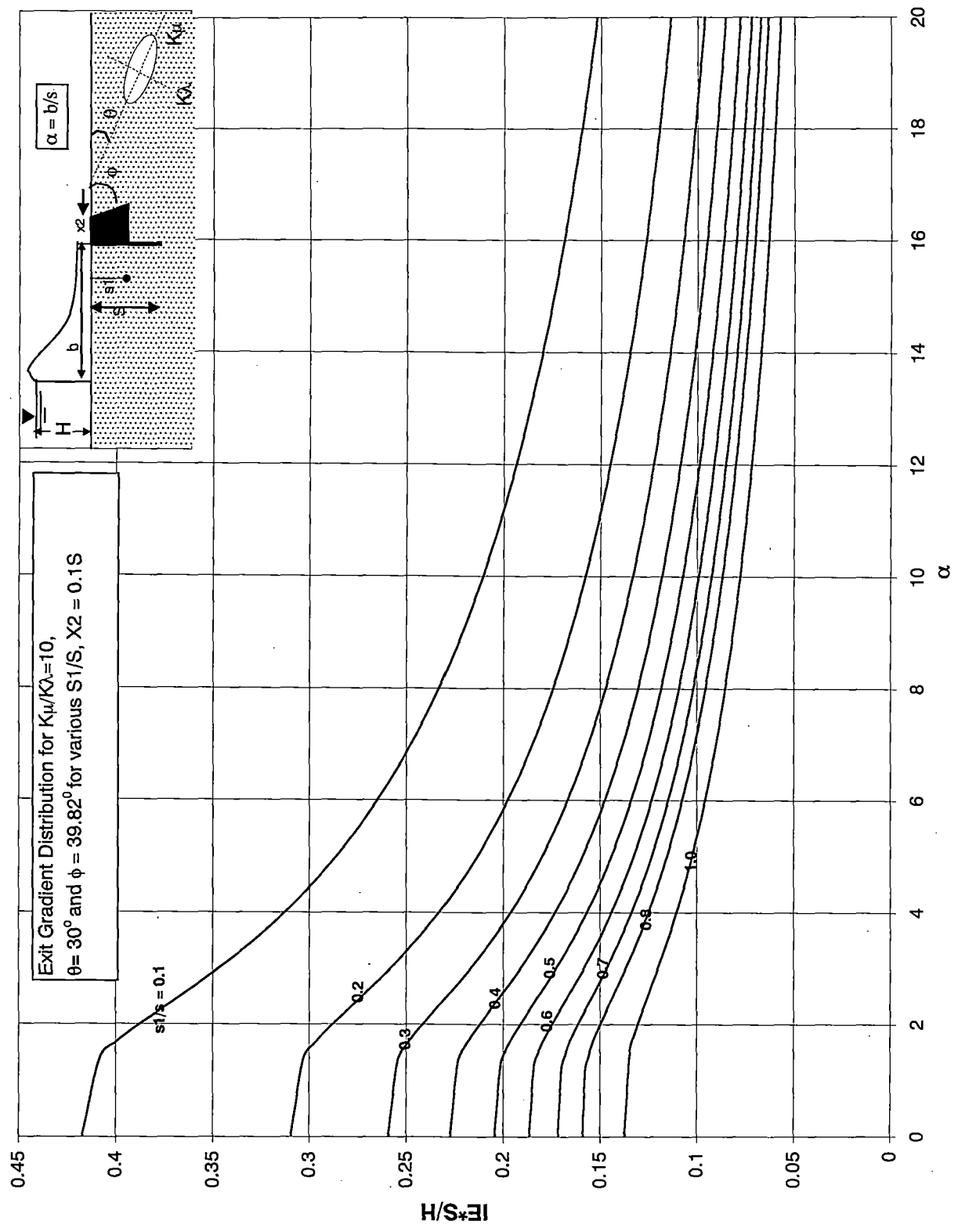


Fig.4.2(a3.2)

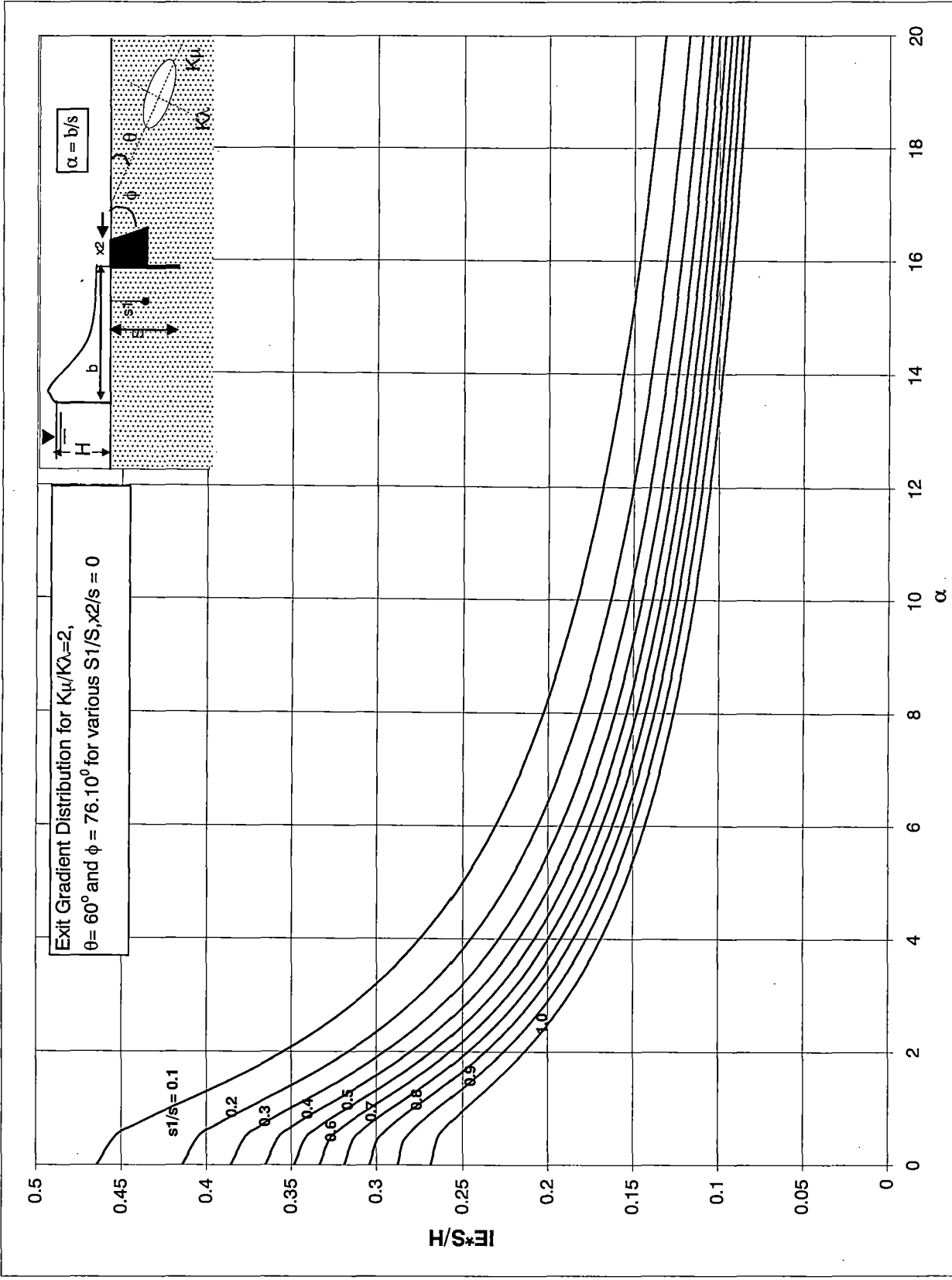


Fig.4.2(b1.1)

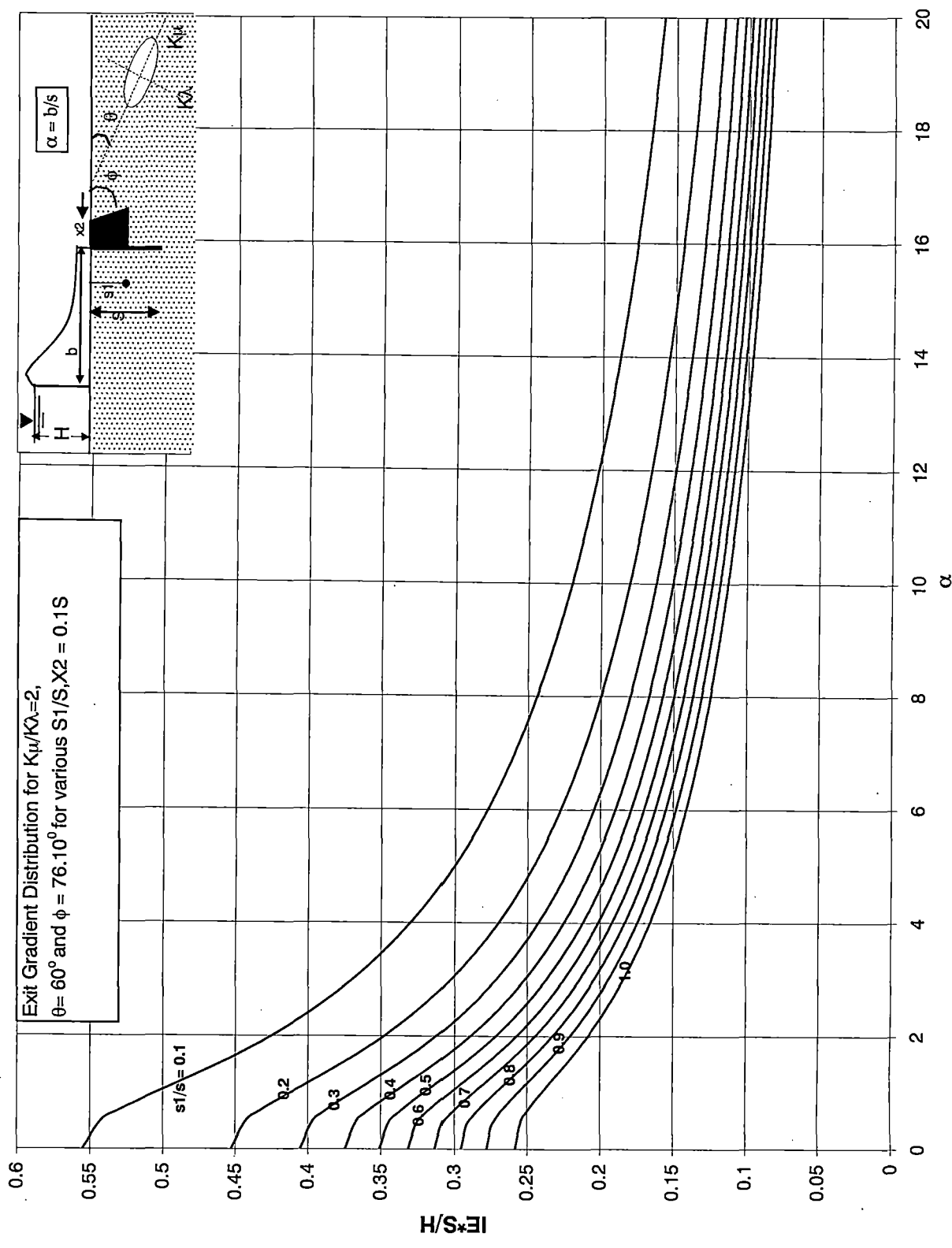


Fig.4.2(b1.2)

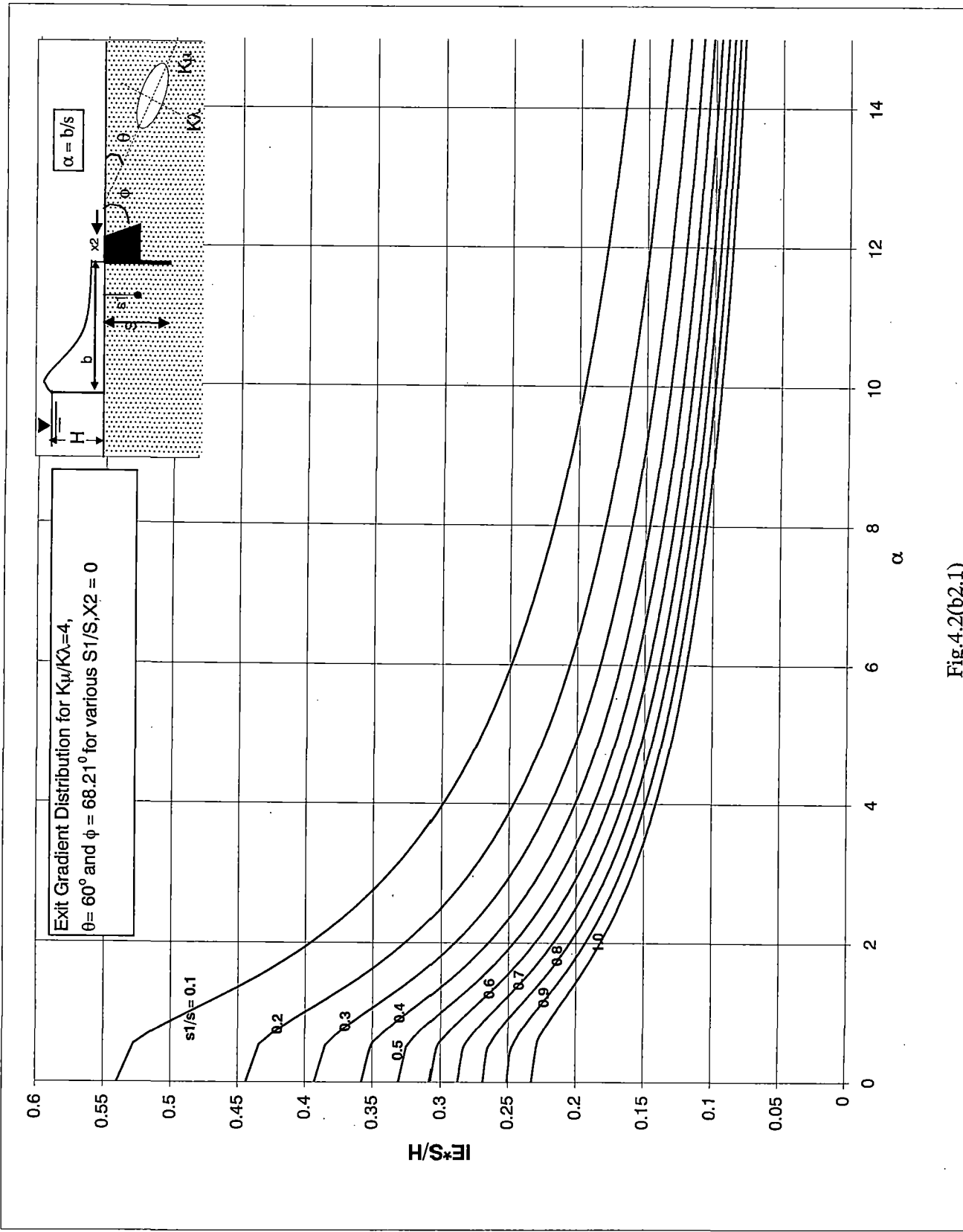


Fig.4.2(b2.1)

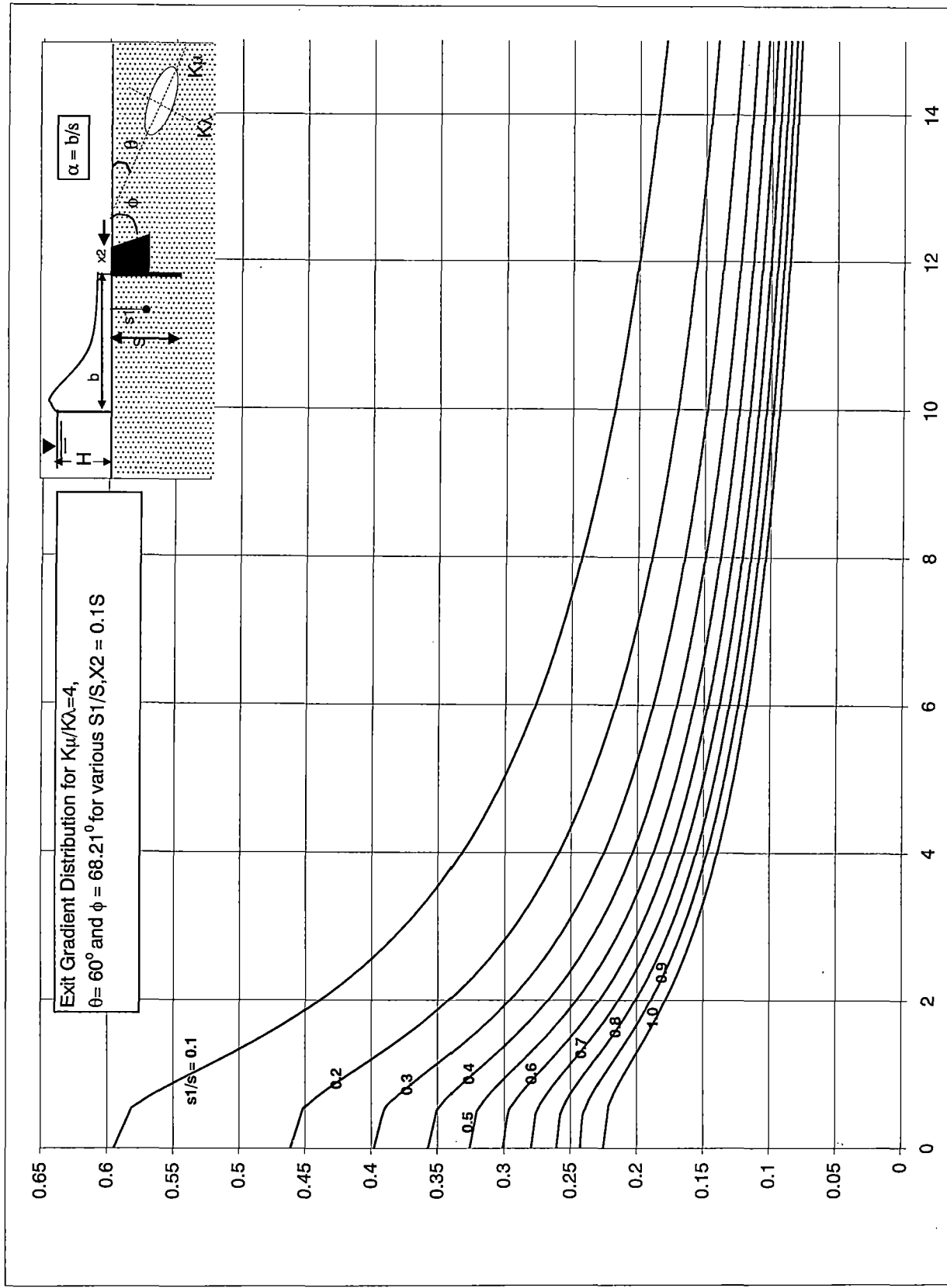


Fig.4.2(b2.2)

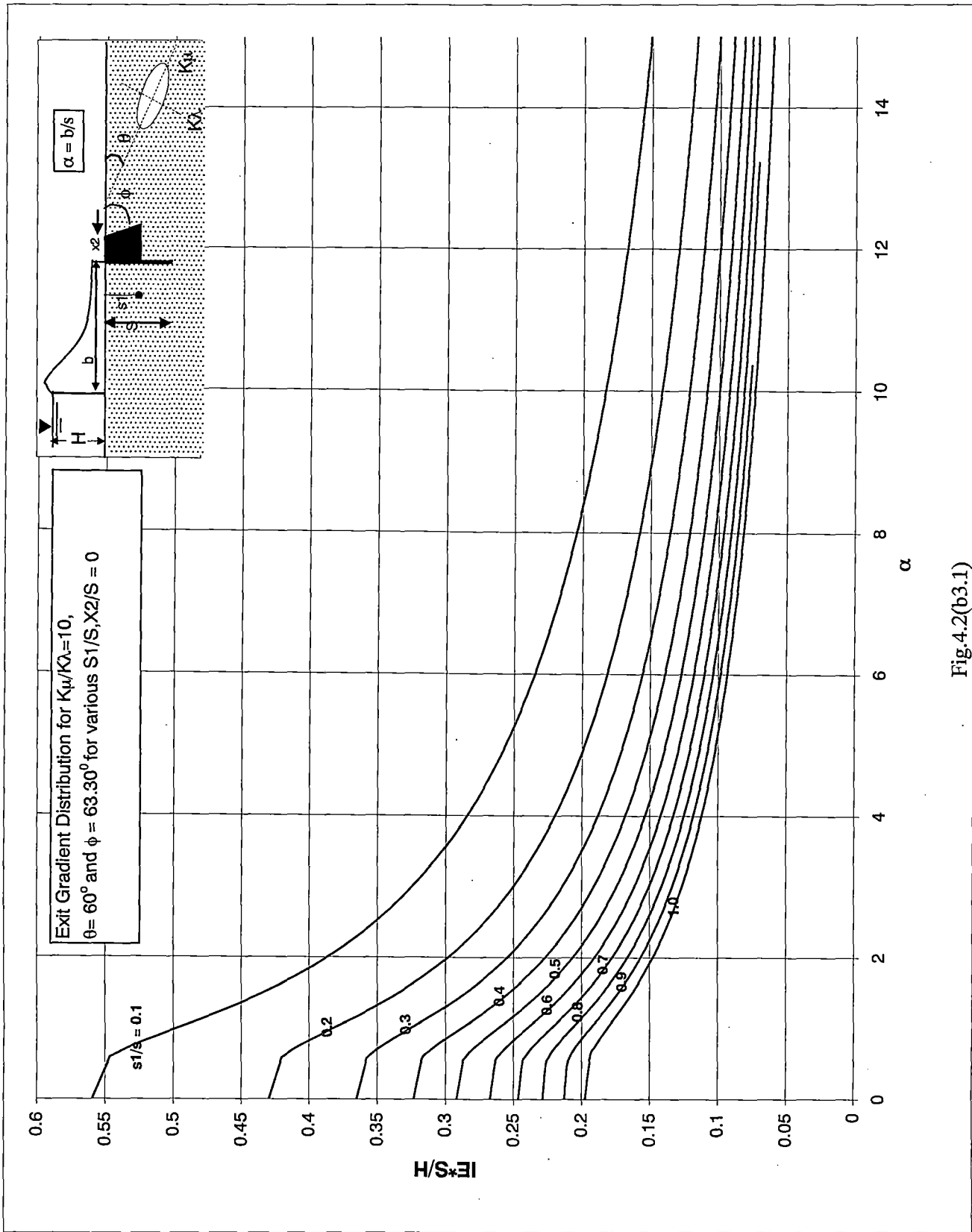


Fig.4.2(b3.1)

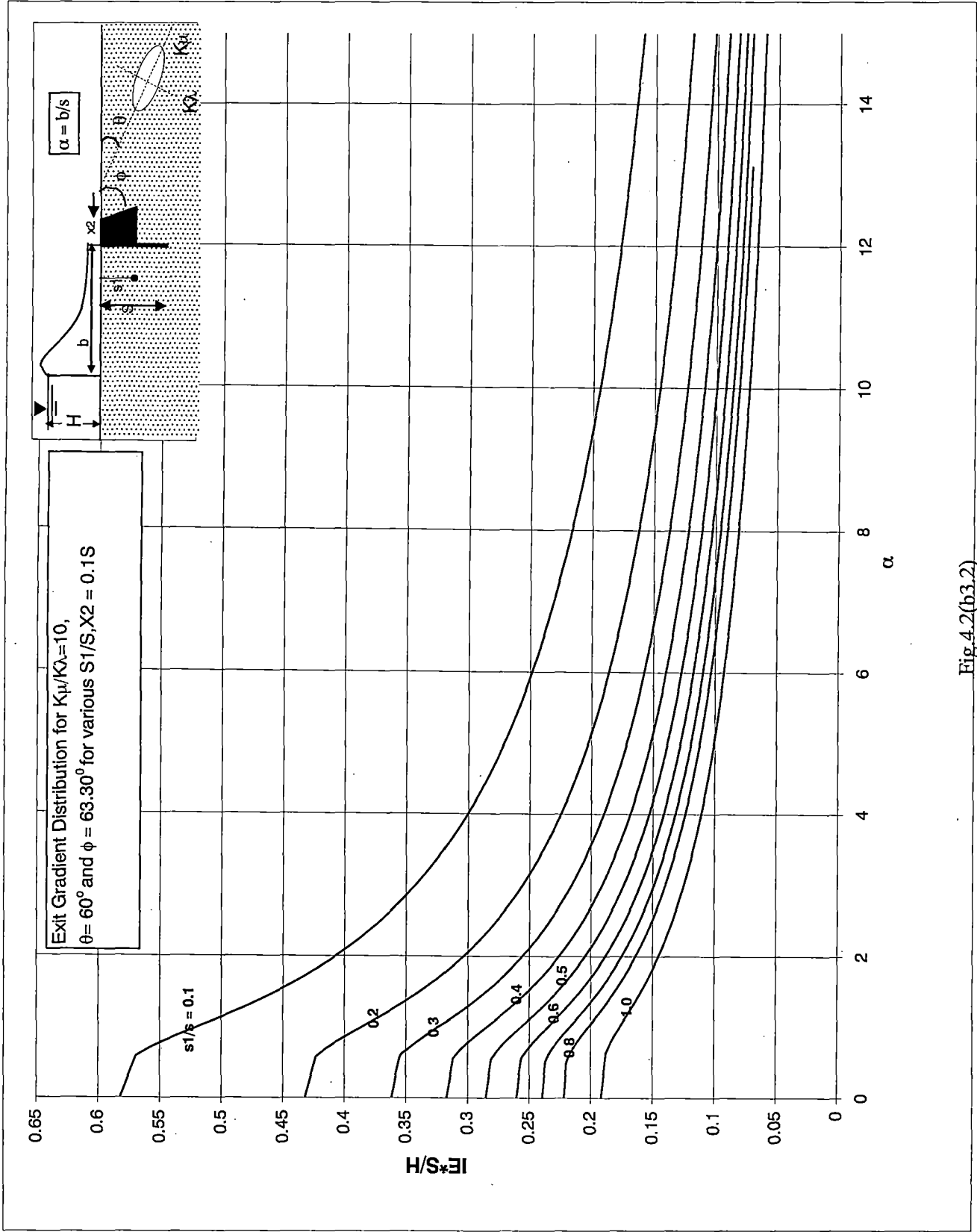


Fig.4.2(b3.2)

CHAPTER 5

DESIGN OF DOWNSTREAM FILTER BLANKET FOR A WEIR.

5.1 General

In any ordinary structure, the critical value of exit gradient is 1 or nearly so, this value of the exit gradient will not be reached if other factors do not intervene. If the exit gradients were considered purely from the academic point of view, failures of any normal structure is not possible. However, in field, various other factors encountered those create conditions leading the development of critical values of exit gradients, these are scour, wave action, sudden application or reduction of head and high spring level etc. Taking these factors into account, Khosla has suggested the following factor of safety to critical Exit gradient:

Shingle	4 to 5
Coarse sand	5 to 6
Fine sand	6 to 7

Generally, in a weir, the value of exit gradient is brought within the safe value by adjusting the dimensions of the weir. Usually, a filter blanket is provided in all hydraulic structures beyond the end sheet pile, even if, the maximum exit gradient is well within the permissible limit because of the provision of the sheet pile. The function of the filter blanket is to provide an adequate cover for the downstream sheet pile line to safe guard against the piping in case of scour. Provision of filter blanket stops the upward movement of the soil particles with the emerging sub-soil flow at exit. Usually, as a thumb rule, the filter blanket is provided for a length of D to $2D$, where D is the anticipated depth of scour measured from the downstream bed of the river.

The shape of eroded bed, downstream of a hydraulic structure, as observed by various investigators in the models and on prototype, resembles arc of a circle or an aerofoil. This change in the boundary of the flow domain will result in redistribution of the exit gradient on downstream side and the factor of safety provided to the exit gradient decreases. In this chapter, an attempt has been made to design the length of the filter (i.e.

to find the required length). The scour profile has been assumed to be linear near the sheet pile.

5.2 Statement of the Problem

Fig.5.1 (a) shows a flat bottomed weir with a vertical sheet pile constructed in an isotropic porous medium of infinite depth. b is the width of the weir and s is the length of the vertical sheet pile. The downstream reservoir boundary is inclined at an angle $\gamma\pi$ with the vertical sheet pile consequent to scour. It is required to find the exit gradient distribution along the downstream reservoir boundary and the length of filter blanket.

5.3 Analysis

The problem is solved applying the Schwarz-Christoffel transformation. First the flow region in z plane is mapped onto the lower half of an auxiliary t plane and then the complex potential plane is also mapped onto the lower half of the auxiliary t plane. From these two conformal mappings, the relationship between w and z plane is obtained. The Schwarz-Christoffel transformation for mapping the polygon ACDEG onto the lower half of the auxiliary t plane shown in fig.5.1 (c) is given by

$$z = M \int \frac{(t-m)}{(t+1)^{1/2} (1-t)^{1-\gamma}} dt + N \quad \dots(5.3.1)$$

the vertices A,C,D,E,G being mapped onto $-\infty, -1, m, 1, \infty$, respectively. In eq. 4.3.1, M and N are the constants to be determined. Let the point B and F be mapped onto the points $t = -\beta_1$ and β_2 , respectively. The values of β_1 and β_2 can be found from eq. 4.3.1 when the constants M, m and N are known. To find the constants M and N and the relationship between the transformation parameters and dimension of the structure, the integration between consecutive vertices are carried out. The constant N is governed by the lower limit of integration. For the point C, $Z = 0$ and $t = -1$, thus equation 5.3.1 can be written as

$$z = M \int_{-1}^t \frac{(1+t) - (1+m)}{(t+1)^{1/2} (1-t)^{1-\gamma}} dt$$

$$\text{or } z = M \int_{-1}^t (1+t)^{1/2} (1-t)^{\gamma-1} dt - M(1+m) \int_{-1}^t (1+t)^{-1/2} (1-t)^{\gamma-1} dt \quad \dots(5.3.2)$$

Using the variable $r = \frac{1+t}{2}$, Eq. 5.3.2 transforms to

$$z = M 2^{\frac{1+2\gamma}{2}} \int_0^{\frac{1+t}{2}} (r)^{1/2} (1-r)^{\gamma-1} dr - M(1+m) 2^{\frac{2\gamma-1}{2}} \int_0^{\frac{1+t}{2}} (r)^{-1/2} (1-r)^{\gamma-1} dr$$

or $z = M 2^{\frac{1+2\gamma}{2}} B_{\frac{1+t}{2}} \left(\frac{3}{2}, \gamma \right) - M(1+m) 2^{\frac{2\gamma-1}{2}} B_{\frac{1+t}{2}} \left(\frac{1}{2}, \gamma \right) \quad \dots(5.3.3)$

In which $B_{\frac{1+t}{2}} \left(\frac{3}{2}, \gamma \right)$ and $B_{\frac{1+t}{2}} \left(\frac{1}{2}, \gamma \right)$ are incomplete Beta functions.

Eq. 5.3.3 governs the relationship between z and t for $-1 \leq t \leq 1$.

For point D, $t = m$ and $Z = is$. Hence, from equation 5.3.3

$$is = M 2^{\frac{1+2\gamma}{2}} B_{\frac{1+m}{2}} \left(\frac{3}{2}, \gamma \right) - M(1+m) 2^{\frac{2\gamma-1}{2}} B_{\frac{1+m}{2}} \left(\frac{1}{2}, \gamma \right) \quad \dots(5.3.4)$$

Hence,

$$M = is / I_1 \quad \dots(5.3.5)$$

For point E, $t = 1$ and $Z = 0$. Hence, from equation 5.3.4

$$0 = M 2^{\frac{1+2\gamma}{2}} B \left(\frac{3}{2}, \gamma \right) - M(1+m) 2^{\frac{2\gamma-1}{2}} B \left(\frac{1}{2}, \gamma \right) \quad \dots(5.3.6)$$

in which $B \left(\frac{3}{2}, \gamma \right)$ and $B \left(\frac{1}{2}, \gamma \right)$ are complete Beta functions.

Now from equation 5.3.6, since $M \neq 0$, m can be found for known value of γ .

Then the constant M can be obtained from eq. 5.3.5

Determination of β_1 and β_2 :

For point B, $Z = Z_B = -b$ and $t = -\beta_1$. Therefore,

$$Z_B = M \int_{-1}^{-\beta_1} \frac{(t-m)}{(t+1)^{1/2} (1-t)^{1-\gamma}} dt \quad \dots(5.3.7)$$

Substituting $t = -\tau$, and $dt = -d\tau$, equation 5.3.7 reduces to

$$Z_B = M \int_1^{\beta_1} \frac{(-)(\tau+m)}{(\tau-1)^{1/2}(\tau+1)^{1-\gamma}} d\tau = \frac{s}{I_1} \int_{-1}^{\beta_1} \frac{(m+\tau)d\tau}{(\tau-1)^{1/2}(1-\tau)^{-\gamma}}$$

$$\text{or } \frac{b}{s} = \frac{I_3}{I_1} \quad \dots(5.3.8)$$

From Equation 5.3.8 for known values of b/s, β_1 can be found by using iterative method.

Integration from E to F

For point E, $Z_E = 0$ and $t = 1$; and for point F, $Z_F = L_2 e^{i\left(\frac{1}{2}-\gamma\right)\pi}$ and $t = \beta_2$.

Applying these conditions in eq. (5.3.1)

$$Z_F = M \int_1^{\beta_2} \frac{(t-m)}{(t+1)^{1/2}(1-t)^{1-\gamma}} dt$$

$$\text{or } Z_F = \frac{M}{(-1)^{1-\gamma}} \int_1^{\beta_2} \frac{(t-m)}{(t+1)^{1/2}(t-1)^{1-\gamma}} dt = \frac{M I_4}{(-1)^{1-\gamma}}$$

in which

$$I_4 = \int_1^{\beta_2} \frac{(t-m)}{(t+1)^{1/2}(1-t)^{1-\gamma}} dt$$

Substituting the value of M and Z_F

$$\frac{L_2}{s} = \frac{I_4}{I_1} \quad \dots(5.3.9)$$

From Equation 5.3.9 for known values of L_2/s , β_2 can be found by using an iteration.

Mapping of w plane onto t plane:

The complex potential w is defined as $w = \phi + i\Psi$ in which ϕ = velocity potential and Ψ = stream function. The velocity potential function ϕ is defined as

$$\phi = -k \left(\frac{P}{\gamma_w} - y \right) + C \quad \dots(5.3.10)$$

The corresponding w plane for the flow domain is shown in fig.5.1(b)

The constant C for the present case is assumed as $C = kh_2$

The mapping of the w plane onto the lower half of the t plane according to the Schwarz-Christoffel transformation is given by

$$\frac{dw}{dt} = 2 \int \frac{dt}{(t+\beta_1)^{1/2} (1-t)^{1/2}} + N_2 \quad \dots(5.3.11)$$

$$w = M_2 \int \frac{dt}{(t+\beta_1)^{1/2} (1-t)^{1/2}} + N_2 \quad \dots(5.3.12(a))$$

$$\text{or } w = M_2 \sin^{-1} \frac{2t + \beta_1 - 1}{\beta_1 + 1} + N_2 \quad (5.3.12(b))$$

in which M_2 and N_2 are constants.

For point E, $t = 1$ and $w = 0$, therefore, $N_2 = -M_2 \pi/2$

For point B, $t = -\beta_1$ and $w = -kH$ gives

$$M_2 = kH/\pi$$

Substituting the values of M_2 and N_2 in eq. 5.3.12(b)

$$w = \frac{kH}{\pi} \sin^{-1} \frac{2t + \beta_1 - 1}{\beta_1 + 1} - \frac{kH}{2} \quad \dots(5.3.13)$$

Exit gradient

The exit gradient I_E is given by

$$I_E = \frac{i}{k} \frac{dw}{dt} \frac{dt}{dz}$$

Replacing $\frac{dw}{dt}$ from eq.5.3.11, and $\frac{dz}{dt}$ from eq.5.3.1, and simplifying

$$I_E = \frac{H}{\pi} \frac{1}{(t+\beta_1)^{1/2} (t-1)^{1/2}} \frac{(1+t)^{1/2} (t-1)^{1-\gamma}}{|M| (t-m)} \quad \dots(5.3.14)$$

Substituting the value of $|M|$ and simplifying

$$I_E \frac{s}{h} = \frac{I_1}{\pi} \frac{1}{(t+\beta_1)^{1/2}} \frac{(1+t)^{1/2} (t-1)^{1/2-\gamma}}{(t-m)}$$

Substituting $t = \beta_2$, in above

$$I_E \frac{s}{h} = \frac{I_1}{\pi} \frac{1}{(t+\beta_1)^{1/2}} \frac{(1+\beta_2)^{1/2} (\beta_2-1)^{1/2-\gamma}}{(\beta_2-m)} \quad \dots(5.3.15)$$

which is the exit gradient at location F.

Now, the exit gradient at any L_2/s can be found substituting the corresponding value of β_2 .

Length of filter blanket:

Water, while moving through porous soil, imparts energy to soil particles through friction. The direction of the seepage force, acting on soil particles, will be along the gradient direction. The seepage force on the soil particles, located at the downstream boundary of the flow domain, which is an equipotential line, will act normal to the downstream surface. The other force acting on the soil particles, located at the downstream boundary of the flow domain is, gravitational force due to the effective weight of the soil particle.

Considering a volume V of soil mass, the effective weight of the soil is given by

$$F_g = V (G-1) (1-n) \gamma_w \quad \dots(5.3.16)$$

Where F_g is the gravitational force acting vertically downwards, G is the specific gravity of the soil, n is the porosity of the soil, and γ_w is the unit weight of water.

The seepage force exerted on the soil mass of volume V , by the hydraulic gradient I_E , is given by (Ceder Green, 1967)

$$F_s = -I_E \gamma_w V \quad \dots(5.3.17)$$

When the boundary of flow domain is horizontal, the seepage force F_s acts vertically upwards. Thus the factor of safety against piping, neglecting cohesion forces, is given by (Khosla, 1936)

$$\text{Factor of safety} = \frac{F_g}{F_s} = -\frac{(G-1)(1-n)}{I_E} \quad \dots(5.3.18)$$

However, with an inclined flow domain boundary, the direction of the hydraulic gradient no longer remains vertical. Fig. 5.2 shows a soil particle at the boundary of flow domain. The assumed inclined scour surface makes an angle δ with the horizontal plane $\{(\delta = (0.5-\gamma)\pi)\}$. The seepage force, being normal to the inclined surface will be at angle δ with the vertical. Therefore, the factor of safety against piping for the soil particle at this point is given by

$$\text{Factor of safety} = \frac{(G-1)(1-n)\text{Cos } \delta}{-I_E} \quad \dots(5.3.19)$$

The value of factor of safety against piping can be evaluated at any point on the assumed inclined scour profile surface using the equations (5.3.15) and (5.3.19).

Depending upon the inclination of the scoured surface with that of the horizontal, for a certain length along the downstream boundary the value of factor of safety may decrease in comparison to no scour situation. Thus, the length up to which factor of safety remains less than the provided (i.e. corresponding to no scour condition) may be considered as the length of the filter blanket.

5.4 Results and Discussion

Numerical results are presented so that the length of filter blanket for a flat bottomed weir with a vertical sheet pile at downstream end, can be obtained easily.

Exit gradient distribution with and without scour is obtained for α (b/s ratio) =1,5,10,15, and 20. The variation of $I_E^*s/H^*\text{cos}\delta$ with L_2/s taking the scoured slope as 1:1 (1 horizontal :1 vertical) is shown in fig.5.3. From these curves, for known value of α the value of L_2/s , up to which the factor of safety becomes less compared to no scour condition, can be obtained. From the figure 5.3, it is seen that for scoured slope 1:1, the value of $I_E^*s/H^*\text{cos}\delta$ is 0 at $L_2 = 0$, increases with increase in L_2/s , attains a maximum value and decreases with further increase in L_2/s . In addition, it is seen that the value of $I_E^*s/H^*\text{cos}\delta$ with scour exceeds the maximum I_E^*s/H corresponding to no scour at $L_2/s =$

0.50 to 2.01, 0.62 to 1.82, 0.78 to 1.52 and 0.88 to 1.23 for $\alpha = 1, 5, 10$ and 15, respectively. In these zones, the factors of safety provided to the maximum exit gradient with no scour will be no longer available with scour condition. Thus, these are the locations up to which the filter blanket needs to be provided. However, to maintain the continuity of the structure the filter blankets are to be placed from the point $L_2 = 0$ itself. As seen in the figure 5.3, when $\alpha = 20$, at no point the value of $I_E*s/H*\cos\delta$ exceeds the maximum I_E*s/H of no scour condition, thus filter blanket is not needed.

From the above results, one can interpret the suitable length of filter blanket to be $2.01*s$, $1.82*s$, $1.52*s$ and $1.23*s$ for $\alpha = 1, 5, 10$ and 15, respectively. Usually, the depth of downstream sheet pile is kept equal to the scour depth, in such condition the range of filter blanket can be taken as $1.23d$ to $2.01d$ that agree with the prevailing practice.

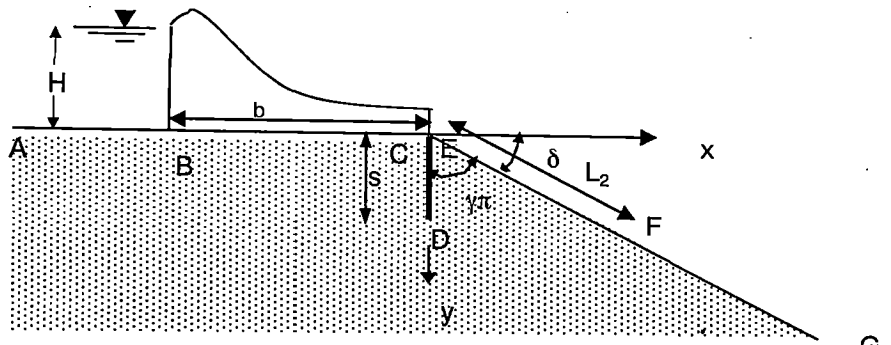
5.4 Conclusion

An analysis for exit gradient distribution for a flat bottomed weir, resting on isotropic porous medium of infinite depth, with straight line scour profile of 1:1 slope commencing from the downstream end of apron, has been obtained, using conformal mapping technique.

The analysis shows that the factor of safety against piping for the straight line scour, described by 1:1 slope, is reduced by 46.3%, 21.8%, 8.6% and 1.3% corresponding to $\alpha = 1, 5, 10$ and 15, respectively in comparison to no scour condition. As α increases the effect of scour decreases. Therefore, as b/s ratio increases the required length of filter blanket decreases.

The suitable length of the filter blanket is $2.0*s$, $1.80*s$, $1.50*s$ and $1.25*s$ for $\alpha = 1, 5, 10$ and 15, respectively.

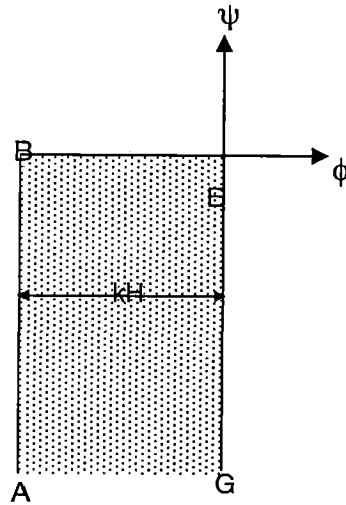
The results obtained are in agreement with the prevailing practice.



Structure with down stream scoured (inclined) boundary.

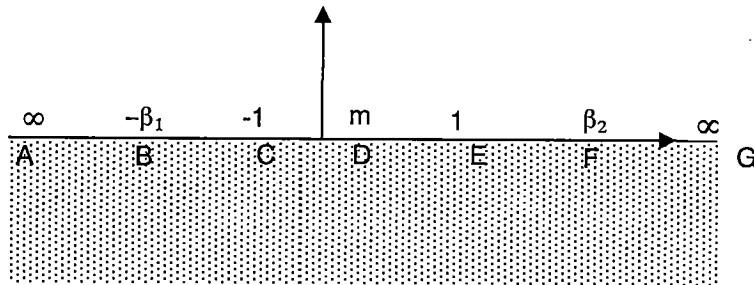
z-Plane

Fig. 5.1(a)



w-Plane

Fig 5.1 (b)



t-Plane

Fig. 5.1(c)

FIG.5.1, STEPS FOR CONFORMAL MAPPING

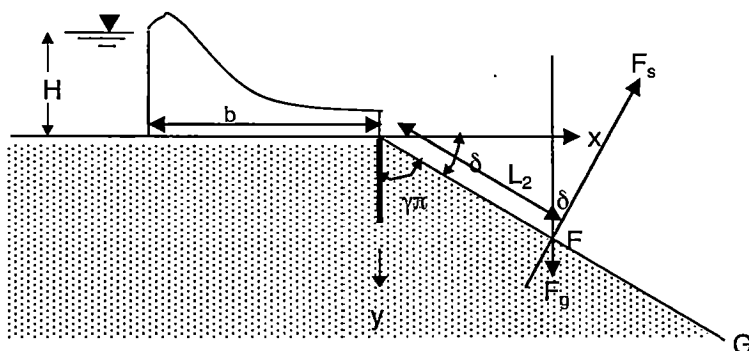
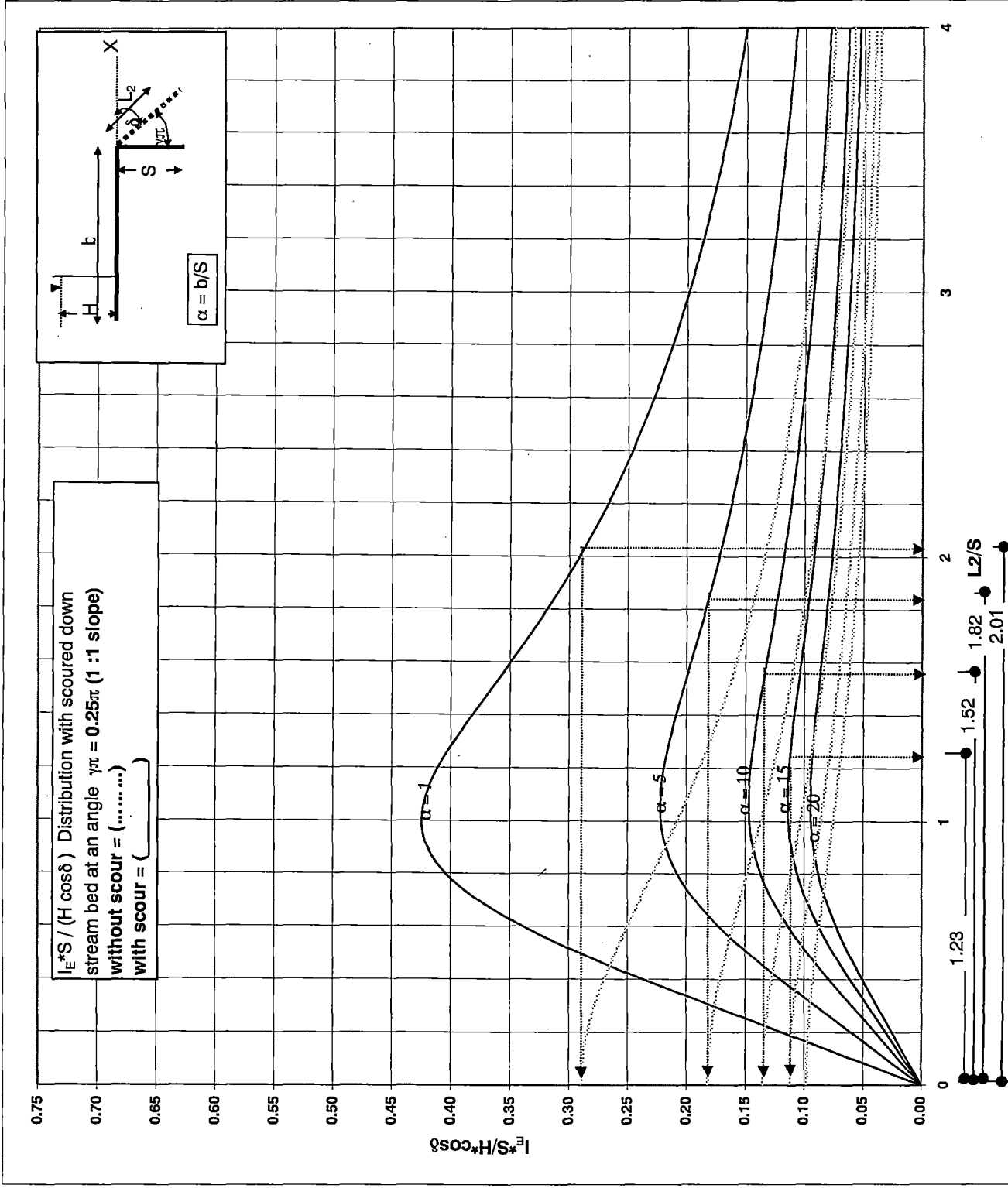


FIG.5.2, FORCES ACTING ON A SOIL PARTICLE AT THE EXIT

Fig.5.3



CHAPTER 6

GENERAL DISCUSSIONS AND CONCLUSIONS

This chapter is devoted to the critical examination of the studies reported in this dissertation and the important conclusions derived from these studies.

The aim of the present study, as stated in chapter 1 of the dissertation, is to develop the design curves for a flat bottomed weir in anisotropic porous medium of infinite depth with a vertical sheet pile line anywhere along its bottom apron. In addition, the study aims to arrive at possible length of downstream filter blanket of a weir on isotropic porous media of infinite depth with inclined profile of scoured surface.

Most natural and man-made soil deposits are anisotropic with respect to permeability to a considerable degree. The field and laboratory tests conducted by many investigators, which show sufficient evidence of anisotropy, are reported in the literature review.

Flow through anisotropic media can be analysed by transforming the anisotropic actual flow domain to a fictitious isotropic flow region by a suitable co-ordinate transformation, for which the Laplace equation is valid and conformal mapping techniques are applicable. From the solution of the problem in the transformed region, the solution for the actual problem in the anisotropic region can be obtained. In the present study, for anisotropic flow domain problem, the analyses are carried out by applying the Schwarz-Christoffel transformation to the corresponding fictitious isotropic flow domain and the obtained results are re-transformed to the actual anisotropic flow domain. The analysis to obtain the length of downstream filter blanket of a weir on isotropic porous media of infinite depth is carried out by directly applying the Schwarz-Christoffel transformation to the actual flow domain.

The analyses and results presented here can be used directly to design the weirs in anisotropic porous media of infinite depth and to obtain the length of downstream filter blanket for a weir in isotropic porous media of infinite depth. The design charts are

presented in the non-dimensional form to enable Engineers to make use of them for any systems of unit.

Chapter 3 deals with the analysis of a flat bottomed weir with a vertical sheet pile anywhere along the apron in actual anisotropic medium. The design charts are obtained and presented for different ratio of maximum and minimum coefficient of permeability, direction of maximum coefficient of permeability, ratio of floor length and vertical sheet pile and position of vertical sheet pile.

Depending upon the degree of anisotropy, the value of $-\phi/kh$ underneath the structure and the maximum exit gradient, may be significantly different in two identical structures of same shape and size but constructed on isotropic and anisotropic porous medium. For the same inclination of the maximum coefficient of permeability, the exit gradient increases as the degree of anisotropy increases.

Compared to the isotropic flow domain, as θ approaches to either 0 or π the horizontal floor becomes less effective while vertical sheet pile becomes more effective in dissipating the total head and as θ approaches to $\pi/2$ an horizontal floor is more effective in dissipating the total head.

For $\theta = 0$, the position of maximum exit gradient is at the downstream end of the structure, and for all $k_\mu/k_\lambda > 1$, the value of maximum exit gradient is always more than that of isotropic flow domain.

For $\pi/2 < \theta < \pi$, the maximum exit gradient is finite but occurs somewhere downstream of the structure. As θ increases the position of maximum exit gradient shifts away from the structure. In this case, the value of maximum exit gradient is always less than that of isotropic medium.

For $0 < \theta < \pi/2$, the exit gradient becomes infinite at the downstream end of the structure, therefore, the structure becomes vulnerable to the piping. Care should be taken to bring the maximum exit gradient within the safe limit.

Design of a weir based on isotropic flow medium may be over or under designed for anisotropic flow medium depending upon θ and k_μ/k_λ .

The results obtained for $k_\mu/k_\lambda = 1$ tally with the results given by Khosla et al.

Chapter 4 deals with the design of a toe structure for controlling the exit gradient for a structure built in anisotropic flow domain with $0 < \theta < \pi/2$.

For $0 < \theta < \pi/2$, the maximum exit gradient, just down stream of the structure becomes infinite, which makes the structure unstable against piping, in such cases the exit gradient can be controlled by providing a suitable toe structure. The inclination of the down stream face of the toe structure with the horizontal should be such that, in transformed fictitious isotropic flow domain, the face makes an angle $\leq \pi/2$ with the transformed x axis. If the inclination of the toe structure is placed in such a way that in transformed fictitious flow domain, it makes an angle $\pi/2$ with the transformed x axis, then the maximum exit gradient is finite and occurs just downstream of the structure.

The value of the maximum exit gradient can be decreased by increasing the depth of toe structure. The effect of increasing the depth of toe structure is more effective for decreasing the exit gradient for small value of α as compared to large value of α .

For small depth of the toe structure, the effect of top width of the toe structure is not preferable, i.e. it increases the exit gradient while for large depth of toe structure, it decreases the exit gradient. Therefore, minimum possible top width of toe structure, feasible from practical point of view, will be appropriate one.

Chapter 5 deals with the design of a filter blanket for a weir on isotropic porous media of infinite depth. In the present study following assumptions are made while arriving the results in this chapter:

- i)The downstream shape of the scoured surface is a straight line and inclined at a slope of 1: 1 (Horizontal: Vertical)
- ii)The filter blanket is provided in the zone where designed factor safety against piping is reduced due to scour.

The analysis shows that the factor of safety against piping for the straight line scour, described by 1:1 slope, is reduced by 46.3%, 21.8%, 8.6% and 1.3% corresponding to $\alpha = 1, 5, 10$ and 15 , respectively in comparison to no scour condition. As α increases the effect of scour decreases. Therefore, as b/s ratio increases the required length of filter blanket decreases.

The suitable length of the filter blanket is $2.0*s$, $1.80*s$, $1.50*s$ and $1.25*s$ for $\alpha = 1, 5, 10$ and 15 , respectively.

The results obtained are in agreement with the prevailing practice.

Using the present solutions, software in FORTRAN is developed which gives the uplift pressure at key points and exit gradient distribution for $\pi/2 < \theta$, maximum exit gradient for $\theta = 0$ or $\pi/2$ and maximum exit gradient with toe structure for $0 < \theta < \pi/2$. The program can be modified as per the requirement.

APPENDIX - I

FLOW REGION TRANSFORMATION

Problems concerned with anisotropic porous media may be solved by transforming the actual anisotropic flow region into a fictitious isotropic region by an appropriate co-ordinate transformation. The required scale of transformation of a two-dimensional flow problem is obtained from the equation of continuity as follows (Harr, 1962):

The equation of continuity for two-dimensional steady flow is

$$\frac{\partial u}{\partial x} + \frac{\partial v}{\partial y} = 0 \quad \dots (A-I.1)$$

in which

u, v = discharge velocity in x and y directions, respectively.

From the generalized Darcy' law,

$$u = -k_x \frac{\partial h}{\partial x} \quad \dots (A-I.2)$$

and

$$v = -k_y \frac{\partial h}{\partial y} \quad \dots (A-I.3)$$

in which k_x, k_y = principal coefficients of permeability in x and y directions, respectively;

$$h = \frac{p}{\gamma_w} + y$$

Where,

p = pressure,

γ_w = unit weight of water , and

x, y = co-ordinates.

substituting the values of u and in equation (A-I.1),

$$\frac{\partial^2 h}{\partial \left[\left(\frac{k_x}{k_y} \right) \right]} + \frac{\partial^2 h}{\partial y^2} = 0 \quad \dots(\text{A-I.4})$$

Substitution of $X = x \left(\frac{k_y}{k_x} \right)^{1/2}$ reduces eq. (A-I.4) to

$$\frac{\partial^2 h}{\partial X^2} + \frac{\partial^2 h}{\partial y^2} = 0 \quad \dots(\text{A-I.5})$$

In a similar manner, substituting $Y = y \left(\frac{k_x}{k_y} \right)^{1/2}$, it is found that

$$\frac{\partial^2 h}{\partial x^2} + \frac{\partial^2 h}{\partial Y^2} = 0 \quad \dots(\text{A-I.6})$$

Thus, by choosing one of the above two scales of transformation, a homogeneous anisotropic region can be transformed into a fictitious isotropic region for which the Laplace equation is applicable.

The mathematical procedure for transformation follows the example of Polubarinova-Kochina as given below:

Figure A-I.1 represents in x, y plane a flat bottomed weir having a vertical sheet pile and resting on an anisotropic porous medium, the direction of maximum coefficient of permeability makes an angle θ with horizontal as shown. The directions of co-ordinate axes, μ and λ , are chosen to coincide with the directions of maximum and minimum coefficients of permeability, respectively. The correspondence between these co-ordinate systems is given by

$$\mu = x \cos\theta - y \sin\theta \quad \dots(\text{A-I.7})$$

$$\lambda = x \sin\theta - y \cos\theta \quad \dots(\text{A-I.8})$$

In order to transform the anisotropic flow region to isotropic one, an expansion in the direction of λ is necessary. As stated earlier the co-ordinate in the direction of λ should be expanded using multiplying factor $\left(\frac{k_\mu}{k_\lambda}\right)^{1/2}$

In which

K_μ and K_λ = principal coefficients of permeability in the direction of μ and λ , respectively.

Designating $\eta = \lambda\left(\frac{k_\mu}{k_\lambda}\right)^{1/2}$ and replacing the value of λ from eq. (A-I.8)

$$\eta = \left(\frac{k_\mu}{k_\lambda}\right)^{1/2} (x \sin \theta + y \cos \theta) \quad \dots \text{(A-I.9)}$$

Thus, the physical anisotropic flow domain in x,y plane to fictitious isotropic flow domain in μ,η using eqs. (A-I.7) and (A-I.9)

The straight line $y = 0$ is transformed to a straight line in μ,η plane, governed by the equation

$$\frac{\eta}{\mu} = \left(\frac{k_\mu}{k_\lambda}\right)^{1/2} \tan \theta \quad \dots \text{(A-I.10)}$$

and a straight line $x = 0$ is transformed to a straight line given by

$$\frac{\eta}{\mu} = -\left(\frac{k_\mu}{k_\lambda}\right)^{1/2} \cot \theta \quad \dots \text{(A-I.11)}$$

if s is the length of a vertical sheet pile in anisotropic medium, its new length, \bar{s} , in fictitious isotropic medium is given by

$$\bar{s} = s \left(\sin^2 \theta + \frac{k_\mu}{k_\lambda} \cos^2 \theta \right)^{1/2} \quad \dots \text{(A-I.12)}$$

A horizontal blanket of width \bar{b} in the physical domain is transformed in the fictitious isotropic flow domain to a blanket of width b , which is given by

$$\bar{b} = b \left(\cos^2 \theta + \frac{k_\mu}{k_\lambda} \sin^2 \theta \right)^{1/2} \quad \dots \text{(A-I.13)}$$

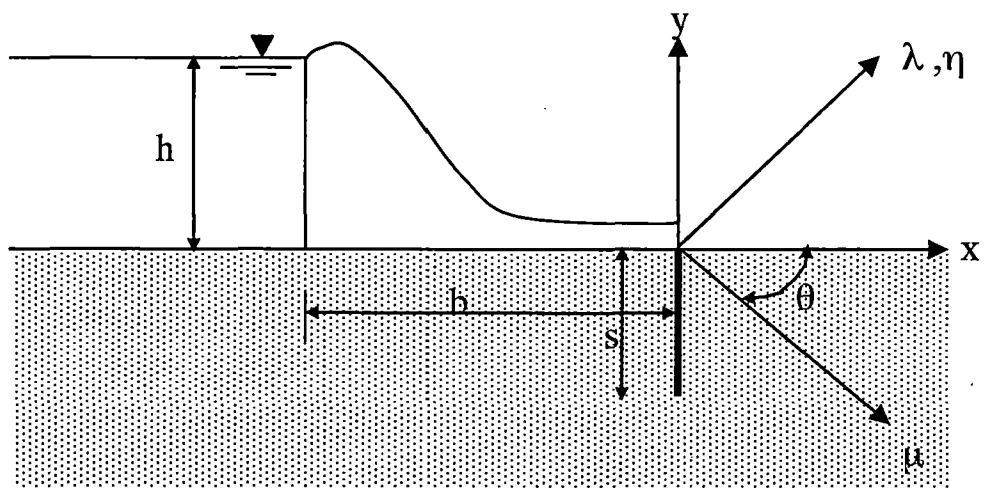


FIG. AI - 1 COORDINATE TRANSFORMATION

APPENDIX - II

RELATIONSHIPS BETWEEN EXIT GRADIENTS IN ORIGINAL AND TRANSFORMED DOMAINS

The mathematical procedure for finding the relationships between i) exit gradients in anisotropic and fictitious isotropic domain; and ii) inclination of flow lines at exit in anisotropic region follow the derivation obtained by Mishra (1972) as given below:

Figure AII.1 shows the section of an anisotropic confined flow region near the downstream surface in x,y co-ordinate system and its corresponding transformed isotropic section in \bar{x},\bar{y} co-ordinate system. The direction of maximum coefficient of permeability makes an angle θ with the direction of x . μ and λ are the axes chosen parallel to the directions of maximum and minimum coefficients of permeability, respectively. The straight line $y = 0$ transforms to the straight line $\bar{o}\bar{x}$ when the anisotropic region is converted into fictitious isotropic region. The \bar{y} axis is perpendicular to the \bar{x} axis. Point Q in fig. AII.1 locates the exit of flow line in the anisotropic flow domain and P is a point on the flow line adjacent to point Q. \bar{P} and \bar{Q} are the corresponding points in the fictitious isotropic flow domain.

The exit gradient at the point Q in actual flow domain is given by $\frac{h_P - h_Q}{ds}$, in which h_P and h_Q are the total heads at the point P and Q respectively, and ds is the elemental length PQ. Since the total head at P and Q are the total head at \bar{P} and \bar{Q} , respectively, the exit gradient in the fictitious region is given by $\frac{h_P - h_Q}{d\bar{s}}$ in which $d\bar{s}$ is the transformed length of ds .

From equation (A-I.8) and (A-I.9) ds is given by

$$ds = \left((dx)^2 + (dy)^2 \right)^{1/2} \quad \dots(\text{A-II.1})$$

$$= \left((d\mu)^2 + N_1 (d\eta)^2 \right)^{1/2} \quad \dots(\text{A-II.2})$$

in which

$$N_1 = \left(\frac{k_\lambda}{k_\mu} \right)$$

The length ds is given by

$$d\bar{s} = \left((d\mu)^2 + (d\eta)^2 \right)^{1/2} \quad \dots(\text{A-II.3})$$

The length ds is equal to the length dy . Therefore, the ratio of the exit gradient at a point in the actual flow domain and the exit gradient at the corresponding point in the fictitious domain is given by

$$\frac{\frac{h_P - h_Q}{ds}}{\frac{h_P - h_Q}{d\bar{s}}} = \frac{d\bar{s}}{ds} \quad \dots(\text{A-II.4})$$

$$= \frac{\left((d\mu)^2 + (d\eta)^2 \right)^{1/2}}{\left((d\mu)^2 + N_1 (d\mu)^2 \right)^{1/2}} \quad \dots(\text{A-II.5})$$

$$= \left[\frac{1 + \tan^2 \delta_1}{N_1 + \tan^2 \delta_1} \right]^{1/2} \quad \dots(\text{A-II.6})$$

$$\text{in which } \delta_1 = \tan^{-1} \left(\frac{1}{\sqrt{N_1}} \tan \theta \right)$$

The inclinations of the stream lines at the exit for the actual flow region are obtained as follows:

From eqs. (A-I.7) and (A-I.9)

$$dx = d\mu \cos \theta + \sqrt{N_1} d\eta \sin \theta \quad \dots(\text{A-II.7})$$

$$dy = \sqrt{N_1} d\eta \cos \theta - d\mu \sin \theta \quad \dots(\text{A-II.8})$$

Therefore, the slope of the stream lines at the exit

$$\tan \phi = \frac{dy}{dx} = \frac{-\sqrt{N_1} \cot \delta_1 - \tan \theta}{1 - \sqrt{N_1} \cot \delta_1 \tan \theta} \quad \dots(\text{A-II.9})$$

$$\text{or } \phi = \tan^{-1} \frac{-\sqrt{N_1} \cot \delta_1 - \tan \theta}{1 - \sqrt{N_1} \cot \delta_1 \tan \theta} \quad \dots(\text{A-II.10})$$

As mentioned earlier, when the actual anisotropic flow domain is transformed to a fictitious isotropic region, a vertical sheet pile in the actual flow domain generally becomes inclined in the transformed region. Using the relationships given above and the results obtained for the weirs in fictitious isotropic domain, the pressure distribution, the pressure at key points, the exit gradient distribution and the maximum exit gradient for the anisotropic case can be found out.

From the above relation it is evident that any line which is inclined at an angle ϕ (as described by the equation A-II.10) with the horizontal in anisotropic flow domain changes into the line normal to the transformed x axis in fictitious isotropic flow domain.

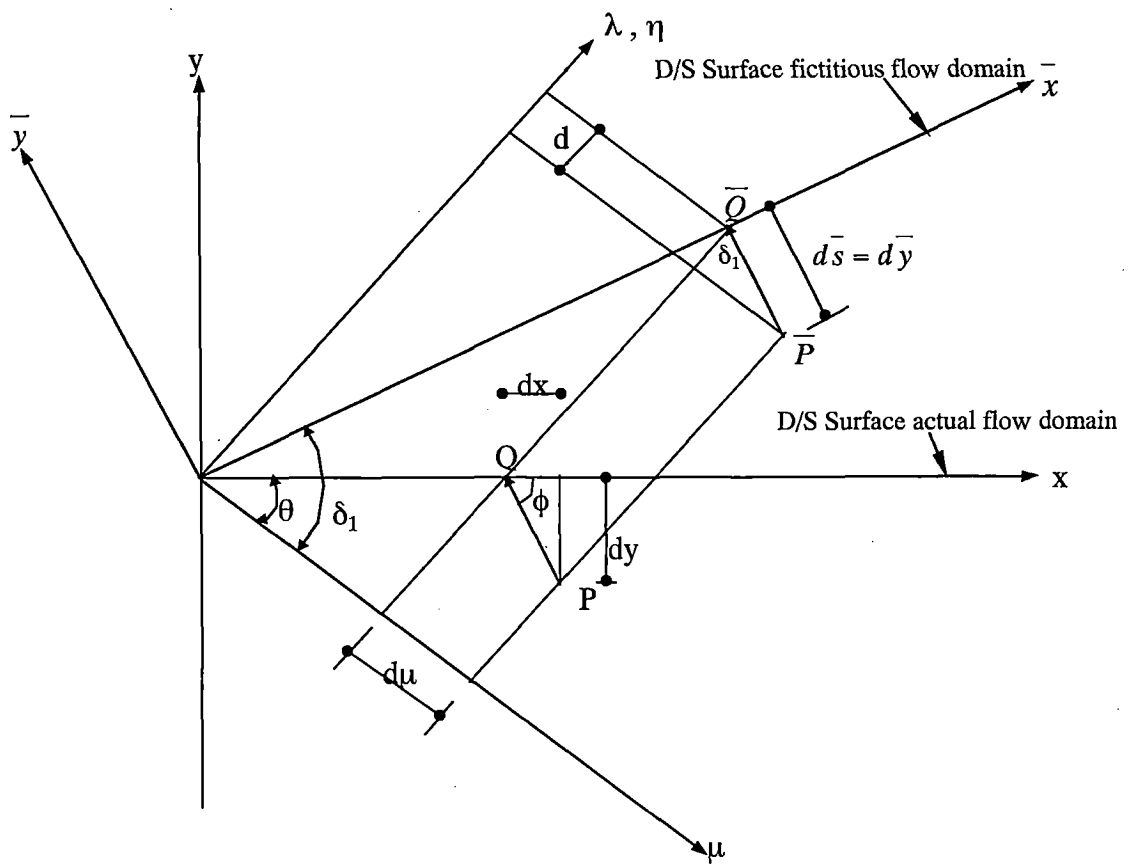


FIG. AII - 1, STEPS FOR DERIVING INCLINATIONS OF STREAM LINES

APPENDIX - III

FORTRAN PROGRAM

```
c PROGRAM LISTINGS AND EXAMPLE OUTPUT FOR
c DESIGN OF WEIRS ON PERMEABLE ANISOTROPIC POROUS MEDIUM
c *****
```

```
c This PROGRAM is a part of the M. Tech. thesis developed by Tek Bahadur Karki
c IWM (2002-4), and submitted to WRDTC,IIT,Roorkee.
c This source code is only intended as a supplement to the thesis
c " Design of Weirs on Permeable Anisotropic Porous Medium".
c See these sources for detailed information.
```

```
C
C *****
```

```
c User's guide for input
```

```
c th = angle theta in degree, direction of maximum coefficient of permeability
c r1 = ratio of maximum and minimum coefficients of permeability
c w = total width of the structure
c s = depth of vertical sheet pile
c x1 = length of upstream blanket
c sx = depth of toe structure in fraction of sheet pile depth
c unit2 is input file for gaussian quadrature coefficient
c unit 1 is input file for weir data and flow domain data
c unit 4 is input file for depth ratio of toe and sheet pile in case theta<90 degree
c Attention is to be paid while choosing initial guesses wherever
c required in the programme.
```

```
C*****
```

```
        DIMENSION WW(96),XX(96),sx(9)
        open(3,file='gauss.dat',status='old')
        open(4,file='sx.dat',status='old')
        open(1,file='weir.dat',status = 'old')
        open(2,file='result.out',status='unknown')
        read(1,*)th,r1
        read(1,*)w,s,x1
        Write(2,*)'*****'
        write(2,*)'The inputs are '
        write(2,*)'-----'
        write(2,601)th,r1,w,s,x1,w-x1
601 format(2x,/' theta = ',f6.2,'degree',2x,/' kmu/klamda = ',2x,f6.2,
```

```

1  2x,/' Total width of weir, w = ',f6.2,1x,/' Length of sheetpile,
2  s = ',f6.2,2x,/' b1 = ',f6.2,',3x,b2 = ',f6.2)
  Write(2,*)'*****'
  write(2,*)' '
  write(2,*)'The outputs are '
  write(2,*)'-----'

      pi=3.141592654
      alpha = w/s
      x2 = w-x1
      r2 = 1/r1
      th = th*pi/180
      c1 = ((sin(th))**2+r1*(cos(th)**2))**0.5
      c2=(cos(th)**2+r1*(sin(th)**2))**0.5
      x1 = x1*c2
      x2 = x2*c2
      cr = c2/c1
      s=s*c1
      w=w*c2
      d1 = atan((tan(th))/(r2**0.5))
      fm=((1+((tan(d1))**2))/(r2+((tan(d1))**2)))**0.5
      if(pi/2-th)222,221,222
      if(th)222,221,222
221   ga = 0.5
      goto 103
222   if(th)221,221,223
223   th1 = atan(((r1)**0.5)*tan(th))
      th2 = atan(-((r1)**0.5)*(1/tan(th)))
300   if(pi/2-th)101,101,102
101   ga = (abs(th1)+abs(th2))/pi
      goto 103
102   ga = (pi-abs(th1)-abs(th2))/pi
      goto 103

103   A1=1.+GA
      B=1.-GA
      A2=GA
C     initial guess values to be supplied by the users are
C     x, b1 and b2. for a dipressed weir write below the value of ratio of depression
C     to the length of sheet pile against variable r.
      delx=0.00001
      r=0
      b1=4.00001
      delb1=0.00001

```

```

b2=1.00001
delb2=0.00001
f2= x1/s
f3 = x2/s

call smodule(a1,b,a2,x,delx,sm,zd,r)
if(x1)107,107,108
107 b1 = 1
goto 112
108 call fx1(ga,b1,zb,sm,delb1,f2,zd)
if(x2)111,111,112
111 b2 = 1
goto 114
112 call fx2(ga,b2,zfe,sm,delb2,f3,zd)
114 call phi(b1,b2,sm,pi,pc,pe,pd)
if(1/2-ga)332,332,333
C if 0 < theta < pi/2, subroutine toex is called, otherwise subroutine ex is called
332 call Ex(ga,b1,sm,zd,cr,fm,pi,c1)
goto 555
333 call toex(n,ww,xx,sx,ga,pi,c1,c2,w,s,exi,fm,d1,th,r2)
goto 555
555 continue
write(2,*)'RESULTS END'

write(2,*)'#####'
Stop
end

c *****
c subroutine to calculate m

Subroutine smodule(a1,b,a2,x,delx,sm,zd,r)
1 CONTINUE
CALL BETAIN(A1,B,X,BETAI)
ZD1=2.*BETAI
CALL BETAIN(A2,B,X,BETAI)
ZD2=2*X*BETAI
ZD=ZD1-ZD2
ZE=2.*betac(A1,B)- 2*X*betac(A2,B)

RESIDUE=r-ZE/ZD
IF(ABS(RESIDUE).LT.0.00001)GOTO 5
X=X+DELX
IF(RESIDUE.GT.0.0) GOTO 1
XR=X-DELX

```

```

2      XL=XR-DELX
      X=(XL+XR)/2.

      CALL BETAIN(A1,B,X,BETAI)
      ZD1=2.*BETAI
      CALL BETAIN(A2,B,X,BETAI)
      ZD2=2*X*BETAI
      ZD=ZD1-ZD2
      ZE=2.*betac(A1,B)-2*X*betac(A2,B)
      RESIDUE=r-ZE/ZD
      IF(ABS(RESIDUE).LT.0.00001)GOTO 5
      X=X+DELX
      IF(RESIDUE.GT.0.0) GOTO 3
      IF(RESIDUE.LT.0.0) GOTO 4
3      XL=X
      GOTO 2
4      XR=X
      GOTO 2
5      CONTINUE
      SM=2*X-1.
      return
      end
c      *****
c      Subroutine to find b1
      subroutine fx1(ga,b1,zb,sm,delb1,f2,zd)
6      CONTINUE

      CALL ZBW(GA,B1,ZB,sm)

      RESIDUE=F2-ZB/ZD
      IF(ABS(RESIDUE).LT.0.00001)GOTO 7
      B1=B1+DELB1
      IF(RESIDUE.GT.0.0) GOTO 6
      B1R=B1-DELB1
      B1L=B1R-DELB1
8      B1=(B1L+B1R)/2.

      CALL ZBW(GA,B1,ZB,sm)

      RESIDUE=F2-ZB/ZD

      IF(ABS(RESIDUE).LT.0.00001)GOTO 7
      IF(RESIDUE.GT.0.0) GOTO 9
      IF(RESIDUE.LT.0.0) GOTO 10
9      B1L=B1

```

```

10      GOTO 8
      B1R=B1
      GOTO 8
7      CONTINUE
      return
      end

c      Subroutine to find b2
      subroutine fx2(ga,b2,zfe,sm,delb2,f3,zd)

21     CONTINUE
      CALL ZfeW(GA,b2,Zfe,sm)

      RESIDUE=F3-abs(Zfe/ZD)
      IF(ABS(RESIDUE).LT.0.00001)GOTO 22
      b2=b2+DELb2
      IF(RESIDUE.GT.0.0) GOTO 21
      b2R=b2-DELb2
      b2L=b2R-DELb2
23     b2=(b2L+b2R)/2.

      CALL ZfeW(GA,b2,Zfe,sm)

      RESIDUE=F3-abs(Zfe/ZD)

      IF(ABS(RESIDUE).LT.0.001)GOTO 22
      IF(RESIDUE.GT.0.0) GOTO 24
      IF(RESIDUE.LT.0.0) GOTO 25
24     b2L=b2
      GOTO 23
25     b2R=b2
      GOTO 23
22     CONTINUE
      return
      end

c      *****
C      gama function to use in complete beta function

      FUNCTION gammln(xx)
      REAL gammln,xx
      INTEGER j
      DOUBLE PRECISION ser,stp,tmp,x,y,cof(6)
      SAVE cof,stp

```



```

DATA cof,stp/76.18009172947146d0,-86.50532032941677d0,
*24.01409824083091d0,-1.231739572450155d0,.1208650973866179d-2,
*-.5395239384953d-5,2.5066282746310005d0/

```

```

11      x=xx
        y=x
        tmp=x+5.5d0
        tmp=(x+0.5d0)*log(tmp)-tmp
        ser=1.000000000190015d0
        do 11 j=1,6
          y=y+1.d0
          ser=ser+cof(j)/y
          continue
        gammln=tmp+log(stp*ser/x)

        return
        END

```

```

c      *****
c      complete beta function

```

```

CU      FUNCTION betac(z,w)
        REAL betac,w,z
        USES gammln
        REAL gammln
        betac=exp(gammln(z)+gammln(w)-gammln(z+w))
        return
        END

```

```

c      *****
c      subroutine for incomplete beta function
        SUBROUTINE BETAIN(P,Q,X,BETA)
        IF(Q.GT.1.)GOTO 100
        C4=P
        C5=1.0-Q
        C6=1.0+P
        C7=1.0
        C9=1.0
        C10=1.0
7        C9=C9*X*C4/C6*C5/C7
        C10=C10+C9
        C4=C4+1.0
        C5=C5+1.0
        C6=C6+1.0
        C7=C7+1.0
        A=ABS(C9)

```

```

IF(A.GT.0.0000001) GOTO 7
BETAI=X**P*C10/P
RETURN
100 X=1.-X
P1=Q
Q1=P
C4=P1
C5=1.0-Q1
C6=1.0+P1
C7=1.0
C9=1.0
C10=1.0
77 C9=C9*X*C4/C6*C5/C7
C10=C10+C9
C4=C4+1.0
C5=C5+1.0
C6=C6+1.0
C7=C7+1.0
A=ABS(C9)
IF(A.GT.0.0000001) GOTO 77
BETAI=X**P*C10/P
RETURN
END
c *****
c subroutine to solve integration for b1
SUBROUTINE ZBW(GA,B1,ZB,sm)
sum1=0.
N=1
5 x1=(1./((ga+n-1)*(ga+n)))*((b1-1)/(b1+1))**(ga+n-1)
N=N+1
sum1=sum1+x1
A1=ABS(X1)
IF(n.lt.20)GOTO 5
sumx=sum1*ga*(1-b1)
sum2=0.
N=1
10 x2=(1./(ga+n-1))*((b1-1)/(b1+1))**(ga+n-1)
N=N+1
sum2=sum2+x2
A2=ABS(X2)
IF(n.lt.20)GOTO 10
sumy=sum2*(1+sm)
ZB = SUMX-SUMY
RETURN
END

```

```

c      *****
c      subroutine to solve integration for b2
          subroutine ZfeW(GA,b2,Zfe,sm)
              sum1=0.
              N=1
30         x1=(1./((n-1-ga)*(n-ga)))*((b2-1)/(b2+1))**(n-1-ga)
              N=N+1
              sum1=sum1+x1
              A1=ABS(X1)
              IF(n.lt.20)GOTO 30
              sumx=sum1*ga*(1-b2)
              sum2=0.
              N=1
40         x2=(1./(n-ga))*((b2-1)/(b2+1))**(n-ga)
              N=N+1
              sum2=sum2+x2
              A2=ABS(X2)
              IF(n.lt.20)GOTO 40
              sumy=sum2*(1+sm)
              Zfe = SUMX-SUMY

              return
              END
c      subroutine to calculate phi
          Subroutine   phi(b1,b2,sm,pi,pc,pe,pd)

              pc = (1/pi)*asin((2+b1-b2)/(b1+b2))-0.5
              pE = (1/pi)*asin((-2+b1-b2)/(b1+b2))-0.5
              pD = (1/pi)*asin((2*sm+b1-b2)/(b1+b2))-0.5
              write(2,*)'The phi values '
              write(2,602)pc,pe,pd

602         format(1x,/1x,'At junc. of floor and D/S face of pile, phiC/kh =',
1f7.3,1x,/1x,'At junc. of floor and U/S face of pile, phiE/kh =',
2f7.3,1x,/1x,'At the tip of sheet pile, phiD/kh =',f7.3)

              write(2,*)'.....'
              return
              end
c      *****
c      subroutine to obtain exit gradient distribution
          Subroutine Ex(ga,b1,sm,zd,cr,fm,pi,c1)
C      initial guesse to be supplied by user is b2

              b2=1.000001

```

```

delb2=0.00001
write(2,*)'The exit gradient distribution is as follows'
write(2,*)' x/s IE*S/H'
c starting value of f4 is to be supplied by user
f4 = 0.01
66 continue
f3=f4*cr
61 CONTINUE
CALL ZfeW(GA,b2,Zfe,sm)
RESIDUE=F3-abs(Zfe/ZD)
IF(ABS(RESIDUE).LT.0.00001)GOTO 62
b2=b2+DELb2
IF(RESIDUE.GT.0.0) GOTO 61
b2R=b2-DELb2
b2L=b2R-DELb2
63 b2=(b2L+b2R)/2.

CALL ZfeW(GA,b2,Zfe,sm)

RESIDUE=F3-abs(Zfe/ZD)
IF(ABS(RESIDUE).LT.0.001)GOTO 62
IF(RESIDUE.GT.0.0) GOTO 64
IF(RESIDUE.LT.0.0) GOTO 65
64 b2L=b2
GOTO 63
65 b2R=b2
GOTO 63
62 CONTINUE

E1=abs(zd)*((1.+b2)**(1.-ga))*(b2-1.)**ga
e2= pi*((b1+b2)**0.5)*((b2-1.)**0.5)*(b2-sm)
Exi=e1/e2
Exi=fm*Exi/c1
write(2,256)f4,Exi

256 format(1x,f7.3,2x,f7.4)
f4=f4+.01
if(f4-.1)66,66,750
750 continue
f4=f4+.09
if(f4-5.1)66,66,950
850 continue
f4=f4+0.9
if(f4-11.)66,66,950
950 continue

```

```

WRITE(2,*)'.....'
WRITE(2,*)' '
return
end
c *****
c      subroutine for controlling the exit gradient
c      if 0<theta<pi/2

      subroutine toex(n,ww,xx,sx,ga,pi,c1,c2,w,s,exi,fm,d1,th,r2)

      DIMENSION WW(96),XX(96),sx(9)
      double precision sm0,gama0,beta0,b1,sm,gama,beta,ent1,
1res1,delsm0,dgama0,dbeta0,delb1,fs

      READ(3,*)N

      READ (3,*)(WW(I),I=1,N)

      READ (3,*)(XX(I),I=1,N)
      read(4,*)(sx(I),i=1,9)
c      different depth of toe structure as fraction of sheet pile length are to be supplied
c      by the user through file 4
      ph=atan( -(r2**0.5)/tan(d1))-tan(th)/
1(1-(r2**0.5)*tan(th)/tan(d1)))
      ph = ph*180/pi
      write(2,*)'Maximum exit gradient with toe structure'

      write(2,603)abs(ph)
      write(*,603)abs(ph)

603      format(1x,/,1x,'Inclination of the D/S face of toe =',f7.2,'deg.')
      x2 = 0.
      write(2,604)x2
      write(*,604)x2

604      format(1x,/,1x,'Top width of toe structure x2/s =',f7.2)
      write(2,*)' '
      write(2,*)'values of max. exit grad.with depth of toe structure'
      write(2,*)' '
      write(2,*)' s1/s  IE max *s /H'

6      FORMAT(8F7.3)

      INDEX=1

```

```

        pi=3.141592654
c      initial guess value for sm0,gama0 and beta0 are to be supplied by the user
        SM0=-0.5d0
        GAMA0=1.1d0
        BETA0=1.12d0
50     continue
        do i=1,9
        s1=sx(i)
        s2=1.
        x1=s1*cos(pi*ga)
        d=s1*sin(pi*ga)

        CALL MAIN(N,WW,XX,SM0,GAMA0,BETA0,
        1res1,s1,s2,ga,x1,x2,d,
        2FA,FB,FC,FF1,FF2,FF3,
        3DELSM0,DGAMA0,DBETA0)
c      initial guess value for b1 is to be supplied by the user.
        b1=3.0000
        sm=sm0
        gama=gama0
        beta=beta0
        ent1=res1
        delb1=0.00001

        call widthu(N,WW,XX,sm,gama,beta,b1,ga,ent1,w,s,delb1,fs)

        fs=-fs

300    format(1x,f7.3,1x,f7.4)
        Exn1=abs(ent1)
        exn2=(beta+1.)**(1.-ga)
        exn3=(beta-1.)**ga
        exn=exn1*exn2*exn3
        exd1=pi*(beta-sm)
        exd2=(beta+b1)**0.5
        exd3=(beta-gama)**0.5
        exd=exd1*exd2*exd3
        ex1=exn/exd
        exi=fm*ex1/c1
        WRITE(2,300)s1/s2,exi
        WRITE(*,300)s1/s2,exi

        end do
        write(2,*)'.....!'

```

return

END

```
c *****
C SUBROUTINE TO SOLVE JACOBIAN MATRIX

      subroutine MAIN(N,WW,XX,SM0,GAMA0,BETA0,
1res1,s1,s2,ga,x1,x2,d,
2FA,FB,FC,FF1,FF2,FF3,
3DELSM0,DGAMA0,DBETA0)
      double precision sm0,gama0,beta0,sm1,gama1,beta1,res1,aa,
1delsm0,dgama0,dbeta0
      DIMENSION WW(96),XX(96)
      DIMENSION AA(3,3),CC(3)

      EPSILON=0.000001d0
10 CONTINUE

      call bx(N,WW,XX,SM0,GAMA0,BETA0,
1res1,s1,s2,ga,x1,x2,d,
2FA,FB,FC,FF1,FF2,FF3)
      CC(1)=-FF1
      CC(2)=-FF2
      CC(3)=-FF3

      DELSM=EPSILON
      DGAMA=EPSILON
      DBETA=EPSILON

      sm1=sm0+Delsm

      call bx(N,WW,XX,SM1,GAMA0,BETA0,
1res1,s1,s2,ga,x1,x2,d,
2FA,FB,FC,FF11,FF22,FF33)
      AA(1,1)=(FF11-FF1)/DELSM
      AA(2,1)=(FF22-FF2)/DELSM
      AA(3,1)=(FF33-FF3)/DELSM

      GAMA1=GAMA0+DGAMA
      call bx(N,WW,XX,SM0,GAMA1,BETA0,
1res1,s1,s2,ga,x1,x2,d,
```

2FA,FB,FC,FF11,FF22,FF33)

AA(1,2)=(FF11-FF1)/DGAMA

AA(2,2)=(FF22-FF2)/DGAMA

AA(3,2)=(FF33-FF3)/DGAMA

BETA1=BETA0+DBETA

call bx(N,WW,XX,SM0,GAMA0,BETA1,
1res1,s1,s2,ga,x1,x2,d,
2FA,FB,FC,FF11,FF22,FF33)

AA(1,3)=(FF11-FF1)/DBETA

AA(2,3)=(FF22-FF2)/DBETA

AA(3,3)=(FF33-FF3)/DBETA

MM=3

CALL MATRIXIN(AA,MM)

SUM=0

DO J=1,3

SUM=SUM+AA(1,J)*CC(J)

ENDDO

DelSM0=SUM

SUM=0

DO J=1,3

SUM=SUM+AA(2,J)*CC(J)

ENDDO

DGAMA0=SUM

SUM=0

DO J=1,3

SUM=SUM+AA(3,J)*CC(J)

ENDDO

Dbeta0=SUM

SM0=DELSM0+SM0

GAMA0=DGAMA0+GAMA0

BETA0=DBETA0+BETA0

INDEX=INDEX+1

IF(INDEX.GT.200)GOTO 20

IF(ABS(DELSM0).GT.0.000001)GOTO 10


```

                IF(ABS(DGAMA0).GT.0.000001)GOTO 10
                IF(ABS(DBETA0).GT.0.000001)GOTO 10
                GOTO 30
20             CONTINUE
                WRITE(2,*)'ITERATRION HAS FAILED'
                GOTO 40
30             CONTINUE

40             CONTINUE

                RETURN
                END
C             *****
C             SUBROUTINE FOR MATRIXINVERSE (LU DECOMPOSITION)

SUBROUTINE MATRIXIN (AA,MM)
  DIMENSION AA(3,3),B(3),C(3)
  double precision aa

  NN=MM-1
  AA(1,1)=1./AA(1,1)
  DO 8 M=1,NN
    K=M+1
    DO 3 I=1,M
      B(I)=0.0
      DO 3 J=1,M
3         B(I)=B(I)+AA(I,J)*AA(J,K)
      D=0.0
      DO 4 I=1,M
4         D=D+AA(K,I)*B(I)
      D=-D+AA(K,K)
      AA(K,K)=1./D
      DO 5 I=1,M
5         AA(I,K)=-B(I)*AA(K,K)
      DO 6 J=1,M
        C(J)=0.0

      DO 6 I=1,M
6         C(J)=C(J)+AA(K,I)*AA(I,J)
      DO 7 J=1,M
7         AA(K,J)=-C(J)*AA(K,K)
      DO 8 I=1,M
      DO 8 J=1,M
8         AA(I,J)=AA(I,J)-B(I)*AA(K,J)

```

RETURN
END

C *****
C SUBROUTINE TO GROUP SUBROUTINES

```
subroutine bx(N,WW,XX,SM0,GAMA0,BETA0,  
1res1,s1,s2,ga,x1,x2,d,  
2FA,FB,FC,FF1,FF2,FF3)  
DIMENSION WW(96),XX(96)  
double precision sm0,gama0,beta0,res1,res2,res3,res4
```

```
CALL Fx11(N,WW,XX,ga,SM0,GAMA0,BETA0,Res 1)  
CALL Fx22(N,WW,XX,ga,SM0,GAMA0,BETA0,Res 2)  
CALL Fx3(N,WW,XX,ga,SM0,GAMA0,BETA0,Res 3)  
CALL Fx4(N,WW,XX,ga,SM0,GAMA0,BETA0,Res 4)
```

```
FA=RES2/RES1  
FB=RES3/RES1  
FC=RES4/RES1  
FF1=((s2-s1)/S2)+FA  
FF2=((x1+x2)/S2)+FB  
FF3=(d/s2)+Fc
```

RETURN
END

C *****
C SUBROUTINE Fx11

```
subroutine Fx11(N,WW,XX,ga,SM0,GAMA0,BETA0,Res 1)  
DIMENSION WW(96),XX(96)  
double precision sm0,gama0,beta0,res1
```

```
SUM=0  
DO I=1,N  
U=XX(I)  
V1=(U+1.)/2.  
v2=(sm0+1.)**(1./10.)  
v=v1*v2  
F2N1=(V**10.)-1.-SM0  
f2n2=v**((10.*ga)-1.)  
f2n3=(gama0+1.-(v**10.))**0.5
```

```

f2n=f2n1*f2n2*f2n3
F2D1=(BETA0+1.-(v**10))**0.5
f2d2=(2.-(v**10))**ga
f2d=f2d1*f2d2
F2=F2N/F2D
SUM=SUM+ WW(I)*F2
ENDDO
Res1=SUM*5*((sm0+1.)*(1./10.))
RETURN
END

```

C *****

C SUBROUTINE Fx22

```

subroutine Fx22(N,WW,XX,ga,SM0,GAMA0,BETA0,Res 2)
  DIMENSION WW(96),XX(96)
  double precision sm0,gama0,beta0,res2

```

```

SUM=0
DO I=1,N
U=XX(I)
V1=(U+1.)/2
v2=(1.-sm0)**(1./10.)
v=v1*v2
F2N1=1.-(V**10.)-SM0
f2n2=(gama0-1.+(V**10.))**0.5
f2n3=v**(9.-(10.*ga))
f2n=f2n1*f2n2*f2n3
F2D1=(BETA0-1.+(v**10))**0.5
f2d2=(2.-(v**10))**(1.-ga)
f2d=f2d1*f2d2
F2=F2N/F2D
SUM=SUM+ WW(I)*F2
ENDDO
Res2=SUM*5*((1.-sm0)**(1./10.))
RETURN
END

```

C *****

C SUBROUTINE Fx3

```

subroutine Fx3(N,WW,XX,ga,SM0,GAMA0,BETA0,Res 3)
  DIMENSION WW(96),XX(96)
  double precision sm0,gama0,beta0,res3

```

```

SUM=0

```

```

DO I=1,N
U=XX(I)
V1=(u+1.)/2.
v2=(gama0-1.)**ga
v=v1*v2
F4N1=(v**(1./ga))+1.-sm0
f4n2=(gama0-1.-(v**(1./ga)))**0.5
f4n3=v**((1.-2*ga)/ga)
f4n=f4n1*f4n2*f4n3
F4D1=(2.+(v**(1./ga)))**(1.-ga)
f4d2=(beta0-1.-(v**(1./ga)))**0.5
f4d=f4d1*f4d2
F4=F4N/F4D
SUM=SUM+WW(I)*F4
ENDDO
Res3=(SUM*((gama0-1.)**ga))/(2.*ga)
RETURN
END

```

C *****

```

C SUBROUTINE Fx4
  subroutine Fx4(N,WW,XX,ga,SM0,GAMA0,BETA0,Res 4)
    DIMENSION WW(96),XX(96)
    double precision sm0,gama0,beta0,res4

```

```

SUM=0
DO I=1,N
U=XX(I)
V1=(u+1.)/2
v2=(beta0-gama0)**0.5
v=v1*v2
F5N1=(beta0-sm0-v**2.)
f5n2=(beta0-gama0-v**2.)**0.5
f5n=f5n1*f5n2
F5D1=(beta0+1.-v**2.)**(1.-ga)
f5d2=(beta0-1.-v**2.)**ga
f5d=f5d1*f5d2
F5=F5N/F5D
SUM=SUM+WW(I)*F5
ENDDO
Res4=SUM*((beta0-gama0)**0.5)
RETURN
END

```

C *****

```

c      SUBROUTINE TO OBTAIN B1
      subroutine widthu(N, WW, XX, sm, gama, beta, b1, ga, ent1, w, s, delb1, fs)

      double precision sm, gama, beta, b1, delb1, ent1, fs

      DIMENSION WW(96), XX(96)

21     CONTINUE
      call fx5(N, WW, XX, sm, gama, beta, b1, ga, ent1, fs)

      RESIDUE=(w/s)+Fs
      IF(ABS(RESIDUE).LT.0.00001)GOTO 22
      b1=b1+DELb1
      IF(RESIDUE.GT.0.0) GOTO 21
      b1R=b1-DELb1
      b1=b1R-DELb1
23     b1=(b1L+b1R)/2.

      call fx5(N, WW, XX, sm, gama, beta, b1, ga, ent1, fs)

      RESIDUE=(w/s)+Fs

      IF(ABS(RESIDUE).LT.0.000001)GOTO 22
      IF(RESIDUE.GT.0.0) GOTO 24
      IF(RESIDUE.LT.0.0) GOTO 25
24     b1L=b1
      GOTO 23
25     b1R=b1
      GOTO 23
22     CONTINUE
      Return
      end

C      *****
C      SUBROUTINE ROUTINE FX5

      SUBROUTINE fx5(N, WW, XX, sm, gama, beta, b1, ga, ent1, fs)
      double precision sm, gama, beta, b1, ent1, ent5, fs

      DIMENSION WW(96), XX(96)

      SUM=0
      DO I=1, N

```

U=XX(I)

v=(U+1.)*((b1-1.)**(1./20))/2.

F1N=(v**20.+1.+sm)*((v**20+1.+gama)**0.5)*
1(v**(20.*ga-1.))
F1D=((v**20+2.)*ga)*((v**20+beta+1.)*0.5)
F1=F1N/F1D
SUM=SUM+WW(I)*F1

ENDDO

ENT5=SUM*10*((b1-1.)**(1./20.))

Fs=ENT5/ENT1

RETURN

END

Sample Output, example 1

The inputs are

theta = 120.00degree

kmu/klamda = 2.00

Total width of weir, w = 25.00

Length of sheetpile, s = 5.00

b1 = 25.00, b2 = .00

The outputs are

The phi values

At junc. of floor and D/S face of pile, $\phi_C/kh = .000$

At junc. of floor and U/S face of pile, $\phi_E/kh = -.351$

At the tip of sheet pile, $\phi_D/kh = -.216$

.....

The exit gradient distribution is as follows

x/s	IE*S/H
.010	.0583
.020	.0696
.030	.0764
.040	.0816
.050	.0858
.060	.0896
.070	.0928
.080	.0957
.090	.0983
.100	.1007
.200	.1171
.300	.1261
.400	.1307
.500	.1320
.600	.1310
.700	.1283
.800	.1245
.900	.1201
1.000	.1154
1.100	.1107
1.200	.1061

1.300	.1017
1.400	.0975
1.500	.0936
1.600	.0899
1.700	.0865
1.800	.0832
1.900	.0802
2.000	.0774
2.100	.0748
2.200	.0724
2.300	.0701
2.400	.0679
2.500	.0659
2.600	.0640
2.700	.0622
2.800	.0605
2.900	.0589
3.000	.0574
3.100	.0560
3.200	.0546
3.300	.0533
3.400	.0521
3.500	.0509
3.600	.0498
3.700	.0488
3.800	.0477
3.900	.0468
4.000	.0458
4.100	.0449
4.200	.0441
4.300	.0433
4.400	.0425
4.500	.0417
4.600	.0410
4.700	.0403
4.800	.0396
4.900	.0389
5.000	.0383

.....
RESULTS END

#####

APPENDIX – IV

REFERENCES

1. Arvin, V.I. , and Numerov, S.N. , (1965), “ Theory of Fluid Flow in Undeformable Porous Media ,” Translated from Russian by Israel Program for Scientific Translation, Jerusalem.
2. Dagan, G. , (1967), “ A Method of Determining the Permeability and Effective Porosity of Unconfined Anisotropic Aquifers,” Water Resources Research, Vol.3, No.4, Fourth Quarter, pp. 1059 – 1071.
3. Davis, N.S., (1969), “ Porosity and Permeability of Natural Materials,” Flow through Porous Media, Edited by Roger J.M. De Weist, Academic Press, New York, p.70.
4. De Weist, R.J.M., (1965), “ Geohydrology, “ John Wiley and Sons, New York.
5. Harr, M.E., (1962), “ Groundwater and Seepage, “ McGraw-Hill Book Company, Inc., New York.
6. Khosla, R.B.A.N., Bose, N.K., and Taylor, E.Mc K., (1954), “Design of Weirs on Permeable Foundations,” Central Board of Irrigation, New Delhi, India.
7. Krizek, R.J., and Anand, V.B., (1968), “Flow Around a Vertical Sheet pile Embedded in an Inclined Stratified Medium,” Water Resources Research, Vol.4,No.1, February, pp. 113-123.
8. Kumar, D., (1982), “ Optimal Design of Barrage on Permeable Foundation”, Ph.D. Thesis, School of Hydrology, University of Roorkee, Roorkee, India.
9. Leliavsky S., (1957), “Irrigation and Hydraulic Design (Vol I and II),” Chapman and Hall Ltd., London
10. Luthin, J.N., (1957), “Drainage of Agricultural Lands,” American Society of Agronomy, Madison, Wisconsin.
11. Mansur, C.I., and Dietrich, R.J., (1965), “Pumping Test to Determine Permeability Ration,” Journal of the Soil Mechanics and Foundations Division, ASCE, Vol.91, No.SM4, Proc. Paper 4415, pp. 151-183

12. Marcus, H., (1962), "The Permeability of a Sample of an Anisotropic Porous Media," Journal of Geophysical Research, Vol.67, No. 13, December, pp.5215-5225.
13. Mishra, G.C., (1972), "Confined and Unconfined Flows through Porous Media." Ph.D. Thesis, Faculty of Engineering, Indian Institute of Science, Bangalore, India.
14. Muskat, M., (1937), "The Flow of Homogeneous Fluids through Porous Media." McGraw-Hill Book Company, New York.
15. Palubarinova-Kochina, P.Ya., (1962), "Theory of Groundwater Movement." Translated from the Russian by J.M. Roger De Weist, Princeton University Press, Princeton, New Jersey.
16. Sharma, H.D, et al, (1972), "Hydraulic Design of Undersluices Bays, the Barrage Bays and Head Regulator for Kosi Barrage near Ramnagar – A Model Study," Technical Memorandum No. 45, R.R. (H₁ – 8/c), IRI, Roorkee.
17. William, H.P., William, T.V., Saul, A.T., Brain, C.F., (1993) "Numerical Recipes in Fortran, The art of Scientific Computing," Cambridge university Press.